THESIS ON NATURAL AND EXACT SCIENCES B134

Interactions of Alzheimer`s Amyloid-ß Peptides with Zn(II) and Cu(II) Ions

ANN TIIMAN

TUT
PRESS

TALLINN UNIVERSITY OF TECHNOLOGY
Faculty of Science
Department of Gene Technology

Dissertation was accepted for the defense of the degree of Doctor of Philosophy in Gene Technology on June 20, 2012.

Supervisors: Associated Professor Vello Tõugu, Department of Gene Technology, Tallinn University of Technology, Estonia

Professor Peep Palumaa, Department of Gene Technology, Tallinn University of Technology, Estonia

Opponents: Professor Astrid Gräslund, Department of Biochemistry and Biophysics, Stockholm University, Sweden

Professor Tiit Land, Tallinn University, Estonia

Defense of the thesis: August, 30, 2012, Tallinn University of Technology.

Declaration:
I hereby declare that this doctoral thesis, my original investigation and achievement, submitted for the doctoral degree at Tallinn University of Technology has not been submitted for any academic degree.

This dissertation was supported by European Social Fund.

Copyright: Ann Tiiman, 2012
ISSN 1406-4723
ISBN 978-9949-23-329-8 (publication)
ISBN 978-9949-23-330-4 (PDF)

LOODUS- JA TÄPPISTEADUSED B134

Alzheimeri amüloid-ß peptiidide interaktsioonid Zn(II) ja Cu(II) ioonidega

ANN TIIMAN

TTÜ
KIRJASTUS

CONTENTS

INTRODUCTION

Taking some time for yourself and for philosophy you look at the world and try to see what it is made of. You find that at the beginning it is all about mathematics – the probability that anything can exist or be talked of. Then you need some physics that tells you how these probabilities are coming to reality and what "forces" things to happen. After the probabilities and different kinds of forces taking effect, you see the interactions between atoms and molecules which brings you to chemistry. Moving on from chemistry, putting together different molecules and complex systems, somewhere and somehow you find yourself in biology with cells and life, functioning in all its complexity, and difficulties that malfunctioning brings with itself. This is where things are getting very complicated and hard to understand.

If you now take a step back and look at the big picture again you find yourself in a world where we have learned so much about the basic building blocks that many aspects of the world we can now manipulate, including our own body. As a result, life expectancy has risen all over the world and if it continues with the current trend then in 2050 more than 10 % of the population in Europe will be over the age of 80. Simply put the population is "graying" and people are living much longer. However, the golden years are not always so golden. A direct result of living longer is that the number of people with various dementias is growing. Alzheimer's disease (AD) is the most common of these accounting for up to 60 % of dementia cases. It has been estimated that one in two people who live up to their mid-80's will get the disease. Therefore new challenges have risen in the world of medicine with the main goal being to make the twilight years of our lives enjoyable.

It is important to understand disease mechanisms, because then it is possible to change its course, to delay the symptoms, or if we are really lucky, eliminate the disease altogether. If you look at a person with AD you see problems in simple everyday functioning – at first there are difficulties in forming new memories, but as the disease progresses new mental problems arise, including impaired judgment and speech. In the end stages of AD a person is no longer able to look after oneself and needs around-the-clock-care. If you compare a brain of a person who has AD with a healthy person's brain you find that in the case of AD there is severe shrinkage which is a result of neurons dying. You can also see the amyloid plaques that are the primary hallmark of the disease which are composed mainly of the amyloid-β (Aβ) peptides that are now considered to be the key molecules in AD pathology. Looking at the brain you find that the deposition of Aβ into amyloid plaques occurs in the presence of various biomolecules and ions that may affect this process. Among these are also zinc and copper, which are found in elevated levels in the amyloid plaques. This has lead to the hypothesis that these biometals have an important role in AD.

This thesis is about the interactions of Zn(II) and Cu(II) ions with the Aβ as well as their role in Aβ fibrillization. The primary interaction is the binding of the metal ion to the peptide molecule. The determination of the dissociation constants of the Cu(II)-Aβ and Zn(II)-Aβ complex is the first step in the long journey of understanding the role of metal ions in AD. We determined the dissociation constants for both complexes, looked at the bigger picture, and found the reasons for the variability of the literature data thus far. The second step we made was to examine the effect of Zn(II) and Cu(II) on Aβ fibrillization. Based on our results we were able to propose a mechanism for the Aβ aggregation in the presence of these metal ions. The results are a big step forward in understanding the role of metal ions in AD pathogenesis, however it is clear that there is still a long road to travel before we fully understand AD.

ABBREVIATIONS

Aβ	Amyloid-beta peptide
ACES	2-(carbamoylmethylamino)ethanesulfonic acid
AD	Alzheimer's disease
APOE	Apolipoprotein E
APP	Amyloid precursor protein
BBB	Blood-brain-barrier
CNS	Central nervous system
CQ	5-chloro-7-iodo-8-hydroxyquinoline
CSF	Cerebrospinal fluid
DFO	Desferroxamine
HEPES	4-(-2-hydroxyethyl)-1-poperazineethanesulfonic acid
HFIP	1,1,1,3,3,3-hexafluoro-2-propanol
K_D	Conditional dissociation constant
K_D^{app}	Apparent dissociation constant
MALDI	Matrix-assisted laser desorption/ionization
Me^{2+}	Metal ion
MS	Mass spectrometry
MT	Metallothionein
NFT	Neurofibrillary tangles
NMR	Nuclear magnetic resonance
P	Protein/peptide
PBS	Phosphate buffer saline
Pipes	1,4-pierazinediethanesulfonic acid
PS1	Presenilin-1
PS2	Presenilin-2
ROS	Reactive oxygen species
TEM	Transmission electron microscopy
ThT	Thioflavin T
Tris	2-amino-2-hydroxymethyl-propane-1,3-diol
UV-Vis	Ultraviolet-visible

ORIGINAL PUBLICATIONS

This thesis is based on the following publications, which will be referred to in the text by their roman numerals.

I. Tõugu, V., **A. Karafin** and P. Palumaa (2008). "Binding of Zinc(II) and Copper(II) to the Full-Length Alzheimer's Amyloid-Beta Peptide." J. Neurochem. 104(5): 1249-1259.

II. Tõugu, V., **A. Karafin**, K. Zovo, R. S. Chung, C. Howells, A. K. West and P. Palumaa (2009). "Zn(II)- and Cu(II)-Induced Non-Fibrillar Aggregates of Amyloid-Beta (1-42) Peptide Are Transformed to Amyloid Fibrils, Both Spontaneously and under the Influence of Metal Chelators." J. Neurochem. 110(6): 1784-1795.

III. **Karafin, A.**, P. Palumaa and V. Tõugu (2009). "Monitoring of Amyloid-Beta Fibrillization Using an Improved Fluorimetric Method." New Trends Alzheimer Parkinson Relat. Disord.: AD/PD 2009, 9th , Medimond 255-261.

IV. Zovo, K., E. Helk, **A. Karafin,** V. Tõugu and P. Palumaa (2010). "Label-Free High-Throughput Screening Assay for Inhibitors of Alzheimer's Amyloid-B Peptide Aggregation Based on MALDI MS." Anal. Chem. 82(20): 8558-8565.

V. Tõugu, V., **A. Tiiman** and P. Palumaa (2011). "Interactions of Zn(II) and Cu(II) Ions with Alzheimer's Amyloid-Beta Peptide. Metal Ion Binding, Contribution to Fibrillization and Toxicity." Metallomics 3(3): 250-261

Author's contribution

Publication I: The author participated in planning and preformed the experimental work, analyzed the data, and participated in the manuscript preparation.
Publication II: The author participated in planning and preformed the experimental work, analyzed the data (except cell experiments), and participated in the manuscript preparation.
Publication III: The author participated in planning and preformed the experimental work, analyzed the data, and participated in the manuscript preparation.
Publication IV: The author participated in planning and preformed the fluorimetric experiments and analyzed the data.
Publication V: The author participated in the writing of the review.

1. REVIEW OF THE LITERATURE

1.1. Amyloid

A living organism may contain as many as 100 000 different proteins (Dobson 2001). The ability of the newly synthesized proteins to fold to their functional states is one of the most remarkable features of biology. Errors in protein folding are connected with serious consequences and a broad range of human diseases arise from incorrectly folded proteins (Thomas et al. 1995; Dobson 2001; Horwich 2002). These conditions are referred to as protein misfolding or protein conformational diseases. The largest group of misfolding diseases is associated with the conversion of peptides or proteins from their functional soluble states into highly regular fibrillar aggregates. The histology of these aggregates was appreciated more than 150 years ago and was termed amyloid (Aguzzi and O'connor 2010), because the aggregated material stains with dyes such as Congo red similarly to starch (*amylum*).

In 1968, for the first time it was demonstrated that amyloid is built up from cross-β structural motifs (Geddes et al. 1968) and the aggregated peptide β-strands were implicated as the key structural feature of amyloids. It is now known that amyloid formation is not necessarily pathological, in some cases it might have a normal physiological function (Berson et al. 2003; Chiti and Dobson 2006; Maji et al. 2009). Furthermore, it appeared that *de novo* designed peptides and some naturally occurring proteins that are not associated with diseases can also be induced to form amyloid fibrils under appropriate conditions (Chiti et al. 1999). This indicates that fibrillization may be a generic property of a polypeptide chain. It should also be noted here that not all proteinaceous aggregates are amyloids. Originally the term amyloid was used only to describe extracellular protein deposits that stain with histological dyes. However, currently the term amyloid describes both extracellular and intracellular aggregates with regular fibrillar structures. All amyloid fibrils have some common structural features despite the primary sequence diversity. Amyloids are unusual in being kinetically stable structures (Dobson 2003; Selkoe 2003) that can persist for long periods. They are elongated, unbranched, ~6-20 nm wide rope like polymers that are physically and chemically robust (e.g., protease-resistant) (Goldsbury et al. 2011). The main characteristic of the amyloid fibril is that the ordered regions adopt the classic cross-β-structure, where the β-strands align perpendicular to the long axis of the fibril and inter-chain β-sheet hydrogen bonds are oriented parallel to the fibril axis (See Fig. 3C) (Tycko 2004; Nelson et al. 2005). In fibrils formed form the amyloid-β (Aβ) peptides the individual strands within the β-sheets can be parallel (Torok et al. 2002; Petkova et al. 2005) or antiparallel (Qiang et al. 2012) depending on the Aβ sequence. The supermolecular structure of the fibrils can be very complex

and the individual fibrils are formed from protofilaments with typically 2 to 9 protofilaments per fibril (Abedini and Raleigh 2009).

The proteinaceous deposits found in patients with any of the amyloid diseases have a major protein component that forms the amyloid core and also additional associated molecules, including glycosaminoglycans, the serum amyloid P component, apolipoprotein E (APOE), collagen as well as metal ions (Chiti and Dobson 2006). These various minor components of the deposits may play an important role in the aggregation process or mediate the cytotoxicity of these aggregates.

Amyloidoses can be grouped as neurodegenerative diseases where aggregation occurs in the brain, nonneuropathic localized amyloidoses, where aggregation occurs in a single tissue other than the brain, and nonneuropathic systemic amyloidoses, where aggregation occurs in multiple tissues (Chiti and Dobson 2006). The neurodegenerative diseases include disorders in which the pathological proteins accumulate within the nucleus (for example Huntington's disease and spinocerebellar ataxias), in the cytoplasm (Parkinson's disease), in the extracellular space (prion diseases), or in multiple locations like in the cytoplasm and in the extracellular space (Alzheimer's disease (AD)) (Aguzzi and O'connor 2010).

1.2. Alzheimer's disease

Dementia is a wide term, describing different diseases and conditions that develop when nerve cells in the brain die or no longer function normally. This in turn causes changes in one's memory, behavior, and ability to think clearly. By 2005, 24.2 million people around the world had dementia and 4.6 million new cases were diagnosed in that year alone (Ferri et al. 2005). It is estimated that the number of people with dementia will rise by 2040 by 80-190 % in Europe, North America, and the developed Western Pacific region, while an increase by more than 300 % is proposed for Latin America, India, China, North Africa, and the Middle Eastern Crescent (Hampel et al. 2011). AD is the main cause of dementia, accounting for 50-60 % of all cases (Hendrie 1998). These dramatic numbers indicate that AD already has and will have a tremendous impact on society and it could be viewed as a modern epidemic.

AD is thought to begin as many as 20 years prior to its clinical diagnosis (Alzheimer's 2012) and it affects people in different ways but the common first symptom of the disease is episodic memory impairment. In the first stages the semantic memory and procedural memory are relatively spared (Jakob-Roetne and Jacobsen 2009). As the disease progresses cognitive abilities decline, including impaired judgment, decision making, and orientation. In later stages psychobehavioral disturbances as well as language impairment often occurs

(Galimberti and Scarpini 2012). In advanced AD, people need help with basic activities of daily living, such as dressing, eating, and using the bathroom, in final stages people become bedbound and reliant on around-the-clock care. AD is ultimately fatal with the mean survival around 4-8 years (Alzheimer's 2012).

Age is the major risk factor for AD with doubling of the risk with every five years after the age of 65 (Cummings et al. 1998). Genetically, AD is divided into two forms: familial and sporadic. Familial AD has a Mendelian inheritance and is predominantly early onset (< 60 years). Three genes have been implicated in the pathophysiology of familial AD: amyloid precursor protein (APP) and presenilin (PS1 and PS2) genes. The genetic heritability of sporadic AD is estimated to be high (Gatz et al. 2006), but it is likely that gene combinations rather than a single gene determine disease occurrence. *APOE* is currently the only established susceptibility gene for late-onset AD. It has been estimated that the four established AD risk genes account for less than 30 % of the genetic variance of the disease, therefore numerous additional risk genes exist (Daw et al. 2000). Several genes are currently under investigation, including *SORL1* (Rogaeva et al. 2007), *GAB2* (Reiman et al. 2007), and *A2M* (Blacker et al. 1998), however these need further validation. Other risk factors that increase disease risk include vascular diseases, diabetes, hypertension, traumatic head injury, smoking, and obesity. Preventive modifiers are anti-inflammatory agents, physical exercise, cognitive activity, and antioxidants (Reitz et al. 2011).

Looking at the brain of an AD patient severe atrophy which is caused by the loss of dendrites and axons, myelin reduction, shrinkage, and the death of neurons can be observed (Sjobeck et al. 2005). For example in the end stages of AD more than 80 % of the neurons in the hippocampus have disappeared and the volume is reduced to less than a half (Bobinski et al. 1996; Smith 2002). The neuropathological hallmarks of the disease are extracellular amyloid beta plaques and intracellular neurofibrillary tangles (NFT). NFTs are composed of the microtubule-associated protein tau, which is hyperphosphorylated and has severe oxidative modifications (Mattson 2004). Amyloid plaques are composed mainly of small, 4 kDa Aβ peptides (Masters et al. 1985; Welander et al. 2009) which are derived from the APP. There are three types of Aβ deposits in AD brains, named diffuse plaques, senile plaques, and cerebrovascular deposits (Morgan et al. 2004). Diffuse plaques are usually smaller than 20 μm in diameter, amorphous and spherical Aβ deposits which might represent an early stage of amyloid formation (Castellani et al. 2010). Senile plaques are also spherical, with a diameter around 50-200 μm, containing an amyloid core and are surrounded by dystrophic neurites (Morgan et al. 2004). The temporal and spatial connections between these two hallmarks of the disease are not well understood. Amyloid plaques appear first in the frontal cortex and then spread through the cortical region. NFTs are first seen in the limbic system and from there progress to the cortical region (Pimplikar 2009).

There are various hypothesis about the cause of AD, including amyloid cascade hypothesis (Hardy and Higgins 1992), neuronal cytoskeletal degeneration hypothesis (De Ferrari and Inestrosa 2000), cholinergic hypothesis (Bartus et al. 1982), inflammation (Galimberti et al. 2008), oxidative damage (Reddy et al. 2009), and mitochondrial dysfunction (Santos et al. 2010). The amyloid cascade hypothesis is currently the best defined and most studied conceptual framework for AD. However, these hypotheses are not mutually exclusive, for example copper in the amyloid plaques may cause oxidative damage which in turn may lead to inflammation or to mitochondrial dysfunction.

1.3. Amyloid cascade hypothesis

In 1992 Hardy and Higgins formalized the amyloid cascade hypothesis, which states that "*deposition of amyloid β protein (AβP), the main component of the plaques, is the causative agent of Alzheimer's pathology and the neurofibrillary tangles, cell loss, vascular damage, and dementia follow as a direct result of this deposition*" (Fig. 1 and Fig. 2) (Hardy and Higgins 1992). This hypothesis has also been implemented for other neurodegenerative diseases, for example Parkinson's disease (Santner and Uversky 2010). The amyloid cascade hypothesis is supported by several lines of evidence, from divergent areas such as genetics, histopathology, and animal models.

Perhaps the strongest evidence for the role of amyloid in AD comes from the genetics. To date, 32 different mutations have been identified in the *APP* gene (Galimberti and Scarpini 2012). Most of these mutations are localized at or near the cleavage sites that give rise to the Aβ peptide and enhance the production of the Aβ peptide or increase the amount of $A\beta_{42}$ (Suzuki et al. 1994; Scheuner et al. 1996; Eckman et al. 1997; Kwok et al. 2003). Those few mutations that are within the Aβ peptide are thought to increase the fibrillization propensity of Aβ (Wisniewski et al. 1991). 182 mutations in *PSEN1* and 13 mutations in *PSEN2* have been described (Galimberti and Scarpini 2012). Mutations in the presenilin genes also enhance the processing of APP to form amyloidogenic Aβ (Scheuner et al. 1996). Moreover essentially all people with Down syndrome (trisomy 21) develop the neuropathological hallmarks of AD after the age of 40 and more than half of the people with Down syndrome show clinical evidence of cognitive decline (Brugge et al. 1994). It is presumed that this is due to a lifelong overexpression of the *APP* gene on chromosome 21, whereas AD was not detected clinically or pathologically in a 78-year-old woman, who had a partial trisomy 21, with no extra copy of the *APP* gene (Prasher et al. 1998). The fourth gene, implicated in AD, *APOE*, codes for a lipid-binding protein that is expressed in humans as one of three isoforms, which are encoded by three different alleles, *APOE ε2, APOE ε3*, and *APOE ε4*. The presence of a single *APOE ε4* allele is associated with a 2-3 fold increase in the risk, while two

copies is associated with a fivefold increase in the risk of getting AD. Each inherited *APOE ε4* allele lowers the onset of the disease by 6-7 years (Corder et al. 1993; Poirier et al. 1993; Kurz et al. 1996). Various roles have been suggested for APOE in AD pathogenesis (Kim et al. 2009), including that APOE isoforms differentially affect Aβ clearance, which results in an APOE isoform-dependent pattern of Aβ accumulation in life (Castellano et al. 2011). Therefore all currently known genetic risk factors influence the disease risk via an Aβ dependent mechanism.

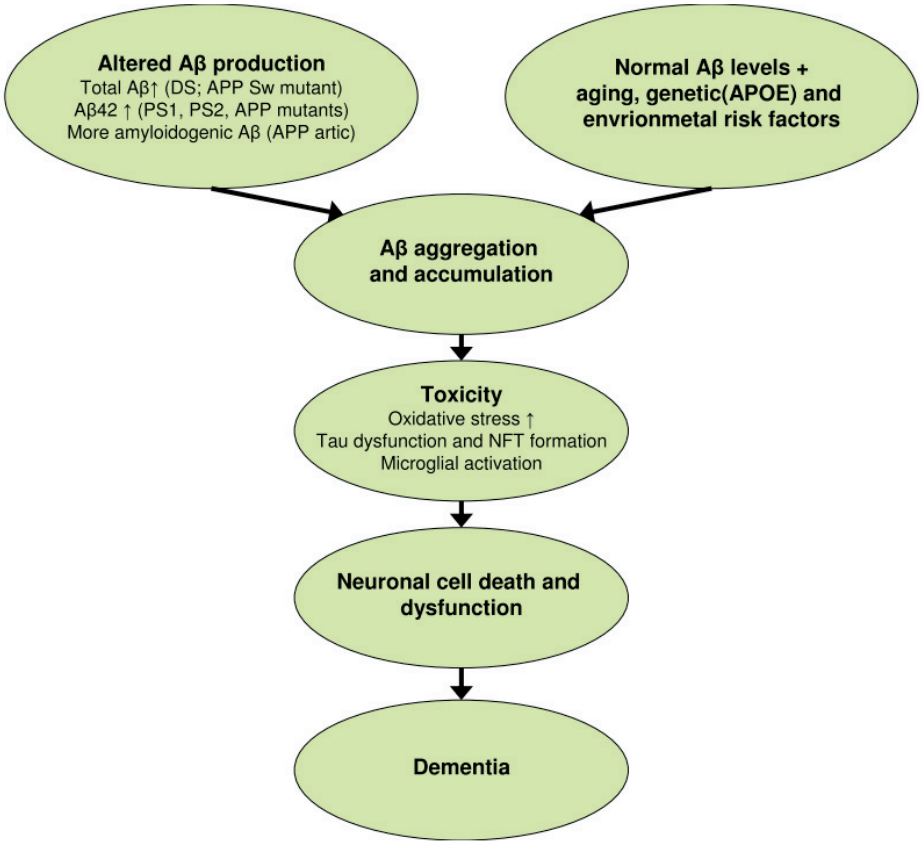

Figure 1. An overview of the amyloid cascade hypothesis in AD, modified from Golde (Golde 2003).

Different AD mouse models have been created that develop Aβ plaques and show memory deficits. For example in APPswe/PS1d9xYFP transgenic mice it was demonstrated that amyloid plaques form quickly and within 1-2 days from the plaque appearance, microglia is activated and recruited to the site. Progressive neuritic changes ensue, leading to increasingly dysmorphic neuritis

over the next days and weeks (Meyer-Luehmann et al. 2008). This shows that amyloid plaques are critical mediators of the neuritic pathology.

By definition amyloid plaques are the key components in AD pathology. Therefore amyloid accumulation should correlate with the degree of dementia. And indeed in one carefully controlled study a correlation between plaque load in the entorhinal cortex and cognitive dysfunction was established (Cummings and Cotman 1995). However, in general there is a poor correlation between plaque load and the degree of dementia (Terry et al. 1991; Braak and Braak 1998). This may be due to different cognitive reserve levels. It is suggested that individuals with greater cognitive reserve exhibit reduced susceptibility to dementia. It has been demonstrated that the correlation between amyloid deposition and cognitive performance is weaker in subjects with higher cognitive reserve (Rentz et al. 2010).

Diffuse amyloid plaques are present also in the brains of many older adults who do not have other pathological or clinical evidence of AD. In general it has been shown that around 20 % of healthy elderly are amyloid positive (Knopman et al. 2003; Mintun et al. 2006; Rowe et al. 2007). However, it is possible that they would have developed dementia, had they lived longer, and the plaques could represent a preclinical stage, that is unaccompanied by sufficient cognitive impairment to yield a diagnosis. Moreover it has been demonstrated that these plaques in nondemented aging associate with declined cognitive performance and therefore it is unlikely that they are benign (Price et al. 2009).

One criticism for the amyloid cascade hypothesis comes from the fact that tangle pathology is much better associated with disease severity and NFT formation seems to predate plaque formation (Braak et al. 1996; Braak and Braak 1998; Giannakopoulos et al. 2003). However in the case of frontotemporal dementia with parkinsonism, there is a severe deposition of tau in NFTs in the brain but no deposition of amyloid (Hardy et al. 1998). Therefore it is clear that profound NFT formation is not sufficient to induce amyloid formation. Moreover, transgenic mice overexpressing mutant human APP and mutant human tau undergo increased formation of tau-positive tangles (compared with mice overexpressing tau alone), whereas the structure and number of amyloid plaques remains unaltered (Lewis et al. 2001). It should be noted also that it has been shown in humans that Aβ levels increase before tau pathology emerges (Naslund et al. 2000). A mechanism, which links amyloid deposition and NFTs has also been suggested, which states that Aβ peptides promote pathological tau filament assembly in neurons by triggering tau cleavage by caspase which generates a proteolytic product with enhanced polymerization kinetics (Gamblin et al. 2003).

There has been a chorus of concern that no cure for AD has been found based on the amyloid cascade hypothesis. Over time it has undergone alterations,

primarily in the description of the pathogenic forms of the Aβ (Hardy and Selkoe 2002; Pimplikar 2009). Probably the most popular variation "the oligomeric hypothesis" suggests that the toxic species is not the fibrillar aggregate but oligomeric Aβ or some other transient form of the peptide aggregates. The second modification, on which my further approach is based on, is that the metal ions that are in abundance in the plaques generate oxidative stress which causes neurotoxicity (Bush 2003; Huang et al. 2004).

1.4. Amyloid-beta peptide

Aβ is derived from a type-1 membrane protein, the APP, which is expressed in various tissues of the organism, both in the periphery and the central nervous system (CNS) (Jakob-Roetne and Jacobsen 2009). It has three common isoforms, APP_{695}, APP_{751}, and APP_{770}, of which the first is abundant in neuronal cells (Selkoe 2001). The function of APP is still elusive and many putative functions have been proposed, including that it could be involved in regulating metal ion transport and homeostasis (Ciuculescu et al. 2005; Gaggelli et al. 2006; Muller and Zheng 2012). APP is proteolytically processed by three proteases: α-, β-, and γ-secretase (Dillen and Annaert 2006). There are two mutually exclusive cleavage pathways for APP processing: the amyloidogenic (considered as the pathogenic pathway) and non-amyloidogenic or constitutive pathway (Fig. 2). In tissues other than the CNS, the APP cleavage is predominantly non-amyloidogenic. But in the CNS, where the expression of β-secretase is highest, the amyloidogenic pathway also has an important role (Jakob-Roetne and Jacobsen 2009). The non-amyloidogenic pathway begins with cleavage by the α-secretase, between K687 and L688 (APP_{770} numbering). The amyloidogenic pathway begins with APP cleavage by the β-secretase between residues M671 and D672. Both cleavages generate a short C-terminal fragment of 83 or 99 amino acids long respectively, which remains anchored in the membrane with its transmembrane domain. These C-terminal fragments can be further processed by the γ-secretase (which requires four protein components for its activity: PS1 or PS2, nicastrin, anterior pharynx defective-1 and presenilin enhancer-2) and this cleavage results in the case of the shorter fragment in the p3 peptides, while the longer C-terminal fragment gives rise to the Aβ peptides. The γ-secretase cuts the APP at several different positions and the resulting Aβ peptides have different lengths. The dominant species is Aβ40 peptide, which normally constitutes 80 to 90 % of all the Aβ peptides. The second major species is Aβ42 (5 to 10 %) (Haass and Selkoe 2007; Jakob-Roetne and Jacobsen 2009; Detoma et al. 2012).

Aβ is a natural byproduct of APP proteolysis in the brains and cerebrospinal fluid (CSF) of normal humans throughout life (Seubert et al. 1992; Shoji et al. 1992). According to some authors it may even serve a physiological function (Zou et al. 2002; Giuffrida et al. 2009). Aβ exists in three fractions in the brain:

membrane-linked, aggregated and soluble. The major soluble form of Aβ in the blood and CSF is Aβ40 (Seubert et al. 1992; Vigopelfrey et al. 1993). However Aβ42, which is less prevalent in biological fluids, is enriched in amyloid plaques (Masters et al. 1985). Moreover Aβ42 has a greater tendency to aggregate and precipitate as amyloid *in vitro* (Harper and Lansbury 1997). Therefore it is clear that Aβ42 is more amyloidogenic. It cannot be overlooked that the amyloid plaques contain various minor isoforms of the Aβ peptides (for example Aβ4-42, Aβ1-43, 3-pyroglutamateAβ3-42, etc.) (Portelius et al. 2010). It has been shown that these isoforms may be more aggregation prone or more neurotoxic (Pike et al. 1995; Portelius et al. 2010), however, their relative importance in the pathogenesis of AD is not fully understood.

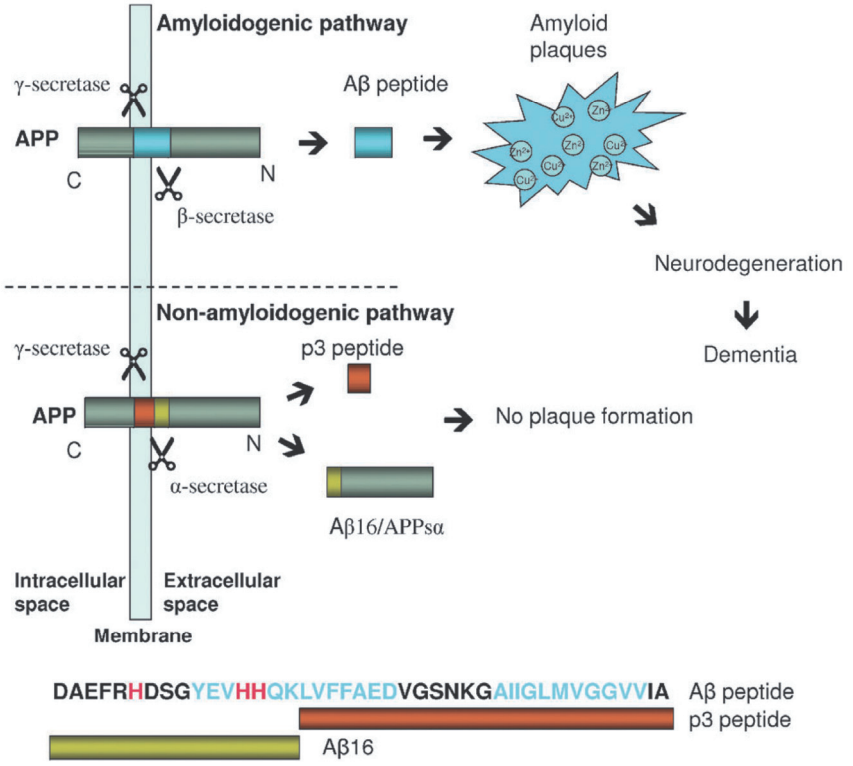

Figure 2. APP proteolytic processing and the cascade of events that leads to dementia. Cleavage of APP by α-, β-, and γ-secretases in the amyloidogenic and non-amyloidogenic pathway are given at the top. The Aβ sequence is shown at the bottom, the amino acid residues given in blue form the β-sheet in Aβ fibrils, histidine residues are shown in red (Publication V).

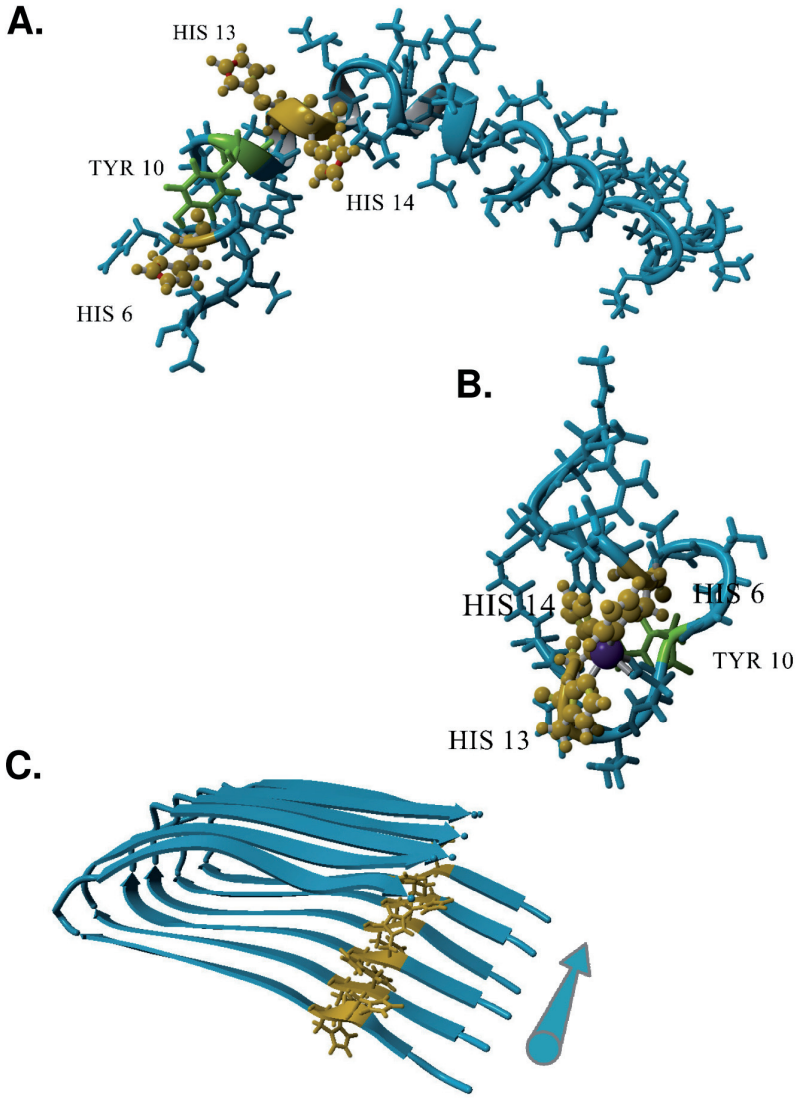

Figure 3. The structures of different Aβ conformations. (a) α-helix of Aβ (PDB code: 1Z0Q) (Tomaselli et al. 2006); (b) the structure of $A\beta_{1\text{-}16}$ upon Zn(II) binding (Zirah et al. 2006) (PDB code: 1ZE9); (c) structure of Aβ protofilament. The fibril axis is indicated by the arrow. The Aβ fibril is composed of a number of protofilaments Atomic coordinates were kindly provided by Dr. Robert Tycko. Histidine residues are depicted in yellow, tyrosine in green and Zn(II) ion in blue. The Yasara modeling program was used for visualization (Krieger et al. 2002).

The amyloid fibrils are characterized by their β-sheet structures. In Aβ40 fibrils residues 12-24 and 30-40 form parallel β-sheets and these are connected by a turn involving residues 25-29 (Petkova et al. 2002). For Aβ42 it has been shown that residues 18-26 and 31-42 form the β-strands (Fig. 2 and Fig. 3C) (Roychaudhuri et al. 2009). Amyloid fibrils are the end product of a complex fibrillization pathway and their formation is preceded both *in vitro* and *in vivo* by numerous on- or off-pathway intermediates. These can include Aβ dimers, oligomers, amyloid-derived diffusible ligands, nuclei and protofibrils (Fig. 5) (Fandrich et al. 2011). The structure of Aβ40 and Aβ42 in buffer at physiological pH is mainly random coil (Riek et al. 2001; Hou et al. 2004). In membrane-mimicking conditions, the conformation is largely α-helical (Fig. 3A) (Morgan et al. 2004) which is an approximation of its structure when it is a part of the APP molecule.

One of the key questions in amyloid deposition is which Aβ forms are toxic. At first it was demonstrated that fibrillar Aβ is neurotoxic (Lorenzo and Yankner 1994; Fukuda et al. 1999). This was also observed *in vivo* when fibrillar Aβ was injected into mouse brains (Pimplikar 2009). The latest idea is that higher soluble aggregates, Aβ oligomers, are the causing pathogenic agents (Walsh and Selkoe 2007). Different biochemically distinct oligomeric species have been identified and shown to be toxic *in vitro* and *in vivo* (Walsh et al. 2002; Ahmed et al. 2010; Balducci et al. 2010; Cizas et al. 2010; Freir et al. 2010). Oligomeric Aβ has also been isolated from the brains of AD model mice (Lesne et al. 2006) and from human AD brains (Shankar et al. 2008). In the latter it was also demonstrated that the isolated oligomers inhibited long-term potentiation. How these oligomers form *in vivo* or how they trigger deleterious changes currently remains unknown. Moreover, the definition of various oligomers depends strongly on the context of their preparation and often they cannot be isolated or easily purified (Broersen et al. 2010). It is clear that in high concentrations oligomeric species of the Aβ are toxic, however, the spontaneous formation of toxic amounts of oligomers *in vivo*, where the concentration of Aβ is low, is highly improbable. What is more, kinetic evidence show, that the minimal structure that initiates fibrillization is a dimer (Hellstrand et al. 2009) and the growth of individual plaques in animal models is fast (Meyer-Luehmann et al. 2008), therefore it is likely that fibrillization would out-compete oligomerization at low peptide concentrations. It has been suggested, however, that toxic oligomers can be a secondary particle, derived from fibrils (Martins et al. 2008). The actual toxicity mechanism in the brain may be a result of various Aβ species and various other molecules that interact with them. For example, the low toxicity of Aβ fibrils *in vitro* may be due to the fact that they do not contain metal ions, therefore they cannot cause oxidative stress. The fibrils in AD brains contain metal ions and these could mediate the toxicity *in vivo*. It has been demonstrated that Cu-Aβ aggregates are cytotoxic in the presence of ascorbic

acid in concentrations similar to those in the CSF (Meloni et al. 2007; Publication II; Chung et al. 2010).

1.5. Metal ions and Alzheimer's disease

Metals can be classified as toxicological or biometals based upon whether they are detrimental to the organism or they have a functional role. However the mismetabolism of any metal ion in the body can lead to disease. In the CNS several biometals such as copper, zinc and iron are needed for many enzymatic activities, mitochondrial function, neurotransmission, learning, and memory. In the healthy brain the metal ion content is stringently regulated and the concentration of free metal ions is kept at a very low level. The metal ion homeostasis in the brain is regulated by the blood-brain-barrier (BBB) (Tamano and Takeda 2011). However with increasing age and/or oxidative stress, the BBB becomes compromised so that metal ions are more easily transported into and out of the brain (Scott and Orvig 2009; Tamano and Takeda 2011).

Copper is a redox-active metal that can exist either in the oxidized (Cu(II)) or in the reduced (Cu(I)) oxidation state. Many enzymes harness the changes in copper oxidation state to catalyze redox chemistry for a wide variety of chemical transformations that are central to biology. However, when electrochemically active copper is not bound to an enzyme as a cofactor, copper ions are able to catalyze the production of potentially dangerous reactive oxygen species (ROS) through Fenton reaction:

$$Me^{n+} + H_2O_2 \rightarrow Me^{(n+1)+} + OH^{\bullet} + OH^{-}$$

or Haber-Weiss reaction:

$$O_2^{\bullet -} + H_2O_2 \xrightarrow{Me^+} OH^- + OH^{\bullet} + O_2,$$

where Me^{2+} is metal ion.

If ROS are not appropriately detoxified, they can react with almost all biomolecules in living cells. This results in extensive impairment of cellular functions through lipid peroxidation, protein oxidation, and nucleic acid cleavage (Halliwell and Gutteridge 1984). The dichotomous nature of copper demands that its concentrations in the organism would be under control and it is essential that the copper transport is tightly regulated. For this reason, the concentration of intracellular free copper is maintained at exceedingly low levels (less than 10^{-18}M) (Rae et al. 1999). The normal extracellular copper concentration is between 0.2 and 1.7 μM (Smith et al. 2007). The healthy human adult brain comprises 2 % of body mass but contains 7.3 % of total copper in the

body, which makes it comparable to the liver (about 9 %), which is a central organ in copper homeostasis (Gaggelli et al. 2006; Hung et al. 2010). Approximately one fifth of the total oxygen is consumed in the brain, what is more, it has disproportionately low levels of antioxidant activity. Moreover, in the glutamate-ergic synapse, in the cortex and hippocampus, copper ions are released into the synaptic cleft. It has been estimated that the concentration of Cu(II) in the synaptic cleft may be as high as 15-100 μM (Hartter and Barnea 1988; Kardos et al. 1989). This makes the brain particularly susceptible to oxidative stress.

Zinc is the most abundant trace element in the body after iron and its highest content is found in the brain. The average of total brain zinc concentration is estimated to be approximately 150 μM (Frederickson et al. 2005). Over 90 % of the zinc in the brain is classified as static (tightly bound to enzymes, transcription factors, metallothioneins (MT), etc.) (Que et al. 2008). Free Zn(II) concentration in the cytosol is in the picomolar range (Frederickson et al. 2005) and approximately 500 nM in the brains extracellular fluid (Vasto et al. 2008). However, high levels of Zn(II) arise in the hippocampus, the amygdala, and the cortex, that contain zinc-ergic synapses, where Zn(II) is concentrated in synaptic vesicles, with the assistance of the zinc transporter Zn-T3 (Frederickson and Bush 2001). It is estimated that Zn(II) concentration in the synaptic cleft may rise up to 300 μM after its release from the vesicles (Assaf and Chung 1984).

Aβ aggregation and toxicity is thought to be connected with metal ions. Since the pioneering paper published by Bush et al. in 1994 where zinc was linked to amyloid (Bush et al. 1994) the possible links between metal ions and AD have been very intensively studied. Dyshomeostasis and imbalance of metal ions is seen in the AD brain. Copper, zinc, and iron are found in high concentrations (~1 mM) in amyloid plaques (Lovell et al. 1998). Moreover, zinc and copper ions are directly coordinated by Aβ (Dong et al. 2003). Iron is predominantly in a ferritin bound form in neuritic processes associated with the plaques (Grundkeiqbal et al. 1990). A number of studies have shown that iron homeostasis is altered in AD, however, it is likely that this is a secondary effect (Smith et al. 2007).

In the context of AD-related metal dyshomeostasis, a role is offered to the nonphysiological aluminium. In the early papers, aluminium was proposed to be the major etiological factor in AD (Crapper et al. 1973; Crapper et al. 1976). However, currently aluminium is assumed to be one of possible co-/aggravating factors, with no convincing proof so far (Zatta 2006).

The significance of metal ions in amyloid formation has also been demonstrated in different animal models. For instance plaque load is reduced by approximately 50 % in transgenic mice, who overexpress human APP, when

they lack the zinc-transporter ZnT3 that transports Zn(II) into synaptic vesicles (Lee et al. 2002). The importance of Cu(II) in plaque formation has been shown on another AD model animal, a cholesterol fed rabbit. Trace amounts of Cu(II) in their drinking water induce the accumulation of Aβ, the formation of senile plaque-like structures, and retardation of the rabbits ability to learn a difficult task (Sparks and Schreurs 2003). However, it has also been shown that Cu(II) has an advantageous effect. Transgenic mice that overexpress human APP carrying the Swedish/London mutation, that were treated with Cu(II) had a detectable reduction of amyloid plaques and did not have the premature lethal phenotype (Bayer et al. 2003). Recently it was demonstrated in *Drosophila*, with an eye-specific expression of human Aβ42, that dietary supplements of zinc and copper enhance cellular damage associated with Aβ42 expression. Positive effects were seen with various metal chelators (Hua et al. 2011).

Metal ions can have various roles in AD, they may influence the pathogenesis directly and indirectly. They can do the latter by altering APP processing (Duce and Bush 2010; Roberts et al. 2012). Metal ions can directly affect the pathogenesis by binding to the Aβ peptide and modulating its behavior. Moreover redox active metal ions like copper and iron can produce ROS that can lead to oxidative stress. Recently it was demonstrated that Cu(II)-Aβ cause the formation of axonal swellings, that contain hyperphosphorylated tau via the production of free radicals and subsequent efflux of K^+ out of neurons (Howells et al. 2012).

1.6. Metal-binding affinity of Aβ

The metal binding affinity of proteins and peptides is an important parameter in biology, and the quantitative determination of the binding affinity of Aβ peptides helps to assess the significance of metal binding as a potential inducer of pathological Aβ aggregation. A binding affinity that is too low may indicate that the peptide is not able to bind the metal ion *in vivo* due to the presence of other ligands with stronger affinities. Understanding the thermodynamics and kinetics of Cu(II) and Zn(II) binding to Aβ peptides is also crucial for rational drug design.

Classically the affinity of a protein/peptide (P) for a metal ion (Me^{2+}) is estimated by calculating the dissociation constant K_D, referring to the equilibrium:

$$P + Me^{2+} \overset{K_D}{\leftrightarrows} Me^{2+}P \qquad (1),$$

$$K_D = \frac{[\mathrm{P}] \times [\mathrm{Me}^{2+}]}{[\mathrm{Me}^{2+}\mathrm{P}]} \qquad (2),$$

where, [P] is the peptide/protein concentration, [Me^{2+}] is the metal ion concentration and [Me^{2+}P] is the concentration of the peptide/protein complex with the metal ion.

The interactions between metal ions and biomolecules are hard to follow directly because biological fluids are complex. One alternative strategy is to determine the binding constants *in vitro* and based on this information discuss about the possibility of this interaction *in vivo*.

Various methods can be used to determine the metal binding affinity of the peptide/protein: potentiometry, calorimetry, equilibrium dialysis, various mass spectrometry (MS) techniques, electron paramagnetic resonance, nuclear magnetic resonance (NMR), and different spectroscopic methods, including ultraviolet-visible (UV-Vis) spectroscopy, circular dichroism, and fluorescence (Faller et al. 2012; Zawisza et al. 2012). All of these methods have different advantages and limitations; the choice of method depends on the metal and peptide/protein used.

If the affinity is high compared with the sensitivity of the applied method, then the measurements should be carried out in the presence of a competing low-affinity ligand:

$$\mathrm{L} + \mathrm{Me}^{2+} \overset{K_L}{\leftrightarrows} \mathrm{Me}^{2+}\mathrm{L} + \mathrm{L} \overset{K_{L2}}{\leftrightarrows} \mathrm{Me}^{2+}\mathrm{L}_2 \qquad (3).$$

In this case the K_D is calculated by the following formula:

$$K_D = K_D^{app} \times \left(1 + \frac{[\mathrm{L}]}{K_L} + \frac{[\mathrm{L}]^2}{K_{L2}}\right) \qquad (4),$$

where K_D is the buffer independent conditional dissociation constant, K_D^{app} is the apparent dissociation constant, [L] is the ligand concentration, K_L is the dissociation constant of the Me^{2+}L complex, and K_{L2} is the dissociation constant of the $Me^{2+}L_2$ complex.

This increases the apparent dissociation constant value so that it fits the detection range of the method. pH buffers (HEPES, Tris, phosphate, etc.) or amino acids (Gly, His) have been used for this purpose. However, it should be

noted here that phosphate buffer is not suitable for studying the effects of Cu(II) and Zn(II) due to the very low solubility of the corresponding phosphates, which may precipitate during the experiment and cause artifacts.

When using competing ligands, the presence or absence of ternary complexes should also be estimated. When ternary complexes occur and they are not accounted for in the model used it leads to a drastic overestimation of the binding affinity. In order to rule out the formation of ternary complexes, the K_D^{qpp} values should be determined at different competing ligand concentrations and the conditional constant should be independent of the ligand concentration. Very good examples of how various ligand concentrations are used to determine the dissociation constant are given by Professor Bal and colleagues (Rozga et al. 2009; Rozga et al. 2010).

Fluorescence measurements have several subtypes, one can measure the intrinsic fluorescence of the peptide, use covalently linked or extrinsic fluorophores. The Aβ molecule contains one tyrosine and no tryptophan (Fig. 2), which makes the affinity measurement system relatively simple. When measuring the changes in its intrinsic fluorescence the formulas used for dissociation constant calculations depend on the metal and peptide concentration. When the apparent dissociation constant is relatively high (K_D^{app} > P) a hyperbolic binding isotherm is used:

$$I = I_0 + \frac{[Me^{2+}] \times (I_\infty - I_0)}{[Me^{2+}] + K_D^{app}} \qquad (5),$$

where I_0, I, and I_∞ are the fluorescence intensities of the peptide sample in the absence, presence, and saturation of metal ions. When a physical characteristic, for instance intrinsic fluorescence intensity, is measured and the dissociation constant is calculated using a binding isotherm it is necessary to demonstrate that the parameter measured responds to the binding of the first metal ion.

However, when the K_D^{app} is relatively low and the metal and peptide concentrations are in the same range then the following equation is used:

$$I = I_0 + \frac{0{,}5 \times (I_0 - I_\infty)}{[P]} \times \left([P] + [Me^{2+}] + K_D^{app} + \sqrt{\left([P] + [Me^{2+}] + K_D^{app} \right)^2 - 4 \times [P] \times [Me^{2+}]} \right) \qquad (6).$$

The usage of Scatchard plot for K_D estimation may be the source of artefacts.

An excellent review about the determination of metal-protein affinities and possible pitfalls in this process is given by Xiao and Wedd (Xiao and Wedd 2010) and about various methods for the detection of these affinities by Faller et al. (Faller et al. 2012).

1.6.1. The affinity of Aβ for Cu(II)

The reported affinity of Aβ towards Cu(II) varies from attomolar (Atwood et al. 2000) to micromolar (Garzon-Rodriguez et al. 1999) (Table 1). This is likely to be caused by different techniques used for the constant determination and due to different experimental conditions. It is important to note that some of the variability in the apparent dissociation constant, K_D^{app}, arises from the fact that measurements are carried out in the presence of various Cu(II) binding ligands. These components can be taken into account and the buffer independent K_D values can be calculated by using the appropriate correction functions (Sokolowska and Bal 2005):

$$\log K_D = \log K_D^{app} + \mathrm{C} \qquad (7),$$

$$\mathrm{C} = \log(1 + \beta_{CuL} \times \frac{\mathrm{c_L}}{1 + 10^{-\mathrm{pH}+\mathrm{pK_a}}}) \qquad (8),$$

where c_L is buffer concentration, K_a is the deprotonization constant of the buffer and β_{CuL} is the dissociation constant for the Cu(II)-ligand complex (Sokolowska and Bal 2005).

Table 1. The dissociation constants of Cu(II)-Aβ complexes from the literature.

Aβ peptide	Buffer/pH	Method	Competitor	K_D^{app} (μM)	K_D (nM)	Ref.
40	10 mM Tris /7.4*	Tyr-10 emission	-	1.6	73	(Garzon-Rodriguez et al. 1999)
42				2.0	91	
40	10 mM Tris /7.5*	Tyr-10 emission	-	11	12	(Karr et al. 2005)
28				28	32	
28	Water/7.8	Tyr-10 emission	Gly, His	0.01 -0.1	10-100	(Syme et al. 2004)

40	50 mM PBS /7.4*	Tyr-10 emission	-	8	120	(Raman et al. 2005)
28	10 mM HEPES /7.2	Tyr-10 emission	-	2.5	77	(Danielsson et al. 2007)
40	10 mM Tris /7.4*	Tyr-10 emission	-	0.47	37	(Publication I)
	20 mM Tris /7.4*			1.21	35	
	50 mM Tris /7.4*			3.82	24	
	100 mM Tris /7.4*			30.1	54	
	20 mM HEPES /7.4*			0.57	36	
	50 mM HEPES /7.4*			0.90	24	
	100 mM HEPES /7.4*			2.5	34	
42	20 mM HEPES /7.4*			0.76	48	
40	20-100 mM HEPES /7.4	Tyr-10 emission	-	-	57	(Rozga et al. 2010)
40	20 mM HEPES /7.2	ITC	Gly	-	0.091	(Hatcher et al. 2008)
	20 mM HEPES /7.4				0.042	
	20 mM Pipes/7.2				0.011	
16	20 mM HEPES /7.2				0.067	
	20 mM HEPES /7.4				0.034	
	20 mM Pipes/7.2				0.033	
16	20 mM ACES /7.4*	ITC	ACES	-	0.909	(Sacco et al. 2012)
	50 mM ACES /7.4*				0.961	
	100 mM ACES /7.4*				0.943	
28	20 mM ACES /7.4*				1.72	

28	100 mM KNO3	Potentio-metry	-	-	0.024	(Kowalik-Jankowska et al. 2003)
16					0.208	
16	200 mM KCl	Potentio-metry	-	-	0.120	(Damante et al. 2008)

* physiological saline

In 2008 we found that the K_D for the Cu(II)-Aβ complex is 35 ± 10 nM (Publication I). This value was confirmed by Rozga et al. in 2010, who found the K_D = 57 nM under slightly different conditions (Rozga et al. 2010). Since then two alternative affinity estimates have been determined. One in the range of 0.01-1 nM (Hatcher et al. 2008; Sarell et al. 2009; Xiao and Wedd 2010) and the other 30-60 nM (Publication I; Rozga et al. 2009; Rozga and Bal 2010; Rozga et al. 2010). In general it is seen that the tyrosine method gives lower values than potentiometry and calorimetry. This difference can be a result of an overestimation of the affinity in potentiometric and calorimetric measurements due to ternary complex formations of Cu(II) with various components that was left unaccounted for in the model used for the constant calculation. Moreover potentiometry and calorimetry are done at higher peptide concentrations where Aβ tends to aggregate while tyrosine fluorescence measurements are carried out at lower peptide concentrations (Fig. 4). It has been hypothesized that these higher affinities that are obtained at higher peptide concentrations represent dimeric/oligomeric complexes (Zawisza et al. 2012).

Several different coordination modes have been proposed for the Cu(II)-Aβ complex. Most likely the complex has a dynamic structure with a mixture of different ligands, in which the three histidine residues are likely to be included (Faller and Hureau 2009; Publication V). Cu(II) forms a 1:1 complex with Aβ (Karr et al. 2005; Jiang et al. 2007), at higher Cu concentrations a second ion binding has also been observed (Ali et al. 2006), however, due to a low binding affinity it is not biologically relevant.

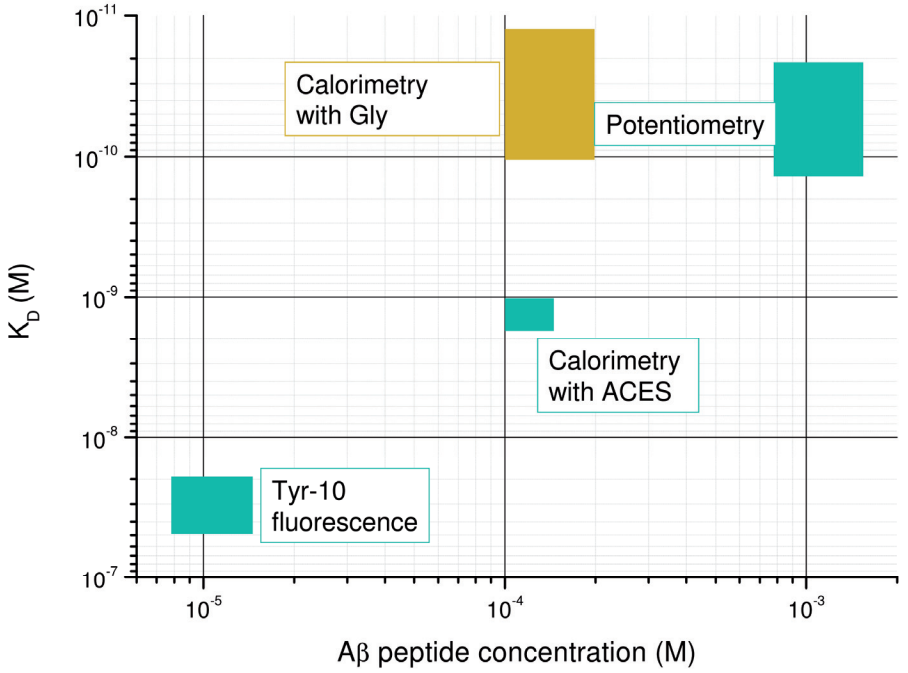

Figure 4. The log-log relationship between Aβ peptide concentrations and reported K_D values for Cu(II) binding, according to various experimental methodologies. Boxes represent the ranges of concentrations and dissociation constants for all peptides. Based on Zawisza et al. (Zawisza et al. 2012).

In summary it can be concluded that the dissociation constant for the monomeric Cu(II)-Aβ complex at pH 7.4 is around 30-60 nM. Professor Bal and colleagues speculated that the affinity in the synaptic cleft could be closer to the higher reported affinity values due to peptide oligomerization and ternary complex formation in the cleft (Zawisza et al. 2012). Nevertheless, it is clear that the Cu(II) binding affinity of Aβ is in a biologically relevant range, Aβ can bind Cu(II) in all forms (monomer, fibril and nonfibrillar aggregates, whereas the affinity of aggregates is considerably higher), but under the equilibrium conditions it cannot compete with strong Cu(II) chelators, such as MT and human serum albumin.

1.6.2. The affinity of Aβ for Zn(II)

The reported K_D values for Zn(II)-Aβ complex vary between 1 and 300 μM (Table 2). Lower affinity values are found from metal-induced changes in tyrosine fluorescence (Clements et al. 1996; Garzon-Rodriguez et al. 1999; Publication I) other method give values in the range of 1-5/20 μM (Clements et

al. 1996; Danielsson et al. 2007; Talmard et al. 2007). In 2008 we estimated that the dissociation constant for the Zn(II)-Aβ complex is approximately 60 μM by using tyrosine fluorescence. In order to see if the Zn(II)-Aβ complex changes with time we used a competing ligand, Zincon. It was demonstrated that the initial low affinity Zn(II)-Aβ complex transformed into a high-affinity complex, with a $K_D \sim 2$ μM in 30 minutes (Publication I). Our results demonstrated for the first time that the change in zinc-binding affinity of Aβ in time occurs concomitantly with zinc-induced Aβ aggregation. Comparing different methods that have been used for affinity measurements it can be seen that radioligand binding, NMR and metal displacement experiments, where higher affinities were detected are all characterized by longer incubation times as compared with measurements of the intrinsic fluorescence of Aβ.

High-resolution NMR studies show that in a 1:1 Zn(II)-Aβ complex Zn(II) is coordinated by Asp1, His6, His13 and His14 (Danielsson et al. 2007). Glu11 has also been shown to contribute energetically to the Zn(II) binding (Fig. 3B) (Zirah et al. 2006; Tsvetkov et al. 2010). The residues 6-14 have been identified as a minimal Zn(II) binding site in Aβ (Tsvetkov et al. 2010).

Table 2. The dissociation constants of Zn(II)-Aβ complexes from the literature.

Aβ peptide	**Buffer/pH**	**Method**	K_D^{app} **(μM)**	**Ref.**
40	10 mM Tris/7.4*	Tyr-10 fluorescence	300	(Garzon-Rodriguez et al. 1999)
42			57	
16	20 mM Tris/7.4*	ITC	22	(Talmard et al. 2007)
28			10	
40			7	
16	20 mM HEPES/7.4*	Zincon competition	14	
28			12	
40			7	
42			7	
28	10 mM HEPES/7.2	Tyr-10 fluorescence, Cu(II) competition	6.6	(Danielsson et al. 2007)
	10 mM Na phosphate/6.5		3.2	
	10 mM Na phosphate/7.2		1.1	
40	10 mM Na phosphate/7.2	NMR, Cu(II) competition	1,2	

40	10 mM Tris/7.4*	Tyr-10 fluorescence	60	(Publication I)
	100 mM Tris/7.4*		184	
	20 mM HEPES/7.4*		65	
42	20 mM HEPES/7.4*		91	
40	10 mM Tris/7.4	$^{65}Zn^{2+}$ displacement	3.2	(Clements et al. 1996)
	10 mM HEPES/7.4		3.2	
40	20 mM Tris/7.4	$^{65}Zn^{2+}$ displacement	5.2	(Bush et al. 1994)
16	50 mM Tris/7.3	ITC	56	(Tsvetkov et al. 2010)

* physiological saline

Therefore it can summarized that the Zn(II) complex with full-length Aβ cannot be characterized by a single dissociation constant. And it can be hypothesized that the Zn (II) binding affinity of Aβ monomer is close to 100 μM which increases to 1-5 μM upon aggregation. This idea that the affinity increases upon aggregation is by now generally accepted (Faller and Hureau 2009; Zawisza et al. 2012). Considering the K_D values it can be concluded that Aβ can directly bind available Zn(II) in certain brain areas which contain zinc-ergic neurons.

1.7. Aβ aggregation

Fibrillization is a process where polypeptides go from their normal fold into a predominantly β-sheet secondary structure which leads to the formation of large, regular fibrillar structures. In general the fibril growth exhibits a typical sigmoidal curve. Numerous different models exist that describe the fibrillization process (Morris et al. 2009). The widest accepted model for fibril growth is the nucleation-elongation model that is composed of three phases: a nucleation phase also called a lag phase, a growth phase, and a stationary phase (Fig. 5). The rate limiting step is the formation of fibrillization nuclei or "seeds" through the self-association of monomers into oligomeric species during the nucleation phase (Harrison et al. 2007). The structure and the thermodynamics of the formulation of seeds remains elusive, however, there is a consensus that these particles are rich in β-sheet secondary structure elements, which form a template for the interaction with incoming peptides through an interchain hydrogen bonding network. A recent kinetic study has revealed that, in the case of Aβ, the critical nuclei may consist of only two peptide molecules (Hellstrand et al. 2009). The nucleation phase is followed by the rapid growth of fibrils through the addition of monomers to preexisting fibrils. Analysis of the kinetics of the self assembly of filamentous structures demonstrates that amyloid growth can often be dominated by secondary rather than primary nucleation events, for instance fragmentation of early fibrils (Knowles et al. 2009). Fibril growth is

followed by maturation (bundling and formation of interfibrillar stabilizing interactions) and finally a steady state when the aggregates and monomers appear to be in equilibrium (Harrison et al. 2007).

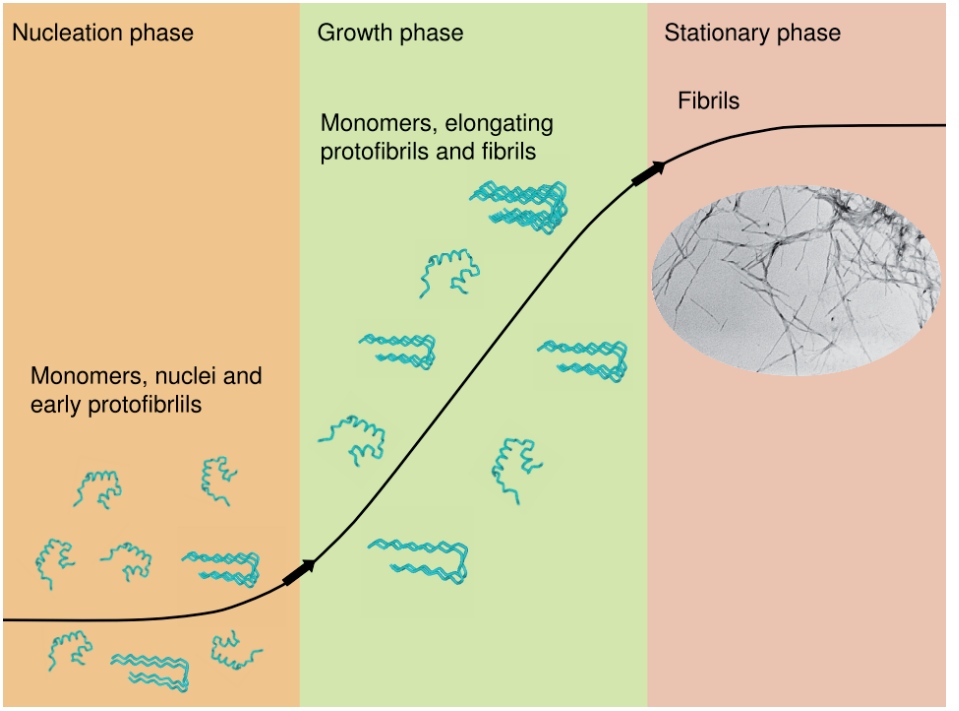

Figure 5. The fibrillization curve. Fibrillization is divided into three phases: nucleation phase were monomers, nuclei and early protofibrils occur; elongation phase, were monomers are added to protofibrils and fibrils; and finally a stationary phase. Various off- and on-pathway intermediates could possibly occur, including various oligomers, and amyloid-derived diffusible ligands.

In order to analyze the fibril formation process kinetically, it is important to have a well characterized peptide/protein preparation and an appropriate monitoring technique. Several different techniques have been used to track the fibrillization, including observing the increased fluorescence of amyloid sensitive dyes (for example Thioflavin T (ThT)), the amount of aggregates is seen by various light scattering and turbidity methods as well as different MS methods (including matrix-assisted laser desorption/ionization (MALDI)), different aggregates can be appreciated by size exclusion chromatography, increased β-sheet secondary structure measured by circular dichroism spectroscopy and Fourier transform infrared spectroscopy, decreased molecular tumbling measured by intrinsic fluorescence anisotropy, or time-lapsed observation of the peptide morphology by atomic force microscopy, morphology of the aggregates can be viewed also by transmission electron microscopy (TEM) (Lomakin et al. 1996; Atwood et al.

1998; Johansson et al. 2006; Lee et al. 2007; Lin et al. 2008; Wahlstrom et al. 2008; Fodera et al. 2009; Publication II; Publication III; Publication IV).

One of the most widely used techniques is ThT fluorescence. The benzothiazole dye fluoresces in the presence of fibrils. It is believed that ThT interacts relatively specifically and rapidly with amyloid fibrils, and the binding is independent of the primary structure of the protein. Only multimeric fibrillar forms, not multiple domains in native proteins fluoresce with ThT (Levine 1995). A drawback for the ThT method is that various components may interfere with ThT binding and fluorescence (Publication IV; Hudson et al. 2009), therefore it is necessary to validate that the observed inhibition is not due to suppression of the binding of ThT to the fibrils or its fluorescence. For instance, we demonstrated that the disappearance of monomers in MALDI spectrum is parallel to fibril formation determined by ThT fluorescence intensity (Publication IV).

Different experimental setups are used with the ThT method. One option is *in situ* real-time ThT assay, where fibrillization is carried out in the presence of ThT (Publication II; Bourhim et al. 2007). Then it is important to first establish that the ThT concentrations used do not interfere with the fibrillization process. We have demonstrated that ThT concentrations of up to 15 μM did not affect the fibrillization kinetics. Moreover, similar fibrillization curves were observed when ThT was added at different time points (Publication III). The other option is to use a discontinuous setup, where aliquots from the aggregation mixture are pipetted into a ThT solution for measurements (Holm et al. 2007; Rangachari et al. 2007). However this is material and time consuming, especially when considering that the fibrillization of defibrillated peptide samples tends to take days if not weeks (Isaacs et al. 2006; Siegel et al. 2007).

Fibrillization of peptides and proteins is relatively difficult to study due to poor reproducibility. Moreover it has been suggested that fibrillization is a stochastic process (Hortschansky et al. 2005; Friedrich et al. 2010) which makes the study almost impossible. This suggestion may be correct for the initial stage of the fibrillization processes under quiescent conditions with defibrillated peptides. However if seed is added to the reaction mixture or it is continuously agitated it speeds up the aggregation and increases the reproducibility of the aggregation process (Lee et al. 2007; Hellstrand et al. 2009; Publication II; Publication III; Publication IV).

It should be mentioned here, that in the earlier studies 1,1,1,3,3,3-hexafluoro-2-propanol (HFIP) pretreatment was not used to disassemble preformed aggregates (Stine et al. 2003) which lead to significant variations in the degree of aggregation in the initial solution which results in experimental irreproducibility.

This problem can be overcome with pretreatment of the Aβ peptide with HFIP in order to get a defibrillized peptide (Publication III; Stine et al. 2003).

Various formulas are used to fit the aggregation data and asses the effect of different compounds on parameters that describe the aggregation process. One example is the Boltzmann equation:

$$y = \frac{A_2 - A_1}{1 + e^{(t - t_0) \times k}} + A_2 \qquad (9),$$

where A_1 is the initial fluorescence level, A_2 is the maximum fluorescence, t_0 is the time when fluorescence has reached half maximum, and k is the rate constant of the fibril elongation. This equation allows to determine two parameters that describe the fibrillization kinetics – the rate constant (k) characterizing the fibril growth and the lag time (lag) characterizing the nucleation. The latter is calculated by the following equation:

$$lag = t_0 - \frac{2}{k} \qquad (10).$$

1.7.1. Metals and Aβ aggregation

The Aβ aggregation and fibrillization are crucial aspects in the development of AD. Studies of the fibrillization kinetics in the presence of metal ions helps to understand the role of endogenous metal ions and metal chelating agents in amyloid plaque formation in the brain.

Based on the belief that metal ions play a role in AD pathology a therapeutic strategy has been developed, called "metal chelation therapy" (Cherny et al. 2001; Bush and Tanzi 2008). This approach relies on the assumption that metal ions, especially Cu(II) and Zn(II) cause Aβ aggregation and hopes that the removal of these metal ions from amyloid plaques by metal chelators should solubilize the plaques. To date, several metal chelators have been used in the metal chelation therapy for AD. Desferrioxamine (DFO) was the first compound used to treat metal overload in the CNS and to dissolve amyloid aggregates (Budimir 2011). It significantly reduced the behavioral and cognitive declines in AD patients (Mclachlan et al. 1991). DFO is still used against aluminium and iron overloading but is no longer being pursued clinically for AD (Hegde et al. 2009). At the same time, different 8-hydroxyquinoline analogues (VK-28, HLA-20 and MA-30) have shown great potential in the treatment of several neurodegenerative diseases (Budimir 2011). Of these clioquinol (5-chloro-7-iodo-8-hydroxyquinoline, CQ) reached phase II clinical trials, where it lowered

the plasma $A\beta_{42}$ levels, but had no cognitive effect in patients with mild AD and a cognitive benefit but no change in plasma $A\beta_{42}$ levels in patients with severe disease (Ritchie et al. 2003). However, the long-term use of CQ is limited by different adverse side-effects and it has been withdrawn from human experimentation (Baran 2010). CQ related compound PBT2 has completed phase IIa trial in AD patients where it reduced $A\beta_{42}$ concentrations in the CSF compared with patients on placebo (Lannfelt et al. 2008). Both CQ and PBT2 are effective in AD mouse models (Cherny et al. 2001; Adlard et al. 2008). However, the effect of these two chelators may be more complex than initially proposed (White et al. 2006; Crouch et al. 2009) and further investigations as well as larger clinical trials are needed to draw conclusions about the effects of "metal chelation therapy".

The influence of zinc and copper ions on the aggregation of Aβ peptides has been intensively studied over the last decade, nevertheless, the results are contradictory about the nature and even the direction of the effects. In first studies it was reported that metal ions enhance Aβ fibrillization rate and metal chelators reversed the effect of metal ions (Bush et al. 1994; Esler et al. 1996; Cherny et al. 1999). However later it has also been demonstrated that metal ions enhance the formation of fibrillar structures (Ricchelli et al. 2005). In addition complex effects have also been observed (Klug et al. 2003) or no influence at all (Mancino et al. 2009).

These inconsistencies may be due to the fact that in earlier studies it was demonstrated that aggregation occurs but the nature of the aggregates was not determined. By now it has been shown that the metal induced aggregates are mainly non-fibrillar (Opazo et al. 2002; Raman et al. 2005; Ha et al. 2007; Chen et al. 2011). However, this does not eliminate the inconsistencies completely as both enhancement of fibril formations (Sarell et al. 2010) as well as inhibition of fibrillization has been observed (Publication II).

Moreover the fibrillization process consists of two different processes: nucleation and fibril elongation (Fig. 5). Therefore the effect of the metal ion on the fibrillization may depend on the experimental setup. If the fibrillization process is slow, in quiescent conditions due to little secondary nucleation, the added metal ions cause the peptide to assemble into metal-induced aggregates. These aggregates are not dead-end products of the aggregation pathway, they can evolve to Aβ fibrils. It has been demonstrated that at first nonfibrillar aggregates are seen in $A\beta_{42}$ samples with added Cu(II) and Zn(II) ions, but if these samples are incubated for one week fibrillar aggregates are seen in TEM images (Publication II). At the same time it has been demonstrated that this fibril formation does not take more than 24 h (Mancino et al. 2009) and the fibrils that formed contained the appropriate metal ion (Chung et al. 2010). Therefore under these conditions metal ions enhance fibril formation. Indeed it has been reported

recently that substoichiometric concentrations of Cu(II) significantly accelerate Aβ fibrillization in conditions where fibrillization in the absence of metal ions is slow (lag period 70-100 h), however, at higher concentrations both Cu(II) and Zn(II) inhibited fibrillization and caused the formation of nonfibrillar aggregates (Sarell et al. 2010). In conditions where the fibrillization is fast (e.g., in the presence of pre-formed seeds and/or agitation (Publication II; Publication IV), metal ions cause fibrillization inhibition by lowering the free peptide concentration due to the formation of the Me(II)-Aβ complex. This inhibitory effect is reversible via the addition of metal chelators (Publication II; Publication IV). In *in vivo* conditions, where Aβ concentration is in the nanomolar range (Sjogren et al. 2001), the fibrillization of the Aβ peptide is an unlikely process. However, metal ions may enhance Aβ aggregation into metal-induced non-fibrillar aggregates. If these metal ions are not removed by natural metal-buffering proteins (for example MT), these aggregates could eventually transform into fibrillar seeds and subsequently into fibrils (Publication II). In AD the levels of the brain-specific Zn(II) binding protein MT-3 are 10 fold lower than in healthy persons (Yu et al. 2001). This in turn lowers the zinc buffering capacity which in turn can increase the availability of Zn(II) to Aβ. In the light of the metal chelation therapy, it is clear, that metal chelators may have a protective role prior to amyloid formation. However after amyloid formation their potential may be limited as chelators are not able to dissolve fibrillar Aβ.

2. AIMS OF THE STUDY

The aim of this study was to investigate the interactions of Zn(II) and Cu(II) ions with Aβ peptides since these interactions may have pivotal role in the molecular mechanism of AD. Based on the analysis of literature carried out before starting the study, the aims of the experimental work were:

1) To measure the K_D values for the Zn(II)-Aβ and Cu(II)-Aβ complexes;
2) To determine the effect of metal ions and their chelators on the Aβ aggregation and fibrillization;
3) Based on the estimated thermodynamic and kinetic parameters to design a schematic model describing the effects of metal ions and their chelation on plaque formation and AD pathogenesis.

3. MATERIALS AND METHODS

Publication I

- ✓ Fluorescence spectrometric measurements
- ✓ Dissociation constant calculations
- ✓ MALDI MS measurements
- ✓ UV-VIS spectroscopy measurements

Publication II

- ✓ Aβ fibrillization monitoring by ThT fluorescence
- ✓ Parameter calculations
- ✓ TEM visualizations

Publication III

- ✓ Aβ fibrillization monitoring by ThT fluorescence
- ✓ Parameter calculations
- ✓ TEM visualizations

Publication IV

- ✓ Aβ fibrillization monitoring by ThT fluorescence
- ✓ Parameter calculations

4. RESULTS

Publication I

- ✓ It was established by fluorimetric titration in the presence of different concentrations of HEPES buffer as a weak copper-chelating compound that Aβ forms a 1:1 complex with Cu(II), with a conditional K_D equal to 35 nM.
- ✓ It was shown, by using a competing fluorescent dye Phen Green, that Aβ does not form any extra high affinity complex with Cu(II) that are invisible in Tyr fluorescence titration.
- ✓ It was shown that Aβ initially forms a low affinity (K_D = 60 μM) complex with Zn(II) which is transformed into a high-affinity complex, with an estimated $K_D \sim 2\mu M$.

Publication II

- ✓ Zn(II) and Cu(II) exhibited an inhibitory effect on the fibrillization of the Aβ peptide.
- ✓ Metal chelators reversed the effects on the metal ions.
- ✓ The inhibitory effect of Zn(II) (IC_{50} = 1.79 μM) was found to be three times stronger than that of Cu(II) (IC_{50} = 4.9 μM).
- ✓ It was demonstrated that metal ions induced the formation of amorphous aggregates and that these aggregates were transformed into fibrils during incubation.
- ✓ It was demonstrated that His13 and His14 but not His6 contribute to the metal-induced inhibition of Aβ fibrillization but none of the His residues were essential to the process.
- ✓ It was demonstrated that copper-induced Aβ aggregates are toxic to neurons only in the presence of the reducing agent ascorbate.
- ✓ Zn induced aggregates were not neurotoxic either in the presence or absence of ascorbate.
- ✓ Based on the effects of metal ions and metal chelators a model of fibrilliogenesis was suggested.

Publication III

- ✓ A fast and reproducible method for monitoring of Aβ fibrillization was established.
- ✓ It was shown that mixing enhances fibrillization rate.
- ✓ It was established that up to 15 μM concentration of ThT does not affect fibrillization.

- ✓ It was demonstrated that the fibrillization rate was independent of the pH range from 7-9, but started to decrease below 7.
- ✓ It was shown that fibrillization rate constant k was independent of the peptide concentration from 2 to 10 μM.

Publication IV

- ✓ The MALDI-TOF MS fibrillization assay was validated by parallel monitoring of the Aβ fibrillization by ThT assay.
- ✓ The effect of various compounds on Aβ fibrillization was demonstrated.
- ✓ It was shown that several compounds interfere with ThT emission in the ThT based fibrillization assay.

Publication V

- ✓ The literature about the Aβ complex formation with Cu(II) and Zn(II) and also the effect of these metal ions on the aggregation was analyzed in detail and critically reviewed.
- ✓ The mechanism of Aβ fibrillization *in vitro* in the presence of metal ions was further elaborated (Fig. 6).

5. DISCUSSION

The dissociations constant values for the Cu(II)-Aβ and Zn(II)-Aβ complex formation determined in this study are both in a biologically relevant range. This means that direct interactions of Zn(II) and Cu(II) with Aβ peptides may occur in certain brain areas and these metal ions may play a role in the pathophysiology of AD via interactions with Aβ. Since the affinity is not too high, the dyshomeostasis of metal ions in AD brain may shift the association equilibrium to the formation of the complex.

The metal ion and protein association is mediated by electrostatic and coordinative interactions between the metal cation and specific protein residues. However, Aβ is not a metal chaperone or a metal binding protein possessing a certain preformed metal binding site and therefore different coexisting metal ion coordination modes are possible. The coordination environment for Cu(II) and Zn(II) in the complex with Aβ has been studied using various methods. It is generally accepted that zinc ions form a 1:1 (Clements et al. 1996) complex with the N-terminal part of the Aβ peptide, where the Zn(II) is coordinated mainly by the three His residues (Fig. 3B) (Danielsson et al. 2007; Gaggelli et al. 2008). Smaller peptide fragments without His6 or His14 show 2:1 binding stoichiometry and dimerization of the peptide upon Zn(II) binding (Tsvetkov et al. 2010). Longer peptides tend to form insoluble aggregates in the presence of Zn(II). This suggest that the Zn(II) binding to full-length Aβ has a dynamic nature where different forms of Zn(II)-Aβ complexes with comparable dissociation constants may co-exist. In some of these complexes the His residues that coordinate the metal ion originate from different Aβ molecules which may induce aggregation of the peptide (Miura et al. 2000; Syme and Viles 2006; Minicozzi et al. 2008; Miller et al. 2010).

Cu(II) forms a more stable soluble 1:1 complex with Aβ than Zn(II) (Karr et al. 2005; Jiang et al. 2007), characterized by a conditional K_D equal to 35 nM (Publication I). At higher Cu(II) concentrations a second ion binding has also been observed (Ali et al. 2006) but this process is not physiologically relevant due to low affinity. Several different coordination modes have been proposed for the Cu(II)-Aβ complex. Most likely the soluble Cu(II)-Aβ complex has a dynamic structure existing as a mixture of species with different ligands (Faller and Hureau 2009; Publication V). At lower pH Cu(II) is coordinated by two His and Asp1 whereas at higher pH the complex is pleiomorphic with all three His residues and main chain nitrogen atoms of Asp1 and Ala2 involved (Shin and Saxena 2008; Drew et al. 2009; Hureau et al. 2009). However, if we take into account that the complex structure is determined at higher Aβ concentrations, where the dissociation constant values determined show increased affinity, it is possible that the Cu(II) is coordinated by ligands from more than one Aβ

molecule simultaneously. This process should also enhance peptide assembly into aggregates.

At neutral pH values Cu(II) and Zn(II) ions compete for the same binding site on the Aβ peptide. However, at lower pH values Zn(II) seems to lack residue specific ligands, while Cu(II) keeps its specificity (Ghalebani et al. 2012). This led the authors to the conclusion that Zn(II) may have a protective role under non-acidic conditions.

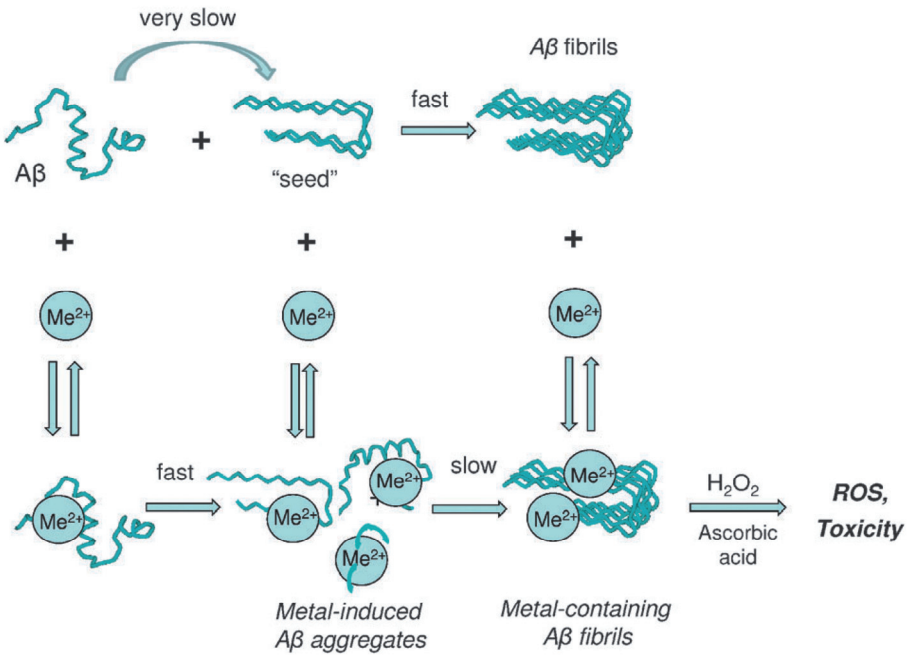

Figure 6. Fibrillization of Aβ peptide in vitro in the presence of metal ions. In the presence of fibrillar nucleus the fibril growth through monomer addition is ‘‘fast’’ (half-life less than one hour). Added metal ions form monomeric complexes with Aβ that precipitate in a non-fibrillar form and also bind to growing fibril ends, thus inhibiting the fast fibrillization process and turning it into a ‘‘slow’’ process that takes a few days. The formation of fibrillar seeds is referred to as ‘‘very slow’’ (it can take several weeks under quiescent conditions). In the absence of seeds the binding of metal ions to Aβ leads to ‘‘slow’’ formation of fibrils, thus increasing the fibrillization rate. Binding of metal ions to fibrils is only partially reversible, the metal ions are ‘‘trapped’’ within matured fibrils (Publication V).

An important aspect to consider related to Aβ metal ion interactions is the affinity of Aβ towards metal ions in different oligomeric and aggregated states. Metal ions cause the peptide assembly into aggregates. It has been shown that these aggregates have a stronger affinity towards Zn(II) than the initial Aβ

monomer (Publication II). A similar conclusion has also been made for Cu(II) from the increase of the apparent affinity at higher peptide concentrations (Zawisza et al. 2012). However, the stability of metal ions bound to fibrils or inside the amyloid plaques may be considerably higher than can be estimated from the affinity since the metal ions may become kinetically trapped inside the aggregates during the aggregation process so that they can no longer be sequestered by different metal chelators.

Based on the fibrillization experiments and analysis of published results we proposed a model for the fibrillization of the Aβ peptide in the presence of metal ions (Fig. 6). In *in vitro* conditions where the fibrillization is fast (due to agitation or addition of seeds) the metal ions inhibit fibril growth by lowering the concentration of the free peptide. Surprisingly, Zn(II) that has lower affinity for Aβ than Cu(II) is a stronger fibrillization inhibitor (Publication II). This may be caused by the fast formation of Zn(II)-Aβ aggregates or by the binding of the Zn(II) to the growing end of the fibril observed recently (Innocenti et al. 2010). Both Zn(II) and Cu(II) induce Aβ aggregation to nonfibrillar aggregates. It is important to notice that the metal-induced aggregates are capable of transforming into Aβ fibrils within days and the metal ions can become kinetically trapped within these fibrils. The inhibiting effect of the metal ions on the fibrillization can be suppressed at least partially by the addition of metal chelators (Publication II), which indicates that metal chelators can dissolve metal-induced Aβ aggregates and release Aβ monomers into solution, where they can participate in fibrillization. It is not excluded that *in vivo* the metal ions can enhance fibril formation through the formation of metal-induced aggregates that evolve into fibrils. In the contexts of the metal chelation therapy it is clear that chelators may have a preventive role against metal-induced aggregates and concomitant fibril formation prior to amyloid deposition. After the formation of amyloid plaques, chelators can have only a limited effect, or they can even accelerate plaque formation because they can dissolve metal-induced Aβ aggregates but they cannot not stop Aβ fibrillization and dissolve Aβ fibrils.

CONCLUSIONS

- It was established that the affinity of Aβ peptide for Zn(II) and Cu(II) is in a biologically relevant range, so that it is probable that these molecules interact *in vivo*.

- It was shown that the metal ions Zn(II) and Cu(II) exert inhibitory effect on fibrillization of Aβ due to formation of metal-induced aggregates and metal chelators are able to eliminate this inhibitory effect.

- It was demonstrated that metal-induced aggregates are amorphous and that during incubation these aggregates are transformed into amyloid fibrils.

- It was suggested that *in vivo* metal ions could induce seed-independent fibrillization of Aβ by formation of metal-induced aggregates that transform into amyloid fibrils.

REFERENCES

Abedini, A. and D. P. Raleigh (2009). "A Role for Helical Intermediates in Amyloid Formation by Natively Unfolded Polypeptides?" Phys. Biol. **6**(1): 15005.

Adlard, P. A., R. A. Cherny, D. I. Finkelstein, et al. (2008). "Rapid Restoration of Cognition in Alzheimer's Transgenic Mice with 8-Hydroxy Quinoline Analogs Is Associated with Decreased Interstitial Abeta." Neuron **59**(1): 43-55.

Aguzzi, A. and T. O'connor (2010). "Protein Aggregation Diseases: Pathogenicity and Therapeutic Perspectives." Nat. Rev. Drug Discov. **9**(3): 237-248.

Ahmed, M., J. Davis, D. Aucoin, et al. (2010). "Structural Conversion of Neurotoxic Amyloid-Beta(1-42) Oligomers to Fibrils." Nat. Struct. Mol. Biol. **17**(5): 561-U556.

Ali, F. E., F. Separovic, C. J. Barrow, et al. (2006). "Copper and Zinc Mediated Oligomerisation of A Beta Peptides." Int. J. Pept. Res. Ther. **12**(2): 153-164.

Alzheimer's Association (2012). "2012 Alzheimer's Disease Facts and Figures." Alzheimers dement. **8**(2): 131-168.

Assaf, S. Y. and S. H. Chung (1984). "Release of Endogenous Zn2+ from Brain Tissue During Activity." Nature **308**(5961): 734-736.

Atwood, C. S., R. D. Moir, X. Huang, et al. (1998). "Dramatic Aggregation of Alzheimer Abeta by Cu(II) Is Induced by Conditions Representing Physiological Acidosis." J.Biol.Chem. **273**(21): 12817-12826.

Atwood, C. S., R. C. Scarpa, X. Huang, et al. (2000). "Characterization of Copper Interactions with Alzheimer Amyloid Beta Peptides: Identification of an Attomolar-Affinity Copper Binding Site on Amyloid Beta1-42." J. Neurochem. **75**(3): 1219-1233.

Balducci, C., M. Beeg, M. Stravalaci, et al. (2010). "Synthetic Amyloid-Beta Oligomers Impair Long-Term Memory Independently of Cellular Prion Protein." Proc. Natl. Acad. Sci. USA **107**(5): 2295-2300.

Baran, E. J. (2010). "Chelation Therapies: A Chemical and Biochemical Perspective." Curr. Med. Chem. **17**(31): 3658-3672.

Bartus, R. T., R. L. Dean, B. Beer, et al. (1982). "The Cholinergic Hypothesis of Geriatric Memory Dysfunction." Science **217**(4558): 408-417.

Bayer, T. A., S. Schafer, A. Simons, et al. (2003). "Dietary Cu Stabilizes Brain Superoxide Dismutase 1 Activity and Reduces Amyloid Abeta Production in APP23 Transgenic Mice." Proc. Natl. Acad. Sci. USA **100**(24): 14187-14192.

Berson, J. F., A. C. Theos, D. C. Harper, et al. (2003). "Proprotein Convertase Cleavage Liberates a Fibrillogenic Fragment of a Resident Glycoprotein to Initiate Melanosome Biogenesis." J. Cell Biol. **161**(3): 521-533.

Blacker, D., M. A. Wilcox, N. M. Laird, et al. (1998). "Alpha-2 Macroglobulin Is Genetically Associated with Alzheimer Disease." Nat. Genet. **19**(4): 357-360.

Bobinski, M., J. Wegiel, H. M. Wisniewski, et al. (1996). "Neurofibrillary Pathology--Correlation with Hippocampal Formation Atrophy in Alzheimer Disease." Neurobiol. Aging **17**(6): 909-919.

Bourhim, M., M. Kruzel, T. Srikrishnan, et al. (2007). "Linear Quantitation of Abeta Aggregation Using Thioflavin T: Reduction in Fibril Formation by Colostrinin." J. Neurosci. Methods **160**(2): 264-268.

Braak, H. and E. Braak (1998). "Evolution of Neuronal Changes in the Course of Alzheimer's Disease." J. Neural Transm. Suppl. **53**: 127-140.

Braak, H., E. Braak, J. Bohl, et al. (1996). "Age, Neurofibrillary Changes, A Beta-Amyloid and the Onset of Alzheimer's Disease." Neurosci. Lett. **210**(2): 87-90.

Broersen, K., F. Rousseau and J. Schymkowitz (2010). "The Culprit Behind Amyloid Beta Peptide Related Neurotoxicity in Alzheimer's Disease: Oligomer Size or Conformation?" Alzheimers Res. Ther. **2**(4): 12.

Brugge, K. L., S. L. Nichols, D. P. Salmon, et al. (1994). "Cognitive Impairment in Adults with Downs-Syndrome - Similarities to Early Cognitive Changes in Alzheimers-Disease." Neurology **44**(2): 232-238.

Budimir, A. (2011). "Metal Ions, Alzheimer's Disease and Chelation Therapy." Acta Pharm. **61**(1): 1-14.

Bush, A. I. (2003). "The Metallobiology of Alzheimer's Disease." Trends Neurosci. **26**(4): 207-214.

Bush, A. I., W. H. Pettingell, G. Multhaup, et al. (1994). "Rapid Induction of Alzheimer A Beta Amyloid Formation by Zinc." Science **265**(5177): 1464-1467.

Bush, A. I. and R. E. Tanzi (2008). "Therapeutics for Alzheimer's Disease Based on the Metal Hypothesis." Neurotherapeutics **5**(3): 421-432.

Castellani, R. J., R. K. Rolston and M. A. Smith (2010). "Alzheimer Disease." DM-Dis. Mon. **56**(9): 484-546.

Castellano, J. M., J. Kim, F. R. Stewart, et al. (2011). "Human ApoE Isoforms Differentially Regulate Brain Amyloid-Beta Peptide Clearance." Sci. Transl. Med. **3**(89): 89ra57

Chen, W. T., Y. H. Liao, H. M. Yu, et al. (2011). "Distinct Effects of Zn2+, Cu2+, Fe3+, and Al3+ on Amyloid-Beta Stability, Oligomerization, and Aggregation: Amyloid-Beta Destabilization Promotes Annular Protofibril Formation." J.Biol.Chem. 286(11): 9649-9656.

Cherny, R. A., C. S. Atwood, M. E. Xilinas, et al. (2001). "Treatment with a Copper-Zinc Chelator Markedly and Rapidly Inhibits Beta-Amyloid Accumulation in Alzheimer's Disease Transgenic Mice." Neuron **30**(3): 665-676.

Cherny, R. A., J. T. Legg, C. A. Mclean, et al. (1999). "Aqueous Dissolution of Alzheimer's Disease Abeta Amyloid Deposits by Biometal Depletion." J.Biol.Chem. **274**(33): 23223-23228.

Chiti, F. and C. M. Dobson (2006). "Protein Misfolding, Functional Amyloid, and Human Disease." Annu. Rev. Biochem. **75**: 333-366.

Chiti, F., P. Webster, N. Taddei, et al. (1999). "Designing Conditions for *in vitro* Formation of Amyloid Protofilaments and Fibrils." Proc. Natl. Acad. Sci. USA **96**(7): 3590-3594.

Chung, R. S., C. Howells, E. D. Eaton, et al. (2010). "The Native Copper- and Zinc- Binding Protein Metallothionein Blocks Copper-Mediated A Beta Aggregation and Toxicity in Rat Cortical Neurons." PLoS ONE **5**(8): e12030.

Cizas, P., R. Budvytyte, R. Morkuniene, et al. (2010). "Size-Dependent Neurotoxicity of Beta-Amyloid Oligomers." Arch. Biochem. Biophys. **496**(2): 84-92.

Ciuculescu, E. D., Y. Mekmouche and P. Faller (2005). "Metal-Binding Properties of the Peptide APP(170-188): A Model of the Zn-II-Binding Site of Amyloid Precursor Protein (APP)." Chem.-Eur. J. **11**(3): 903-909.

Clements, A., D. Allsop, D. M. Walsh, et al. (1996). "Aggregation and Metal-Binding Properties of Mutant Forms of the Amyloid A Beta Peptide of Alzheimer's Disease." J. Neurochem. **66**(2): 740-747.

Corder, E. H., A. M. Saunders, W. J. Strittmatter, et al. (1993). "Gene Dose of Apolipoprotein E Type 4 Allele and the Risk of Alzheimer's Disease in Late Onset Families." Science **261**(5123): 921-923.

Crapper, D. R., S. S. Krishnan and A. J. Dalton (1973). "Brain Aluminum Distribution in Alzheimer's Disease and Experimental Neurofibrillary Degeneration." Science **180**(4085): 511-513.

Crapper, D. R., S. S. Krishnan and S. Quittkat (1976). "Aluminium, Neurofibrillary Degeneration and Alzheimer's Disease." Brain **99**(1): 67-80.

Crouch, P. J., D. J. Tew, T. Du, et al. (2009). "Restored Degradation of the Alzheimer's Amyloid-Beta Peptide by Targeting Amyloid Formation." J. Neurochem. **108**(5): 1198-1207.

Cummings, B. J. and C. W. Cotman (1995). "Image Analysis of Beta-Amyloid Load in Alzheimer's Disease and Relation to Dementia Severity." Lancet **346**(8989): 1524-1528.

Cummings, J. L., H. V. Vinters, G. M. Cole, et al. (1998). "Alzheimer's Disease: Etiologies, Pathophysiology, Cognitive Reserve, and Treatment Opportunities." Neurology **51**(1 Suppl 1): S2-17; discussion S65-17.

Damante, C. A., K. Osz, Z. Nagy, et al. (2008). "The Metal Loading Ability of Beta-Amyloid N-Terminus: A Combined Potentiometric and Spectroscopic Study of Copper(II) Complexes with Beta-Amyloid(1-

16), Its Short or Mutated Peptide Fragments, and Its Polyethylene Glycol (PEG)-ylated Analogue." Inorg. Chem. **47**(20): 9669-9683.

Danielsson, J., R. Pierattelli, L. Banci, et al. (2007). "High-Resolution NMR Studies of the Zinc-Binding Site of the Alzheimer's Amyloid Beta-Peptide." FEBS J. **274**(1): 46-59.

Daw, E. W., H. Payami, E. J. Nemens, et al. (2000). "The Number of Trait Loci in Late-Onset Alzheimer Disease." Am. J. Hum. Genet. **66**(1): 196-204.

De Ferrari, G. V. and N. C. Inestrosa (2000). "Wnt Signaling Function in Alzheimer's Disease." Brain Res. Rev. **33**(1): 1-12.

Detoma, A. S., S. Salamekh, A. Ramamoorthy, et al. (2012). "Misfolded Proteins in Alzheimer's Disease and Type II Diabetes." Chem. Soc. Rev. **41**(2): 608-621.

Dillen, K. and W. Annaert (2006). "A Two Decade Contribution of Molecular Cell Biology to the Centennial of Alzheimer's Disease: Are We Progressing Toward Therapy?" Int. Rev. Cytol. **254**: 215-300.

Dobson, C. M. (2001). "The Structural Basis of Protein Folding and Its Links with Human Disease." Philos. Trans. R. Soc. Lond. B. Biol. Sci. **356**(1406): 133-145.

Dobson, C. M. (2003). "Protein Folding and Misfolding." Nature **426**(6968): 884-890.

Dong, J., C. S. Atwood, V. E. Anderson, et al. (2003). "Metal Binding and Oxidation of Amyloid-Beta within Isolated Senile Plaque Cores: Raman Microscopic Evidence." Biochemistry **42**(10): 2768-2773.

Drew, S. C., C. L. Masters and K. J. Barnham (2009). "Alanine-2 Carbonyl Is an Oxygen Ligand in Cu2+ Coordination of Alzheimer's Disease Amyloid-Beta Peptide--Relevance to N-Terminally Truncated Forms." J. Am. Chem. Soc. **131**(25): 8760-8761.

Duce, J. A. and A. I. Bush (2010). "Biological Metals and Alzheimer's Disease: Implications for Therapeutics and Diagnostics." Prog. Neurobiol. **92**(1): 1-18.

Eckman, C. B., N. D. Mehta, R. Crook, et al. (1997). "A New Pathogenic Mutation in the APP Gene (I716V) Increases the Relative Proportion of A Beta 42(43)." Hum. Mol. Genet. **6**(12): 2087-2089.

Esler, W. P., E. R. Stimson, J. M. Jennings, et al. (1996). "Zinc-Induced Aggregation of Human and Rat Beta-Amyloid Peptides *in vitro*." J. Neurochem. **66**(2): 723-732.

Faller, P. and C. Hureau (2009). "Bioinorganic Chemistry of Copper and Zinc Ions Coordinated to Amyloid-Beta Peptide." Dalton Trans.(7): 1080-1094.

Faller, P., C. Hureau, P. Dorlet, et al. (2012). "Methods and Techniques to Study the Bioinorganic Chemistry of Metal–Peptide Complexes Linked to Neurodegenerative Diseases." Coordin. Chem. Rev. (*in press*).

Fandrich, M., M. Schmidt and N. Grigorieff (2011). "Recent Progress in Understanding Alzheimer's Beta-Amyloid Structures." Trends Biochem. Sci. **36**(6): 338-345.

Ferri, C. P., M. Prince, C. Brayne, et al. (2005). "Global Prevalence of Dementia: A Delphi Consensus Study." Lancet **366**(9503): 2112-2117.

Fodera, V., S. Cataldo, F. Librizzi, et al. (2009). "Self-Organization Pathways and Spatial Heterogeneity in Insulin Amyloid Fibril Formation." J. Phys. Chem. B **113**(31): 10830-10837.

Frederickson, C. J. and A. I. Bush (2001). "Synaptically Released Zinc: Physiological Functions and Pathological Effects." Biometals **14**(3-4): 353-366.

Frederickson, C. J., J. Y. Koh and A. I. Bush (2005). "The Neurobiology of Zinc in Health and Disease." Nature Rev. Neurosci. **6**(6): 449-462.

Freir, D. B., R. Fedriani, D. Scully, et al. (2010). "Abeta Oligomers Inhibit Synapse Remodelling Necessary for Memory Consolidation." Neurobiol. Aging **32**(12): 2211-2218.

Friedrich, R. P., K. Tepper, R. Ronicke, et al. (2010). "Mechanism of Amyloid Plaque Formation Suggests an Intracellular Basis of A Beta Pathogenicity." Proc. Natl. Acad. Sci. USA **107**(5): 1942-1947.

Fukuda, H., T. Shimizu, M. Nakajima, et al. (1999). "Synthesis, Aggregation, and Neurotoxicity of the Alzheimer's Abeta1-42 Amyloid Peptide and Its Isoaspartyl Isomers." Bioorg. Med. Chem. Lett. **9**(7): 953-956.

Gaggelli, E., A. Janicka-Klos, E. Jankowska, et al. (2008). "NMR Studies of the Zn2+ Interactions with Rat and Human Beta-Amyloid (1-28) Peptides in Water-Micelle Environment." J. Phys. Chem. B **112**(1): 100-109.

Gaggelli, E., H. Kozlowski, D. Valensin, et al. (2006). "Copper Homeostasis and Neurodegenerative Disorders (Alzheimer's, Prion, and Parkinson's Diseases and Amyotrophic Lateral Sclerosis)." Chem. Rev. **106**(6): 1995-2044.

Galimberti, D., C. Fenoglio and E. Scarpini (2008). "Inflammation in Neurodegenerative Disorders: Friend or Foe?" Curr. Aging Sci. **1**(1): 30-41.

Galimberti, D. and E. Scarpini (2012). "Progress in Alzheimer's Disease." J. Neurol. **259**(2): 201-211.

Gamblin, T. C., F. Chen, A. Zambrano, et al. (2003). "Caspase Cleavage of Tau: Linking Amyloid and Neurofibrillary Tangles in Alzheimer's Disease." Proc. Natl. Acad. Sci. USA **100**(17): 10032-10037.

Garzon-Rodriguez, W., A. K. Yatsimirsky and C. G. Glabe (1999). "Binding of Zn(II), Cu(II), and Fe(II) Ions to Alzheimer's A Beta Peptide Studied by Fluorescence." Bioorg. Med. Chem. Lett. **9**(15): 2243-2248.

Gatz, M., C. A. Reynolds, L. Fratiglioni, et al. (2006). "Role of Genes and Environments for Explaining Alzheimer Disease." Arch. Gen. Psychiat. **63**(2): 168-174.

Geddes, A. J., K. D. Parker, E. D. Atkins, et al. (1968). ""Cross-Beta" Conformation in Proteins." J. Mol. Biol. **32**(2): 343-358.

Ghalebani, L., A. Wahlström, J. Danielsson, et al. (2012). "pH-Dependence of the Specific Binding of Cu(II) and Zn(II) Ions to the Amyloid-B Peptide." Biochem. Bioph. Res. Co.(*in press*).

Giannakopoulos, P., F. R. Herrmann, T. Bussiere, et al. (2003). "Tangle and Neuron Numbers, but Not Amyloid Load, Predict Cognitive Status in Alzheimer's Disease." Neurology **60**(9): 1495-1500.

Giuffrida, M. L., F. Caraci, B. Pignataro, et al. (2009). "Beta-Amyloid Monomers Are Neuroprotective." J. Neurosci. **29**(34): 10582-10587.

Golde, T. E. (2003). "Alzheimer Disease Therapy: Can the Amyloid Cascade Be Halted?" J. Clin. Invest. **111**(1): 11-18.

Goldsbury, C., U. Baxa, M. N. Simon, et al. (2011). "Amyloid Structure and Assembly: Insights from Scanning Transmission Electron Microscopy." J. Struct. Biol. **173**(1): 1-13.

Grundkeiqbal, I., J. Fleming, Y. C. Tung, et al. (1990). "Ferritin Is a Component of the Neuritic (Senile) Plaque in Alzheimer Dementia." Acta Neuropathol. **81**(2): 105-110.

Ha, C., J. Ryu and C. B. Park (2007). "Metal Ions Differentially Influence the Aggregation and Deposition of Alzheimer's Beta-Amyloid on a Solid Template." Biochemistry **46**(20): 6118-6125.

Haass, C. and D. J. Selkoe (2007). "Soluble Protein Oligomers in Neurodegeneration: Lessons from the Alzheimer's Amyloid Beta-Peptide." Nat. Rev. Mol. Cell Biol. **8**(2): 101-112.

Halliwell, B. and J. M. C. Gutteridge (1984). "Oxygen-Toxicity, Oxygen Radicals, Transition-Metals and Disease." Biochem. J. **219**(1): 1-14.

Hampel, H., D. Prvulovic, S. Teipel, et al. (2011). "The Future of Alzheimer's Disease: The Next 10 Years." Prog. Neurobiol. **95**(4): 718-728.

Hardy, J., K. Duff, K. G. Hardy, et al. (1998). "Genetic Dissection of Alzheimer's Disease and Related Dementias: Amyloid and Its Relationship to Tau." Nat. Neurosci. **1**(5): 355-358.

Hardy, J. and D. J. Selkoe (2002). "The Amyloid Hypothesis of Alzheimer's Disease: Progress and Problems on the Road to Therapeutics." Science **297**(5580): 353-356.

Hardy, J. A. and G. A. Higgins (1992). "Alzheimer's Disease: The Amyloid Cascade Hypothesis." Science **256**(5054): 184-185.

Harper, J. D. and P. T. Lansbury, Jr. (1997). "Models of Amyloid Seeding in Alzheimer's Disease and Scrapie: Mechanistic Truths and Physiological Consequences of the Time-Dependent Solubility of Amyloid Proteins." Annu. Rev. Biochem. **66**: 385-407.

Harrison, R. S., P. C. Sharpe, Y. Singh, et al. (2007). "Amyloid Peptides and Proteins in Review." Rev. Physiol. Biochem. Pharmacol. **159**: 1-77.

Hartter, D. E. and A. Barnea (1988). "Evidence for Release of Copper in the Brain: Depolarization-Induced Release of Newly Taken-up 67copper." Synapse **2**(4): 412-415.

Hatcher, L. Q., L. Hong, W. D. Bush, et al. (2008). "Quantification of the Binding Constant of Copper(II) to the Amyloid-Beta Peptide." J. Phys. Chem. B **112**(27): 8160-8164.

Hegde, M. L., P. Bharathi, A. Suram, et al. (2009). "Challenges Associated with Metal Chelation Therapy in Alzheimer's Disease." J. Alzheimers Dis. **17**(3): 457-468.

Hellstrand, E., B. Boland, D. M. Walsh, et al. (2009). "Amyloid B-Protein Aggregation Produces Highly Reproducible Kinetic Data and Occurs by a Two-Phase Process." ACS Chem. Neurosci. **1**(1): 13-18.

Hendrie, H. C. (1998). "Epidemiology of Dementia and Alzheimer's Disease." Am. J. Geriat. Psychiat. **6**(2): S3-S18.

Holm, N. K., S. K. Jespersen, L. V. Thomassen, et al. (2007). "Aggregation and Fibrillation of Bovine Serum Albumin." Biochim. Biophys. Acta. **1774** (9): 1128-1138.

Hortschansky, P., V. Schroeckh, T. Christopeit, et al. (2005). "The Aggregation Kinetics of Alzheimer's Beta-Amyloid Peptide Is Controlled by Stochastic Nucleation." Protein Sci. **14**(7): 1753-1759.

Horwich, A. (2002). "Protein Aggregation in Disease: A Role for Folding Intermediates Forming Specific Multimeric Interactions." J. Clin. Invest. **110**(9): 1221-1232.

Hou, L., H. Shao, Y. Zhang, et al. (2004). "Solution NMR Studies of the A Beta(1-40) and A Beta(1-42) Peptides Establish That the Met35 Oxidation State Affects the Mechanism of Amyloid Formation." J. Am. Chem. Soc. **126**(7): 1992-2005.

Howells, C., K. Saar, E. Eaton, et al. (2012). "Redox-Active Cu(II)-Aβ Causes Substantial Changes in Axonal Integrity in Cultured Cortical Neurons in an Oxidative-Stress Dependent Manner." Exp. Neurol. (*in press*).

Hua, H. Q., L. Munter, A. Harmeier, et al. (2011). "Toxicity of Alzheimer's Disease-Associated A Beta Peptide Is Ameliorated in a *Drosophila* Model by Tight Control of Zinc and Copper Availability." Biol. Chem. **392**(10): 919-926.

Huang, X., R. D. Moir, R. E. Tanzi, et al. (2004). "Redox-Active Metals, Oxidative Stress, and Alzheimer's Disease Pathology." Ann. N. Y. Acad. Sci. **1012**: 153-163.

Hudson, S. A., H. Ecroyd, T. W. Kee, et al. (2009). "The Thioflavin T Fluorescence Assay for Amyloid Fibril Detection Can Be Biased by the Presence of Exogenous Compounds." FEBS J. **276**(20): 5960-5972.

Hung, Y. H., A. I. Bush and R. A. Cherny (2010). "Copper in the Brain and Alzheimer's Disease." J. Biol. Inorg. Chem. **15**(1): 61-76.

Hureau, C., Y. Coppel, P. Dorlet, et al. (2009). "Deprotonation of the Asp1-Ala2 Peptide Bond Induces Modification of the Dynamic Copper(II)

Environment in the Amyloid-Beta Peptide near Physiological pH." Angew. Chem. Int. Edit. **48**(50): 9522-9525.

Innocenti, M., E. Salvietti, M. Guidotti, et al. (2010). "Trace Copper(II) or Zinc(II) Ions Drastically Modify the Aggregation Behavior of Amyloid-Beta 1-42: An AFM Study." J. Alzheimer's Dis. **19**(4): 1223-1229.

Isaacs, A. M., D. B. Senn, M. Yuan, et al. (2006). "Acceleration of Amyloid Beta -Peptide Aggregation by Physiological Concentrations of Calcium." J.Biol.Chem. **281**: 27916-27923.

Jakob-Roetne, R. and H. Jacobsen (2009). "Alzheimer's Disease: From Pathology to Therapeutic Approaches." Angew. Chem. Int. Ed. Engl. **48**(17): 3030-3059.

Jiang, D., L. Men, J. Wang, et al. (2007). "Redox Reactions of Copper Complexes Formed with Different Beta-Amyloid Peptides and Their Neuropathalogical Relevance." Biochemistry **46**(32): 9270-9282.

Johansson, A. S., F. Berglind-Dehlin, G. Karlsson, et al. (2006). "Physiochemical Characterization of the Alzheimer's Disease-Related Peptides A Beta 1-42arctic and A Beta 1-42wt." FEBS J. **273**(12): 2618-2630.

Kardos, J., I. Kovacs, F. Hajos, et al. (1989). "Nerve Endings from Rat Brain Tissue Release Copper Upon Depolarization. A Possible Role in Regulating Neuronal Excitability." Neurosci. Lett. **103**(2): 139-144.

Karr, J. W., H. Akintoye, L. J. Kaupp, et al. (2005). "N-Terminal Deletions Modify the Cu2+ Binding Site in Amyloid-Beta." Biochemistry **44**(14): 5478-5487.

Kim, J., J. M. Basak and D. M. Holtzman (2009). "The Role of Apolipoprotein E in Alzheimer's Disease." Neuron **63**(3): 287-303.

Klug, G. M., D. Losic, S. S. Subasinghe, et al. (2003). "Beta-Amyloid Protein Oligomers Induced by Metal Ions and Acid pH Are Distinct from Those Generated by Slow Spontaneous Ageing at Neutral pH." Eur. J. Biochem. **270**(21): 4282-4293.

Knopman, D. S., J. E. Parisi, A. Salviati, et al. (2003). "Neuropathology of Cognitively Normal Elderly." J. Neuropath. Exp. Neur. **62**(11): 1087-1095.

Knowles, T. P. J., C. A. Waudby, G. L. Devlin, et al. (2009). "An Analytical Solution to the Kinetics of Breakable Filament Assembly." Science **326**(5959): 1533-1537.

Kowalik-Jankowska, T., M. Ruta, K. Wisniewska, et al. (2003). "Coordination Abilities of the 1-16 and 1-28 Fragments of Beta-Amyloid Peptide Towards Copper(II) Ions: A Combined Potentiometric and Spectroscopic Study." J. Inorg. Biochem. **95**(4): 270-282.

Krieger, E., G. Koraimann and G. Vriend (2002). "Increasing the Precision of Comparative Models with Yasara Nova - a Self-Parameterizing Force Field." Proteins **47**(3): 393-402.

Kurz, A., K. Altland, N. Lautenschlager, et al. (1996). "Apolipoprotein E Type 4 Allele and Alzheimer's Disease: Effect on Age at Onset and Relative Risk in Different Age Groups." J. Neurol. **243**(6): 452-456.

Kwok, J. B., G. M. Halliday, W. S. Brooks, et al. (2003). "Presenilin-1 Mutation L271V Results in Altered Exon 8 Splicing and Alzheimer's Disease with Non-Cored Plaques and No Neuritic Dystrophy." J.Biol.Chem. **278**(9): 6748-6754.

Lannfelt, L., K. Blennow, H. Zetterberg, et al. (2008). "Safety, Efficacy, and Biomarker Findings of PBT2 in Targeting Abeta as a Modifying Therapy for Alzheimer's Disease: A Phase IIa, Double-Blind, Randomised, Placebo-Controlled Trial." Lancet Neurol. **7**(9): 779-786.

Lee, J. Y., T. B. Cole, R. D. Palmiter, et al. (2002). "Contribution by Synaptic Zinc to the Gender-Disparate Plaque Formation in Human Swedish Mutant APP Transgenic Mice." Proc. Natl. Acad. Sci. USA **99**(11): 7705-7710.

Lee, S., E. J. Fernandez and T. A. Good (2007). "Role of Aggregation Conditions in Structure, Stability, and Toxicity of Intermediates in the Abeta Fibril Formation Pathway." Protein Sci. **16**(4): 723-732.

Lesne, S., M. T. Koh, L. Kotilinek, et al. (2006). "A Specific Amyloid-Beta Protein Assembly in the Brain Impairs Memory." Nature **440**(7082): 352-357.

Levine, H. (1995). "Thioflavine-T Interaction with Amyloid Beta-Sheet Structures." Amyloid-Int. J. Exp. Clin. Investig. **2**(1): 1-6.

Lewis, J., D. W. Dickson, W. L. Lin, et al. (2001). "Enhanced Neurofibrillary Degeneration in Transgenic Mice Expressing Mutant Tau and APP." Science **293**(5534): 1487-1491.

Lin, M. S., L. Y. Chen, H. T. Tsai, et al. (2008). "Investigation of the Mechanism of Beta-Amyloid Fibril Formation by Kinetic and Thermodynamic Analyses." Langmuir **24**(11): 5802-5808.

Lomakin, A., D. S. Chung, G. B. Benedek, et al. (1996). "On the Nucleation and Growth of Amyloid Beta-Protein Fibrils: Detection of Nuclei and Quantitation of Rate Constants." Proc. Natl. Acad. Sci. USA **93**(3): 1125-1129.

Lorenzo, A. and B. A. Yankner (1994). "Beta-Amyloid Neurotoxicity Requires Fibril Formation and Is Inhibited by Congo Red." Proc. Natl. Acad. Sci. USA **91**(25): 12243-12247.

Lovell, M. A., J. D. Robertson, W. J. Teesdale, et al. (1998). "Copper, Iron and Zinc in Alzheimer's Disease Senile Plaques." J. Neurol. Sci. **158**(1): 47-52.

Maji, S. K., M. H. Perrin, M. R. Sawaya, et al. (2009). "Functional Amyloids as Natural Storage of Peptide Hormones in Pituitary Secretory Granules." Science **325**(5938): 328-332.

Mancino, A. M., S. S. Hindo, A. Kochi, et al. (2009). "Effects of Clioquinol on Metal-Triggered Amyloid-Beta Aggregation Revisited." Inorg. Chem. **48**(20): 9596-9598.

Martins, I. C., I. Kuperstein, H. Wilkinson, et al. (2008). "Lipids Revert Inert Abeta Amyloid Fibrils to Neurotoxic Protofibrils That Affect Learning in Mice." EMBO J. **27**(1): 224-233.

Masters, C. L., G. Simms, N. A. Weinman, et al. (1985). "Amyloid Plaque Core Protein in Alzheimer-Disease and Down Syndrome." Proc. Natl. Acad. Sci. USA **82**(12): 4245-4249.

Mattson, M. P. (2004). "Pathways Towards and Away from Alzheimer's Disease." Nature **430**(7000): 631-639.

Mclachlan, D. R. C., A. J. Dalton, T. P. A. Kruck, et al. (1991). "Intramuscular Desferrioxamine in Patients with Alzheimers-Disease." Lancet **337**(8753): 1304-1308.

Meloni, G., P. Faller and M. Vasak (2007). "Redox Silencing of Copper in Metal-Linked Neurodegenerative Disorders: Reaction of Zn7metallothionein-3 with Cu2+ Ions." J.Biol.Chem. **282**(22): 16068-16078.

Meyer-Luehmann, M., T. L. Spires-Jones, C. Prada, et al. (2008). "Rapid Appearance and Local Toxicity of Amyloid-Beta Plaques in a Mouse Model of Alzheimer's Disease." Nature **451**(7179): 720-U725.

Miller, Y., B. Ma and R. Nussinov (2010). "Zinc Ions Promote Alzheimer Abeta Aggregation Via Population Shift of Polymorphic States." Proc. Natl. Acad. Sci. USA **107**(21): 9490-9495.

Minicozzi, V., F. Stellato, M. Comai, et al. (2008). "Identifying the Minimal Copper- and Zinc-Binding Site Sequence in Amyloid-Beta Peptides." J.Biol.Chem. **283**(16): 10784-10792.

Mintun, M. A., G. N. Larossa, Y. I. Sheline, et al. (2006). "[11C]PIB in a Nondemented Population: Potential Antecedent Marker of Alzheimer Disease." Neurology **67**(3): 446-452.

Miura, T., K. Suzuki, N. Kohata, et al. (2000). "Metal Binding Modes of Alzheimer's Amyloid Beta-Peptide in Insoluble Aggregates and Soluble Complexes." Biochemistry **39**(23): 7024-7031.

Morgan, C., M. Colombres, M. T. Nunez, et al. (2004). "Structure and Function of Amyloid in Alzheimer's Disease." Prog. Neurobiol. **74**(6): 323-349.

Morris, A. M., M. A. Watzky and R. G. Finke (2009). "Protein Aggregation Kinetics, Mechanism, and Curve-Fitting: A Review of the Literature." BBA-Proteins Proteom. **1794**(3): 375-397.

Muller, U. C. and H. Zheng (2012). "Physiological Functions of APP Family Proteins." Cold Spring Harb. Perspect. Med. **2**(2): a006288.

Naslund, J., V. Haroutunian, R. Mohs, et al. (2000). "Correlation between Elevated Levels of Amyloid Beta-Peptide in the Brain and Cognitive Decline." Jama **283**(12): 1571-1577.

Nelson, R., M. R. Sawaya, M. Balbirnie, et al. (2005). "Structure of the Cross-Beta Spine of Amyloid-Like Fibrils." Nature **435**(7043): 773-778.

Opazo, C., X. Huang, R. A. Cherny, et al. (2002). "Metalloenzyme-Like Activity of Alzheimer's Disease Beta-Amyloid. Cu-Dependent Catalytic Conversion of Dopamine, Cholesterol, and Biological Reducing Agents to Neurotoxic H(2)O(2)." J.Biol.Chem. **277**(43): 40302-40308.

Petkova, A. T., Y. Ishii, J. J. Balbach, et al. (2002). "A Structural Model for Alzheimer's Beta-Amyloid Fibrils Based on Experimental Constraints from Solid State NMR." Proc. Natl. Acad. Sci. USA **99**(26): 16742-16747.

Petkova, A. T., R. D. Leapman, Z. H. Guo, et al. (2005). "Self-Propagating, Molecular-Level Polymorphism in Alzheimer's Beta-Amyloid Fibrils." Science **307**(5707): 262-265.

Pike, C. J., M. J. Overman and C. W. Cotman (1995). "Amino-Terminal Deletions Enhance Aggregation of Beta-Amyloid Peptides *in vitro*." J.Biol.Chem. **270**(41): 23895-23898.

Pimplikar, S. W. (2009). "Reassessing the Amyloid Cascade Hypothesis of Alzheimer's Disease." Int. J. Biochem. Cell B. **41**(6): 1261-1268.

Poirier, J., J. Davignon, D. Bouthillier, et al. (1993). "Apolipoprotein E Polymorphism and Alzheimer's Disease." Lancet **342**(8873): 697-699.

Portelius, E., N. Bogdanovic, M. K. Gustavsson, et al. (2010). "Mass Spectrometric Characterization of Brain Amyloid Beta Isoform Signatures in Familial and Sporadic Alzheimer's Disease." Acta Neuropathol. **120**(2): 185-193.

Prasher, V. P., M. J. Farrer, A. M. Kessling, et al. (1998). "Molecular Mapping of Alzheimer-Type Dementia in Down's Syndrome." Ann. Neurol. **43**(3): 380-383.

Price, J. L., D. W. Mckeel, V. D. Buckles, et al. (2009). "Neuropathology of Nondemented Aging: Presumptive Evidence for Preclinical Alzheimer Disease." Neurobiol. Aging **30**(7): 1026-1036.

Qiang, W., W. M. Yau, Y. Q. Luo, et al. (2012). "Antiparallel Beta-Sheet Architecture in Iowa-Mutant Beta-Amyloid Fibrils." Proc. Natl. Acad. Sci. USA **109**(12): 4443-4448.

Que, E. L., D. W. Domaille and C. J. Chang (2008). "Metals in Neurobiology: Probing Their Chemistry and Biology with Molecular Imaging." Chem. Rev. **108**(5): 1517-1549.

Rae, T. D., P. J. Schmidt, R. A. Pufahl, et al. (1999). "Undetectable Intracellular Free Copper: The Requirement of a Copper Chaperone for Superoxide Dismutase." Science **284**(5415): 805-808.

Raman, B., T. Ban, K. Yamaguchi, et al. (2005). "Metal Ion-Dependent Effects of Clioquinol on the Fibril Growth of an Amyloid Beta Peptide." J.Biol.Chem. **280**(16): 16157-16162.

Rangachari, V., B. D. Moore, D. K. Reed, et al. (2007). "Amyloid-Beta(1-42) Rapidly Forms Protofibrils and Oligomers by Distinct Pathways in Low

Concentrations of Sodium Dodecylsulfate." Biochemistry **46**(43): 12451-12462.
Reddy, V. P., X. W. Zhu, G. Perry, et al. (2009). "Oxidative Stress in Diabetes and Alzheimer's Disease." J. Alzheimers Dis. **16**(4): 763-774.
Reiman, E. M., J. A. Webster, A. J. Myers, et al. (2007). "GAB2 Alleles Modify Alzheimer's Risk in APOE Epsilon 4 Carriers." Neuron **54**(5): 713-720.
Reitz, C., C. Brayne and R. Mayeux (2011). "Epidemiology of Alzheimer Disease." Nat. Rev. Neurol. **7**(3): 137-152.
Rentz, D. M., J. J. Locascio, J. A. Becker, et al. (2010). "Cognition, Reserve, and Amyloid Deposition in Normal Aging." Ann. Neurol. **67**(3): 353-364.
Ricchelli, F., D. Drago, B. Filippi, et al. (2005). "Aluminum-Triggered Structural Modifications and Aggregation of Beta-Amyloids." Cell. Mol. Life Sci. **62**(15): 1724-1733.
Riek, R., P. Guntert, H. Dobeli, et al. (2001). "NMR Studies in Aqueous Solution Fail to Identify Significant Conformational Differences between the Monomeric Forms of Two Alzheimer Peptides with Widely Different Plaque-Competence, A Beta(1-40)(Ox) and A Beta(1-42)(Ox)." Eur. J. Biochem. **268**(22): 5930-5936.
Ritchie, C. W., A. I. Bush, A. Mackinnon, et al. (2003). "Metal-Protein Attenuation with Iodochlorhydroxyquin (Clioquinol) Targeting Abeta Amyloid Deposition and Toxicity in Alzheimer Disease: A Pilot Phase 2 Clinical Trial." Arch. Neurol. **60**(12): 1685-1691.
Roberts, B. R., T. M. Ryan, A. I. Bush, et al. (2012). "The Role of Metallobiology and Amyloid-ss Peptides in Alzheimer's Disease." J. Neurochem. **120**: 149-166.
Rogaeva, E., Y. Meng, J. H. Lee, et al. (2007). "The Neuronal Sortilin-Related Receptor SORL1 Is Genetically Associated with Alzheimer Disease." Nat. Genet. **39**(2): 168-177.
Rozga, M. and W. Bal (2010). "The Cu(II)/A Beta/Human Serum Albumin Model of Control Mechanism for Copper-Related Amyloid Neurotoxicity." Chem. Res. Toxicol. **23**(2): 298-308.
Rozga, M., M. Kloniecki, M. Dadlez, et al. (2010). "A Direct Determination of the Dissociation Constant for the Cu(II) Complex of Amyloid Beta 1-40 Peptide." Chem. Res. Toxicol. **23**(2): 336-340.
Rozga, M., A. M. Protas, A. Jablonowska, et al. (2009). "The Cu(II) Complex of Abeta40 Peptide in Ammonium Acetate Solutions. Evidence for Ternary Species Formation." Chem. Commun. (Camb.)(11): 1374-1376.
Rowe, C. C., S. Ng, U. Ackermann, et al. (2007). "Imaging Beta-Amyloid Burden in Aging and Dementia." Neurology **68**(20): 1718-1725.
Roychaudhuri, R., M. Yang, M. M. Hoshi, et al. (2009). "Amyloid Beta-Protein Assembly and Alzheimer Disease." J.Biol.Chem. **284**(8): 4749-4753.
Sacco, C., R. Skowronsky, S. Gade, et al. (2012). "Calorimetric Investigation of Copper(II) Binding to Aβ Peptides: Thermodynamics of Coordination Plasticity." J. Biol. Inorg. Chem. **17**(4): 531-541.

Santner, A. and V. N. Uversky (2010). "Metalloproteomics and Metal Toxicology of Alpha-Synuclein." Metallomics **2**(6): 378-392.

Santos, R. X., S. C. Correia, X. L. Wang, et al. (2010). "Alzheimer's Disease: Diverse Aspects of Mitochondrial Malfunctioning." Int. J. Clin. Exp. Pathol. **3**(6): 570-581.

Sarell, C. J., C. D. Syme, S. E. Rigby, et al. (2009). "Copper(II) Binding to Amyloid-Beta Fibrils of Alzheimer's Disease Reveals a Picomolar Affinity: Stoichiometry and Coordination Geometry Are Independent of Abeta Oligomeric Form." Biochemistry **48**(20): 4388-4402.

Sarell, C. J., S. R. Wilkinson and J. H. Viles (2010). "Substoichiometric Levels of Cu2+ Ions Accelerate the Kinetics of Fiber Formation and Promote Cell Toxicity of Amyloid-Beta from Alzheimer Disease." J.Biol.Chem. **285**(53): 41533-41540.

Scheuner, D., C. Eckman, M. Jensen, et al. (1996). "Secreted Amyloid Beta-Protein Similar to That in the Senile Plaques of Alzheimer's Disease Is Increased i*n vivo* by the Presenilin 1 and 2 and APP Mutations Linked to Familial Alzheimer's Disease." Nat. Med. **2**(8): 864-870.

Scott, L. E. and C. Orvig (2009). "Medicinal Inorganic Chemistry Approaches to Passivation and Removal of Aberrant Metal Ions in Disease." Chem. Rev. **109**(10): 4885-4910.

Selkoe, D. J. (2001). "Alzheimer's Disease: Genes, Proteins, and Therapy." Physiol. Rev. **81**(2): 741-766.

Selkoe, D. J. (2003). "Folding Proteins in Fatal Ways." Nature **426**(6968): 900-904.

Seubert, P., C. Vigopelfrey, F. Esch, et al. (1992). "Isolation and Quantification of Soluble Alzheimers Beta-Peptide from Biological-Fluids." Nature **359**(6393): 325-327.

Shankar, G. M., S. Li, T. H. Mehta, et al. (2008). "Amyloid-Beta Protein Dimers Isolated Directly from Alzheimer's Brains Impair Synaptic Plasticity and Memory." Nat. Med. **14**(8): 837-842.

Shin, B. K. and S. Saxena (2008). "Direct Evidence That All Three Histidine Residues Coordinate to Cu(II) in Amyloid-Beta1-16." Biochemistry **47**(35): 9117-9123.

Shoji, M., T. E. Golde, J. Ghiso, et al. (1992). "Production of the Alzheimer Amyloid-Beta Protein by Normal Proteolytic Processing." Science **258**(5079): 126-129.

Siegel, S. J., J. Bieschke, E. T. Powers, et al. (2007). "The Oxidative Stress Metabolite 4-Hydroxynonenal Promotes Alzheimer Protofibril Formation." Biochemistry **46**(6): 1503-1510.

Sjobeck, M., M. Haglund and E. Englund (2005). "Decreasing Myelin Density Reflected Increasing White Matter Pathology in Alzheimer's Disease - a Neuropathological Study." Int. J. Geriatr. Psych. **20**(10): 919-926.

Sjogren, M., H. Vanderstichele, H. Agren, et al. (2001). "Tau and Abeta42 in Cerebrospinal Fluid from Healthy Adults 21-93 Years of Age: Establishment of Reference Values." Clin. Chem. **47**(10): 1776-1781.

Smith, A. D. (2002). "Imaging the Progression of Alzheimer Pathology through the Brain." Proc. Natl. Acad. Sci. USA **99**(7): 4135-4137.

Smith, D. G., R. Cappai and K. J. Barnham (2007). "The Redox Chemistry of the Alzheimer's Disease Amyloid Beta Peptide." Biochim. Biophys. Acta **1768**(8): 1976-1990.

Sokolowska, M. and W. Bal (2005). "Cu(II) Complexation By "Non-Coordinating" N-2-Hydroxyethylpiperazine-N'-2-Ethanesulfonic Acid (Hepes Buffer)." J. Inorg. Biochem. **99**(8): 1653-1660.

Sparks, D. L. and B. G. Schreurs (2003). "Trace Amounts of Copper in Water Induce Beta-Amyloid Plaques and Learning Deficits in a Rabbit Model of Alzheimer's Disease." Proc. Natl. Acad. Sci. USA **100**(19): 11065-11069.

Stine, W. B., Jr., K. N. Dahlgren, G. A. Krafft, et al. (2003). "*In vitro* Characterization of Conditions for Amyloid-Beta Peptide Oligomerization and Fibrillogenesis." J.Biol.Chem. **278**(13): 11612-11622.

Suzuki, N., T. T. Cheung, X. D. Cai, et al. (1994). "An Increased Percentage of Long Amyloid Beta Protein Secreted by Familial Amyloid Beta Protein Precursor (Beta APP717) Mutants." Science **264**(5163): 1336-1340.

Syme, C. D., R. C. Nadal, S. E. Rigby, et al. (2004). "Copper Binding to the Amyloid-Beta (Abeta) Peptide Associated with Alzheimer's Disease: Folding, Coordination Geometry, pH Dependence, Stoichiometry, and Affinity of Abeta-(1-28): Insights from a Range of Complementary Spectroscopic Techniques." J.Biol.Chem. **279**(18): 18169-18177.

Syme, C. D. and J. H. Viles (2006). "Solution (1)H NMR Investigation of Zn(2+) and Cd(2+) Binding to Amyloid-Beta Peptide (Abeta) of Alzheimer's Disease." Biochim. Biophys. Acta **1764**(2): 246-256.

Zatta, P. (2006). "Aluminum and Alzheimer's Disease: A *Vexata Questio* between Uncertain Data and a Lot of Imagination." J. Alzheimers Dis. **10**(1): 33-37.

Zawisza, I., M. Rózga and W. Bal (2012). "Affinity of Copper and Zinc Ions to Proteins and Peptides Related to Neurodegenerative Conditions (Aβ, APP, A-Synuclein, PrP)." Coordin. Chem. Rev.(in press).

Zirah, S., S. A. Kozin, A. K. Mazur, et al. (2006). "Structural Changes of Region 1-16 of the Alzheimer Disease Amyloid Beta-Peptide Upon Zinc Binding and *in vitro* Aging." J.Biol.Chem. **281**(4): 2151-2161.

Zou, K., J. S. Gong, K. Yanagisawa, et al. (2002). "A Novel Function of Monomeric Amyloid Beta-Protein Serving as an Antioxidant Molecule against Metal-Induced Oxidative Damage." J. Neurosci. **22**(12): 4833-4841.

Talmard, C., A. Bouzan and P. Faller (2007). "Zinc Binding to Amyloid-Beta: Isothermal Titration Calorimetry and Zn Competition Experiments with Zn Sensors." Biochemistry **46**(47): 13658-13666.

Tamano, H. and A. Takeda (2011). "Dynamic Action of Neurometals at the Synapse." Metallomics **3**(7): 656-661.

Terry, R. D., E. Masliah, D. P. Salmon, et al. (1991). "Physical Basis of Cognitive Alterations in Alzheimers-Disease - Synapse Loss Is the Major Correlate of Cognitive Impairment." Ann. Neurol. **30**(4): 572-580.

Thomas, P. J., B.-H. Qu and P. L. Pedersen (1995). "Defective Protein Folding as a Basis of Human Disease." Trends Biochem. Sci. **20**(11): 456-459.

Tomaselli, S., V. Esposito, P. Vangone, et al. (2006). "The Alpha-to-Beta Conformational Transition of Alzheimer's Abeta-(1-42) Peptide in Aqueous Media Is Reversible: A Step by Step Conformational Analysis Suggests the Location of Beta Conformation Seeding." Chembiochem **7**(2): 257-267.

Torok, M., S. Milton, R. Kayed, et al. (2002). "Structural and Dynamic Features of Alzheimer's Abeta Peptide in Amyloid Fibrils Studied by Site-Directed Spin Labeling." J.Biol.Chem. **277**(43): 40810-40815.

Tsvetkov, P. O., A. A. Kulikova, A. V. Golovin, et al. (2010). "Minimal Zn(2+) Binding Site of Amyloid-Beta." Biophys. J. **99**(10): L84-86.

Tycko, R. (2004). "Progress Towards a Molecular-Level Structural Understanding of Amyloid Fibrils." Curr. Opin. Struc. Biol. **14**(1): 96-103.

Wahlstrom, A., L. Hugonin, A. Peralvarez-Marin, et al. (2008). "Secondary Structure Conversions of Alzheimer's Abeta(1-40) Peptide Induced by Membrane-Mimicking Detergents." FEBS J. **275**(20): 5117-5128.

Walsh, D. M., I. Klyubin, J. V. Fadeeva, et al. (2002). "Naturally Secreted Oligomers of Amyloid Beta Protein Potently Inhibit Hippocampal Long-Term Potentiation *in vivo*." Nature **416**(6880): 535-539.

Walsh, D. M. and D. J. Selkoe (2007). "A Beta Oligomers - a Decade of Discovery." J. Neurochem. **101**(5): 1172-1184.

Vasto, S., G. Candore, F. Listi, et al. (2008). "Inflammation, Genes and Zinc in Alzheimer's Disease." Brain Res. Rev. **58**(1): 96-105.

Welander, H., J. Franberg, C. Graff, et al. (2009). "A Beta 43 Is More Frequent Than A Beta 40 in Amyloid Plaque Cores from Alzheimer Disease Brains." J. Neurochem. **110**(2): 697-706.

White, A. R., T. Du, K. M. Laughton, et al. (2006). "Degradation of the Alzheimer Disease Amyloid Beta-Peptide by Metal-Dependent up-Regulation of Metalloprotease Activity." J.Biol.Chem. **281**(26): 17670-17680.

Vigopelfrey, C., D. Lee, P. Keim, et al. (1993). "Characterization of Beta-Amyloid Peptide from Human Cerebrospinal-Fluid." J. Neurochem. **61**(5): 1965-1968.

Wisniewski, T., J. Ghiso and B. Frangione (1991). "Peptides Homologous to the Amyloid Protein of Alzheimers-Disease Containing a Glutamine for Glutamic-Acid Substitution Have Accelerated Amyloid Fibril Formation." Biochem. Bioph. Res. Co. **179**(3): 1247-1254.

Xiao, Z. and A. G. Wedd (2010). "The Challenges of Determining Metal-Protein Affinities." Nat. Prod. Rep. **27**(5): 768-789.

Yu, W. H., W. J. Lukiw, C. Bergeron, et al. (2001). "Metallothionein III Is Reduced in Alzheimer's Disease." Brain Res. **894**(1): 37-45.

ACKNOWLEDGEMENT

This study was carried out at the Department of Gene Technology, Tallinn University of Technology (TUT), Estonia, during 2006-2012.

I would like to express my sincere gratitude to all the people who helped and encouraged me in various ways during all the years in the university and while preparing this thesis. There are some people I would like to mention in particular.

It is difficult to overstate my gratitude to my supervisor Vello Tõugu for his encouragement and advice throughout all the years in the Proteomics lab. I can truthfully say that he has been the best supervisor that one can have.

I owe my thanks to my supervisor Professor Peep Palumaa for giving me the opportunity to work in the Proteomics laboratory, for his help, detailed and constructive comments.

I share the credit of my work with all the coauthors from the Proteomics laboratory at TUT and from the NeuroRepair Group at the University of Tasmania.

I must also acknowledge Valdek Mikli and Kairit Zovo for all their help with the transmission electron microscopy experiments.

I am thankful to all the people who have been a part of our laboratory group through the years.

I thank Professor Nigulas Samel for reviewing the thesis.

I would like to thank The World Federation of Scientists for financial support. I am also grateful to TTÜ Arengufond and Tiina Mõis for awarding me with the Tiina Mõis scholarship. I am indebted to the Archimedes Foundation and the DoRa program for enabling me to gain knowledge at different conferences.

And last but not least I would like to express my sincerest gratitude to my family, for their understanding and support. Without your help it would have been impossible to finish this work, so thank you for taking Tom on long walks and tractor rides, and for reading the thesis. My loving thanks go to Margo for everything and more.

SUMMARY

Alzheimer's disease (AD) is a progressive brain disorder that is the most prevalent cause of dementia in the elderly population and the third leading cause of death in developed countries. The molecular events that trigger neurodegeneration in AD, the likelihood of which rises fast with aging, is not completely understood. This makes it more difficult to find a cure for the disease. There is increasing evidence showing that the triggers of this cascade of events are the amyloid- β (Aβ) peptides that make up the amyloid deposits characteristic to the disease. In addition to the fibrillar forms of the peptides these deposits contain in high levels biometals copper, zinc, and iron. It has been established out of these three at least Zn(II) and Cu(II) interact with the Aβ peptides with considerable affinity and affect their fibrillization and toxicity on neurons.

The complex formation of full-length $A\beta_{40}$ peptide with Cu(II) and Zn(II) ions was studied. It was found that Cu(II) forms a stable, reversible complex with Aβ and for the first time, the buffer independent dissociation constant value for this interaction was determined. The K_D^{app} value equal to 35 nM at pH 7.4 suggest that this interaction occur at physiologically relevant Cu(II) concentrations in the brain. The interaction of Aβ with Zn(II) is more complex. $A\beta_{40}$ monomers and Zn(II) are forming an initial complex with the K_D^{app} value of 63 μM that transforms into a tighter complex with affinity close to 2μM within 30 minutes. The reasons for a huge variation of the affinity constants of these complexes in literature are discussed.

A new approach for Aβ aggregation monitoring was established and used for the studies of the effects of Zn(II) and Cu(II) on the Aβ aggregation. This approach was also used to validate a high-throughput screening assay for the search of inhibitors of Aβ aggregation based on MALDI MS. It was shown that the effects of metal ions on Aβ aggregation depend on the aggregation conditions. In conditions where the aggregation is fast metal ions inhibit fibrillization in a concentration dependent manner by lowering the concentration of free peptide. However, under the conditions where aggregation is slow, metal ions enhance fibrillization by causing the formation of metal-induced aggregates which trasnform into amyloid fibrils. These results suggest that the metal induced aggregates may fom in the synaptic cleft which in turn migth spontaneously be transformed into amyloid fibrils.

To sum up it can be concluded that the interactions of the Aβ peptide with Zn(II) and Cu(II) ions was extensively studied and the results indicate that these metal ions may play an important role in the pathophysiology of AD.

KOKKUVÕTE

Alzheimeri tõbi (AD) on aeglaselt süvenev neurodegeneratiivne haigus, mis on peamine nõdrameelsuse põhjus eakate hulgas ja sageduselt kolmas surma põhjus arenenud maades. Molekulaarsel tasemel toimuvad sündmused, mis AD korral vallandavad neurodegeneratsiooni, ei ole veel lõplikult selged, kuid nende toimumise tõenäosus suureneb kiiresti inimese vanuse kasvades. Teadmatus haigust otseselt käivitavate tegurite osas raskendab oluliselt AD ravimite väljatöötamist. Viimastel aastakümnetel tehtud uurimused näitavad valdavalt, et neuronite suremiseni viiva kaskaadi esmaseks vallandajaks on amüloid-β (Aβ) peptiidid, mis moodustavad ajus haigusele iseloomulikke amüloidi deposiite. Lisaks fibrillaarses vormis peptiidile sisaldavad nood moodustised kõrgenenud kontsentratsioonides kõige levinumaid biometalle – vaske, tsinki ja rauda. On kindaks tehtud, et nendest metallioonidest vähemalt Zn(II) ja Cu(II) interakteeruvad Aβ peptiididega arvestatava afiinsusega ja mõjutavad nende fibrillisatsiooni ning toksilisust närvirakkudele.

Käesolevas töös näidati, et Cu(II) moodustab stabiilse, pöörduva kompleksi Aβ-ga, mida iseloomustab puhvrist sõltumatu dissotsiatsioonikonstant väärtusega 35 nM pH 7,4 juures. Aβ vastasmõjud Zn(II)-ga on keerulisemad. Nimelt moodustavad Aβ40 monomeerid Zn(II)-ga algse kompleksi K_D^{app} väärtusega 60 µM, mis muundub tugevamaks kompleksiks, mille afiinsus on ligikaudu 2 µM. Saadud tulemused lubavad analüüsida kirjanduses toodud afiinsuskonstantide väärtuste ülisuure varieeruvuse põhjuseid.

Aβ agregatsiooni jälgimiseks töötati välja uus lähenemine ja seda kasutati Zn(II) ja Cu(II) mõju uurimiseks Aβ agregatsioonile. Seda lähenemist kasutati ka suure läbilaskevõimega MALDI MS-l baseeruva Aβ agregatsiooni inhibiitorite sõeluuringu metoodika valideerimiseks. Näidati, et metallioonide mõju Aβ agregatsioonile sõltub agregatsiooni kulgemise kiirusest. Kiire agregatsiooni toimumise korral metallioonid inhibeerivad fibrillisatsiooni kontsentratsioonist sõltuvalt, vähendades vaba peptiidi kontsentratsiooni. Samal ajal on metallioonid võimelised indutseerima mittefibrillaarsete Aβ agregaatide teket, mis omakorda aja jooksul omandavad fibrillaarse struktuuri. Tingimustes kus amüloidi moodustumine on aeglane võib see viimase teket oluliselt kiirendada. Need tulemused viitavad, et metallioonide poolt indutseeritud agregaatide võimalik moodustumine sünaptilises pilus, kus Zn(II) ja Cu(II) esinevad kõrgendatud kontsentratsioonis, võib olla isegi amüloidsete naastude moodustumise käivitajaks.

Kokkuvõtvalt saab öelda, et käesolevas töös uuriti põhjalikult Aβ peptiidide interaktsioone Zn(II)- ja Cu(II)-ioonidega ja saadud tulemused viitavad, et need metallioonide olulisele rollile AD patogeneesis.

PUBLICATION I

Tõugu, V., **A. Karafin** and P. Palumaa (2008)
"Binding of Zinc(II) and Copper(II) to the Full-Length Alzheimer's Amyloid-Beta Peptide."
J. Neurochem. **104**(5): 1249-1259

JOURNAL OF NEUROCHEMISTRY | 2008 | 104 | 1249–1259 doi: 10.1111/j.1471-4159.2007.05061.x

Binding of zinc(II) and copper(II) to the full-length Alzheimer's amyloid-β peptide

Vello Tõugu, Ann Karafin and Peep Palumaa

Department of Gene Technology, Tallinn University of Technology, Akadeemia tee, Tallinn, Estonia

Abstract

There is evidence that binding of metal ions like Zn^{2+} and Cu^{2+} to amyloid beta-peptides (Aβ) may contribute to the pathogenesis of Alzheimer's disease. Cu^{2+} and Zn^{2+} form complexes with Aβ peptides *in vitro*; however, the published metal-binding affinities of Aβ vary in an enormously large range. We studied the interactions of Cu^{2+} and Zn^{2+} with monomeric $A\beta_{40}$ under different conditions using intrinsic Aβ fluorescence and metal-selective fluorescent dyes. We showed that Cu^{2+} forms a stable and soluble 1 : 1 complex with $A\beta_{40}$, however, buffer compounds act as competitive copper-binding ligands and affect the apparent K_D. Buffer-independent conditional K_D for Cu(II)-$A\beta_{40}$ complex at pH 7.4 is equal to 0.035 μmol/L. Interaction of $A\beta_{40}$ with Zn^{2+} is more complicated as partial aggregation of the peptide occurs during zinc titration experiment and in the same time period (within 30 min) the initial Zn-$A\beta_{40}$ complex (K_D = 60 μmol/L) undergoes a transition to a more tight complex with $K_D \sim 2$ μmol/L Competition of $A\beta_{40}$ with ion-selective fluorescent dyes Phen Green and Zincon showed that the K_D values determined from intrinsic fluorescence of Aβ correspond to the binding of the first Cu^{2+} and Zn^{2+} ions to the peptide with the highest affinity. Interaction of both Zn^{2+} and Cu^{2+} ions with Aβ peptides may occur in brain areas affected by Alzheimer's disease and Zn^{2+}-induced transition in the peptide structure might contribute to amyloid plaque formation.

Keywords: Alzheimer's disease, amyloid-β peptide, binding constants, copper, zinc.

J. Neurochem. (2008) **104**, 1249–1259.

Alzheimer's disease (AD) is a neurodegenerative disease characterized by deposits of extracellular amyloid plaques and intracellular neurofibrillary tangles in the brain. The principal components of the plaques are fibrils formed of 40–42 residues long amyloid β-peptides (Aβ) derived from cleavage of amyloid precursor protein (APP) by β- and γ-secretases (Tanzi and Bertram 2005; Blennow *et al.* 2006; Haass and Selkoe 2007).

Aβ aggregation is an established pathogenic mechanism of AD and therefore factors influencing the Aβ aggregation are of high interest. Aggregation of Aβ peptides is primarily affected by a variety of genetic and dietary factors leading to increased concentrations of Aβ peptides or to the excessive formation of Aβ peptides with increased tendency for aggregation in the brain (Tanzi and Bertram 2005; Blennow *et al.* 2006; Haass and Selkoe 2007). Moreover, it has been demonstrated that the interaction of Aβ peptides with zinc (Mantyh *et al.* 1993; Bush *et al.* 1994b; Esler *et al.* 1996; Brown *et al.* 1997; Bush 2003; Cuajungco and Faget 2003) and copper (Atwood *et al.* 1998; Bush *et al.* 2003; Adlard and Bush 2006; Gaggelli *et al.* 2006) ions may induce the aggregation of Aβ peptides and these ligands may act as seeding factors in the formation of amyloid plaques. Indeed, the levels of Zn^{2+} and Cu^{2+} are elevated in the amyloid deposits (Lovell *et al.* 1998; Miller *et al.* 2006) and the homeostasis of these metals is mis-regulated in the AD brain (Adlard and Bush 2006).

The availability of zinc and copper in the brain varies in a large range. In the majority of brain regions extracellular concentrations of Cu^{2+} and Zn^{2+} are very low (Masuoka and Saltman 1994; Frederickson *et al.* 2006). However, certain brain regions like the hippocampus, the amygdala, and the cortex are rich in specific zinc-enriched synapses, where Zn^{2+} ions are concentrated into synaptic vesicles by a specific zinc transporter Zn-T3 (Frederickson and Bush

Received June 29, 2007; revised manuscript received October 2, 2007; accepted October 4, 2007.

Address correspondence and reprint requests to Dr Vello Tõugu, Department of Gene Technology, Tallinn University of Technology, Akadeemia tee 15, 19086 Tallinn, Estonia. E-mail: vello.tougu@ttu.ee

Abbreviations used: AD, Alzheimer's disease; Aβ, amyloid-β; APP, amyloid precursor protein; BCS, bathocuprinedisulfonic acid; HFIP, 1,1,1,3,3,3-hexafluoro-2-propanol; NP, Newport Green; PG, Phen Green; ThT, thioflavin T; TSPP, tetrakis-(4-sulfophenyl)porphine.

© 2007 The Authors
Journal Compilation © 2007 International Society for Neurochemistry,

2001). The role of synaptic zinc is largely unknown, yet, the estimate of its maximal local concentration in the synaptic cleft upon activation is as high as 300 μmol/L (Assaf and Chung 1984; Howell *et al.* 1984). As zinc-enriched synapses are present mainly in the brain regions most affected in AD, many authors have suggested the causative role of synaptic zinc in AD (Deibel *et al.* 1996; Adlard and Bush 2006; Konoha *et al.* 2006). In animal experiments lowering the concentration of synaptic zinc by the knock-out of Zn-transporter Zn-T3 leads to a reduced plaque formation in AD model mice suggesting that synaptic zinc might contribute to plaque formation also in the case of AD (Lee *et al.* 2002).

There is evidence suggesting that similarly to zinc, copper ions are also released from vesicles of neurons during synaptic transmission (Hartter and Barnea 1988; Kardos *et al.* 1989; Schlief *et al.* 2005). Recently, it was demonstrated that activation of NMDA-type of glutamate receptors of hippocampal neurons leads to the release of copper ions from post-synaptic neurites, however, the molecular and cellular basis for functioning of copper ions within the nervous system is not well understood (Schlief *et al.* 2005).

The primary interaction of Aβ peptides with metal ions, the reversible formation of metal-Aβ complexes, is extensively studied; however, the estimates for the affinity of Aβ towards both Zn^{2+} and Cu^{2+} ions vary in an enormously large range. Dissociation constant (K_D), values for Zn(II)-$A\beta_{40}$ complexes lie between 100 nmol/L (Bush *et al.* 1994a) and 300 μmol/L (Garzon-Rodriguez *et al.* 1999), and those for Cu(II)-$A\beta_{40}$ complexes between 0.1 nmol/L (Atwood *et al.* 2000) and 10 μmol/L (Karr *et al.* 2005). Similar variability in the estimates of K_D values (0.1–47 μmol/L) is observable also in the case of shorter $A\beta_{28}$ and $A\beta_{16}$ peptides (Karr *et al.* 2005; Guilloreau *et al.* 2006; Ma *et al.* 2006). Stoichiometry of the interactions of Aβ with metal ions is also elusive: the presence of up to four binding sites for metal ions in the peptide molecule is proposed. Recent NMR studies demonstrate that $A\beta_{28}$ forms a 1 : 1 complex with Cu(II) ions via histidine residues, (Karr *et al.* 2005; Syme and Viles 2006). Formation of 1 : 1 Cu(II)-$A\beta_{42}$ complexes was confirmed also by ESI-FTICR-MS (Jiang *et al.* 2007). However, at high copper concentrations binding of the second Cu^{2+} to the Aβ molecule has also been detected (Ali *et al.* 2006; Guilloreau *et al.* 2006; Ma *et al.* 2006). For Zn(II)-Aβ complexes stoichiometry from 1 : 1 (Clements *et al.* 1996) to 3 : 1 (Atwood *et al.* 2000) have been reported. The formation of different oligomeric Zn(II)-Aβ complexes with the involvement of metal and His residues from two different Aβ molecules have also been suggested (Miura *et al.* 2000; Curtain *et al.* 2001; Syme and Viles 2006).

Inconsistency between published metal-binding parameters for Aβ may arise from many reasons including different composition of peptide samples used in the experiments (presence of oligomers in the sample of monomeric Aβ), different reaction conditions (nature and concentration of buffer, which acts as competitive metal-binding agent, pH, incubation time) as well as from differences in methodology used for determination of binding constants etc.

In the present study, we paid special attention to the generation of monomeric and relatively stabile $A\beta_{40}$ and $A\beta_{42}$ samples and to the determination of the reliable thermodynamic parameters for reversible 1 : 1 complex formation of Aβ with Zn^{2+} and Cu^{2+} ions. These parameters are necessary for understanding the biological role of metal ions in the aggregation of Aβ peptides and in the formation of amyloid plaques characteristic for AD. We demonstrated that the type of buffer and its concentration have a substantial influence on the apparent affinity of Aβ towards Cu^{2+} ions and derived the value for the conditional (buffer independent) dissociation constant for Cu(II)-Aβ complex. In the case of zinc we showed that some peptide aggregation occurs during metal-binding experiment and the initial and weak Zn(II)-Aβ complex transforms relatively fast to a complex with an affinity in the micromolar range.

Experimental procedures

Materials

Lyophilized $A\beta_{40}$ and $A\beta_{42}$ peptides, NaOH salts (ultra pure, recombinant) were purchased from rPeptide (Bogart, GA, USA). Fluorogenic metal chelators Newport Green (NG) and Phen Green (PG) were from Invitrogen Molecular Probes (Eugene, OR, USA). Tris and HEPES, both Ultrapure, MB Grade were from USB Corporation (Cleveland, OH, USA), 1,1,1,3,3,3-hexafluoro-2-propanol (HFIP), Zincon, Thioflavin T (ThT), α-cyano-4-hydroxycinnamic acid, trifluoroacetic acid, $CuCl_2 \times 2H_2O$ and histidine hydrochloride were from Sigma–Aldrich (St. Louis, MO, USA); bathocuprinedisulfonic acid disodium salt (BCS) was from Fluka Biochemika (Milwaukee, WI, USA), $ZnCl_2$ and NaCl were extra pure from Scharlau (City, Spain). All solutions were prepared in fresh MilliQ water.

Sample preparation

Stock solution of Aβ peptides was prepared as follows: 50–80 μg of the peptide was dissolved in HFIP at a concentration 500 μmol/L to disassemble preformed aggregates (Stine *et al.* 2003). HFIP was evaporated in vacuum and the dissolving/evaporation procedure was repeated also for a second time. The obtained Aβ HFIP film was dissolved in water containing 0.02% NH_3 at a concentration of 50–100 μmol/L. After 30 min the Aβ solution was sonicated for 30 s. The $A\beta_{40}$ stock solution was kept in a refrigerator and used for experiments during the same day. The experiments with $A\beta_{42}$ were carried out immediately after solubilization because of concerns about the stability of the stock solution.

The fluorescent dyes were dissolved and their concentrations measured as described in the catalogue from Molecular Probes.

Fluorescence spectroscopy

Fluorescence spectra were collected on a Perkin–Elmer LS-45 fluorescence spectrophotometer equipped with a magnetic stirrer

© 2007 The Authors
Journal Compilation © 2007 International Society for Neurochemistry,

(Perkin Elmer, Waltham, MA, USA). For the detection of intrinsic tyrosine fluorescence of Aβ peptides, excitation at 270 nm was used and the emission spectra were recorded in the range of 290–360 nm. The excitation wavelengths for fluorescent dyes Newport Green and Phen Green were 506 and 492 nm and the fluorescence intensities were determined at 535 and 517 nm, respectively. ThT fluorescence at 490 nm was measured with 3.3 μmol/L ThT solution in 50 mmol/L glycine buffer pH 9.0 using excitation at 445 nm.

The titration of Aβ and fluorescence ligands with copper and zinc ions was carried out in a 0.5 cm path length quartz cell with a magnetic stirrer by adding of 1–2 μL aliquots of stock solutions of the respective metal salt to the 400 μL of the peptide solution. After each metal addition the solution was stirred until the stabilization of the fluorescence (1–2 min) and the average fluorescence intensity was measured over a 30 s period. In the control experiments the intrinsic fluorescence of the peptide was constant for at least 30 min. Thus, the peptide solution is stabile and the changes in the fluorescence upon addition of metal salts are caused by the binding of metal ions to Aβ. At the end of the metal titration experiments the reversibility of the fluorescence changes was checked by adding 50 μmol/L histidine as a metal complexing agent to the reaction mixture. To check the presence of aggregates at the end of metal-titration experiments the solution was centrifuged at 10 000 *g* for 15 min, 50 μmol/L histidine was added to the supernatant and Aβ fluorescence was measured and compared to that of the initial sample.

MALDI mass spectroscopy

An $A\beta_{40}$ peptide sample was checked by MALDI-MS before and after experiments with Cu^{2+} ions on a Voyager STR instrument (Applied Biosystems, Foster City, CA, USA) using 10 mg/mL α-cyano-4-hydroxycinnamic acid matrix in 50% acetonitrile/water containing 0.1% trifluoroacetic acid.

UV–VIS spectroscopy

Colorimetric determination of metal ions was performed on a Shimadzu UV-2401PC spectrophotometer (Shimadzu Corp., Kyoto, Japan). Concentration of free Zn^{2+} ions was determined by using a colorimetric zinc-specific dye Zincon. Zincon forms a 1 : 1 complex with Zn^{2+}, which absorbs at 620 nm (ε = 23 500 cm/mol/L at pH 7.4) and has a K_D = 12.7 μmol/L (Shaw *et al.* 1990). Aliquots of Zincon solution were subsequently added to the 10 μmol/L solution of Zn^{2+} in 50 mmol/L HEPES/100 mmol/L NaCl in the absence and presence of 12 μmol/L of Aβ and the OD values at 620 nm were recorded. Cu^{+} ions were determined by using a specific high-affinity dye BCS forming a complex with Cu^{+} absorbing at 483 nm (ε = 13 300/cm/mol/L) (Xiao *et al.* 2004).

Calculation of dissociation constants

The dissociation constants and stoichiometry of the Cu(II)-Aβ complexes were calculated by fitting the titration data to the following equation:

$$I = I_0 + \frac{0.5 \times (I_0 - I_\infty)}{[A]} \times \left([A] + \left[Cu^{2+}\right] + K_D - \sqrt{\left([A] + \left[Cu^{2+}\right] + K_D\right)^2 - 4 \times [A] \times \left[Cu^{2+}\right]}\right) \quad (1)$$

where [A] and $[Cu^{2+}]$ are the total concentrations of the peptide and Cu^{2+} ions, K_D is the dissociation constant of Cu(II)-Aβ complex and I_0, I and I_∞ are the fluorescence intensities of the peptide sample in the absence, the presence, and the saturation of Cu^{2+} ions.

Dissociation constants for the complexes of fluorogenic ion-specific ligands with metal ions were calculated according to a similar equation:

$$I = I_0 + \frac{0.5 \times (I_0 - I_\infty)}{[L]} \times \left([L] + \left[Me^{2+}\right] + K_D - \sqrt{\left([L] + \left[Me^{2+}\right] + K_D\right)^2 - 4 \times [L] \times \left[Me^{2+}\right]}\right) \quad (2)$$

where [L] and $[Me^{2+}]$ are the concentrations of the ligand and metal ion respectively, I, I_0 and I_∞ correspond to the fluorescence intensities of the sample, free dye, and metal-complexed dye, respectively.

The dissociation constants for the Aβ complexes with Zn^{2+} and those for binding of Cu^{2+} at higher Tris buffer concentrations were calculated by fitting the fluorescence titration data to the hyperbolic binding isotherm since in these experiments the concentration of the Aβ peptide as a ligand was lower than K_D:

$$I = I_0 + \frac{\left[Me^{2+}\right] \times (I_\infty - I_0)}{\left[Me^{2+}\right] + K_D} \quad (3)$$

Non-linear least-square fitting and statistical analysis of data was performed by using KyPlot 2.0 program (Koichi Yoshiaka, Japan).

Results

Determination of the conditional dissociation constant of Cu(II)-Aβ(1–40) complex by intrinsic fluorescence titration

Addition of $CuCl_2$ leads to the decrease in the intrinsic fluorescence of the single tyrosine residue in Aβ molecule (Fig. 1). Fitting the data to Eqn. (1) resulted in K_D^{app} = 0.57 μmol/L and binding stoichiometry close to 1 : 1 in 20 mmol/L HEPES, pH 7.4 considered as the standard conditions. The binding of Cu^{2+} to Aβ was completely reversible, since the fluorescence intensity returned to its starting value after addition of 50 μmol/L of histidine. Centrifugation of the sample after the titration with subsequent addition of 50 μmol/L histidine to the supernatant exposed more than 80% of initial Aβ fluorescence confirming that most of the peptide was in a non-precipitated form after the copper titration experiments. Similar results (K_D^{app} = 0.62 μmol/L) were observed when $A\beta_{40}$ was solubilized in 0.02% NH_3 without HFIP pre-treatment. However, the stability of the peptide stock solution without HFIP pre-treatment was poor: its fluorescence decreased significantly within 1 h incubation, whereas fluorescence of HFIP treated sample was stable. Considering this, we used the HFIP pre-treated peptide solutions throughout the study. We found that the K_D^{app} values observed vary in a large range when different buffers are used. For instance, the affinity of Aβ towards Cu^{2+} in 100 mmol/L Tris buffer at pH

© 2007 The Authors

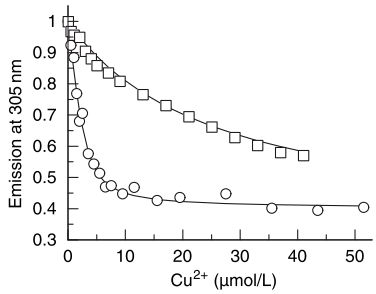

Fig. 1 Intensity of the intrinsic fluorescence of $A\beta_{40}$ as a function of added Cu^{2+}. Reaction conditions: pH 7.4 in 20 mmol/L HEPES (○) and in 100 mmol/L Tris (□) containing 100 mmol/L NaCl; 4 μmol/L $A\beta_{40}$. Excitation at 270 nm.

7.4 was approximately 70 times lower than that in 10 mmol/L Tris at the same pH. The experimental K_D^{app} values for Cu(II)-Aβ complexes together with the data from the literature are presented in Table 1. Addition of calcium ions (3 mmol/L) in the buffer in the concentration close to that in extracellular space, did not affect the Cu^{2+} binding neither in HEPES nor in Tris buffer. The affinity of $A\beta_{42}$ towards Cu^{2+} ions in 20 mmol/L HEPES was similar to that of $A\beta_{40}$.

In order to explain the buffer-dependent variability of K_D^{app} we accounted for the concentrations and type of metal-binding compounds in the reaction mixture. It is known that Tris base forms relatively weak 1 : 1 and 2 : 1 complexes with Cu^{2+} ions, characterized by the stability constants 5.78×10^3/mol/L and 4.46×10^6/mol/L^2, respectively (Takahashi *et al.* 1981). Recently, it was demonstrated that the 'non-coordinating' HEPES buffer also associates with Cu^{2+}: the buffer anion forms a 1 : 1 complex with the stability constant equal to 1.66×10^3/mol/L (Sokolowska and Bal 2005). Since HEPES does not form ternary complexes with metal ions, it is still recommended for copper binding studies; however, its influence to the binding equilibrium should be taken into account by calculating the binding/dissociation constants at zero buffer concentration (conditional binding/dissociation constant) (Sokolowska and Bal 2005).

Conditional constants K_D in HEPES can be calculated from the apparent dissociation constants using the appropriate correction functions (Sokolowska and Bal 2005):

$$\log K_D = \log K_D^{app} + C \quad (4)$$

$$C = \log(1 + \beta_{CuL} \times \frac{c_L}{1 + 10^{-pH+pK_a}}) \quad (5)$$

where c_L is the buffer concentration, K_a is the deprotonization constant of the buffer and β_{CuL} is the dissociation constant for the Cu(II)-HEPES complex (Sokolowska and Bal 2005). We used analogous expressions for the calculation of conditional dissociation constants for Cu(II)-Aβ complex presented in Table 1. With the exception of phosphate buffer, the conditional K_D values were in good agreement suggesting that the differences in the K_D^{app} values for Cu(II)-Aβ originate mainly from the copper binding properties of the buffer species. We also found that the addition of 10–20 μmol/L Cu^{2+} to 10 mmol/L phosphate buffer leads to a sharp increase in the light scattering of the solution indicating the appearance of insoluble particles in the buffer solution

Table 1 The values for apparent (K_D^{app}) and conditional (K_D) dissociation constants of the Cu(II)-$A\beta_{40}$ complexes in various buffer solutions determined by intrinsic fluorescence measurements

K_D^{app} (μmol/L)	Conditions	C	K_D (μmol/L)	References
1.6 2.0[a]	10 mmol/L Tris 100 mmol/L NaCl, pH 7.4	1.34	0.073 0.091	(Garzon-Rodriguez *et al.* 1999)
11 28[b]	100 mmol/L Tris 150 mmol/L NaCl pH 7.5	2.94	0.012 0.032	(Karr *et al.* 2005)
8	50 mmol/L PBS, 100 mmol/L NaCl, pH 7.4	1.82	0.12	(Raman *et al.* 2005)
2.5[b]	50 mmol/L HEPES, pH 7.2 10 mmol/L HEPES, pH 7.2	0.87 1.51	0.370.077	(Danielsson *et al.* 2007)
0.01–0.1[b]	Water, pH 7.8	0	0.01–0.1	(Syme *et al.* 2004)
0.47 ± 0.23	pH 7.3, 10 mmol/L Tris, 100 mmol/L NaCl	1.10	0.037	
1.21 ± 0.41	20 mmol/L Tris, 100 mmol/L NaCl	1.53	0.035	
3.82 ± 0.89	50 mmol/L Tris, 100 mmol/L NaCl	2.20	0.024	
30.1 ± 5.7	100 mmol/L Tris, 100 mmol/L NaCl	2.74	0.054	
0.57 ± 0.23	20 mmol/L HEPES, 100 mmol/L NaCl	1.19	0.036	
0.90 ± 21	50 mmol/L HEPES, 100 mmol/L NaCl	1.57	0.024	
2.5 ± 0.6	100 mmol/L HEPES, 100 mmol/L NaCl	1.86	0.034	
0.76 ± 1.0[a]	20 mmol/L HEPES, 100 mmol/L NaCl	1.19	0.048	

[a]$A\beta_{42}$: [b]$A\beta_{28}$.

© 2007 The Authors
Journal Compilation © 2007 International Society for Neurochemistry,

and disturbing spectroscopic measurements of Cu^{2+} binding constants. Such a behavior is a result of very low solubility of copper(II)phosphate.

The K_D value for Cu(II)-Aβ_{40} equal to 0.035 ± 0.010 μmol/L was calculated from our data as an average and this value should be used for the comparison of the Cu-binding properties of Aβ with that of competing metabolites and proteins.

Determination of Aβ(1–40) affinity towards Cu^{2+} using Phen Green as a fluorescent dye

Theoretically Aβ molecule can bind multiple metal ions and it is possible that the binding of the first Cu^{2+} ion with the highest affinity does not affect fluorescence of the tyrosine residue. In order to exclude this possibility and to confirm the K_D value determined from intrinsic fluorescence, the ability of Aβ to compete for Cu^{2+} with a copper-selective fluorescence dye Phen Green was also studied. Phen Green molecule binds a single Cu^{2+} ion with submicromolar affinity and this process leads to the disappearance of its fluorescence. Addition of a competing ligand (Aβ) to the reaction mixture should shift the fluorescence decrease of Phen Green to higher Cu^{2+} concentrations while the K_D^{app} value and (or) binding stoichiometry for the competing ligand can be determined by regression analysis.

Titration of Phen Green with Cu^{2+} ions in the absence and presence of different concentrations of Aβ_{40} is shown in Fig. 2a. The K_D^{app} value for Cu(II)-PG complex determined by fitting the results to Eqn (2) is equal to 0.015 μmol/L. Presence of Aβ_{40} shifts the titration curve towards higher copper concentrations indicating the ability of the peptide to compete with the dye for metal ions. K_D^{app} value for Cu(II)-PG complex depended linearly on the concentration of Aβ (Fig. 2b), and assuming 1 : 1 stoichiometry of the Cu(II)-Aβ complex, K_D^{app} value equal to 0.5 μmol/L was estimated from this dependence. The K_D^{app} value observed is similar to the K_D^{app} = 0.9 μmol/L determined from the Cu^{2+}-induced changes of intrinsic fluorescence of Aβ_{40} under similar conditions. Formation of a small amount of Cu(II)$_2$-Aβ complex at high copper concentrations cannot be excluded. Binding of the second Cu^{2+} ion with low affinity would decrease the K_D value estimated from competition experiments and increase the value of the K_D determined from direct measurements.

Determination of the Cu(I) ions and oxidized Aβ forms

Copper ion is electrochemically active when bound to Aβ (Huang *et al.* 1999a; Lynch *et al.* 2000), which may rise concerns that Cu^{+} may accumulate and the peptide may get oxidized during copper titration experiments. In order to check the occurrence of redox processes under our experimental conditions, we have performed following tests. Figure 3a shows that when BCS was added to the solution containing Cu^{2+} and HEPES the OD_{483} increased because of

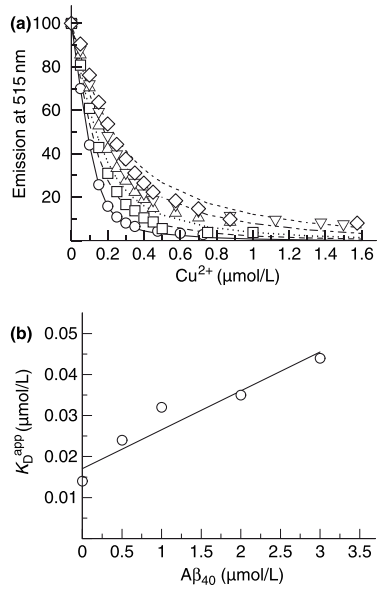

Fig. 2 Estimation of the affinity of Cu^{2+} towards Aβ_{40} by competition with the fluorescent dye Phen Green. (a) Fluorescence of Phen Green with addition of increasing amounts of copper in the absence (○) and presence of 0.5 (□); 1 (△); 2 (▽) and 3 (◇) μmol/L of Aβ in 50 mmol/L HEPES and 100 mmol/L NaCl, pH 7.4, excitation at 492 nm. Lines correspond to the simulated curves assuming K_D = 0.5 μmol/L. (b) Influence of Aβ on the apparent dissociation constant of Cu(II)-PG complex estimated by fitting of experimental data to Eqn. (2).

BCS-assisted reduction of Cu^{2+} in HEPES buffer, which was observed also earlier (Hegetschweiler and Saltman 1986). The rate of the increase in the OD_{483} corresponds to the copper reduction, since the association of Cu^{+} with the dye is almost instant and reduction of Cu^{2+} under aerobic conditions occurs only in the presence of strong Cu^{+} stabilizing agents like BCS (Hegetschweiler and Saltman 1986; Sayre 1996). When Cu^{2+} ions are pre-incubated with Aβ_{40} before addition of BCS, the OD_{483} increases with the same rate without any 'burst' phase, which is indicative for absence of Cu^{+} ions in the system. Separate MALDI MS experiment (Fig. 3b) demonstrated that after 2 h incubation of Aβ_{40} with Cu^{2+} ions there are no oxidized Aβ_{40} products formed. Obtained results together confirm that Cu^{2+} is not reduced and Aβ_{40} is not oxidized under our experimental conditions.

Determination of the dissociation constant of Zn-Aβ(1–40) complex using intrinsic fluorescence

Addition of Zn^{2+} to the solution of 2–5 μmol/L of Aβ without continuous stirring resulted in an increase in the intrinsic fluorescence of the tyrosine residue similar to that observed in the literature (Garzon-Rodriguez *et al.* 1999;

© 2007 The Authors

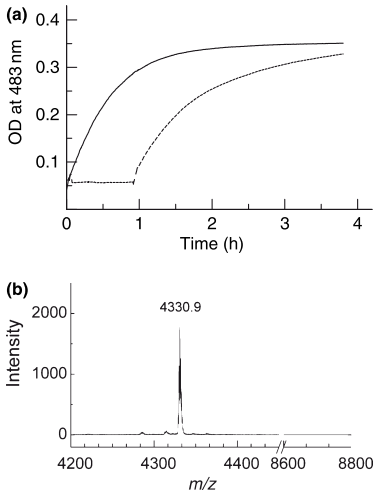

Fig. 3 Reduction of copper ions in the presence on $A\beta_{40}$ (a) Reaction of BCS with 25 μmol/L copper ions without $A\beta_{40}$ (solid line) and with 1 h pre-incubation with 4 μmol/L $A\beta_{40}$ (dotted line) in 50 mmol/L HEPES, 100 mmol/L NaCl, pH 7.3. (b) MALDI-TOF MS spectrum of the 4 μmol/L $A\beta_{40}$ peptide after the 2 h incubation with 25 μmol/L Cu^{2+} ions in 50 mmol/L HEPES, 100 mmol/L NaCl, pH 7.3.

Ricchelli *et al.* 2005). However, the reproducibility of the results was very poor. Literature data about the effect of Zn^{2+} on the intrinsic fluorescence of Aβ is also not in agreement: zinc increases the fluorescence of $A\beta_{40}$ in 10 mmol/L Tris/0.1 mol/L NaCl, pH 7.4 by a factor of 2.16 and binding was characterized by K_D^{app} = 300 μmol/L (Garzon-Rodriguez *et al.* 1999), whereas similar measurements in 100 mmol/L Tris/150 mmol/L NaCl, pH 7.4 revealed only a 1.3-fold increase in fluorescence intensity with an estimate for K_D^{app} lower than 20 μmol/L (Ricchelli *et al.* 2005). Moreover, zinc had no effect on intrinsic fluorescence of Aβ in phosphate buffer (Raman *et al.* 2005).

In search for reproducibility, we observed that stirring of the solution has a substantial influence on the fluorescence of Aβ in the presence of Zn^{2+} ions. Since mixing the samples seemed to be critical we carried out the zinc-binding experiments using continuous stirring, which also substantially improved the reproducibility of the experiments. In contrast to Cu(II)-Aβ showing stable fluorescence for at least 20 min, the fluorescence intensity of Aβ in the presence of Zn^{2+} ions showed substantially lower stability. The initial stabilization occurring within 1.5–2.5 min was followed by a slow decrease in the intensity, which formally corresponds to increased metal-binding and might be also connected to aggregation phenomena. We determined K_D^{app} values from readings taken after 3 min incubation with stirring giving stabile readings.

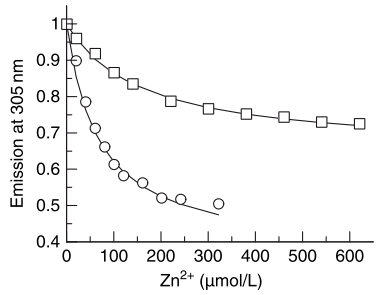

Fig. 4 Intensity of the intrinsic fluorescence of 4 μmol/L $A\beta_{40}$ as a function of added Zn^{2+}. Reaction conditions: 4 μmol/L $A\beta_{40}$ at pH 7.4 in 20 mmol/L HEPES (○) and in 100 mmol/L Tris (□) containing 100 mmol/L NaCl. Excitation at 270 nm.

Decrease in the intrinsic fluorescence of $A\beta_{40}$ at increasing concentrations of Zn^{2+} ions under the conditions of continuous stirring is shown in Fig. 4. K_D values calculated from the respective titration curves according to Eqn. (3) are listed in Table 2. Table 2 shows that K_D^{app} for Zn(II)-Aβ complex is higher at higher concentrations of Tris, but there is no difference between the K_D^{app} values in 20 mmol/L HEPES, and in 10 mmol/L Tris. The K_D^{app} value for $A\beta_{42}$ in 20 mmol/L HEPES was also similar to that of $A\beta_{40}$. The Zn(II)-Aβ complex formation was reversible since the Aβ fluorescence returned to the initial level after the adding of 50 μmol/L of histidine. However, centrifugation of the reaction mixture and separation of the supernatant before addition of histidine showed that a substantial fraction of $A\beta_{40}$ (up to 50%) was aggregated at the end of the titration, indicating that zinc in contrast to copper induces aggregation of Aβ peptides during metal-titration experiment. The absence of ThT fluorescence in the corresponding tests showed that despite the aggregation, no fibrillar $A\beta_{40}$ aggregates were formed during metal ion titration experiments.

Table 2 The values for apparent (K_D^{app}) for the Zn(II)-$A\beta_{40}$ complexes in various buffer solutions determined by intrinsic fluorescence measurements

K_D^{app}(μmol/L)	Conditions
65 ± 3	20 mmol/L HEPES, 100 mmol/L NaCl, pH 7.4
124 ± 32[a]	
91 ± 16[b]	
60 ± 14	10 mmol/L Tris, 100 mmol/L NaCl, pH 7.4
184 ± 30	100 mmol/L Tris, 100 mmol/L NaCl, pH 7.4
300[c]	10 mmol/L Tris, 100 mmol/L NaCl, pH 7.4[b]

[a]Emission was measured immediately after zinc addition; [b]$A\beta_{42}$; [c]From Garzon-Rodriguez *et al.* (1999).

© 2007 The Authors
Journal Compilation © 2007 International Society for Neurochemistry,

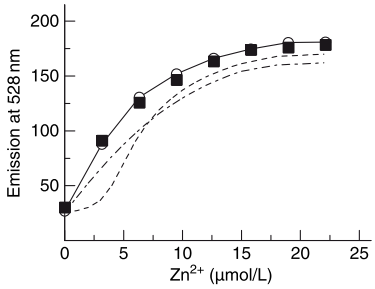

Fig. 5 Influence of Zn^{2+} on the fluorescence of Newport Green. Experimental data in the absence (○) and presence of 5 μmol/L of $A\beta_{40}$ (■). 20 mmol/L HEPES, 100 mmol/L NaCl, pH 7.4, 0.55 μmol/L NG. Simulated curves corresponding to the values of K_D = 0.107 μmol/L (–·–·–) and K_D = 3.2 μmol/L (– – –). Excitation at 506 nm.

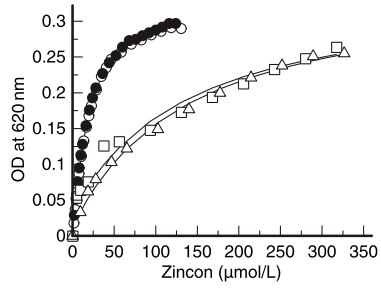

Fig. 6 Titration of 12 μmol/L Zn^{2+} in the absence (filled circles) and presence (open symbols) of 12 μmol/L $A\beta_{40}$ with Zincon. pH 7.3 in 50 mmol/L HEPES, 100 mmol/L NaCl. The peptide was pre-incubated with Zn^{2+} ions for 0 min (○); 30 min (□) and 4 h (△) before titration with Zincon.

Titration of Newport Green with Zn^{2+} in the absence and presence of Aβ(1–40)

Interaction of Aβ with Zn^{2+} ion was also studied with a zinc-specific fluorescent dye Newport Green. Upon binding Zn^{2+} ions, the fluorescence of the dye increases. K_D value for the Zn(II)-NG complex is equal to 1.0 μmol/L (Catalogue of Molecular Probes). Titration curves of the NG with Zn^{2+} in the absence and presence of 5 μmol/L of Aβ determined without pre-incubation of Aβ with Zn^{2+} ions are shown in Fig. 5. The K_D^{app} value for the Zn(II)-NG complex constant was found to be equal to 3.5 μmol/L in 20 mmol/L HEPES/100 mmol/L NaCl at pH 7.4. Fig. 5 shows that 5 μmol/L of $A\beta_{40}$ did not affect the fluorescence intensity of NG in the presence of increasing amounts of Zn^{2+}. Thus, $A\beta_{40}$ is not able to compete with NG for Zn^{2+} ions and its affinity towards zinc is substantially lower than that of NG. We simulated the effects of Aβ on zinc titration of NG by using the high-affinity binding constants and stoichiometry proposed in the literature (Bush *et al.* 1994a), and the resulting curves are also presented in Fig. 5. Disagreement between simulated and experimental data indicates that the fast binding of Zn^{2+} ions to Aβ in a micromolar range is not observed. A control experiment showed that the binding of Zn^{2+} by Tricine buffer [c = 10 μmol/L; K_D = 10 μmol/L (Paoletti *et al.* 1997)] was clearly detectable under similar experimental conditions.

The K_D^{app} value for the Zn(II)-NG complex increased to 20 μmol/L in 50 mmol/L Tris, thus, it is more influenced by buffer than the K_D^{app} value for Zn(II)-$A\beta_{40}$ complex.

Determination of the time-dependent binding of Zn^{2+} to Aβ

In the presence of Zn^{2+} ions we observed a time-dependent decrease in the intrinsic fluorescence of Aβ, which suggests that the initial fast-forming Zn(II)-Aβ complex may undergo a slow transformation and/or aggregation. In order to estimate the K_D value for the resulting complexes we carried out the titrations of Zn^{2+} containing Aβ solutions with Zincon after different incubation times. The titration curves presented in Fig. 6 show that the K_D value for the fast forming initial Zn(II)-$A\beta_{40}$ complex (incubation time 3 min) is higher than that for the complex of Zn^{2+} with Zincon (K_D = 11.5 μmol/L). However, when $A\beta_{40}$ was incubated in a solution containing 10 μmol/L Zn^{2+} for 30 min or for a longer period before titration with Zincon, the titration curve was shifted towards higher Zincon concentrations suggesting that upon incubation the initial weak Zn(II)-$A\beta_{40}$ complex was transformed into a high-affinity complex with affinity ~ 2 μmol/L. Similar curves were observed also with $A\beta_{42}$. The binding of Zn^{2+} ions to $A\beta_{40}$ is still reversible as all zinc was extracted from Zn(II)-$A\beta_{40}$ complexes at high concentrations of Zincon. A similar result was obtained also after a 4-h incubation of Zn(II)-$A\beta_{40}$ solution before titration with Zincon suggesting that the process of transformation is almost complete within 30 min.

Discussion

Our results demonstrate that despite the apparent similarity in chemical properties of Zn^{2+} and Cu^{2+} their mode of interaction with $A\beta_{40}$ is substantially different: interaction of Cu^{2+} with $A\beta_{40}$ is limited to a fast and reversible formation of a stable complex, whereas the formation of initial weak Zn(II)-$A\beta_{40}$ complex is followed by its relatively fast transition to high-affinity complexes.

Interaction of Aβ with Cu(II) ions

Although the interaction of Cu^{2+} ions with $A\beta_{40}$ is described by a simple reversible 1 : 1 complex formation, the apparent binding constant values vary in a very large range under different experimental conditions (Table 1). Making use of

© 2007 The Authors
Journal Compilation © 2007 International Society for Neurochemistry,

the appropriate correction functions that take into account the metal-binding properties of buffers, we demonstrated that, with the exception of the phosphate buffer, the values for the calculated conditional K_D in different buffers are close to 0.035 μmol/L. The very low solubility of copper(II)phosphate makes phosphate buffer unsuitable for metal-binding experiments. Thus, we concluded that the large variability in the K_D^{app} values for Cu(II)-Aβ complex determined here and reported in the literature is mainly caused by interactions of the Cu^{2+} ions with buffer components. Experiments with competing fluorescent dye Phen Green resulted in a K_D^{app} value similar to that determined from intrinsic fluorescence of $A\beta_{40}$ and showed no evidence for the ability of $A\beta_{40}$ to bind copper with extra high-affinity (K_D = 0.1 nmol/L) suggested in the literature (Atwood *et al.* 1998). It should be noted that Atwood and colleagues used prolonged (24 h) incubation of Aβ peptide with Cu^{2+} ions: it is likely that during prolonged incubation the peptide oligomerizes and aggregates in the presence of metal ions, or even undergoes oxidative modifications, which may lead to the formation high-affinity binding sites for copper ions. Latter hypothesis is supported by the observation that during prolonged incubation the initial soluble 1 : 1 Cu(II)-Aβ complex is transformed to sodium dodecyl sulfate-resistance aggregates and the peptide can undergo chemical modifications, for instance, tyrosine cross-linking after 3 days incubation at 37°C (Atwood *et al.* 2004). In our experimental conditions there was no Cu^{+} accumulation in the $A\beta_{40}$ solution and according to MALDI MS analysis the peptide was not oxidized during the *in vitro* experiments. Our data are in agreement with recent ESI-FTICR-MS results showing that $A\beta_{42}$ forms a soluble monomeric 1 : 1 complex with Cu^{2+} ions whereas the tyrosine and methionine residues are not oxidized during the experiment and the bound copper is in the Cu^{2+} oxidation state (Jiang *et al.* 2007).

There is substantial evidence in the literature that at high concentrations of Aβ and Cu^{2+} the formation of Cu(II)-Aβ complexes with 1 : 2 and 2 : 1 stoichiometry can also occur (Ali *et al.* 2006; Guilloreau *et al.* 2006; Ma *et al.* 2006). These complexes, if present, may complicate the determination of binding constants; however, because of the low concentrations of copper ions and Aβ *in vivo*, such complexes are practically absent in physiological conditions. Taken together, the fast-forming reversible 1 : 1 Cu(II)-$A\beta_{40}$ complex is characterized by buffer independent conditional K_D value equal to 0.035 μmol/L at pH 7.4. This K_D value is applicable for the comparison of copper-binding affinity of Aβ with that of other peptides, proteins and biological ligands. The affinity of $A\beta_{42}$ towards Cu^{2+} was very similar to that of $A\beta_{40}$.

Interaction of Aβ with Zn(II) ions

The hypothesis on the physiological importance of the interaction between Zn^{2+} ions and Aβ and the role of zinc in AD often rely on the assumption that $A\beta_{40}$ binds one Zn^{2+} ion with high-affinity (K_D = 100 nmol/L) and two additional Zn^{2+} ions with somewhat lower affinity (K_D = 5 μmol/L) (Bush *et al.* 1994a). These values were obtained from the binding of radioactive Zn^{2+} ions to the $A\beta_{40}$ immobilized onto polyvinylidene difluoride membranes. However, later results obtained by a similar method showed the formation of only 1 : 1 complex with K_D = 3.2 μmol/L (Clements *et al.* 1996). Micromolar affinity for the binding of Zn^{2+} to $A\beta_{40}$ was obtained also from NMR-studies and from fluorimetric experiments where Aβ bound Zn^{2+} was displaced by Cu^{2+} (Danielsson *et al.* 2007). At the same time, the K_D values for Zn-$A\beta_{40}$ determined from zinc-induced changes in the intrinsic fluorescence of Aβ are substantially higher and lie in the range from 20 μmol/L (Ricchelli *et al.* 2005) to 300 μmol/L (Garzon-Rodriguez *et al.* 1999).

By using the intrinsic fluorescence of $A\beta_{40}$ and zinc-specific dye Zincon, we demonstrated that $A\beta_{40}$ formed an initial low-affinity Zn(II)-$A\beta_{40}$ complex (K_D = 60 μmol/L), which was transformed to a high-affinity complex with $K_D \sim 2$ μmol/L in a period of 30 min. Our results demonstrate for the first time the change of zinc-binding affinity of Aβ with time occurring concomitantly with zinc-induced Aβ aggregation. It can be suggested that K_D = 60 μmol/L represents the relatively low 'true' affinity of monomeric $A\beta_{40}$-peptide towards Zn^{2+} ion, whereas micromolar Zn^{2+} binding affinity is characteristic for metal-binding sites in zinc-induced oligomers or aggregates of $A\beta_{40}$.

The fact that the interaction of Zn^{2+} with $A\beta_{40}$ depends on the incubation time (in the timescale of performing experiments) and mixing conditions should be taken into account in experimental studies of the formation of this complex. Comparing different methods used in zinc-binding studies, we noticed that radioligand binding, NMR and metal displacement experiments, where binding constants values in the micromolar range were detected (Bush *et al.* 1994a; Clements *et al.* 1996; Danielsson *et al.* 2007), are all characterized by longer incubation times of Aβ with Zn^{2+} ions as compared with measurements of intrinsic fluorescence of Aβ, from which K_D values 60 μmol/L or larger (Garzon-Rodriguez *et al.* 1999) were obtained.

The changes in the K_D^{app} value for Zn(II)-$A\beta_{40}$ complex in different buffers were not parallel to the changes in those for Zn–NG complex. Thus, in contrast to the Cu(II)-$A\beta_{40}$ complexes, the interaction of Zn^{2+} with the amyloid peptides cannot be characterized by a single conditional K_D value. This behavior might be caused by the formation of ternary Zn(II)-Aβ-buffer complexes. Moreover, considering the instability of the fluorescence intensity, partial aggregation of Aβ in zinc-containing solutions and relatively fast transformation of the initial complex to high-affinity complex, it is likely that in the case of zinc the K_D value does not belong to a single and well-defined Zn(II)-Aβ complex, but is an average value characterizing the heterogeneous mixture

© 2007 The Authors
Journal Compilation © 2007 International Society for Neurochemistry,

of monomeric Zn(II)-Aβ and various Zn(II)-Aβ oligomeric complexes and aggregates. This conclusion is in agreement with the results of NMR and CD studies of metal-Aβ complexes indicating that Zn^{2+} coordination is dominated by intermolecular coordination and formation of polymeric species (Syme and Viles 2006). Dynamic changes in the composition of such species might cause a 100-fold difference in the 'apparent' zinc-binding affinities of $A\beta_{40}$ as follows from the K_D measurements at different incubation times. Recent observation that Zn^{2+} ions can precipitate out soluble aggregates of $A\beta_{40}$, also indicate their increased affinity towards zinc ions (Garai *et al.* 2007).

Biological context

The availability of zinc ions in the brain varies in a large scale. The tonic level of free Zn^{2+} in the extracellular fluid of the rat, rabbit, and human brain is as low as 19 nmol/L (Frederickson *et al.* 2006), however, concentration of free zinc ions in the regions of zinc-enriched neurons is much higher. The theoretical upper limit of Zn^{2+} ions in the synaptic clefts of zinc-enriched neurons (Madsen and Gitlin 2007) reaches 300 μmol/L (Assaf and Chung 1984; Howell *et al.* 1984) and the experimentally determined level of Zn^{2+} during the release of pre-synaptic zinc into the extracellular space is 10–30 μmol/L [for review, see Frederickson and Bush (2001)]. Considering the values of K_D for Zn(II)-Aβ complex, it can be concluded that the probability for the Zn(II)-Aβ complex formation is high only in certain brain areas containing synapses of zincergic neurons. However, interaction of Zn^{2+} with Aβ is not limited to the fast reversible binding: initial binding of zinc to Aβ induces transformation of the peptide to an oligomeric or a polymeric complex with increased zinc-binding affinity. The latter phenomenon potentiates the effect of zinc on Aβ and might enable zinc to act as a seeding factor in the process of amyloid plaque formation. Recently, it has been demonstrated that Zn^{2+} ions precipitate out soluble oligomeric Aβ forms and lower their toxicity (Garai *et al.* 2007), which indicates that Zn^{2+} might be protective against oligomeric Aβ species, which are considered to be most toxic to neurons (Klein *et al.* 2001).

The conditional dissociation constant for the Cu(II)-$A\beta_{40}$ complex, equal to 0.035 μmol/L, is close to the affinity of copper towards amino acids and other low-affinity ligands and proteins present in extra-cellular environment (Masuoka and Saltman 1994). The extracellular copper concentration is generally low, however, there is evidence that in upon excitation of certain neurons copper ions are released into synaptic clefts in concentrations up to 15–100 μmol/L (Hartter and Barnea 1988; Kardos *et al.* 1989) and may also play a role in synaptic transmission (Madsen and Gitlin 2007). Recently the release of Cu^{2+} from synaptosomes was detected using *tetrakis*-(4-sulfophenyl)porphine (TSPP) (Hopt *et al.* 2003). Since the K_D^{app} value for Cu(II)-TSPP complex (K_D^{app} = 0.44 μmol/L) is very similar to that of Cu(II)-$A\beta_{40}$ complex, in 10 mmol/L HEPES, this observation suggests that concentration of synaptically released copper ions might be sufficient for the formation of Cu(II)-$A\beta_{40}$ complex. This complex formation may significantly affect the homeostasis and metabolism of Aβ peptides and may lead to the insertion of Cu^{2+} ions to amyloid plaques. As Aβ associated copper is electrochemically active, it might also induce the production of reactive oxygen species causing oxidative stress in AD (Huang *et al.* 1999b).

Acknowledgments

The work was supported by Grants No. 6840 and 7191 from Estonian Science Foundation and project EU 19685 from Enterprise Estonia.

References

Adlard P. A. and Bush A. I. (2006) Metals and Alzheimer's disease. *J. Alzheimers Dis.* **10**, 145–163.

Ali F. E., Separovic F., Barrow C. J., Yao S. G. and Barnham K. J. (2006) Copper and zinc mediated oligomerisation of A beta peptides. *Int. J. Pept. Res. Ther.* **12**, 153–164.

Assaf S. Y. and Chung S. H. (1984) Release of endogenous Zn^{2+} from brain tissue during activity. *Nature* **308**, 734–736.

Atwood C. S., Moir R. D., Huang X., Scarpa R. C., Bacarra N. M., Romano D. M., Hartshorn M. A., Tanzi R. E. and Bush A. I. (1998) Dramatic aggregation of Alzheimer abeta by Cu(II) is induced by conditions representing physiological acidosis. *J. Biol. Chem.* **273**, 12817–12826.

Atwood C. S., Scarpa R. C., Huang X., Moir R. D., Jones W. D., Fairlie D. P., Tanzi R. E. and Bush A. I. (2000) Characterization of copper interactions with alzheimer amyloid beta peptides: identification of an attomolar-affinity copper binding site on amyloid beta1-42. *J. Neurochem.* **75**, 1219–1233.

Atwood C. S., Perry G., Zeng H. *et al.* (2004) Copper mediates dityrosine cross-linking of Alzheimer's amyloid-beta. *Biochemistry* **43**, 560–568.

Blennow K., de Leon M. J. and Zetterberg H. (2006) Alzheimer's disease. *Lancet* **368**, 387–403.

Brown A. M., Tummolo D. M., Rhodes K. J., Hofmann J. R., Jacobsen J. S. and Sonnenberg-Reines J. (1997) Selective aggregation of endogenous beta-amyloid peptide and soluble amyloid precursor protein in cerebrospinal fluid by zinc. *J. Neurochem.* **69**, 1204–1212.

Bush A. I. (2003) The metallobiology of Alzheimer's disease. *Trends Neurosci.* **26**, 207–214.

Bush A. I., Pettingell W. H. Jr, Paradis M. D. and Tanzi R. E. (1994a) Modulation of A beta adhesiveness and secretase site cleavage by zinc. *J. Biol. Chem.* **269**, 12152–12158.

Bush A. I., Pettingell W. H., Multhaup G., d Paradis M., Vonsattel J. P., Gusella J. F., Beyreuther K., Masters C. L. and Tanzi R. E. (1994b) Rapid induction of Alzheimer A beta amyloid formation by zinc. *Science* **265**, 1464–1467.

Bush A. I., Masters C. L. and Tanzi R. E. (2003) Copper, beta-amyloid, and Alzheimer's disease: tapping a sensitive connection. *Proc. Natl Acad. Sci. U. S. A.* **100**, 11193–11194.

Clements A., Allsop D., Walsh D. M. and Williams C. H. (1996) Aggregation and metal-binding properties of mutant forms of the

© 2007 The Authors
Journal Compilation © 2007 International Society for Neurochemistry,

amyloid A beta peptide of Alzheimer's disease. *J. Neurochem.* **66**, 740–747.

Cuajungco M. P. and Faget K. Y. (2003) Zinc takes the center stage: its paradoxical role in Alzheimer's disease. *Brain Res. Brain Res. Rev.* **41**, 44–56.

Curtain C. C., Ali F., Volitakis I., Cherny R. A., Norton R. S., Beyreuther K., Barrow C. J., Masters C. L., Bush A. I. and Barnham K. J. (2001) Alzheimer's disease amyloid-beta binds copper and zinc to generate an allosterically ordered membrane-penetrating structure containing superoxide dismutase-like subunits. *J. Biol. Chem.* **276**, 20466–20473.

Danielsson J., Pierattelli R., Banci L. and Gräslund A. (2007) High-resolution NMR studies of the zinc-binding site of the Alzheimer's amyloid beta-peptide. *FEBS J.* **274**, 46–59.

Deibel M. A., Ehmann W. D. and Markesbery W. R. (1996) Copper, iron, and zinc imbalances in severely degenerated brain regions in Alzheimer's disease: possible relation to oxidative stress. *J. Neurol. Sci.* **143**, 137–142.

Esler W. P., Stimson E. R., Jennings J. M., Ghilardi J. R., Mantyh P. W. and Maggio J. E. (1996) Zinc-induced aggregation of human and rat beta-amyloid peptides in vitro. *J. Neurochem.* **66**, 723–732.

Frederickson C. J. and Bush A. I. (2001) Synaptically released zinc: physiological functions and pathological effects. *Biometals* **14**, 353–366.

Frederickson C. J., Giblin L. J., Krezel A. *et al.* (2006) Concentrations of extracellular free zinc (pZn)e in the central nervous system during simple anesthetization, ischemia and reperfusion. *Exp. Neurol.* **198**, 285–293.

Gaggelli E., Kozlowski H., Valensin D. and Valensin G. (2006) Copper homeostasis and neurodegenerative disorders (Alzheimer's, prion, and Parkinson's diseases and amyotrophic lateral sclerosis). *Chemical Reviews* **106**, 1995–2044.

Garai K., Sahoo B., Kaushalya S. K., Desai R. and Maiti S. (2007) Zinc Lowers Amyloid-beta Toxicity by Selectively Precipitating Aggregation Intermediates. *Biochemistry* **46**, 10655–10663.

Garzon-Rodriguez W., Yatsimirsky A. K. and Glabe C. G. (1999) Binding of Zn(II), Cu(II), and Fe(II) ions to Alzheimer's A beta peptide studied by fluorescence. *Bioorg. Med. Chem. Lett.* **9**, 2243–2248.

Guilloreau L., Damian L., Coppel Y., Mazarguil H., Winterhalter M. and Faller P. (2006) Structural and thermodynamical properties of Cu(II) amyloid-beta16/28 complexes associated with Alzheimer's disease. *J. Biol. Inorg. Chem.* **11**, 1024–1038.

Haass C. and Selkoe D. J. (2007) Soluble protein oligomers in neurodegeneration: lessons from the Alzheimer's amyloid beta-peptide. *Nat. Rev. Mol. Cell Biol.* **8**, 101–112.

Hartter D. E. and Barnea A. (1988) Evidence for release of copper in the brain: depolarization-induced release of newly taken-up 67copper. *Synapse* **2**, 412–415.

Hegetschweiler K. and Saltman P. (1986) Interaction of Copper(Ii) with N-(2-Hydroxyethyl)Piperazine-N'-Ethanesulfonic Acid (Hepes). *Inorg. Chem.* **25**, 107–109.

Hopt A., Korte S., Fink H., Panne U., Niessner R., Jahn R., Kretzschmar H. and Herms J. (2003) Methods for studying synaptosomal copper release. *J. Neurosci. Methods* **128**, 159–172.

Howell G. A., Welch M. G. and Frederickson C. J. (1984) Stimulation-induced uptake and release of zinc in hippocampal slices. *Nature* **308**, 736–738.

Huang X., Atwood C. S., Hartshorn M. A. *et al.* (1999a) The A beta peptide of Alzheimer's disease directly produces hydrogen peroxide through metal ion reduction. *Biochemistry* **38**, 7609–7616.

Huang X., Cuajungco M. P., Atwood C. S. *et al.* (1999b) Cu(II) potentiation of alzheimer abeta neurotoxicity. Correlation with cell-free hydrogen peroxide production and metal reduction. *J. Biol. Chem.* **274**, 37111–37116.

Jiang D., Men L., Wang J., Zhang Y., Chickenyen S., Wang Y. and Zhou F. (2007) Redox Reactions of Copper Complexes Formed with Different beta-Amyloid Peptides and Their Neuropathalogical Relevance. *Biochemistry* **46**, 9270–9282.

Kardos J., Kovacs I., Hajos F., Kalman M. and Simonyi M. (1989) Nerve endings from rat brain tissue release copper upon depolarization. A possible role in regulating neuronal excitability. *Neurosci. Lett.* **103**, 139–144.

Karr J. W., Akintoye H., Kaupp L. J. and Szalai V. A. (2005) N-Terminal deletions modify the Cu^{2+} binding site in amyloid-beta. *Biochemistry* **44**, 5478–5487.

Klein W. L., Krafft G. A. and Finch C. E. (2001) Targeting small Abeta oligomers: the solution to an Alzheimer's disease conundrum? *Trends Neurosci.* **24**, 219–224.

Konoha K., Sadakane Y. and Kawahara M. (2006) Zinc neurotoxicity and its role in neurodegenerative diseases. *J. Health. Sci.* **52**, 1–8.

Lee J. Y., Cole T. B., Palmiter R. D., Suh S. W. and Koh J. Y. (2002) Contribution by synaptic zinc to the gender-disparate plaque formation in human Swedish mutant APP transgenic mice. *Proc. Natl Acad. Sci. U. S. A.* **99**, 7705–7710.

Lovell M. A., Robertson J. D., Teesdale W. J., Campbell J. L. and Markesbery W. R. (1998) Copper, iron and zinc in Alzheimer's disease senile plaques. *J. Neurol. Sci.* **158**, 47–52.

Lynch T., Cherny R. A. and Bush A. I. (2000) Oxidative processes in Alzheimer's disease: the role of abeta-metal interactions. *Exp. Gerontol.* **35**, 445–451.

Ma Q., Li Y., Du J., Liu H., Kanazawa K., Nemoto T., Nakanishi H. and Zhao Y. (2006) Copper binding properties of a tau peptide associated with Alzheimer's disease studied by CD, NMR, and MALDI-TOF MS. *Peptides* **27**, 841–849.

Madsen E. and Gitlin J. D. (2007) Copper and iron disorders of the brain. *Annu. Rev. Neurosci.* **30**, 317–337.

Mantyh P. W., Ghilardi J. R., Rogers S., DeMaster E., Allen C. J., Stimson E. R. and Maggio J. E. (1993) Aluminum, iron, and zinc ions promote aggregation of physiological concentrations of beta-amyloid peptide. *J. Neurochem.* **61**, 1171–1174.

Masuoka J. and Saltman P. (1994) Zinc(II) and copper(II) binding to serum albumin. A comparative study of dog, bovine, and human albumin. *J. Biol. Chem.* **269**, 25557–25561.

Miller L. M., Wang Q., Telivala T. P., Smith R. J., Lanzirotti A. and Miklossy J. (2006) Synchrotron-based infrared and X-ray imaging shows focalized accumulation of Cu and Zn co-localized with beta-amyloid deposits in Alzheimer's disease. *J. Struct. Biol.* **155**, 30–37.

Miura T., Suzuki K., Kohata N. and Takeuchi H. (2000) Metal binding modes of Alzheimer's amyloid beta-peptide in insoluble aggregates and soluble complexes. *Biochemistry* **39**, 7024–7031.

Paoletti P., Ascher P. and Neyton J. (1997) High-affinity zinc inhibition of NMDA NR1-NR2A receptors. *J. Neurosci.* **17**, 5711–5725.

Raman B., Ban T., Yamaguchi K., Sakai M., Kawai T., Naiki H. and Goto Y. (2005) Metal Ion-dependent Effects of Clioquinol on the Fibril Growth of an Amyloid {beta} Peptide. *J. Biol. Chem.* **280**, 16157–16162.

Ricchelli F., Drago D., Filippi B., Tognon G. and Zatta P. (2005) Aluminum-triggered structural modifications and aggregation of beta-amyloids. *Cell Mol. Life Sci.* **62**, 1724–1733.

Sayre L. M. (1996) Alzheimer's precursor protein and the use of bathocuproine for determining reduction of copper(II). *Science* **274**, 1933–1934.

Schlief M. L., Craig A. M. and Gitlin J. D. (2005) NMDA receptor activation mediates copper homeostasis in hippocampal neurons. *J. Neurosci.* **25**, 239–246.

Shaw C. F., Laib J. E., Savas M. M. and Petering D. H. (1990) Biphasic Kinetics of Aurothionein Formation from Gold Sodium Thiomalate

© 2007 The Authors
Journal Compilation © 2007 International Society for Neurochemistry,

- a Novel Metallochromic Technique to Probe Zn-2+ and Cd-2+ Displacement from Metallothionein. *Inorg. Chem.* **29**, 403–408.

Sokolowska M. and Bal W. (2005) Cu(II) complexation by 'non-coordinating' N-2-hydroxyethylpiperazine-N'-2-ethanesulfonic acid (HEPES buffer). *J. Inorg. Biochem.* **99**, 1653–1660.

Stine W. B. Jr, Dahlgren K. N., Krafft G. A. and LaDu M. J. (2003) In vitro characterization of conditions for amyloid-beta peptide oligomerization and fibrillogenesis. *J. Biol. Chem.* **278**, 11612–11622.

Syme C. D. and Viles J. H. (2006) Solution (1)H NMR investigation of Zn(2+) and Cd(2+) binding to amyloid-beta peptide (Abeta) of Alzheimer's disease. *Biochim. Biophys. Acta* **1764**, 246–256.

Syme C. D., Nadal R. C., Rigby S. E. and Viles J. H. (2004) Copper binding to the amyloid-beta (Abeta) peptide associated with Alzheimer's disease: folding, coordination geometry, pH dependence, stoichiometry, and affinity of Abeta-(1-28): insights from a range of complementary spectroscopic techniques. *J. Biol. Chem.* **279**, 18169–18177.

Takahashi M.-a., Takano M. and Asada K. (1981) Tris-Induced Cross-Linking of Thylakoid Peptides; Thiol Oxidation Catalyzed by Tris-Cu^{2+} Complexes as a Possible Mechanism. *J. Biochem. (Tokyo)* **90**, 87–94.

Tanzi R. E. and Bertram L. (2005) Twenty years of the Alzheimer's disease amyloid hypothesis: a genetic perspective. *Cell* **120**, 545–555.

Xiao Z., Loughlin F., George G. N., Howlett G. J. and Wedd A. G. (2004) C-terminal domain of the membrane copper transporter Ctr1 from Saccharomyces cerevisiae binds four Cu(I) ions as a cuprous-thiolate polynuclear cluster: sub-femtomolar Cu(I) affinity of three proteins involved in copper trafficking. *J. Am. Chem. Soc.* **126**, 3081–3090.

© 2007 The Authors
Journal Compilation © 2007 International Society for Neurochemistry,

PUBLICATION II

Tõugu, V., **A. Karafin**, K. Zovo, R. S. Chung, C. Howells, A. K. West and P. Palumaa (2009)
"Zn(II)- and Cu(II)-Induced Non-Fibrillar Aggregates of Amyloid-Beta (1-42) Peptide Are Transformed to Amyloid Fibrils, Both Spontaneously and under the Influence of Metal Chelators."
J. Neurochem. **110**(6): 1784-1795

Journal of Neurochemistry

JOURNAL OF NEUROCHEMISTRY | 2009 | 110 | 1784–1795 doi: 10.1111/j.1471-4159.2009.06269.x

Zn(II)- and Cu(II)-induced non-fibrillar aggregates of amyloid-β (1–42) peptide are transformed to amyloid fibrils, both spontaneously and under the influence of metal chelators

Vello Tõugu,* Ann Karafin,* Kairit Zovo,* Roger S. Chung,† Claire Howells,† Adrian K. West† and Peep Palumaa*

*Department of Gene Technology, Tallinn University of Technology, Tallinn, Estonia

†NeuroRepair Group, Menzies Research Institute, University of Tasmania, Hobart, Tasmania, Australia

Abstract

Aggregation of amyloid-β (Aβ) peptides is a central phenomenon in Alzheimer's disease. Zn(II) and Cu(II) have profound effects on Aβ aggregation; however, their impact on amyloidogenesis is unclear. Here we show that Zn(II) and Cu(II) inhibit $A\beta_{42}$ fibrillization and initiate formation of non-fibrillar $A\beta_{42}$ aggregates, and that the inhibitory effect of Zn(II) (IC_{50} = 1.8 μmol/L) is three times stronger than that of Cu(II). Medium and high-affinity metal chelators including metallothioneins prevented metal-induced $A\beta_{42}$ aggregation. Moreover, their addition to preformed aggregates initiated fast $A\beta_{42}$ fibrillization. Upon prolonged incubation the metal-induced aggregates also transformed spontaneously into fibrils, that appear to represent the most stable state of $A\beta_{42}$. H13A and H14A mutations in $A\beta_{42}$ reduced the inhibitory effect of metal ions, whereas an H6A mutation had no significant impact. We suggest that metal binding by H13 and H14 prevents the formation of a cross-β core structure within region 10–23 of the amyloid fibril. Cu(II)-$A\beta_{42}$ aggregates were neurotoxic to neurons *in vitro* only in the presence of ascorbate, whereas monomers and Zn(II)-$A\beta_{42}$ aggregates were non-toxic. Disturbed metal homeostasis in the vicinity of zinc-enriched neurons might pre-dispose formation of metal-induced Aβ aggregates, subsequent fibrillization of which can lead to amyloid formation. The molecular background underlying metal-chelating therapies for Alzheimer's disease is discussed in this light.

Keywords: aggregation, Alzheimer's disease, amyloid-β, fibrillization, metal chelating therapy, zinc and copper ions.

J. Neurochem. (2009) **110**, 1784–1795.

Alzheimer's disease (AD) is a devastating neurodegenerative disorder and leading cause of senile dementia. One of the main histopathological hallmarks of the AD brain is the formation of extracellular amyloid plaques, composed mainly of fibrillar amyloid-β (Aβ) peptide, small amounts of other proteins (Liao *et al.* 2004), and transition metal ions (Lovell *et al.* 1998; Miller *et al.* 2006). According to the amyloid cascade hypothesis, Aβ aggregation and the subsequent age-related accumulation of amyloid plaques triggers a cascade of molecular and cellular events leading ultimately to neurodegeneration (Hardy and Selkoe 2002; Walsh and Selkoe 2007). Within the plaques, Aβ molecules are organized into insoluble fibrils with a diameter approximately 6–10 nm and similar amyloid fibrils are also formed by synthetic Aβ *in vitro* (Castano *et al.* 1996). According to current opinion, the fibrillization of Aβ *in vitro* involves nucleation dependent polymerization where an initial slow nucleation ('seeding') period is followed by a rapid fibril growth and final fibril maturation (Lomakin *et al.* 1996; Harper and Lansbury 1997). There is consensus that the extended β-conformation seen in fibrils is pivotal to their formation, and that interchain hydrogen bonds with neighboring Aβ units forms the cross-β amyloid core of the fibril (Tycko 2003; Petkova *et al.* 2006).

The formation of plaques *in vivo* may also involve molecules and ions other than Aβ. Importantly, Aβ interacts

Received March 23, 2009; revised manuscript received June 26, 2009; accepted June 30, 2009.

Address correspondence and reprint requests to Vello Tõugu, Department of Gene Technology, Tallinn University of Technology, Akadeemia 15, 12618 Tallinn, Estonia. E-mail: vello.tougu@ttu.ee

Abbreviations used: Aβ, amyloid-β; AD, Alzheimer's disease; CQ, clioquinol; HFIP, 1,1,1,3,3,3-hexafluoro-2-propanol; MT, metallothionein; TEM, transmission electron microscopy; ThT, thioflavin T.

© 2009 The Authors

with Zn(II) and Cu(II) ions and their binding can initiate peptide aggregation (Bush *et al.* 1994; Atwood *et al.* 1998). The content of extracellular zinc and copper in the brain is generally low. However, high levels of zinc are present in the hippocampus, the amygdala, and the cortex that are rich in specific zinc-ergic synapses, where Zn(II) is concentrated in synaptic vesicles with the assistance of a specific zinc transporter Zn-T3 (Frederickson and Bush 2001). Strikingly, Zn-T3 knock-out transgenic AD model mice do not develop amyloid plaques in the brain (Lee *et al.* 2002), which indicates that synaptic zinc may have a causative role in amyloid formation and pathology of AD (Deibel *et al.* 1996; Adlard and Bush 2006; Konoha *et al.* 2006). As with zinc, copper ions are also released from vesicles into the synaptic cleft of hippocampal neurons (Schlief *et al.* 2005). The affinity of full-length Aβ for Zn(II) and Cu(II) is in the same concentration range as synaptic levels of these metal ions in the brain (Tougu *et al.* 2008), further suggesting that Aβ-metal interactions may be significant *in viv*o. Zn(II) and Cu(ii) are also elevated in amyloid plaques (Lovell *et al.* 1998; Miller *et al.* 2006).

The putative role of metal ions in promoting AD pathology underlies a therapeutic approach called 'metal chelating therapy' (Cherny *et al.* 2001; Bush and Tanzi 2008) which in part, suggests that removal of Cu(II) and Zn(II), from amyloid plaques leads to their solubilization. This approach has been tested by using weak metal chelators like clioquinol (CQ) and its second generation derivatives (PBT2), which reduce plaque load in transgenic mice models of AD (Cherny *et al.* 2001; Adlard *et al.* 2008). PTB2 promoted improvement in cognitive efficacy of AD patients in phase IIa clinical tests, however, the clinical effectiveness of the drug remains to be finally established (Lannfelt *et al.* 2008). Several studies demonstrate that the mechanism of metal chelating therapy is more complex than initially proposed (White *et al.* 2006; Crouch *et al.* 2009). It has been demonstrated that besides metal chelating ability, CQ has other systematic effects both in cell culture models and in whole animal experiments (White *et al.* 2006). Recently it was observed that CQ promotes rather than inhibits the formation of Aβ fibrils *in vitro* and the authors have proposed a careful reconsideration of the potential of CQ-based chelation therapy (Bolognin *et al.* 2008). It is evident that further evaluation of the metal chelators as potential therapeutics should rely on the proper understanding of two fundamental aspects – (i) the effect of metal ions on the aggregation of Aβ; (ii) the effect of metal chelators on metal-induced Aβ aggregates, both of which are currently incompletely understood.

The influence of zinc and copper ions on aggregation of Aβ has been intensively studied over the last decade; nevertheless, many important aspects like the effect of metal ions on aggregation kinetics and the effect of chelators on metal-induced aggregation of Aβ are still elusive. In early studies metal ions have been reported to enhance the rate of Aβ fibrillization and metal chelators acted in an opposite direction by reversing the aggregation (Bush *et al.* 1994; Esler *et al.* 1996; Cherny *et al.* 1999). Later it was found that the metal-induced Aβ aggregates are predominantly non-fibrillar (Yoshiike *et al.* 2001; Raman *et al.* 2005), however, enhanced fibril formation in the presence of metal ions has also been observed (Klug *et al.* 2003; Ricchelli *et al.* 2005). It has even been suggested that the presence of trace levels of metal ions is absolutely necessary for Aβ fibrillization (Huang *et al.* 2004). Reasons for the inconsistency from different studies are unknown.

In this work, we have systematically studied the effect of Zn(II) and Cu(II) on the aggregation of $A\beta_{42}$ and its His to Ala mutants, and the transition between insoluble aggregates and fibrils. We further examined the effect of metal chelators on these processes, and the subsequent neuronal toxicity of fibrils and aggregates. Our results allow us to propose a model which reconciles the interaction of Zn(II) and Cu(II) with $A\beta_{42}$ under physiological conditions, and the emergence of different forms of polymerized Aβ over time.

Experimental procedures

Materials

Lyophilized $A\beta_{42}$ peptide and its H6A, H13A and H14A mutants (ultra pure, recombinant) were purchased from rPeptide (Bogart, GA, USA) as 1,1,1,3,3,3-hexafluoro-2-propanol (HFIP) form. HEPES Ultrapure, MB Grade was from USB Corporation (Cleveland, OH, USA). EDTA, HFIP, Zincon, Thioflavin T, $CuCl_2 \times 2H_2O$ and, glycine, cysteine and histidine hydrochloride were from Sigma-Aldrich (St. Louis, MO, USA); $ZnCl_2$ and NaCl were extra pure from Scharlau (Barcelona, Spain). All solutions were prepared in fresh MilliQ water. Metallothionein-3 (MT-3) was expressed and purified as reported previously (Eriste *et al.* 2003).

Sample preparation

Stock solutions of Aβ were prepared as follows: Aβ HFIP film was dissolved in water containing 0.02% NH_3 at a concentration of 10–20 μM. After 10 min of incubation the Aβ stock solution was diluted with buffer and used for experiments.

Monitoring $A\beta_{42}$ fibrillization by thioflavin T fluorescence

Freshly prepared stock solutions of $A\beta_{42}$ were diluted to a final concentration of 5 μmol/L in 20 mmol/L HEPES and 100 mmol/L NaCl, pH 7.4 containing 3.3 μmol/L of thioflavin T (ThT) and an appropriate amount of Zn(II) or Cu(II). 400 μL of each sample was incubated in a 0.5 cm path length quartz cell and agitated with a magnetic stirrer at 250 rpm. The increase in ThT fluorescence was measured at 480 nm using excitation at 445 nm on a Perkin-Elmer LS-45 fluorescence spectrophotometer (Perkin-Elmer, Waltham, MA, USA) equipped with a magnetic stirrer.

Aggregation parameters were determined by fitting the fluorescence intensity versus time to Boltzmann sigmoid curve

$$y = \frac{A_2 - A_1}{1 + e^{(t - t_0) \times k}} + A_2 \quad (1)$$

where A_1 is the initial fluorescence level, A_2 is the maximum fluorescence, t_0 is the time when fluorescence has reached half

© 2009 The Authors
Journal Compilation © 2009 International Society for Neurochemistry,

maximum and k is the rate constant of the fibril elongation. IC_{50} values were calculated according to hyperbolic dose-response curves.

Conditional dissociation constants for Cu(II)-Aβ_{42} were determined by intrinsic tyrosine fluorescence of Aβ as described in (Tougu *et al.* 2008). Parameter values are given with ± SD.

Transmission electron microscopy

The grids were placed on an adhesive solid surface and 3 μL of previously centrifuged (30 min, 12 000 *g*) peptide solution was pipetted on each grid and allowed to air-dry. Then drops of 2% uranylacetate were spotted on a parafilm plate and grids were placed on them with the upper side down (to bring the probe and the contrasting solution in contact). Probes were kept in uranylacetate for 10 min, then removed and washed with milliQ water. Excess water was then removed with filter paper and the grids were placed into a special carrier. Transmission electron microscopy (TEM) images from the samples were created on SELMI-SUMY EM-125 instrument at 75 kV accelerating voltage and recorded onto high resolution, 60 × 90 mm negative film.

Rat cortical neuron toxicity assay

Cortical neuron cultures were prepared as reported previously (Chung *et al.* 2004) and described in Appendix S1. At 3 days *in vitro*, rat cortical neurons were treated with 5 μmol/L of monomeric Aβ_{42}, Zn(II)-, and Cu(II)-induced Aβ_{42} aggregates, in the presence or absence of 300 μmol/L ascorbate (Sigma). After 24 h, the cells were washed three times with pre-warmed culture medium and incubated with 10% (v/v) alamar Blue® (Invitrogen, Carlsbad, CA, USA) in culture medium for 1 h. Cell viability was measured by the degree of cellular metabolic reduction of alamar Blue®. The degree of reduction was determined by fluorescence (λ_{ex} = 535 nm and λ_{em} = 595 nm) using the Tecan GENios™ microplate reader (Tecan, Männedorf, Switzerland). Neuronal viability was expressed as the percentage of the signal obtained from vehicle-treated cultures (Page *et al.* 1993; Chung *et al.* 2004). In parallel experiments we confirmed using direct cell counts of neuronal survival following Aβ treatments that a reduction in cell number correlated proportionately with decreased levels in alamar Blue reduction. Treatments were tested in at least five duplicate wells per experiment. Statistical analysis was completed using SPSS 16.0 (Chicago, IL, USA). Statistical significance was calculated using one-way ANOVA with Tukey's *post hoc* test. Statistical significance was considered as $p < 0.05$.

Results

Monitoring the *in vitro* formation of Aβ_{42} fibrils

First, we established experimental conditions for fast and reproducible monitoring of Aβ_{42} fibrillization. For this purpose HFIP treated, non-fibrillated peptide was used and the fibrillization process was continuously monitored by an increase in detection of fluorescence of the dye ThT present in the incubation mixture. A fast increase in ThT fluorescence was observed in accordance with a typical two-phase growth curve (Fig. 1), but only when the incubation mixture was agitated. When Aβ_{42} was incubated without agitation the fibrillization process was extremely slow and only a slight

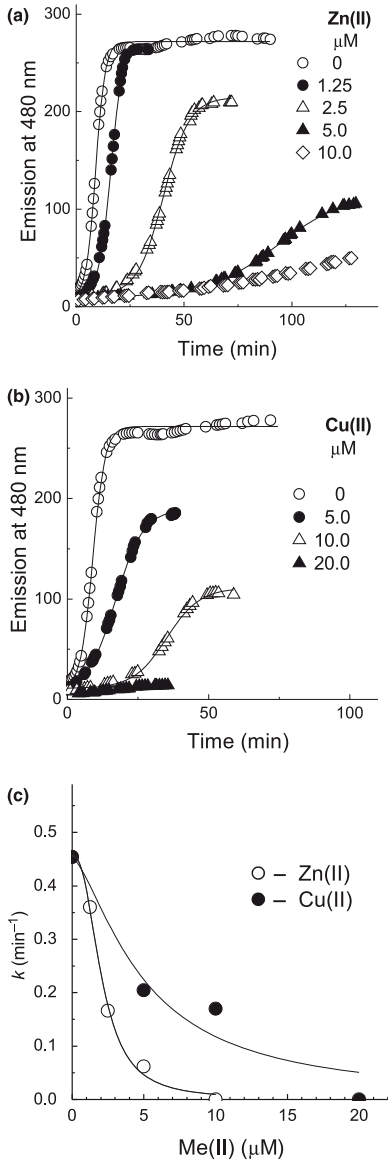

Fig. 1 Effect of metal ions on fibrillization of Aβ_{42} as followed by ThT fluorescence in the presence of (a) Zn(II) and (b) Cu(II). Conditions: 5 μmol/L of Aβ_{42} in 20 mmol/L HEPES, 100 mmol/L NaCl at pH 7.3 was incubated at 25°C in a quartz cell with continuous agitation in the presence of 3.3 μmol/L ThT. Solid lines correspond to fits of the data to Boltzmann equation (eqn 1).

increase in ThT fluorescence was observed during prolonged incubation (3–5 days). A positive correlation was observed between fibrillization rate and stirring intensity, and remained

© 2009 The Authors

constant at stirring rates above 200 rpm. The kinetic curves of fibrillization were fitted to several sigmoidal functions including Avrami, Gompertz and Boltzmann equations and it was found that the latter (eqn 1) provides the best fit of the experimental data and allows calculation of rate constants for the fibrillization process ($k = 0.45 \pm 0.09$ per minute). We established that k did not change when ThT concentration was varied in the range from 3.3 μmol/L to 15 μmol/L indicating that ThT does not affect the fibrillization at the concentrations used. All further fibrillization measurements were carried out at 250 rpm in the presence of 3.3 μmol/L ThT. In these conditions the value of the fibrillization rate constant $k = 0.51 \pm 0.20$ per minute was also independent of the Aβ concentration in the range of 2–10 μM, confirming that it is a reliable kinetic constant useful for quantitative characterization of the fibrillization process.

Effects of Zn(II) and Cu(II) on the formation of $A\beta_{42}$ fibrils

Both Zn(II) and Cu(II) inhibited $A\beta_{42}$ fibrillization (Fig. 1). Metal ions decreased the fibrillization rate constant, and increased the lag period of the process in a concentration dependent manner, whilst at high Zn(II) and Cu(II) levels the maximal level of ThT fluorescence was also reduced. In the case of Zn(II) a twofold decrease of the fibrillization rate constant (considered as IC_{50}), was observed in the presence of 1.8 μmol/L Zn(II), whereas addition of two molar equivalents of Zn(II) almost completely suppressed the formation of ThT-reactive fibrils. The inhibitory effect of Cu(II) was characterized by $IC_{50} = 4.9$ μmol/L showing that Cu(II) is approximately a three times weaker suppressor of $A\beta_{42}$ fibrillization than Zn(II). Our results are consistent with earlier data indicating that Zn(II) and Cu(II) suppress the final level of ThT-reactive Aβ fibrils (Yoshiike *et al.* 2001; Smith *et al.* 2006).

We demonstrated that as well as suppression of $A\beta_{42}$ fibrillization, metal ions initiated fast assembly of $A\beta_{42}$ into insoluble aggregates that sediment during centrifugation at 10 000 *g*. Zn(II)-mediated aggregation of Aβ as near-instantaneous whereas precipitate formation with Cu(II) occurred within 30 min. Continuous agitation was not necessary to ensure the fast metal-induced peptide aggregation. As 4.2 ± 0.2 μmol/L of copper or 4.3 ± 0.3 μmol/L zinc co-precipitated with 4 μmol/L of $A\beta_{42}$ we can conclude that metal to peptide ratio in the aggregates formed in the presence of excess metal ions is approximately 1 : 1.

Effect of metal chelators on the inhibition of Aβ fibrillization by Zn(II) and Cu(II)

In order to study the reversibility of the effects of Cu(II) and Zn(II) upon Aβ fibrillization, and evaluate the strength of metal-amyloid interactions, we examined these processes in the presence of different metal chelating reagents. In the presence of 40 μmol/L glycine, 5 μmol/L Zn(II) still inhibited fibrillization of $A\beta_{42}$ (Fig. 2a). However, partial fibrillization was observed in the presence of 40 μmol/L glutamate or histidine, showing that Glu and His compete with $A\beta_{42}$ for Zn(II). Cysteine also prevented Zn(II)-induced inhibition of $A\beta_{42}$ fibrillization, however, the process was delayed. Addition of high affinity chelators like EDTA ($K_D^{ZnL} = 3.2$ aM) and apo-MT, ($K_D^{Zn} = 0.14$ pM) (Kägi 1993) completely abolished the inhibitory effect of Zn(II) on $A\beta_{42}$ fibrillization. The chelating effect of amino acids correlates well with their metal binding affinities, characterized by constant β (logarithm of the stability constant of the corresponding MeL_2 complex) for Zn(II) binding: β(Gly) = 9.2, β(Glu) = 9.5 β(His) = 11.8 and β(Cys) = 18.2 (Dawson *et al.* 1986). The metal chelators also prevented Cu(II)-induced inhibition of $A\beta_{42}$ fibrillization (Fig. 2b). In fact, their effect was more pronounced than in case of Zn(II): even Gly was able to reverse the inhibitory effect of 10 μmol/L Cu(II) on fibrillization of $A\beta_{42}$.

These results indicate that metal chelators prevent metal-induced $A\beta_{42}$ aggregation, however, it is also important to establish the effect of metal chelators on pre-existing metal-induced $A\beta_{42}$ aggregates. Figure 2(c) shows that addition of the high-affinity metal chelators to freshly prepared Zn(II)-induced $A\beta_{42}$ aggregates gave rise to a fast increase in ThT fluorescence, reflecting the conversion of the aggregates into amyloid fibrils. Zn(II)-induced aggregates were also converted to fibrils in the presence of higher (mmol/L) concentrations of His.

Aggregation of $A\beta_{42}$ was also carried out in an environment mimicking putative *in vivo* conditions in regions of zinc-enriched glutamate-ergic synapses, composed from saline buffer, pH 7.4, Zn(II) and glutamate that are co-released into the synaptic cleft. Figure 2(d) shows that 5 μmol/L Zn(II) inhibits the fibrillization of $A\beta_{42}$ in the presence of 10 μmol/L glutamate. On the other hand, in the presence of 1 μmol/L brain specific *apo*-MT-3, 5 μmol/L Zn(II) had no effect on Aβ fibrillization. Moreover, addition of apo-MT-3 to the Zn(II)-induced $A\beta_{42}$ aggregates induced rapid formation of ThT-reactive $A\beta_{42}$ fibrils.

We similarly examined the effect of CQ in this system (Fig. 2e). We found that CQ alone had no effect on $A\beta_{42}$ fibrillization at concentrations up to 50 μmol/L. In the presence of 10 μmol/L CQ, 5 μmol/L Zn(II) still inhibited fibrillization of the $A\beta_{42}$. However, inhibition was weaker than in the absence of CQ, indicating that CQ can partially prevent Zn(II)-induced aggregation of $A\beta_{42}$. Addition of 10 μmol/L CQ to the Zn(II)-induced $A\beta_{42}$ aggregates induced a limited fibrillization of the peptide, demonstrating that CQ acts similarly to medium affinity metal chelators.

Our results show that the inhibitory effect of Zn(II) and Cu(II) on fibrillization of $A\beta_{42}$ is reversible, and that removal of metal ions from metal-induced $A\beta_{42}$ aggregates initiates peptide fibrillization in our experimental conditions. Only medium and high-affinity metal chelators were able to reverse the effects of metal ion on the $A\beta_{42}$ fibrillization,

© 2009 The Authors
Journal Compilation © 2009 International Society for Neurochemistry,

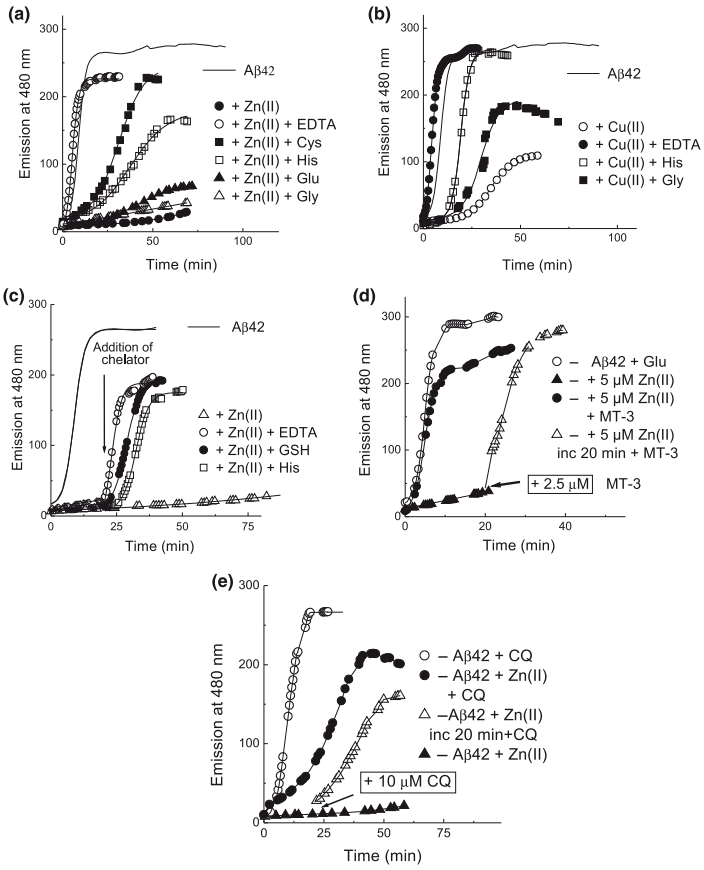

Fig. 2 Effect of metal chelating agents on fibrillization of $A\beta_{42}$ in the presence of Zn(II) and Cu(II) ions. The chelators were added in the beginning of the fibrillization reaction (a,b) or after 20 min incubation of $A\beta_{42}$ in the presence of 10 μmol/L Zn(II) (c); (d) Effect of apo-MT-3 on the fibrillization of $A\beta_{42}$ in the presence of 10 μmol/L glutamate and 10 μmol/L glutamate and 5 μmol/L Zn(II). In the second experiment 2.5 μmol/L MT-3 was added at the point indicated by an arrow. (e) Effect of CQ on the fibrillization of $A\beta_{42}$ alone and in the presence of 5 μmol/L Zn(II). Time of CQ addition is indicated by an arrow. All reactions were carried out with 5 μmol/L of $A\beta_{42}$ in 20 mmol/L HEPES, 100 mmol/L NaCl, 3.3 μmol/L ThT at pH 7.3, 25°C. Solid lines correspond to fits of the data to Boltzmann equation (eqn 1).

indicating that the effect of metal chelators is non-specific and depends mainly on their metal binding affinity.

Affinity of His to Ala mutants of $A\beta_{42}$ to metal ions

The affinity of $A\beta_{42}$ mutants towards Cu(II) was determined by monitoring the intrinsic fluorescence of Y10, which in the case of wild-type peptides is quenched by addition of metal ions (Garzon-Rodriguez *et al.* 1999; Tougu *et al.* 2008). Addition of Cu(II) also decreased the intrinsic fluorescence of the mutant peptides, and fitting the data to the quadratic binding equation resulted in apparent dissociation constant (K_D^{app}) values for Cu(II)-peptide complexes equal to K_D^{app}(H6A) = 2.55 ± 0.60 μmol/L, K_D^{app}(H13A) = 0.88 ± 0.20 μmol/L, and K_D^{app}(H14A) = 3.59 ± 0.60 μmol/L. The K_D^{app} values for H14A and H6A mutant peptides are considerably higher than the K_D^{app} = 0.76 μmol/L for wild-type $A\beta_{42}$ under similar conditions (Tougu *et al.* 2008), confirming their involvement in the formation of metal-peptide complex. However, the contribution of H13 to the Cu(II) binding affinity of $A\beta_{42}$ is surprisingly low as the K_D^{app} value for H13A mutant is similar to that for wild-type $A\beta_{42}$. The affinity of monomeric His-Ala mutant peptides towards Zn(II) could not be determined by this method as there were no substantial changes observed in the intrinsic fluorescence of mutant $A\beta_{42}$ up to 500 μM concentration of Zn(II) and fast aggregation of peptides occurred in these conditions.

Fibrillization of His to Ala mutants of $A\beta_{42}$ in the absence and presence of Zn(II) and Cu(II)

In order to determine the role of His residues in the metal-induced aggregation of $A\beta_{42}$, we studied the fibrillization of all three His to Ala mutants of $A\beta_{42}$ and compared the obtained results with the wild-type peptide (Table 1 and Fig. S1). In the absence of metal ions the fibrillization rate of H13A and H14A peptides was similar to that for wild-type $A\beta_{42}$, whereas H6A mutant fibrillated approximately two times faster. The fibrillization rates of all mutant peptides in the presence of metal ions were similar. The IC_{50}(Zn) and IC_{50}(Cu) values were higher for the H13A and H14A mutant

© 2009 The Authors

Table 1 Effect of metal ions on fibrillization of $A\beta_{42}$ and its His to Ala mutants

$A\beta_{42}$ peptide	k_0* per minute	Zn(II) IC_{50}, μmol/L	Cu(II) IC_{50}, μmol/L
Wild-type	0.45 ± 0.09	1.8 ± 0.9	4.9 ± 1.1
H13A	0.60 ± 0.01	5.2 ± 1.4	43 ± 16
H14A	0.37 ± 0.01	11 ± 6	78 ± 25
H6A	1.16 ± 0.05	1.75 ± 0.1	7.5 ± 1.6

*k_0 was calculated by fitting the fibrillization curve to Boltzmann equation (eqn 1) in the absence of metal ions and IC_{50} values from the metal-induced decrease in the k values. Parameters are given with ± SD.

peptides in comparison with the IC_{50} values for wild-type $A\beta_{42}$ (Table 1). In the case of the H6A mutant, the IC_{50} values for Zn(II) and Cu(II) were similar to those for wild-type peptide because of higher fibrillization rate in the absence of metal ions. The inhibitory effect of metal ions on the fibrillization of mutant peptides was also reversed by the addition of high-affinity metal-chelating agents like EDTA, which induced fast formation of ThT-reactive fibrils as observed for wild-type peptide.

Characterization of Aβ complexes with TEM

To confirm results obtained by ThT fluorescence, $A\beta_{42}$ fibrils and metal-induced $A\beta_{42}$ aggregates were studied by TEM. No fibrils were detected in the samples of $A\beta_{42}$ before the appearance of ThT fluorescence (~5 min). However, $A\beta_{42}$ samples showing high ThT fluorescence (agitation for 30 min) showed a high content of fibrils (Fig. 3) confirming that the increase of ThT fluorescence reflects peptide fibrillization in our assay. In $A\beta_{42}$ samples with added Cu(II) and Zn(II), only a small amount of non-fibrillar aggregates was detected after short (~30 min) incubation. After prolonged incubation (~1 week) $A\beta_{42}$ samples with added Cu(II) and Zn(II) also exhibited fibrils in TEM (Fig. 3), confirming that the metal-induced $A\beta_{42}$ aggregates are converted slowly to fibrils.

Toxicity of metal-induced Aβ complexes in rat cortical neuron toxicity assay

Treatment with monomeric $A\beta_{42}$ in the absence of ascorbate had no neurotoxic effect on cultured rat cortical neurons, but instead resulted in a substantial increase in cellular metabolism relative to vehicle-treated cultures (Fig. 4a). Similar

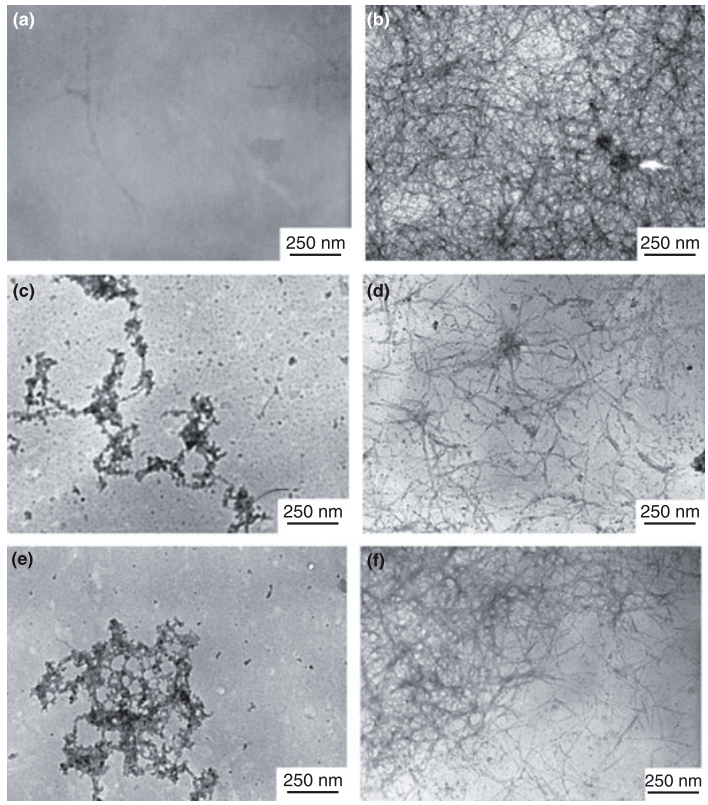

Fig. 3 TEM images of Aβ42 samples. (a) $A\beta_{42}$ agitated for 5 min; (b) $A\beta_{42}$ agitated for 30 min; (c) $A\beta_{42}$ agitated with 5 μmol/L Zn(II) for 30 min; (d) same sample as in (c) incubated for 1 week; (e) $A\beta_{42}$ agitated with 5 μmol/L Cu(II) for 30 min; (f) same sample as in (e) incubated for 1 week. Incubation conditions: 20 mmol/L HEPES and 100 mmol/L NaCl, at pH 7.3, 25°C.

© 2009 The Authors
Journal Compilation © 2009 International Society for Neurochemistry,

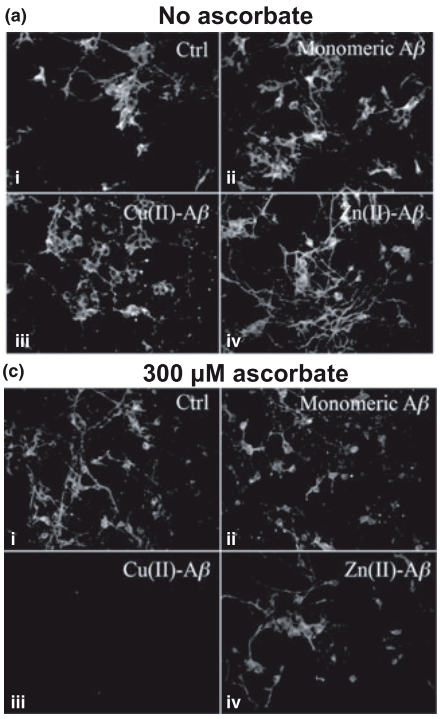

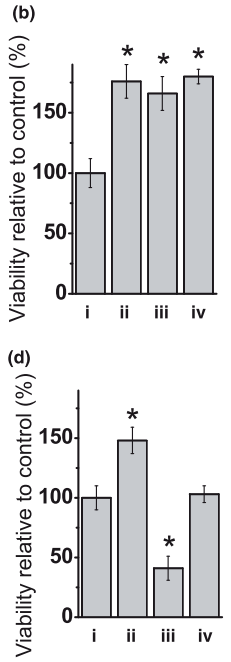

Fig. 4 Toxic effects of metal and non-metal complexed $A\beta_{42}$ in cultured rat cortical neurons. (a) Immunocytochemical labelling of *in vitro* cultured cortical neurons for the cytoskeletal protein tau without treatment (i) and after treatment with 5 μM monomeric $A\beta_{42}$ (ii), Cu(II)- (iii), or Zn(II)-induced $A\beta_{42}$ aggregates (iv) in the absence of ascorbate. (b) Cellular metabolism measured by the reduction of Alamar Blue of *in vitro* cultured cortical neurons without treatment (i) and after treatment with 5 μM monomeric $A\beta_{42}$ (ii), Cu(II)- (iii), or Zn(II)-induced $A\beta_{42}$ aggregates (iv) in the absence of ascorbate. (c) and (d) Same as (a) and (b) in the presence of 300 μM ascorbate. $^*p < 0.01$ compared to vehicle treated cultures. All data are means ± SEM; $n = 6$, except control $n = 5$.

results were observed in the presence of ascorbate (Fig. 4b). In the absence of ascorbate, the Zn(II)-$A\beta_{42}$ and Cu(II)-$A\beta_{42}$ aggregates induced a similar increase in cellular metabolism as monomeric $A\beta_{42}$. However, in the presence of ascorbate, the Cu(II)-Aβ aggregates became highly neurotoxic and caused a significant decrease in neuronal metabolism (and subsequently neuronal viability) relative to the vehicle-treated neuron cultures (Fig. 4a). Furthermore, in the presence of ascorbate, the Zn(II)-Aβ aggregates were not neurotoxic. Immunocytochemical labelling of neuronal cultures for the cytoskeletal protein tau indicated that there was no discernable degeneration in any of the treatments in the absence of ascorbate. In the presence of ascorbate, however, treatment with Cu(II)-$A\beta_{42}$ aggregates caused substantial neuron death and loss of tau immunostaining (Fig. 4b-iii).

Discussion

Cerebral accumulation of Aβ is central to AD pathology, and can be affected by numerous endogenous factors including metal ions. Our study of the aggregation of wild-type $A\beta_{42}$ and its His to Ala mutants in the presence of Zn(II), Cu(II), and metal chelating agents has elucidated several new aspects about the influence of metal ions on the Aβ fibrillization *in vitro* that may also help to understand the role of endogenous metal ions and metal chelating agents in amyloid plaque formation in brain.

In our study, $A\beta_{42}$ fibrillization was monitored by using continuous detection of the fluorescence of ThT, where fast and reproducible fibril growth was catalyzed by agitating the solutions in a quartz cell. We suggest that agitation accelerates peptide fibrillization by multiplying the number of growing ends of the fibrillar seeds by disruption of the early linear fibrils into smaller pieces.

Both Zn(II) and Cu(II) exhibited a pronounced inhibitory effect on $A\beta_{42}$ fibrillization. The concentration-dependent inhibitory effect of Zn(II) (IC_{50} = 1.8 μmol/L) was three times stronger than that of Cu(II) (IC_{50} = 4.9 μmol/L). This is in contrast to their relative binding affinities towards the $A\beta_{42}$ monomer, which is 75-fold higher for Cu(II) (Tougu *et al.* 2008). However, we have observed earlier that the affinity of Zn(II) towards Aβ is enhanced more than tenfold (reaching to ~1 μM) during partial aggregation of $A\beta_{40}$ (Tougu *et al.* 2008), which might explain the appearance of the inhibitory effect of Zn(II) at low micromolar concentration. Both metal ions induced formation of insoluble $A\beta_{42}$ aggregates containing stoichiometric amounts of metal ions. We suggest that the inhibitory effect of metal ions is caused by the decrease in the concentration of free soluble $A\beta_{42}$, necessary for the growth of fibrils. In the case of Cu(II) the affinity of Aβ monomers towards copper is

© 2009 The Authors

sufficiently high ($K_D^{app} << IC_{50}$) to cause inhibition of the fibrillization because of Cu(II)-Aβ formation. Metal-induced aggregation of Aβ occurs most probably according to a conformational change induced aggregation mechanism as suggested in (Talmard *et al.* 2007). Our work and earlier results (Huang *et al.* 1997; Noy *et al.* 2008) indicate that Zn(II)-induced aggregation of Aβ is almost immediate, and therefore it is reasonable to suggest that metal complexes of Aβ aggregate because of fast-forming hydrophobic interactions.

The suppression of $Aβ_{42}$ fibrillization by metal ions was confirmed by TEM, where only a small amount of amorphous $Aβ_{42}$ aggregates was observed in the samples incubated with metal ions. However, after prolonged incubation (1 week) amyloid fibrils were also detected in the samples of metal-induced $Aβ_{42}$ aggregates. Thus, fibrillization of $Aβ_{42}$ also occurs in the presence of metal ions and it follows that the metal-induced $Aβ_{42}$ aggregates are not dead-end products of $Aβ_{42}$ assembly but rather intermediary components of a dynamic system of various Aβ molecular forms (Fig. 5), of which the fibrillar state is the most stable one. These observations can partially explain the contradiction between published results on the effect of metal ions on fibrillization of Aβ. In the conditions where the growth of fibrils is fast (as it was in our experiments) metal ions inhibit the fibrillization by lowering the concentration of free peptide. However, under conditions where the fibrillization is slow metal ions can enhance the fibrillization process by causing peptide assembly to metal-induced aggregates that can further transform to fibrils.

We found that metal chelators with medium and high affinity suppress the inhibitory effect of metal ions on $Aβ_{42}$ fibrillization, and their addition to metal-induced $Aβ_{42}$ aggregates stimulate fibrillization of $Aβ_{42}$. These results also confirm that fibrillar $Aβ_{42}$ is the most stable biochemical form of $Aβ_{42}$. We have recently reported that the metal-induced $Aβ_{40}$ aggregates became fully soluble when the metal ions are sequestered by metal chelators (Tougu *et al.* 2008). In the case of $Aβ_{42}$ the dissociated peptide monomers can subsequently participate in fibrillization through a

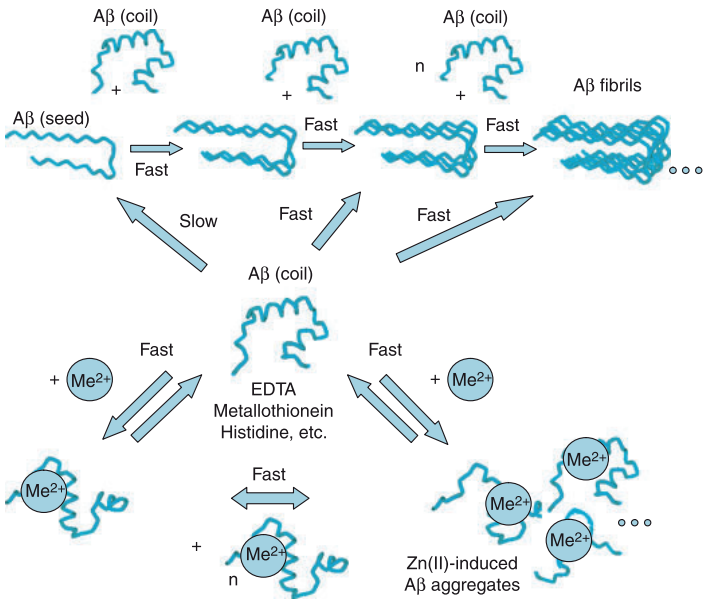

Fig. 5 Mechanisms for assembly and fibrillogenesis of $Aβ_{42}$ in the presence of Zn(II) or Cu(II) ions. $Aβ_{42}$ monomer can bind metal ion or align with preformed fibrillar seeds. Ends of the growing fibrils serve as templates for monomer addition seeds, whereas the origin of the primary seeds is unknown. The number of fibril ends acting as seeds can be increased by fragmentation of linear fibrils in agitated solution. Zn(II)-Aβ monomer formation affects the peptide conformation making it insoluble and they collapse into non-fibrillar aggregates possibly because of hydrophobic contacts (in the presence of excess peptide, free $Aβ_{42}$ can partially co-precipitate with Zn(II)-$Aβ_{42}$ into these aggregates). Loss of metal-free $Aβ_{42}$ from solution causes the inhibition of the fibrillization. Metal chelators can sequester Zn(II) from the aggregates leading to dissociation of $Aβ_{42}$ monomers, which contribute to fibril growth. Metal-induced aggregates acquire fibrillar structure also without addition of chelators during prolonged incubation. It is not clear whether during this incubation the Zn(II) induced $Aβ_{42}$ aggregates can be transformed to fibrillar form through monomeric state, which is always present at low equilibrium concentration, or also directly by rearrangement of its structure. A scheme for the Cu(II) effect can be drawn by replacement of Zn(II) by Cu(II) in the Figure.

© 2009 The Authors
Journal Compilation © 2009 International Society for Neurochemistry,

monomer addition process. Kinetic results also indicate that metal ions do not prevent fibrillization but only inhibit the process by lowering the concentration of soluble monomer. A schematic model describing the effect of metal ions on the fibrillization of $A\beta_{42}$, consistent with our experimental results is presented in Fig. 5.

The study of His-Ala mutants of full-length $A\beta_{42}$ demonstrated His13 and His14 but not His6 contribute to the metal-induced inhibition of Aβ fibrillization. In soluble Zn(II)-Aβ and Cu(II)-Aβ complexes all three His residues participate in metal binding (Syme and Viles 2006; Zirah *et al.* 2006) and therefore we predict that His-mediated metal-binding inhibits fibrillization of Aβ. The current model of fibrillar Aβ, constructed on the basis of experimentally derived NMR parameters, shows that the structural unit of the Aβ protofilament consists of two juxtaposed Aβ molecules, which is replicated along the fibril axis (Fig. 6) (Nelson *et al.* 2005; Petkova *et al.* 2006). Within the Aβ molecule the residues 10–23 and 30–40 are in β conformational state and form hydrogen bonds with the adjoining juxtaposed Aβ units by forming the cross-β amyloid core of the fibril (Fig. 6c). It follows that in Aβ fibrils His 13 and 14 residues should adapt extended β-conformation, where their imidazole units are located on the opposite sides of the peptide backbone (Fig. 6b). Such an arrangement differs substantially from the conformation of this segment in metal-Aβ complexes, where all His residues coordinate a single metal ion. Thus, it is evident that metal binding hinders the adoption of β-conformation in region 13–14 which is necessary for Aβ fibrillization. The structural analysis indicates that metal ions might exert their inhibitory effect on fibrillization of $A\beta_{42}$ by preventing the adoption of extended β-conformation in region 10–14, which has also been suggested on the basis of molecular dynamic calculations of Cu(II)-Aβ complexes (Jiao and Yang 2007). According to this conclusion the effect of mutation on His6, which is not directly involved in β-sheet formation, should be less pronounced as compared to the effect of mutation of His13 and His14. This was also observed in our experiments (Table 1). It is known that binding of metal ions affects fibrillization of other amyloidogenic peptides as well as proteins such as prion protein (Bocharova *et al.* 2005) and superoxide dismutase (Banci *et al.* 2009), indicating that binding of metal ions and metal-induced conformational changes might play a general role in protein fibrillization.

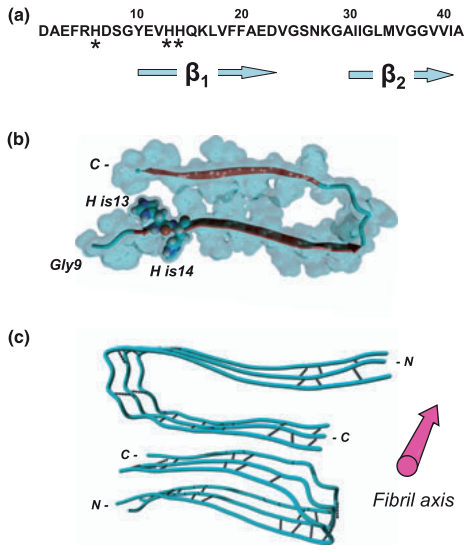

Fig. 6 Structure of Aβ in the protofilament according to Petkova *et al.* (2006). (a) Sequence of human $A\beta_{42}$ showing His residues (indicated by asterisk) and two beta regions (indicated by arrows). (b) Positions of His 13 and His 14 in the extended beta sheet region of fibrillar Aβ. The first nine residues are mobile and their positions are not known. (c) Aβ protofilament repeating unit consists of two juxtaposed Aβ molecules, which form hydrogen bonds with the adjoining juxtaposed Aβ peptide units and form cross-β amyloid core structure of the fibril. Fibril axis is indicated by an arrow.

Aggregation of Aβ *in vivo* occurs in the presence of endogenous metal ions as well as various metal-chelating ligands. The content of zinc in the brain is highest in hippocampus and cortex in the region of the zinc-enriched glutamate-ergic neurons, where up to 300 μmol/L Zn(II) is concentrated into synaptic vesicles. Upon release, together with glutamate, the levels of extracellular zinc can transiently rise to 10–30 μmol/L or higher in the synaptic region (Frederickson *et al.* 2006). It is important to note that the brain regions containing zinc-enriched neurons are also the sites of primary amyloid deposition in AD (Bush 2003). In an environment mimicking the putative *in vivo* conditions in the regions of zinc-enriched synapses (5 μmol/L Zn(II), 20 μmol/L glutamate) Zn(II) induces rapid formation of metal-induced $A\beta_{42}$ aggregates and inhibits $A\beta_{42}$ fibrillization in our experimental conditions. Thus, glutamate cannot effectively compete with $A\beta_{42}$ for Zn(II) binding. However, the brain-specific Zn(II)-binding protein MT-3 in its apo form can block formation of Zn(II)-$A\beta_{42}$ aggregates. MT-3 is released by astrocytes and it may participate in the binding and uptake of Zn(II) ions from the synaptic cleft (Uchida *et al.* 2002; Barnham and Bush 2008). The high zinc-buffering capacity of MTs might stabilize fluctuations in concentration of free Zn(II) and avoid Zn(II)-induced Aβ aggregation. MT-3 can also solubilize $A\beta_{42}$ from metal-induced Aβ aggregates by removing Zn(II). The removal of Zn(II) induced Aβ fibrillization in our experiments. However, at low physiological Aβ concentrations 0.11 nmol/L in brain (Sjogren *et al.* 2001) the fibrillization of monomeric Aβ is a slow and unlikely process. It is repeatedly demonstrated that introduction of $A\beta_{42}$ into brain cannot induce amyloid formation *in vivo* (Meyer-Luehmann *et al.*

© 2009 The Authors

2006). However, if environmental metal buffering capacity is low, metal-induced Aβ aggregates could be formed in the brain and eventually transform to Aβ fibrils. It follows that metal buffering and uptake mechanisms might play a crucial role in the formation of metal-induced Aβ aggregates and defining their fate in the brain. It is known that the levels of MT-3 are substantially (10-fold) lower in AD patient's brains as compared with normal brains (Tsuji *et al.* 1992; Yu *et al.* 2001). In the light of current results it is feasible that lower levels of MT-3 might reduce zinc buffering capacity thus promoting the formation of Zn(II)-induced Aβ aggregates followed by their spontaneous transformation into fibrils, which start to grow by trapping Aβ monomers and thus forming amyloid plaques. The proposed scenario is also supported by elevated concentration of zinc and copper in the cores of pathological amyloid plaques isolated from the brains of AD patients (Lovell *et al.* 1998; Hutchinson *et al.* 2005).

By using a rat cortical neuron toxicity assay we demonstrate that micromolar concentrations of copper-induced $A\beta_{42}$ aggregates are toxic to neurons *in vitro* only in the presence of the reducing agent ascorbate. However, Zn(II)-$A\beta_{42}$ aggregates had no neurotoxic action, either in the presence or absence of ascorbate, which indicates that toxic action of copper-induced $A\beta_{42}$ aggregates arises from copper-catalyzed redox reactions that generate toxic reactive oxygen species. These results are in accordance with previous studies (Multhaup *et al.* 1997). It has also be shown that Aβ can reduce Cu(II) to Cu(I) in the presence of biological reducing substrates *in vitro*, with parallel production of H_2O_2 (Huang *et al.* 1999). The formation of toxic reactive oxygen species is believed to be a major cause of neurodegeneration in AD, and accordingly a substantial component of oxidative stress might be induced from copper ions bound to metal-induced $A\beta_{42}$ aggregates or fibrils (Donnelly *et al.* 2007; Meloni *et al.* 2008).

Our results show that the first generation metal chelating drug candidate CQ itself has no direct effect on $A\beta_{42}$ fibrillization and it acts as a medium affinity metal chelator that can partially prevent or reverse the formation of Zn(II)-induced $A\beta_{42}$ assembly. However, enhanced peptide fibrillization was observed in our experimental conditions. As we discussed earlier, the metal ions apparently can inhibit or enhance the fibril formation depending on the limiting step of the process. The same must also hold for metal chelators that convert metal-induced Aβ aggregates to monomeric peptides, which can be cleared or enhance fibrillization in the presence of fibrillar seeds. Consequently the outcome of metal-chelation therapy might vary between two opposite scenarios: First – prevention of the formation of metal-induced Aβ aggregation and subsequent fibrillization and secondly – removal of metal ions especially of Cu(II) and reduction of their toxicity, however, solubilization of metal-induced Aβ aggregates might lead to parallel promotion of Aβ fibrillization and amyloid formation under certain conditions. The beneficial effect of CQ in animal trials may arise also from ionophore properties of CQ or from the activation of Aβ degradation (White *et al.* 2006; Crouch *et al.* 2009).

In summary, we conclude that the concentration of free Zn(II) and zinc-buffering capacity in regions of zinc-enriched neurons may play a crucial role in amyloid formation. Subsequently, any age- or stress-related disturbance in zinc homeostasis and zinc-buffering capacity in the brain can increase the risk for rapid and amplified Zn(II)-induced Aβ aggregation and further fibrillization leading to the formation of amyloid plaques and downstream AD pathology. From the viewpoint of Aβ fibrillization and amyloid formation, the metal-chelating therapy for AD can have potential only as a preventive measure; thus, alternative mechanisms should be applied to stop amyloidogenesis and reduce amyloid load of AD patients.

Acknowledgements

This work was supported by Estonian Science Foundation grants 6840 (V.T.) and 7191 (P.P.), World Federation of Scientists scholarship to Kairit Zovo, and Alzheimer's Australia Research (Jack and Ethel Goldin Foundation). We thank Dr. Valdek Mikli for help with TEM experiments, and Dr. Robert Tycko for providing the atomic coordinates of Aβ fibrils

Supporting Information

Additional Supporting Information may be found in the online version of this article:

Figure S1. Fibrillization of His to Ala mutants of $A\beta_{42}$ in the presence of metal ions.

Appendix S1. Rodent cortical neural cell cultures.

As a service to our authors and readers, this journal provides supporting information supplied by the authors. Such materials are peer-reviewed and may be re-organized for online delivery, but are not copy-edited or typeset. Technical support issues arising from supporting information (other than missing files) should be addressed to the authors.

References

Adlard P. A. and Bush A. I. (2006) Metals and Alzheimer's disease. *J. Alzheimers Dis.* **10**, 145–163.

Adlard P. A., Cherny R. A., Finkelstein D. I. *et al.* (2008) Rapid restoration of cognition in Alzheimer's transgenic mice with 8-hydroxy quinoline analogs is associated with decreased interstitial Abeta. *Neuron* **59**, 43–55.

Atwood C. S., Moir R. D., Huang X., Scarpa R. C., Bacarra N. M., Romano D. M., Hartshorn M. A., Tanzi R. E. and Bush A. I. (1998) Dramatic aggregation of Alzheimer abeta by Cu(II) is induced by conditions representing physiological acidosis. *J. Biol. Chem.* **273**, 12817–12826.

Banci L., Bertini I., Boca M., Calderone V., Cantini F., Girotto S. and Vieru M. (2009) Structural and dynamic aspects related to oligo-

© 2009 The Authors
Journal Compilation © 2009 International Society for Neurochemistry,

merization of apo SOD1 and its mutants. *Proc. Natl Acad. Sci. USA* **106**, 6980–6985.

Barnham K. J. and Bush A. I. (2008) Metals in Alzheimer's and Parkinson's diseases. *Curr. Opin. Chem. Biol.* **12**, 222–228.

Bocharova O. V., Breydo L., Salnikov V. V. and Baskakov I. V. (2005) Copper(II) inhibits in vitro conversion of prion protein into amyloid fibrils. *Biochemistry* **44**, 6776–6787.

Bolognin S., Zatta P., Drago D., Parnigotto P. P., Ricchelli F. and Tognon G. (2008) Mutual stimulation of beta-amyloid fibrillogenesis by clioquinol and divalent metals. *Neuromol. Med.* **10**, 322–332.

Bush A. I. (2003) The metallobiology of Alzheimer's disease. *Trends Neurosci.* **26**, 207–214.

Bush A. I. and Tanzi R. E. (2008) Therapeutics for Alzheimer's disease based on the metal hypothesis. *Neurotherapeutics* **5**, 421–432.

Bush A. I., Pettingell W. H., Multhaup G., d Paradis M., Vonsattel J. P., Gusella J. F., Beyreuther K., Masters C. L. and Tanzi R. E. (1994) Rapid induction of Alzheimer A beta amyloid formation by zinc. *Science* **265**, 1464–1467.

Castano E. M., Prelli F., Soto C., Beavis R., Matsubara E., Shoji M. and Frangione B. (1996) The length of amyloid-beta in hereditary cerebral hemorrhage with amyloidosis, Dutch type. Implications for the role of amyloid-beta 1-42 in Alzheimer's disease. *J. Biol. Chem.* **271**, 32185–32191.

Cherny R. A., Legg J. T., McLean C. A. *et al.* (1999) Aqueous dissolution of Alzheimer's disease Abeta amyloid deposits by biometal depletion. *J. Biol. Chem.* **274**, 23223–23228.

Cherny R. A., Atwood C. S., Xilinas M. E. *et al.* (2001) Treatment with a copper-zinc chelator markedly and rapidly inhibits beta-amyloid accumulation in Alzheimer's disease transgenic mice. *Neuron* **30**, 665–676.

Chung R. S., Adlard P. A., Dittmann J., Vickers J. C., Chuah M. I. and West A. K. (2004) Neuron-glia communication: metallothionein expression is specifically up-regulated by astrocytes in response to neuronal injury. *J. Neurochem.* **88**, 454–461.

Crouch P. J., Tew D. J., Du T. *et al.* (2009) Restored degradation of the Alzheimer's amyloid-beta peptide by targeting amyloid formation. *J. Neurochem.* **108**, 1198–1207.

Dawson D. C. E., Elliott W. H. and Jones K. M. (1986) *Data for Biochemical Research*, p. 544. Oxford University Press, Oxford.

Deibel M. A., Ehmann W. D. and Markesbery W. R. (1996) Copper, iron, and zinc imbalances in severely degenerated brain regions in Alzheimer's disease: possible relation to oxidative stress. *J. Neurol. Sci.* **143**, 137–142.

Donnelly P. S., Xiao Z. and Wedd A. G. (2007) Copper and Alzheimer's disease. *Curr. Opin. Chem. Biol.* **11**, 128–133.

Eriste E., Kruusel K., Palumaa P., Jornvall H. and Sillard R. (2003) Purification of recombinant human apometallothionein-3 and reconstitution with zinc. *Protein Expr. Purif.* **31**, 161–165.

Esler W. P., Stimson E. R., Jennings J. M., Ghilardi J. R., Mantyh P. W. and Maggio J. E. (1996) Zinc-induced aggregation of human and rat beta-amyloid peptides in vitro. *J. Neurochem.* **66**, 723–732.

Frederickson C. J. and Bush A. I. (2001) Synaptically released zinc: physiological functions and pathological effects. *Biometals* **14**, 353–366.

Frederickson C. J., Giblin L. J. 3rd, Rengarajan B. *et al.* (2006) Synaptic release of zinc from brain slices: factors governing release, imaging, and accurate calculation of concentration. *J. Neurosci. Methods* **154**, 19–29.

Garzon-Rodriguez W., Yatsimirsky A. K. and Glabe C. G. (1999) Binding of Zn(II), Cu(II), and Fe(II) ions to Alzheimer's A beta peptide studied by fluorescence. *Bioorg. Med. Chem. Lett.* **9**, 2243–2248.

Hardy J. and Selkoe D. J. (2002) The amyloid hypothesis of Alzheimer's disease: progress and problems on the road to therapeutics. *Science* **297**, 353–356.

Harper J. D. and Lansbury P. T. Jr (1997) Models of amyloid seeding in Alzheimer's disease and scrapie: mechanistic truths and physiological consequences of the time-dependent solubility of amyloid proteins. *Annu. Rev. Biochem.* **66**, 385–407.

Huang T. H., Fraser P. E. and Chakrabartty A. (1997) Fibrillogenesis of Alzheimer Abeta peptides studied by fluorescence energy transfer. *J. Mol. Biol.* **269**, 214–224.

Huang X., Cuajungco M. P., Atwood C. S. *et al.* (1999) Cu(II) potentiation of Alzheimer abeta neurotoxicity. Correlation with cell-free hydrogen peroxide production and metal reduction. *J. Biol. Chem.* **274**, 37111–37116.

Huang J., Yao Y., Lin J., Ye Y. H., Sun W. Y. and Tang Dagger W. X. (2004) The solution structure of rat Abeta-(1-28) and its interaction with zinc ion: insights into the scarcity of amyloid deposition in aged rat brain. *J. Biol. Inorg. Chem.* **9**, 627–635.

Hutchinson R. W., Cox A. G., McLeod C. W., Marshall P. S., Harper A., Dawson E. L. and Howlett D. R. (2005) Imaging and spatial distribution of beta-amyloid peptide and metal ions in Alzheimer's plaques by laser ablation-inductively coupled plasma-mass spectrometry. *Anal. Biochem.* **346**, 225–233.

Jiao Y. and Yang P. (2007) Mechanism of Copper(II) inhibiting Alzheimer's amyloid beta-peptide from aggregation: a molecular dynamics investigation. *J. Phys. Chem. B.* **111**, 7646–7655.

Kägi J. H. R. (1993) Evolution, structure and chemical activity of class-I metallothioneins: an overview, in *Methallothionein-III: Biological Roles and Medical Implications* (Suzuki K. T., Imura N. and Kimura M., eds), pp. 29–56. Birkhäuser, Basel; Boston; Berlin.

Klug G. M., Losic D., Subasinghe S. S., Aguilar M. I., Martin L. L. and Small D. H. (2003) Beta-amyloid protein oligomers induced by metal ions and acid pH are distinct from those generated by slow spontaneous ageing at neutral pH. *Eur. J. Biochem.* **270**, 4282–4293.

Konoha K., Sadakane Y. and Kawahara M. (2006) Zinc neurotoxicity and its role in neurodegenerative diseases. *J. Health Sci.* **52**, 1–8.

Lannfelt L., Blennow K., Zetterberg H. *et al.* (2008) Safety, efficacy, and biomarker findings of PBT2 in targeting Abeta as a modifying therapy for Alzheimer's disease: a phase IIa, double-blind, randomised, placebo-controlled trial. *Lancet Neurol.* **7**, 779–786.

Lee J. Y., Cole T. B., Palmiter R. D., Suh S. W. and Koh J. Y. (2002) Contribution by synaptic zinc to the gender-disparate plaque formation in human Swedish mutant APP transgenic mice. *Proc. Natl Acad. Sci. USA* **99**, 7705–7710.

Liao L., Cheng D., Wang J. *et al.* (2004) Proteomic characterization of postmortem amyloid plaques isolated by laser capture microdissection. *J. Biol. Chem.* **279**, 37061–37068.

Lomakin A., Chung D. S., Benedek G. B., Kirschner D. A. and Teplow D. B. (1996) On the nucleation and growth of amyloid beta-protein fibrils: detection of nuclei and quantitation of rate constants. *Proc. Natl Acad. Sci. USA* **93**, 1125–1129.

Lovell M. A., Robertson J. D., Teesdale W. J., Campbell J. L. and Markesbery W. R. (1998) Copper, iron and zinc in Alzheimer's disease senile plaques. *J. Neurol. Sci.* **158**, 47–52.

Meloni G., Sonois V., Delaine T., Guilloreau L., Gillet A., Teissie J., Faller P. and Vasak M. (2008) Metal swap between Zn7-metallothionein-3 and amyloid-beta-Cu protects against amyloid-beta toxicity. *Nat. Chem. Biol.* **4**, 366–372.

Meyer-Luehmann M., Coomaraswamy J., Bolmont T. *et al.* (2006) Exogenous induction of cerebral beta-amyloidogenesis is governed by agent and host. *Science* **313**, 1781–1784.

Miller L. M., Wang Q., Telivala T. P., Smith R. J., Lanzirotti A. and Miklossy J. (2006) Synchrotron-based infrared and X-ray imaging shows focalized accumulation of Cu and Zn co-localized with beta-amyloid deposits in Alzheimer's disease. *J. Struct. Biol.* **155**, 30–37.

© 2009 The Authors
Journal Compilation © 2009 International Society for Neurochemistry,

Multhaup G., Ruppert T., Schlicksupp A., Hesse L., Beher D., Masters C. L. and Beyreuther K. (1997) Reactive oxygen species and Alzheimer's disease. *Biochem. Pharmacol.* **54**, 533–539.

Nelson R., Sawaya M. R., Balbirnie M., Madsen A. O., Riekel C., Grothe R. and Eisenberg D. (2005) Structure of the cross-beta spine of amyloid-like fibrils. *Nature* **435**, 773–778.

Noy D., Solomonov I., Sinkevich O., Arad T., Kjaer K. and Sagi I. (2008) Zinc-amyloid beta interactions on a millisecond time-scale stabilize non-fibrillar Alzheimer-related species. *J. Am. Chem. Soc.* **130**, 1376–1383.

Page B., Page M. and Noel C. (1993) A new fluorometric assay for cytotoxicity measurements in-vitro. *Int. J. Oncology* **3**, 473–476.

Petkova A. T., Yau W. M. and Tycko R. (2006) Experimental constraints on quaternary structure in Alzheimer's beta-amyloid fibrils. *Biochemistry* **45**, 498–512.

Raman B., Ban T., Yamaguchi K., Sakai M., Kawai T., Naiki H. and Goto Y. (2005) Metal ion-dependent effects of clioquinol on the fibril growth of an amyloid-beta peptide. *J. Biol. Chem.* **280**, 16157–16162.

Ricchelli F., Drago D., Filippi B., Tognon G. and Zatta P. (2005) Aluminum-triggered structural modifications and aggregation of beta-amyloids. *Cell. Mol. Life Sci.* **62**, 1724–1733.

Schlief M. L., Craig A. M. and Gitlin J. D. (2005) NMDA receptor activation mediates copper homeostasis in hippocampal neurons. *J. Neurosci.* **25**, 239–246.

Sjogren M., Vanderstichele H., Agren H. *et al.* (2001) Tau and Abeta42 in cerebrospinal fluid from healthy adults 21-93 years of age: establishment of reference values. *Clin. Chem.* **47**, 1776–1781.

Smith D. P., Smith D. G., Curtain C. C. *et al.* (2006) Copper-mediated amyloid-beta toxicity is associated with an intermolecular histidine bridge. *J. Biol. Chem.* **281**, 15145–15154.

Syme C. D. and Viles J. H. (2006) Solution (1)H NMR investigation of Zn(2+) and Cd(2+) binding to amyloid-beta peptide (Abeta) of Alzheimer's disease. *Biochim. Biophys. Acta* **1764**, 246–256.

Talmard C., Guilloreau L., Coppel Y., Mazarguil H. and Faller P. (2007) Amyloid-beta peptide forms monomeric complexes with Cu(II) and Zn(II) prior to aggregation. *Chembiochem* **8**, 163–165.

Tougu V., Karafin A. and Palumaa P. (2008) Binding of zinc(II) and copper(II) to the full-length Alzheimer's amyloid-beta peptide. *J. Neurochem.* **104**, 1249–1259.

Tsuji S., Kobayashi H., Uchida Y., Ihara Y. and Miyatake T. (1992) Molecular cloning of human growth inhibitory factor cDNA and its down-regulation in Alzheimer's disease. *EMBO J.* **11**, 4843–4850.

Tycko R. (2003) Insights into the amyloid folding problem from solid-state NMR. *Biochemistry* **42**, 3151–3159.

Uchida Y., Gomi F., Masumizu T. and Miura Y. (2002) Growth inhibitory factor prevents neurite extension and the death of cortical neurons caused by high oxygen exposure through hydroxyl radical scavenging. *J. Biol. Chem.* **277**, 32353–32359.

Walsh D. M. and Selkoe D. J. (2007) A beta oligomers – a decade of discovery. *J. Neurochem.* **101**, 1172–1184.

White A. R., Du T., Laughton K. M. *et al.* (2006) Degradation of the Alzheimer disease amyloid beta-peptide by metal-dependent up-regulation of metalloprotease activity. *J. Biol. Chem.* **281**, 17670–17680.

Yoshiike Y., Tanemura K., Murayama O., Akagi T., Murayama M., Sato S., Sun X., Tanaka N. and Takashima A. (2001) New insights on how metals disrupt amyloid beta-aggregation and their effects on amyloid-beta cytotoxicity. *J. Biol. Chem.* **276**, 32293–32299.

Yu W. H., Lukiw W. J., Bergeron C., Niznik H. B. and Fraser P. E. (2001) Metallothionein-III is reduced in Alzheimer's disease. *Brain Res.* **894**, 37–45.

Zirah S., Kozin S. A., Mazur A. K., Blond A., Cheminant M., Segalas-Milazzo I., Debey P. and Rebuffat S. (2006) Structural changes of region 1-16 of the Alzheimer disease amyloid beta-peptide upon zinc binding and in vitro aging. *J. Biol. Chem.* **281**, 2151–2161.

© 2009 The Authors
Journal Compilation © 2009 International Society for Neurochemistry,

PUBLICATION III

Karafin, A., P. Palumaa and V. Tõugu (2009)
"Monitoring of Amyloid-Beta Fibrillization Using an Improved Fluorimetric Method."
New Trends Alzheimer Parkinson Relat. Disord.: AD/PD 2009, 9th , Medimond 255-261.

Monitoring of Aβ fibrillization using an improved fluorimetric method.

Karafin A., Palumaa P. and Tõugu V.

Department of Gene Technology, Tallinn University of Technology, Tallinn, Estonia

Abstract

Fast Abeta fibrillation was achieved in agitated solutions of defibrillized peptide monitored by increase of ThT fluorescence present in the mixture. The elaborated protocol can be applied for physico-chemical studies of the fibrillation process as well as for screening of fibrillation inhibitors.

Introduction

Alzheimer's disease (AD) is a progressive neurodegenerative disease characterized by amyloid deposits in the brain that are composed mainly from fibrillar amyloid-β (Aβ) peptides (*1*). The mechanism for amyloid formation is suggested to occur through a nucleation-dependent polymerization of Aβ peptides and formation of cross-β amyloid core (*2-5*).

Thioflavin T (ThT) is a fluorogenic dye widely used in the studies of protein fibrillation. The protocols used for the studies of Aβ fibrillation are often time and material consuming and poorly reproducible. On the other hand, there is data indicating that agitation can sufficiently accelerate Aβ fibrillation and ThT dye has a weak effect on the fibrillation (*6, 7*). The aim of the present study was to elaborate a fast and reliable method for monitoring the fibrillation of Aβ, which can be used for the determination of the effect of various endogenic and exogenic factors on Aβ fibrillation.

Materials and Methods.

$A\beta_{42}$ peptide (1 mg) from rPeptide (Athens, USA) was treated with 1,1,1,3,3,3-hexafluoro-2-propanol (HFIP) to disassemble preformed aggregates.

Fibrillation of 5 μM $A\beta_{42}$ was monitored by an increase in the ThT fluorescence intensity at 480 nm (λex=445 nm) on a Perkin-Elmer LS-45 fluorimeter equipped with a magnetic stirrer (250 rpm) in 20 mM HEPES and 100 mM NaCl, pH 7.4 containing 3.3 μM of ThT.

©2009 by MEDIMOND s.r.l.

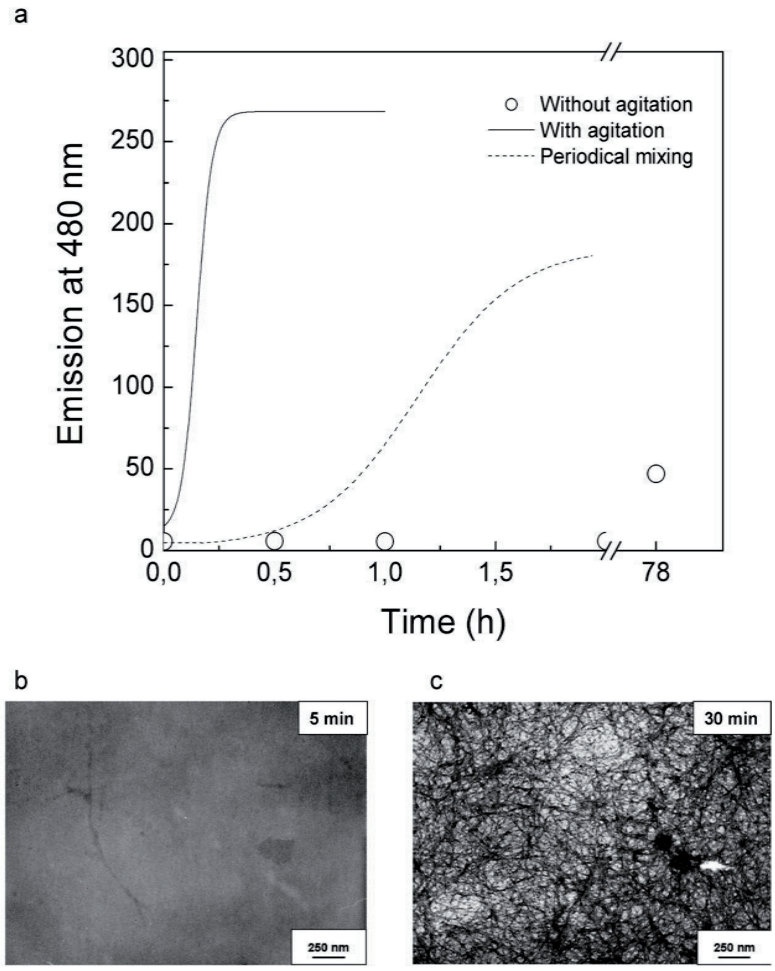

Figure 1. Effect of mixing on Aβ42 fibrillation followed by ThT fluorescence (a) and TEM images are taken after 5 min (b) and 30 min (c) of incubation with agitation.

The kinetic parameters for fibrillation were determined by fitting the time curve of fluorescence intensity to Boltzmann equation:

$$y = \frac{A_2 - A_1}{1 + e^{(t-to)\cdot k}} + A_2 \qquad (1)$$

where A_1 is the initial fluorescence level, A_2 – maximal fluorescence intensity, t_0 – is the time when fluorescence is reached half maximum and k – is the rate constant of the fibril elongation.

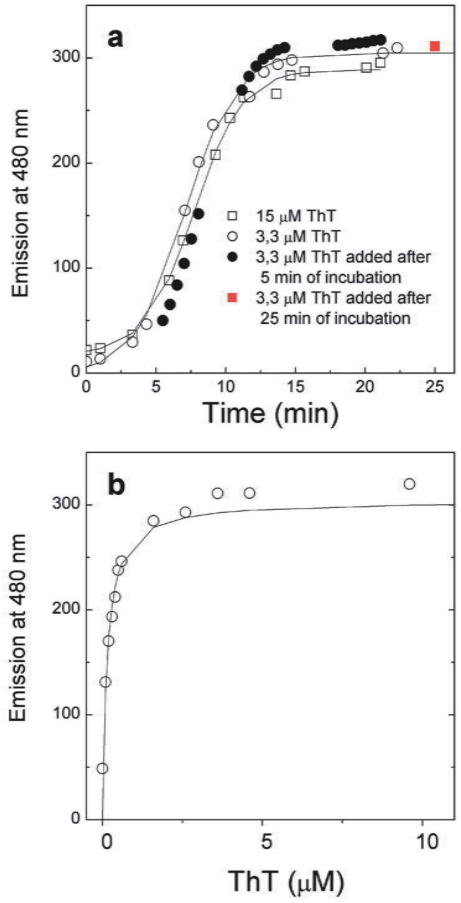

Figure 2. Effect of ThT on Aβ42 aggregation. Aβ42 was incubated in a quartz cell with continuous agitation with 3.3 μM or 15 μM ThT. In a separate experiment ThT was added at different time points. Solid lines correspond to Eq. 1. - (a). Titration of 5 μM Aβ42 solution preincubated for 30 min under agitated conditions with ThT - (b)

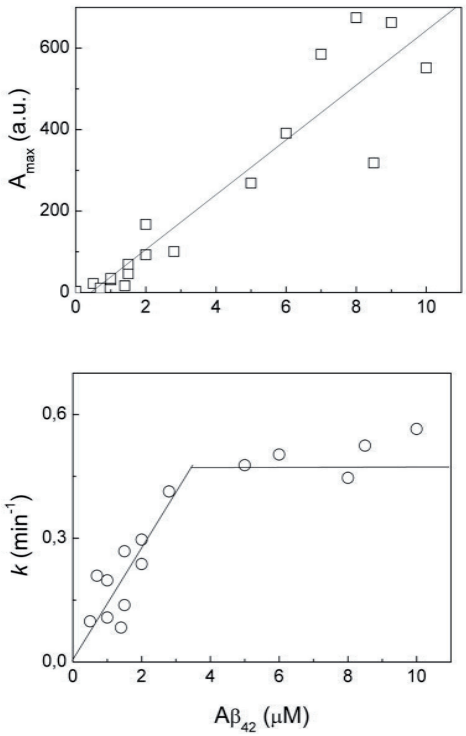

Figure 3. Effect of Aβ concentration on the peptide aggregation. Amax and k values were calculated according to Eq. 1.

Results

First, we established experimental conditions for fast and reproducible monitoring of $A\beta_{42}$ fibrillation. For this purpose the fibrillation process was continuously monitored by an increase in ThT fluorescence present in the incubation mixture. Fast fibrillation of "unseeded" Aβ was observed only in agitated solutions (Fig.1a). The typical sigmoidal growth curves observed could be described by Boltzmann equation (Eq.1). In quiescent Aβ solutions the fibrillation process was extremely slow and only

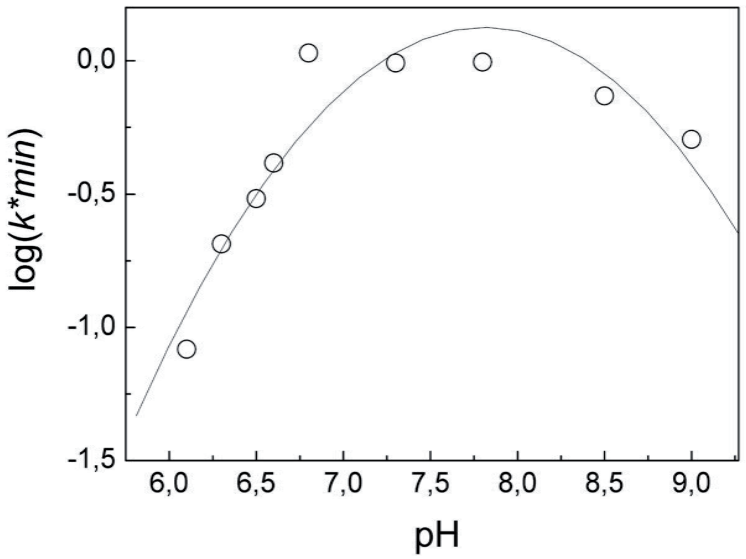

Figure 4. Effect of pH on the Aβ42 aggregation rate. k values were calculated from fits of the data to Boltzmann equation (Eq. 1).

a slight increase in the ThT fluorescence was observed during prolonged incubation (3-5 days). The presence of Aβ fibrils in the growth phase and in the end phase of fibrillation was checked with TEM (Fig.1b,c).

We found that ThT concentration of 3.3 μM is sufficient to monitor the fibrillation (Fig.2b) as increase of ThT concentrations up to 15 μM did not affect the kinetics of $A\beta_{42}$ fibrillation (Fig.2a). Also there was no difference in the kinetics if ThT was added to the aliquots of fibrillization mixture and thus, the fibrillation of $A\beta_{42}$ can be monitored continuously using ThT signal. All further fibrillation measurements were carried out with agitations on magnetic stirrer at 250 rpm in the presence of 3.3 μM ThT.

The intensity of the ThT fluorescence in the end of the incubation depended linearly on the Aβ concentration (Fig.3). The fibrillation rate constant *k* was independent on the peptide concentration in the range from 2 to 10 μM which confirms that it is a reliable kinetic constant useful for quantitative characterization of the fibrillation process (Fig.3).

The fibrillation rate constant *k* did not change in the pH range from 7 to 9, but started to decrease below 7 (Fig.4). The decrease arises most likely due to protonation of His residues.

Conclusions

The influence of different Aβ aggregation effectors and environmental factors on the peptide fibrillation can be studied in a fast and reproducible way in well-agitated solutions by monitoring the fluorescence intensity of ThT dye present in the reaction

mixture. The knowledge about Aβ aggregation mechanism is required for understanding the pathogenic mechanism of amyloidogenesis in AD.

References

1. L. Liao *et al.*, Proteomic characterization of postmortem amyloid plaques isolated by laser capture microdissection *J Biol Chem* **279**, 37061-37068 2004.
2. E. M. Castano *et al.*, The length of amyloid-beta in hereditary cerebral hemorrhage with amyloidosis, Dutch type. Implications for the role of amyloid-beta 1-42 in Alzheimer's disease *J Biol Chem* **271**, 32185-32191 1996.
3. A. Lomakin, D. S. Chung, G. B. Benedek, D. A. Kirschner, D. B. Teplow, On the nucleation and growth of amyloid beta-protein fibrils: detection of nuclei and quantitation of rate constants *Proc Natl Acad Sci U S A* **93**, 1125-1129 1996.
4. J. D. Harper, P. T. Lansbury, Jr., Models of amyloid seeding in Alzheimer's disease and scrapie: mechanistic truths and physiological consequences of the time-dependent solubility of amyloid proteins *Annu Rev Biochem* **66**, 385-407 1997.
5. W. P. Esler *et al.*, Alzheimer's disease amyloid propagation by a template-dependent dock-lock mechanism *Biochemistry* **39**, 6288-6295 2000.
6. D. P. Smith *et al.*, Copper-mediated amyloid-beta toxicity is associated with an intermolecular histidine bridge *J Biol Chem* **281**, 15145-15154 2006.
7. G. T. Dolphin, M. Ouberai, P. Dumy, J. Garcia, Designed Amyloid beta Peptide Fibril-A Tool for High-Throughput Screening of Fibril Inhibitors *ChemMedChem* **2**, 1613-1623 2007.

PUBLICATION IV

Zovo, K., E. Helk, **A. Karafin**, V. Tõugu and P. Palumaa (2010)
"Label-Free High-Throughput Screening Assay for Inhibitors of Alzheimer's Amyloid-B Peptide Aggregation Based on MALDI MS."
Anal. Chem. **82**(20): 8558-8565.

Anal. Chem. **2010,** *82,* 8558–8565

Label-Free High-Throughput Screening Assay for Inhibitors of Alzheimer's Amyloid-β Peptide Aggregation Based on MALDI MS

Kairit Zovo, Eneken Helk, Ann Karafin, Vello Tõugu, and Peep Palumaa*

Department of Gene Technology, Tallinn University of Technology, Akadeemia tee 15, Tallinn 12618, Estonia

Aggregation of amyloid-β (Aβ) peptides is causatively linked to Alzheimer's disease (AD); thus, suppression of this process by small molecule inhibitors is a widely accepted therapeutic and preventive strategy for AD. Screening of the inhibitors of Aβ aggregation deserves much attention; however, despite intensive efforts, there are only a few high-throughput screening methods available, all of them having drawbacks related to the application of external fluorescent probes or artificial Aβ derivatives. We have developed a label-free MALDI MS-based screening test for inhibitors of Aβ_{42} fibrillization that exhibits high sensitivity, speed, and automation possibilities suitable for high-throughput screening. The test was evaluated by transmission electron microscopy and compared with a fluorimetric thioflavin-based assay, where interference of a number of tested compounds with thioflavin T binding and/or fluorescence caused false-positive results. The MALDI MS-based method can significantly speed up in vitro screening of compound libraries for inhibitors of Aβ_{42} fibrillization.

Alzheimer's disease (AD) is an age-dependent neurodegenerative disorder, affecting almost every fifth person at the age of 75−85 years and every other person aged over 85 years. As the population in developed countries ages, the number of people afflicted by AD is expected to increase dramatically. Currently there is still no effective treatment available for AD patients, and their nursing is associated with high and increasing care and medication costs.[1] Given these trends, there is a tremendous need to develop effective therapeutics or preventive tools for AD.

The description of AD pathology by Alois Alzheimer in 1906[2] and the definitive diagnosis of AD nowadays imply the presence of proteinaceous aggregates in the brain.[3] Major extracellular aggregates called amyloid plaques are composed mainly of amyloid-β (Aβ) peptides[4] produced by the proteolytic cleavage of amyloid precursor protein (APP) by β- and γ-secretases.[3a] Major Aβ peptides are composed of 40 and 42 amino acid residues. Aβ_{40} is produced in great abundance in the brain, but Aβ_{42} forms aggregates more readily and comprises the major component of amyloid plaques.[5] Numerous genetic and biochemical studies confirm that Aβ aggregation in the brain triggers a cascade of events leading to the development of intracellular neurofibrillar tangles and neurodegeneration.[3,6] Thus, compounds that inhibit the production and/or aggregation of Aβ are attractive candidates as therapeutics for the prevention and/or treatment of AD as they target the underlying molecular cause of AD.[7]

Since the discovery of the amyloid pathway and the formulation of the amyloid cascade hypothesis, many efforts have been made to find inhibitors of Aβ aggregation/fibrillization.[8] During the recent decade many small molecules that inhibit aggregation/fibrillization of Aβ in vitro have been identified,[7,9] and it has been shown that such types of compounds inhibit Aβ aggregation/fibrillization also in transgenic animal models.[10] Moreover, small molecule methylene blue, which exerts a broad spectrum of pharmacological actions including inhibition of Aβ_{42} oligomerization[11] and fibrillization of other amyloidogenic proteins such as τ,[12] has also been successfully tested in phase II clinical trials, where it slowed cognitive decline of AD patients.[13]

Despite the relative success, the search for effective inhibitors of Aβ aggregation/fibrillization is still complicated by two major hindrances: First, application of structure-based rational drug design is limited since Aβ peptides are conformationally labile and

* To whom correspondence should be addressed. E-mail: peepp@staff.ttu.ee. Phone: +372 6204410. Fax: +372 6204401.

(1) Foster, J. K.; Verdile, G.; Bates, K. A.; Martins, R. N. *Mol. Psychiatry* **2009**, *14*, 239–251.
(2) Alzheimer, A. *Allg. Z. Psychiatr. Psych.-Gerichtl. Med.* **1907**, *64*, 146–148.
(3) (a) Blennow, K.; de Leon, M. J.; Zetterberg, H. *Lancet* **2006**, *368*, 387–403. (b) Hardy, J. *Neuron* **2006**, *52*, 3–13.
(4) Liao, L.; Cheng, D.; Wang, J.; Duong, D. M.; Losik, T. G.; Gearing, M.; Rees, H. D.; Lah, J. J.; Levey, A. I.; Peng, J. *J. Biol. Chem.* **2004**, *279*, 37061–37068.
(5) (a) Roher, A. E.; Lowenson, J. D.; Clarke, S.; Woods, A. S.; Cotter, R. J.; Gowing, E.; Ball, M. J. *Proc. Natl. Acad. Sci. U.S.A.* **1993**, *90*, 10836–10840. (b) Gravina, S. A.; Ho, L.; Eckman, C. B.; Long, K. E.; Otvos, L., Jr.; Younkin, L. H.; Suzuki, N.; Younkin, S. G. *J. Biol. Chem.* **1995**, *270*, 7013–7016. (c) Jarrett, J. T.; Berger, E. P.; Lansbury, P. T., Jr. *Biochemistry* **1993**, *32*, 4693–4697.
(6) (a) Hardy, J. A.; Higgins, G. A. *Science* **1992**, *256*, 184–185. (b) Hardy, J. *J. Alzheimer's Dis.* **2006**, *9*, 151–153.
(7) Estrada, L. D.; Soto, C. *Curr. Top. Med. Chem.* **2007**, *7*, 115–126.
(8) (a) LeVine, H., III. *J. Alzheimer's Dis.* **2004**, *6*, 303–314. (b) Ritchie, C. W.; Bush, A. I.; Masters, C. L. *Expert Opin. Invest. Drugs* **2004**, *13*, 1585–1592. (c) Rochet, J. C. *Expert Rev. Mol. Med.* **2007**, *9*, 1–34.
(9) (a) Hamaguchi, T.; Ono, K.; Yamada, M. *Cell. Mol. Life Sci.* **2006**, *63*, 1538–1552. (b) LeVine, H., III. *Amyloid* **2007**, *14*, 185–197. (c) Necula, M.; Kayed, R.; Milton, S.; Glabe, C. G. *J. Biol. Chem.* **2007**, *282*, 10311–10324.
(10) Hamaguchi, T.; Ono, K.; Murase, A.; Yamada, M. *Am. J. Pathol.* **2009**, *175*, 2557–2565.
(11) Necula, M.; Breydo, L.; Milton, S.; Kayed, R.; van der Veer, W. E.; Tone, P.; Glabe, C. G. *Biochemistry* **2007**, *46*, 8850–60.
(12) Wischik, C. M.; Edwards, P. C.; Lai, R. Y.; Roth, M.; Harrington, C. R. *Proc. Natl. Acad. Sci. U.S.A.* **1996**, *93*, 11213–8.
(13) (a) Gura, T. *Nat. Med.* **2008**, *14*, 894. (b) Oz, M.; Lorke, D. E.; Petroianu, G. A. *Biochem. Pharmacol.* **2009**, *78*, 927–32.

10.1021/ac101583q © 2010 American Chemical Society
Published on Web 09/21/2010

the structure of the Aβ conformer(s) crucial for aggregation is not known. Accordingly, the inhibitors of Aβ aggregation can mainly be searched for by extensive screening of large libraries rather than by rational design. Second, Aβ aggregation is a complicated multistep process that may be affected by subtle changes in the structure of Aβ peptides, external ligands, and environmental conditions, and the success in identifying effective inhibitors depends largely on the reliability and performance of the screening test used.

Screening for the inhibitors of Aβ aggregation has been conducted using several different methods characterized by inherent advantages and disadvantages.[7] The most common techniques for in vitro monitoring of the Aβ aggregation apply amyloid-binding dyes such as thioflavin T (ThT), Congo red, and others, exhibiting spectral changes upon binding to amyloid fibrils.[14] Although these dyes have proven useful in aggregation studies, their mechanism of action and possible contribution to the aggregation are not fully understood. Moreover, their signals can be substantially affected by the compounds tested as potential inhibitors, which may lead to unreliable results.[15] As a rule, a common ThT-based screening test requires prolonged periods of time reaching up to 12 h or use of artificial peptide sequences.[16] Several cell-based assays have also been developed for searching the inhibitors of Aβ aggregation.[17] These methods make use of fusion proteins such as GFP−Aβ; however, the aggregation properties of fusion proteins might differ from those of native Aβ peptide. Moreover, potential drug candidates that do not pass cellular membranes or bacterial cell walls cannot be detected in the cell-based assays.

Mass spectrometry is a contemporary and very promising technique for high-throughput screening; however, its application for the screening of the inhibitors of Aβ aggregation has been quite limited. An attempt has been made to use LC−ESI MS for screening of Aβ aggregation inhibitors;[18] however, LC−MS analysis is a relatively slow and expensive technique that is not very suitable for high-throughput screening. At the same time, MALDI-TOF MS, which has superior potential for development of high-throughput screening tests, has not been used for this purpose yet.

In the present study we developed a highly sensitive, fast, and automated screening assay for inhibitors of Aβ aggregation based on monitoring of the loss of $A\beta_{42}$ monomer from solution by MALDI-TOF MS. The assay provides a unique possibility to work in a label-free system containing only native $A\beta_{42}$ peptide and the compounds tested. The applicability of the test was evaluated using 80 compounds including known inhibitors of Aβ aggregation, and comparison of the obtained results with the fluorimetric ThT assay identified several false-positive responses in the ThT-based test. The elaborated screening test can significantly speed up and increase the reliability of the initial in vitro screening of AD drug candidates and identify active compounds suitable for further detailed studies.

EXPERIMENTAL SECTION

Materials. Lyophilized $A\beta_{42}$ peptide (ultra pure, recombinant) was purchased from rPeptide (Bogart, GA) in the HFIP (1,1,1,3,3,3-hexafluoro-2-propanol) form. HEPES (ultrapure, MB grade) was from USB Corp. (Cleveland, OH). Insulin, ThT, and $CuCl_2 \cdot 2H_2O$ were from Sigma-Aldrich (St. Louis, MO); $ZnCl_2$ and NaCl were extrapure from Scharlau (Barcelona, Spain). α-Cyano-4-hydroxycinnamic acid (CHCA), 3,5-dimethoxy-4-hydroxycinnamic acid (SA), and 2,5-dihydroxybenzoic acid (DHB) were from Fluka (Buchs, Switzerland). Trifluoroacetic acid (TFA) was from Riedel de-Haën (Seelze, Germany), and acetonitrile (AcN) was from Rathburn (Walkerburn, U.K.). The list of compounds tested as putative inhibitors of the fibrillization is presented in Supporting Information Table S-1. All solutions were prepared in fresh Milli-Q water. Electron microscopy grids were obtained from Ted Pella, Inc. (Redding, CA).

Preparation of MALDI Matrixes. Several commercial MALDI MS matrixes (CHCA, SA, and DHB) in solution with different AcN and TFA contents were tested for quantitative determination of $A\beta_{42}$. Matrix compounds (10 mg/mL) were dissolved in 50−70% AcN−water containing 0.1−0.3% TFA. After vortexing, the solutions were centrifuged for 3 min at 6000 rpm, and the supernatant was collected. From the matrixes tested, the highest sensibility and the best reproducibility were observed with 10 mg/mL CHCA matrix dissolved in 60% AcN and 0.3% TFA, which was used throughout the following study.

MALDI-TOF MS Measurements. $A\beta_{42}$ solution was mixed with matrix solution at a ratio of 1:2 on 100-well MALDI plates by using an Ettan Spotter (Amersham Biosciences, Sweden), and the spots were air-dried. MALDI MS spectra were registered on a Voyager DE STR BioSpectrometry workstation (Applied Biosystems, Foster City, CA) in the linear mode. Instrument parameters in the reflector mode: accelerating voltage, 25000 V; grid voltage, 65%; delay time, 500 ns; shots per spectrum, 100 (CHCA), 50 (DHB), 30 (SA); mass range, 1500−10000 Da; low mass gate, 600 Da; laser intensity, 2250 V; number of spectra accumulated, 10. Instrument parameters in the linear mode: accelerating voltage, 25000 V; grid voltage, 93%; delay time, 485 ns; shots per spectrum, 40; mass range, 1500−10000 Da; low mass gate, 1000 Da; laser intensity, 1900 V; number of spectra accumulated, 10. Spectra were recorded in the automatic regime controlled by the program Sequence Control (Applied Biosystems). The spectra were processed with Data Explorer software (version 4, Applied Biosystems).

MALDI-TOF MS Calibration Curves. To elaborate the conditions for the quantitative MALDI-TOF MS measurements, first a series of MALDI MS measurements at a 0.1−2 μM concentration of insulin were recorded and the corresponding MS peak intensity was correlated with the peptide concentration. In another series of experiments, the concentration of $A\beta_{42}$ was varied between 0.0625 and 12 μM and the concentration of insulin was kept constant (0.3 μM). Insulin was added to the matrix solution before automatic spotting. MS measurements were performed in the linear mode as described above, and

(14) (a) Esler, W. P.; Stimson, E. R.; Ghilardi, J. R.; Felix, A. M.; Lu, Y. A.; Vinters, H. V.; Mantyh, P. W.; Maggio, J. E. *Nat. Biotechnol.* **1997**, *15*, 258–263. (b) Blanchard, B. J.; Chen, A.; Rozeboom, L. M.; Stafford, K. A.; Weigele, P.; Ingram, V. M. *Proc. Natl. Acad. Sci. U.S.A.* **2004**, *101*, 14326–14332.

(15) Hudson, S. A.; Ecroyd, H.; Kee, T. W.; Carver, J. A. *FEBS J.* **2009**, *276*, 5960–72.

(16) Dolphin, G. T.; Ouberai, M.; Dumy, P.; Garcia, J. *ChemMedChem* **2007**, *2*, 1613–1623.

(17) (a) Kim, W.; Kim, Y.; Min, J.; Kim, D. J.; Chang, Y. T.; Hecht, M. H. *ACS Chem. Biol.* **2006**, *1*, 461–9. (b) Hong, H. S.; Maezawa, I.; Yao, N.; Xu, B.; Diaz-Avalos, R.; Rana, S.; Hua, D. H.; Cheng, R. H.; Lam, K. S.; Jin, L. W. *Brain Res.* **2007**, *1130*, 223–34.

(18) Cheng, X.; van Breemen, R. B. *Anal. Chem.* **2005**, *77*, 7012–7015.

the concentration of $A\beta_{42}$ was correlated with the fractional content of $A\beta_{42}$ in the MALDI MS spectra, calculated from the peak heights after automatic baseline correction (intensities).

$A\beta_{42}$ Aggregation Assay. A stock solution of $A\beta_{42}$ peptides was prepared as follows: An $A\beta_{42}$ HFIP film was dissolved in water containing 0.02% NH_3 at a concentration of 10−20 μM and vortexed for 1 min. After 10 min of incubation the $A\beta_{42}$ stock solution was diluted in HEPES buffer with a final concentration of 20 mM, pH 7.3, containing a fixed concentration of tested compounds. Aggregation of HFIP-treated $A\beta$ peptide was induced by addition of 2−10% (v/v) $A\beta_{42}$ fibrillar seeds. $A\beta_{42}$ fibrils were prepared by stirring a 5 μM $A\beta_{42}$ solution in 20 mM HEPES, 0.1 M NaCl, pH 7.3, for 1 h, which is sufficient to complete $A\beta_{42}$ fibrillization under the particular conditions.[19] The fibril formation was also confirmed by ThT fluorescence measurements of an aliquot from the fibrillization mixture. $A\beta_{42}$ seeds were obtained from the fibrils by sonication of the solution at 130 W, 20 kHz, and amplitude 50% pulse 05:10 for 1 min (Sonics Vibra-Cell, Newtown, CT). The seeds were used within 1 h of their preparation.

Monitoring $A\beta_{42}$ Fibrillization by ThT Fluorescence. ThT fluorescence assay to monitor $A\beta_{42}$ fibrillization was performed as described earlier.[19] Briefly, 5 μM $A\beta_{42}$ in 20 mM HEPES, 0.1 M NaCl, pH 7.3, containing 3.3 μM ThT was incubated in a 0.5 cm path length quartz cell and agitated with a magnetic stirrer at 250 rpm. The ThT fluorescence measurements were performed on a Perkin-Elmer LS-45 fluorescence spectrometer at $\lambda_{ex} = 440$ nm and $\lambda_{em} = 480$ nm.

Validation of the MALDI MS screening assay was performed by diluting an aliquot of the $A\beta_{42}$ solution in 20 mM HEPES, pH 7.3, incubated with added seeds under quiescent conditions in the fluorescence microcuvette containing 0.1 mL of 3.3 μM ThT solution. The curves were fitted to first-order rate equations using the program Origin 6 (OriginLab, Northhampton, MA).

Transmission Electron Microscopy. $A\beta_{42}$ incubation mixtures were centrifuged (30 min, 12000*g*), 3 μL of the sedimented probe was pipetted into electron microscopy grids, and the probes were air-dried. The grids were brought into contact with 2% (w/v) uranyl acetate, incubated for 10 min, and washed with Milli-Q water. Transmission electron microscopy (TEM) images from the samples were created on a SELMI-SUMY EM-125 instrument at a 75 kV accelerating voltage and recorded onto high-resolution, 60 × 90 mm negative film.

RESULTS

Determination of the $A\beta_{42}$ Concentration by MALDI-TOF MS. $A\beta_{42}$ aggregation can be monitored by quantitative detection of the concentration of soluble $A\beta_{42}$ during aggregation. At the level of individual measurements the MALDI MS technique is generally not quantitative; we observed variation in the intensities of the MALDI MS peaks, which is common for MALDI-TOF measurements and is caused by many factors such as (i) the quality of the individual MALDI spot, (ii) the microstructure of the laser-excited location on the spot, and (iii) the laser intensity used, among other factors. However, quantitative data can be obtained by using a special approach. First, the data must be averaged from different randomly chosen locations in the spot. MALDI MS experiments with different peptides (insulin, insulin β-chain) demonstrated that computing an average of 10 individual measurements from different locations in the spot chosen by a predefined pattern gives a relatively good linear correlation between the peak intensity and the concentration of the peptide in the sample. This procedure was used in all following MALDI MS experiments. Further, to eliminate matrix-dependent variations and to improve reproducibility, an internal standard was introduced. Although deuterated $A\beta_{42}$ and an $A\beta_{42}$ with one or more modified residues are most suitable as internal standards for determination of the $A\beta_{42}$ concentration, these peptides have several disadvantages in application as internal standards in the fibrillization assay: (i) solutions of deuterated or modified $A\beta$ are unstable as they have a tendency for fibrillization; (ii) to get MALDI peaks with similar intensities, these internal standards must be used at micromolar concentrations similar to those of native $A\beta_{42}$, where they can cofibrillize with the probe during spot drying or within the matrix solution; (iii) the use of deuterized $A\beta_{42}$ would considerably increase the cost of the test. After testing of several peptides we have selected insulin as the internal standard as it has a molecular weight close to that of $A\beta_{42}$ and exhibits a good ionization efficiency and solutions of insulin showed the best stability and reproducibility of MALDI MS spectra. The optimal concentration of insulin was 0.3 μM. To achieve better automation, the insulin was added to the matrix solution before spotting. MALDI MS spectra from samples with different concentrations of $A\beta_{42}$ and 0.3 μM insulin are presented in Figure 1a. The correlation between the relative peak intensity of $A\beta_{42}$ compared to the sum of the peak intensities for $A\beta_{42}$ and insulin and the concentration of $A\beta_{42}$ in the sample is provided in Figure 1b. The obtained linear dependence demonstrates the applicability of MALDI-TOF MS for quantitative determination of the $A\beta_{42}$ concentration in the micromolar range suitable for performing fibrillization experiments. The small *y*-intercept value in Figure 1b arises because of the noise in the baseline that makes a small contribution to peak heights after automatic baseline correction.

Monitoring of $A\beta_{42}$ Fibrillization by MALDI-TOF MS. To ensure the reproducibility of the fibrillization process, an alkaline solution of HFIP-treated $A\beta_{42}$ was used as a stock solution. Fibrillization of $A\beta_{42}$ was initiated by diluting the alkaline stock solution of HFIP-treated $A\beta_{42}$ with HEPES buffer at a physiological pH value containing an appropriate amount (0.25 μM) of $A\beta_{42}$ seeds. $A\beta_{42}$ seeds that are seen as short fibril fragments in TEM images (Figure S-1a, Supporting Information) were prepared by sonication of preformed $A\beta_{42}$ fibrils. At different time points aliquots from the reaction mixture were spotted together with an insulin-containing matrix solution onto MALDI plates and analyzed by MALDI-TOF MS. Figure 2a shows that in the absence of seeds the 5 μM $A\beta_{42}$ solution was stable at least for 1 h, whereas after addition of $A\beta_{42}$ seeds a relatively fast decrease in the peak intensity of $A\beta_{42}$ was observed (Figure 2b). Disappearance of the $A\beta_{42}$ monomer peak in MALDI-TOF MS experiments occurs according to first-order kinetics characterized by the rate constant $k = 0.044 \pm 0.008$ min^{-1} ($\tau_{1/2}$

(19) Tõugu, V.; Karafin, A.; Zovo, K.; Chung, R. S.; Howells, C.; West, A. K.; Palumaa, P. *J. Neurochem.* **2009**, *110*, 1784–1795.

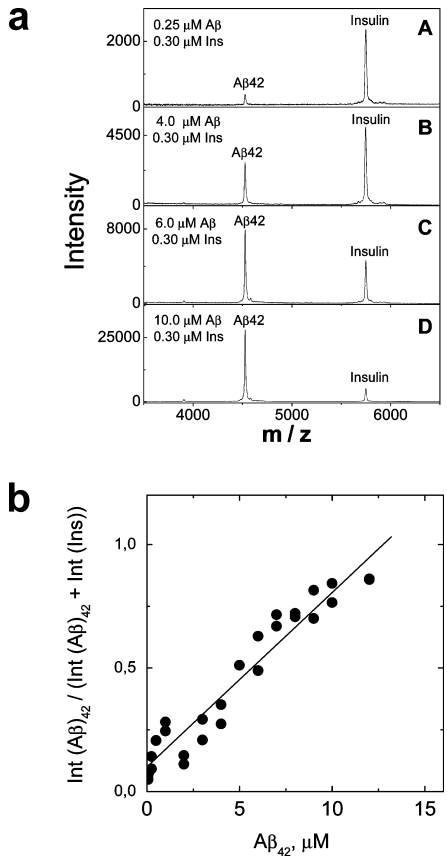

Figure 1. MALDI MS spectra of Aβ_{42}: (a) averaged spectra of different concentrations of Aβ_{42} in the presence of 0.3 μM insulin (A, 0.25 μM Aβ_{42}; B, 4 μM Aβ_{42}; C, 6 μM Aβ_{42}; D, 10 μM Aβ_{42}); (b) correlation between the concentration of Aβ_{42} and the ratio of the Aβ_{42} peak intensity to the sum of Aβ_{42} and insulin peak intensities in the MALDI MS spectra. The solid line corresponds to the linear fit.

$= 15.2 \pm 3.5$ min) (Figure 3a). After 60 min of incubation of 5 μM Aβ_{42} with seeds, the peak intensity decreased to 10% of the initial value and the presence of typical amyloid fibrils in the sample was detected by TEM (Figure S-1b). As a rule, Aβ_{42} preparations without HFIP pretreatment aggregated spontaneously without the addition of external Aβ_{42} seeds; however, batch to batch and day to day variation of the initial height of the peptide peak in MALDI MS spectra was large, and the reproducibility of the results on a quantitative level was poor. Therefore, HFIP-pretreated peptide and Aβ_{42} seeds were used in further experiments. Under the conditions used the seed-induced Aβ_{42} aggregation was almost completed within 60 min, which is suitable for fast screening.

The kinetics of seed-free Aβ_{42} fibrillization monitored by ThT fluorescence could be described as sigmoid curves, and the aggregation parameters were determined by fitting the plot of fluorescence intensity versus time to a Boltzmann curve:

$$y = \frac{A_2 - A_1}{1 + e^{(x - x_0)k}} + A_2 \quad (1)$$

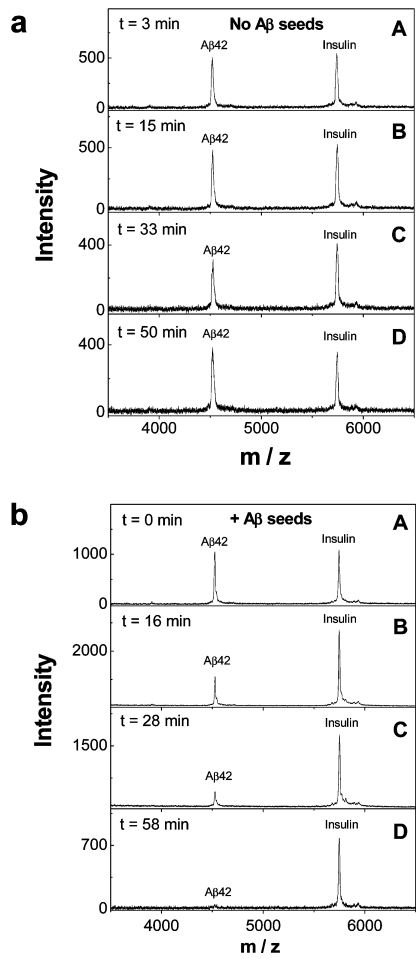

Figure 2. Dynamics of the Aβ_{42} peak in MALDI MS spectra: (a) averaged spectra of 5 μM Aβ_{42} registered at different incubation times in the presence of 0.3 μM insulin as an internal standard; (b) averaged spectra of 5 μM Aβ_{42} after addition of 0.25 μM Aβ_{42} fibrillar seeds registered in the presence of 0.3 μM insulin as an internal standard. Incubation conditions: 20 mM HEPES, pH 7.3, 25 °C.

where A_1 is the initial fluorescence level, A_2 corresponds to the fluorescence at the maximal fibrillization level, x_0 is the time when fluorescence reaches the half-maximum, and k is the rate constant of fibril growth. Fitting of the data was performed using the program Origin 6.

Validation of the MALDI-TOF MS Fibrillization Assay. To confirm that the disappearance of monomer peaks in MALDI-TOF MS experiments (Figure 3a) reflects the fibrillization of Aβ_{42}, the process was in parallel monitored by a ThT assay, which is a widely accepted method for quantitative determination of amyloid fibrils. For this purpose aliquots from the Aβ_{42} incubation mixture were diluted in a fluorescence cuvette containing 0.5 mL of 3.3 μM ThT solution, and the ThT fluorescence was registered. The results in Figure 3b show that the time-dependent increase in the fluorescence intensity is parallel to the decrease in the relative intensity of the Aβ_{42} peak in MALDI MS spectra, and they are characterized by similar

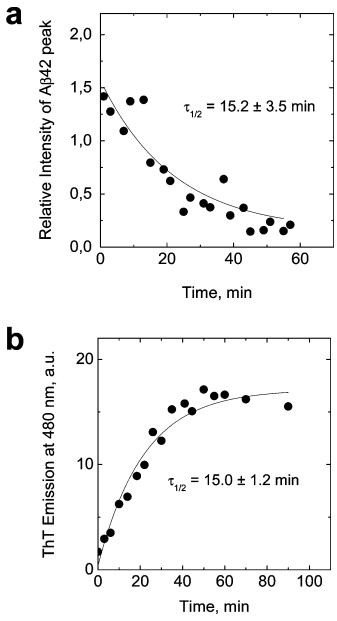

Figure 3. Kinetics of seed-induced $A\beta_{42}$ fibrillization: (a) monitored by a decrease of the intensity of the $A\beta_{42}$ peak in MALDI MS spectra; (b) monitored by an increase of ThT fluorescence. Incubation conditions: 20 mM HEPES, pH 7.3, 25 °C. Excitation at 440 nm and emission at 480 nm were used in the fluorescence experiment with 3.3 μM ThT. Solid lines correspond to first-order kinetic curves with *k* values.

values of the first-order rate constant $k = 0.042 \pm 0.006$ min^{-1} ($\tau_{1/2} = 15.0 \pm 1.2$ min). The obtained results confirm that $A\beta_{42}$ monomer loss in the MALDI MS assay occurs due to peptide fibrillization. This also suggests that $A\beta_{42}$ fibrils do not dissociate in the course of MALDI MS sample preparation.

Screening of the Inhibitors of *Aβ* Aggregation by MALDI-TOF MS. Using the elaborated MALDI MS assay, we performed seven test runs with a set of 80 compounds, including substances that have been reported to interfere with fibrillization of $A\beta_{42}$. A complete list of the tested compounds and the results of screening are provided in Table S-1 (Supporting Information) and in Figure 4. Representative MALDI MS spectra in the presence of some tested compounds are presented in Supporting Information Figures S-2 and S-3. Ten of the tested compounds showed a statistically relevant (95%) inhibitory effect on the fibril growth in our test. The first group of compounds that tested positive consisted of metal ions Zn(II), Cu(II), and Ni(II). According to recent publications, Cu(II) and Zn(II) inhibit fibrillization of $A\beta_{42}$ by inducing formation of nonfibrillar $A\beta_{42}$ aggregates.[19,20] The inhibitory effect of metal ions on the fibrillization of $A\beta_{42}$ is clearly seen in our assay, which means that the metal-induced nonfibrillar $A\beta_{42}$ aggregates dissociate to monomers during the preparation of samples for MALDI MS.

Seven of the organic compounds also tested positive in our screening. Already known inhibitors of $A\beta$ aggregation such as azure C, hemin, basic blue 41 (BB),[21] and tannic acid[22] suppressed the aggregation of $A\beta_{42}$ at a 5 μM concentration in our test

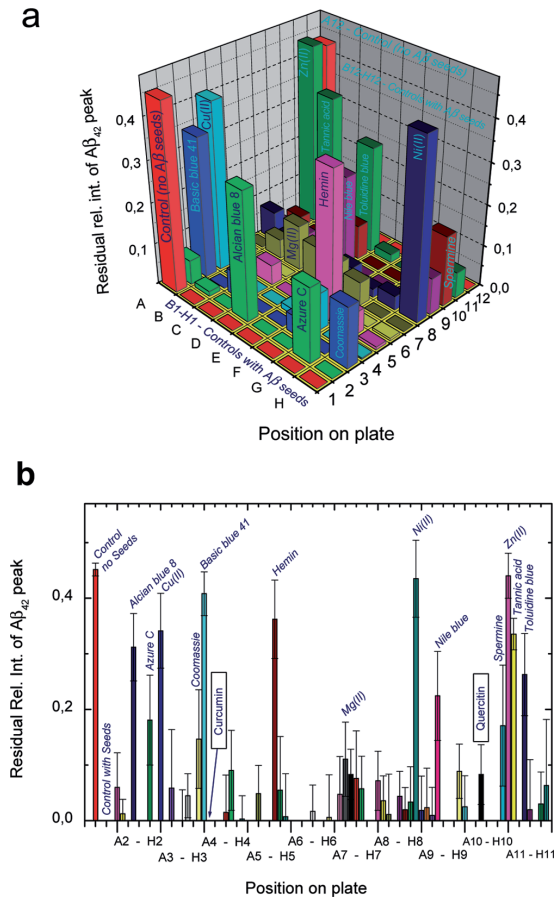

Figure 4. Effect of selected compounds on the aggregation of $A\beta_{42}$ monitored by MALDI-TOF MS (control, relative intensity of the $A\beta_{42}$ monomer peak after 1 h of incubation without additional substances; other columns, intensity of the 5 μM $A\beta_{42}$ monomer peak after 1 h of incubation with a 5 μM concentration of the tested substance): (a) diagram for all tested compounds (a list of compounds together with the fraction of soluble $A\beta_{42}$ together with ±SE is given in Supporting Information Table S-1); (b) effect of selected compounds.

(Figure 4). Moreover, alcain blue 8, Nile blue, and toluidine blue also suppressed fibrillization of $A\beta_{42}$. It is noteworthy that some compounds that were identified as inhibitors of $A\beta_{42}$ fibrillization in ThT tests, such as curcumin[23] and quercetin,[24] did not inhibit the fibrillization of $A\beta_{42}$ at a 5 μM concentration in the MALDI MS assay.

Inhibition of *Aβ* Aggregation According to the ThT Assay. To elucidate reasons for the discrepancy between earlier results obtained by ThT-based methods and our results obtained by MALDI-TOF MS, we performed two types of control experiments. First, we tested representative compounds BB and cur-

(20) Lee, S.; Ryu, J.; Park, C. *Anal. Chem.* **2009**, 812751–2759.

(21) Taniguchi, S.; Suzuki, N.; Masuda, M.; Hisanaga, S.; Iwatsubo, T.; Goedert, M.; Hasegawa, M. *J. Biol. Chem.* **2005**, *280*, 7614–7623.

(22) Ono, K.; Hasegawa, K.; Naiki, H.; Yamada, M. *Biochim. Biophys. Acta* **2004**, *1690*, 193–202.

(23) Ono, K.; Hasegawa, K.; Naiki, H.; Yamada, M. *J. Neurosci. Res.* **2004**, *75*, 742–50.

(24) Ono, K.; Yoshiike, Y.; Takashima, A.; Hasegawa, K.; Naiki, H.; Yamada, M. *J. Neurochem.* **2003**, *87*, 172–81.

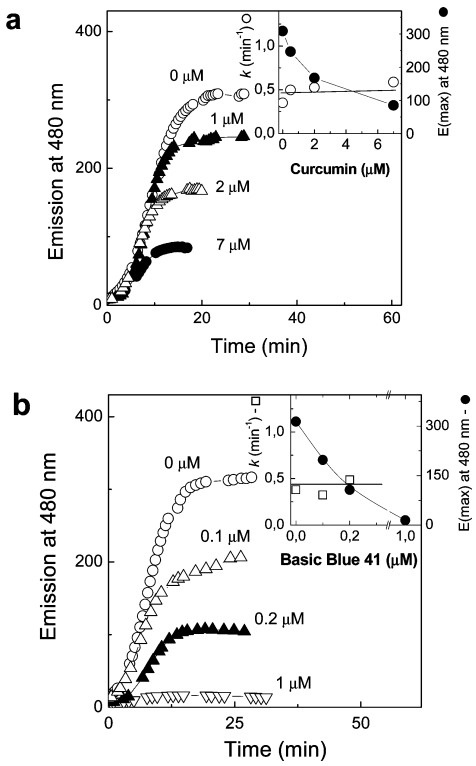

Figure 5. Effects of curcumin and BB on Aβ_{42} fibrillization. Suppression of the time-dependent increase of ThT fluorescence in an agitated solution of seed-free Aβ_{42} (○), by 1 μM (▲), 2 μM (Δ), and 7 μM (●) curcumin (a) and by 0.1 μM (Δ), 0.2 μM (▲), and 1 μM (▽) BB (b). Solid lines correspond to the fitted curves. Insets: dependence of the calculated kinetic constant of fibril growth (*k*) and maximal level of ThT emission from the concentration of the tested compounds.

cumin with the ThT test according to the protocol described in ref 19, and second, we tested putative interference of selected compounds with ThT fluorescence using preformed Aβ_{42} fibrils. Figure 5 shows that BB and curcumin suppress the time-dependent increase in ThT fluorescence whereas total suppression was achieved at 1 μM BB and 10 μM curcumin in conformity with data presented in the literature.[22,24] However, quantitative analysis of the kinetic curves shows that curcumin and BB do not affect the kinetic constant of fibril growth but lower only the final level of ThT fluorescence (Figure 5 insets), which makes the inhibition data obtained by ThT tests highly suspicious.

It has been demonstrated recently that the decrease in the fluorescence intensity in the ThT test might also be caused by interference of the tested compounds with binding of ThT to the fibrils or with ThT fluorescence.[15,16] We tested putative interference of selected compounds with ThT binding and fluorescence by adding 1 and 5 μM concentrations of the selected compounds to preformed Aβ_{42} fibrils labeled with ThT. Figure 6 shows that the addition of 1 or 5 μM ascorbic acid, imidazole, nicotinic acid, phenolphthalein, riboflavin, clioquinol, Zn(II), and Cu(II) did not affect the fluorescence intensity of ThT bound to the preformed Aβ_{42} fibrils, demonstrating that these compounds do not interfere with ThT binding and fluorescence at the concentrations used. At the same time, addition of tannic acid, azure C, Nile blue, curcumin, and BB led to a fast and concentration-dependent decrease in the ThT fluorescence intensity (Figure 6a) that can be explained by competitive displacement of ThT from its binding sites on the fibrils or quenching of the fluorescence of bound ThT by the compounds studied as suggested earlier.[15] The effect of BB was studied in a wide concentration range (Figure 6b), and it was established that a 50% decrease of the ThT fluorescence intensity occurs already at a 0.1 μM concentration of BB, which is similar to the effect of BB in the ThT fibrillization assay (Figure 5b).

Quantitative Determination of Inhibitory Potency by MALDI-TOF MS. The potential of selected compounds such as BB and Zn(II) to inhibit Aβ_{42} fibrillization has been determined by MALDI MS by performing Aβ_{42} fibrillization assay in the presence of different concentrations of these substances. In the case of BB 50% inhibition was observed at a 1.6 μM concentration of the compound, which is 20 times larger than the apparent IC_{50} value determined by the ThT assay. In the case of Zn(II) 50% inhibition occurred at a 3 μM concentration, which is in agreement with the IC_{50} value of 1.8 μM determined earlier by using the ThT assay.[19]

DISCUSSION

The aggregation of Aβ peptides is considered to be a key factor in the development of AD. According to the current knowledge, the fibrillization of Aβ and other amyloidogenic peptides/proteins is a multistep process initiated by the formation of oligomers acting as nucleation seeds that self-propagate and grow into amyloid fibrils through sequential addition of monomers.[25] The fibrillization mechanism and cytotoxicity of different aggregation states of Aβ are still under debate; at the same time, it is widely accepted that inhibition of Aβ fibrillization and amyloid formation is the main strategy for the prevention, control, and therapy of AD.

An initial search of Aβ fibrillization inhibitors can be performed by using in vitro screening assays. These assays should adequately reflect fibrillization of native Aβ and meet the highest criteria for reliability and reproducibility. It is desirable to use unmodified Aβ_{42} peptide in these tests since it is considered to have a crucial role in the formation of amyloid plaques in the brain. To guarantee reproducibility and eliminate batch to batch variations in peptide quality, the materials used in the test should be standardized. We achieved this by using defibrillated Aβ_{42} monomers and initiating the fibrillization process by addition of a controlled amount of preformed Aβ_{42} fibrils as fibrillization seeds. In the design of the MALDI MS screening assay we paid special attention to the solubilization and monomerization of synthetic Aβ_{42} peptide: commercial Aβ_{42} peptides were always treated with HFIP prior to use. SEC analysis on a Superdex 75 column indicated that HFIP-treated Aβ_{42} stock solution was predominantly monomeric. Under quiescent conditions the HFIP-treated monomeric Aβ_{42} is stable at least for 1 day before fibrillization begins; however, its fibrillization can be started by intensive stirring of the peptide solution[19] or by addition of fibrillar seeds. We demonstrated that seed-initiated Aβ_{42} fibrillization assay is well controlled,

(25) Esler, W. P.; Stimson, E. R.; Jennings, J. M.; Vinters, H. V.; Ghilardi, J. R.; Lee, J. P.; Mantyh, P. W.; Maggio, J. E. *Biochemistry* **2000**, *39*, 6288–6295.

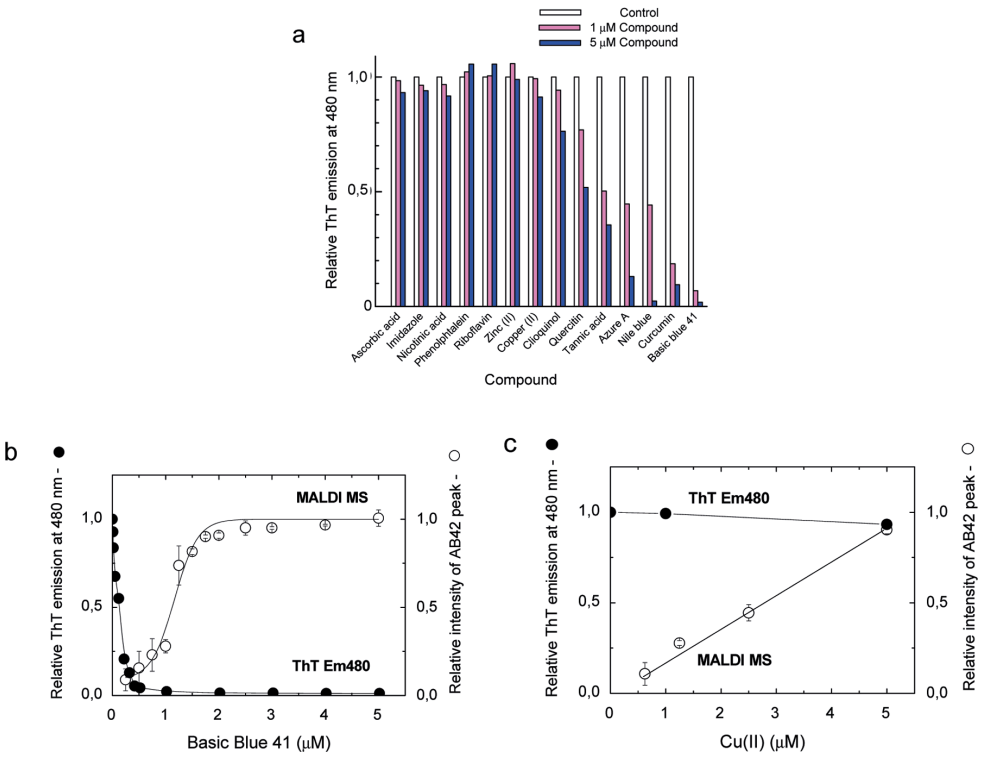

Figure 6. Effects of selected compounds on the ThT fluorescence of preformed fibrils: (a) effects of 1 and 5 μM concentrations of the compounds on the ThT fluorescence of preformed fibrils; (b) effects of different concentrations of BB on the ThT fluorescence of preformed fibrils and the relative intensity of the Aβ_{42} peak in MALDI MS spectra; (c) effects of different concentrations of Cu(II) on the ThT fluorescence of preformed fibrils and the relative intensity of the Aβ_{42} peak in MALDI MS spectra.

gives reproducible results, and could be performed on multiwell plates necessary for high-throughput tests. This assay detects inhibitors of the fibril growth phase of the overall fibrillization process that may affect the process by two mechanisms: (i) stabilization of monomeric Aβ_{42} by complex formation; (ii) blocking the growing ends of the fibrils. Our assay does not detect inhibitors of Aβ_{42} oligomerization and fibril nucleation. However, we think that this shortcoming is common for most in vitro fibrillization tests. In principle, agitation-induced Aβ fibrillization tests can identify additionally compounds that block early seeding steps; however, it is very likely that nucleation processes in agitated solutions where shearing can induce significant secondary seeding are totally different from seeding processes occurring in vivo.

Comparison of the elaborated MALDI MS-based screening test for inhibitors of Aβ_{42} fibrillization with alternative tests allows highlighting the following advantages. Foremost, MALDI MS-based assay relies on the use of a well-defined label-free system containing only native Aβ_{42} peptide and the putative inhibiting substance. Many alternative assays make use of modified Aβ[26] or artificial peptides,[16] which might behave differently from the native Aβ_{42}. Common fluorimetric tests make use of reporter compounds, which change their emission intensity upon binding to fibrillar structures. It has been shown recently that several putative fibrillization inhibitors such as curcumin and quercetin interfere with ThT binding and fluorescence, which generates false-positive results in the particular tests.[15,16] In the current study we confirmed these findings for curcumin and quercetin. Moreover, we also demonstrated that the interference of tested low-molecular-weight compounds with ThT fluorescence is a rather common phenomenon and occurs also in the case of tannic acid, azure A, Nile blue, and BB. In the case of fibrillization inhibitors that do not interfere with ThT binding and fluorescence such as Zn(II) and Cu(II), the MALDI MS assay yielded apparent inhibitory constant values similar to those of the ThT assay.[19] The inhibitory constant value for BB obtained by MALDI MS (IC_{50} = 1.6 μM) is substantially higher than that determined by the ThT test (apparent IC_{50} = 0.1 μM) (Figure 5b), demonstrating that its inhibitory efficiency is overestimated in ThT-based studies due to the interference with ThT emission. On the basis of the presented results, we can conclude that the efficiency of a wide series of inhibitors of the fibrillization of Aβ_{42} should be critically revised. A putative drug candidate, methylene blue, also did not show an inhibitory effect in our test; however, this compound is shown to inhibit formation of Aβ oligomers but not fibrils.[11]

(26) (a) Kim, W.; Kim, Y.; Min, J.; Kim, D. J.; Chang, Y. T.; Hecht, M. H. *ACS Chem. Biol.* **2006**, *1*, 461–469. (b) Hong, H. S.; Maezawa, I.; Yao, N.; Xu, B.; Diaz-Avalos, R.; Rana, S.; Hua, D. H.; Cheng, R. H.; Lam, K. S.; Jin, L. W. *Brain Res.* **2007**, *1130*, 223–234. (c) Chang, P. T.; Kung, F. L.; Talekar, R. S.; Chen, C. S.; Lai, S. Y.; Lee, H. Y.; Chern, J. W. *Anal. Chem.* **2009**, *81*, 6944–6951.

MALDI MS-based assay can be characterized as a fast method. Using automatic spotting from 96-well plates combined with automated MALDI MS measurements enables testing of 80 samples in approximately 2.5 h. The elaborated MALDI-TOF MS assay consumes considerably smaller amounts of peptide for individual measurements than most of the ThT tests as each individual assay can be performed in 25 μL of solution.

In summary, the elaborated MALDI MS-based screening test can significantly speed up in vitro screening of large compound libraries for reliable identification of the inhibitors of Aβ_{42} fibrillization, and MALDI-MS can be also used for quantitative characterization of their inhibitory potential necessary for selection of lead compounds suitable for AD drug development.

ACKNOWLEDGMENT

This work was supported by Estonian Ministry of Education and Research Grant SF0140055s08 (P.P.), Estonian Science Foundation Grants 9171 (P.P.) and 6840 (V.T.), and World Federation of Scientists scholarships to K.Z. and A.K. We thank Dr. Valdek Mikli for help with the TEM experiments and Ingrid Kikkas and Marina Tuuling for their technical assistance and experimental contribution at different stages of this work.

SUPPORTING INFORMATION AVAILABLE

Additional information as noted in the text. This material is available free of charge via the Internet at http://pubs.acs.org.

Received for review June 15, 2010. Accepted September 7, 2010.

AC101583Q

PUBLICATION V

Tõugu, V., **A. Tiiman** and P. Palumaa (2011)
"Interactions of Zn(II) and Cu(II) Ions with Alzheimer's Amyloid-Beta Peptide. Metal Ion Binding, Contribution to Fibrillization and Toxicity."
Metallomics **3**(3): 250-261.

Metallomics

Dynamic Article Links

Cite this: *Metallomics*, 2011, **3**, 250–261

www.rsc.org/metallomics

CRITICAL REVIEW

Interactions of Zn(II) and Cu(II) ions with Alzheimer's amyloid-beta peptide. Metal ion binding, contribution to fibrillization and toxicity†

Vello Tõugu,* Ann Tiiman and Peep Palumaa

Received 10th November 2010, Accepted 7th February 2011
DOI: 10.1039/c0mt00073f

Amyloid-β peptides (Aβ) are key molecules in Alzheimer's disease (AD) pathology as they form amyloid plaques that are primary hallmarks of AD. There is increasing evidence demonstrating that the biometals zinc(II) and copper(II) interact with Aβ peptides and have an influence on their fibrillization and toxicity. Zinc and copper ions are abundantly present in the synaptic areas of the brain, and it is likely that the age-related dyshomeostasis of these biometals is associated with AD pathology. In this review we summarize the knowledge of the interactions of zinc and copper ions with Aβ peptides, their role in Aβ fibrillization and toxicity and provide a critical analysis of the conflicting results in the field. Copper ions entrapped in Aβ fibrils are electrochemically active and can generate ROS in the presence of hydrogen peroxide and reducing agents. This might provide a key for understanding the putative role of copper in Aβ toxicity and AD pathology.

Introduction

Alzheimer's disease (AD) is the most common neurodegenerative disease, comprising more than 50% of dementia in the elderly. The disease is characterized by the extracellular deposition of amyloid-β peptides (Aβ) in the form of senile plaques and the intracellular deposition of hyperphosphorylated tau protein, oxidative damage and neuronal death in the brain. The progressive loss of neurons and synapses throughout the brain during the disease slowly destroys memory and cognitive skills and eventually leads to death. According to the amyloid cascade hypothesis, the Aβ aggregation and formation of amyloid plaques is the key upstream event, which in turn causes formation of intracellular neurofibrillary tangles and cell death.[1]

The Aβ peptide is derived from amyloid precursor protein (APP) through its limited proteolysis. The APP can be cleaved in two alternative ways: the non-amyloidogenic and the amyloidogenic (Fig. 1). In the non-amyloidogenic pathway APP cleavage by α-secretase prevents Aβ formation and subsequent cleavage by γ-secretase liberates the P3 peptide

Department of Gene Technology, Tallinn University of Technology, Akadeemia tee 15, Tallinn 12618, Estonia. E-mail: vello.tougu@ttu.ee
† This article is published as part of a themed issue on Metals in Neurodegenerative Diseases, Guest Edited by David Brown.

Vello Tõugu

*Dr. **Vello Tõugu** is a senior research scientist in the Department of Gene Technology at the Tallinn University of Technology. He got his diploma in chemistry from Tartu University and studied the reaction mechanisms of hydrolytic enzymes and their application in synthesis at the National Institute of Chemical Physics and Biophysics for several years. He received his PhD in chemistry from the Institute of Chemistry of the Estonian Academy of Science in 1991. Since 2005 his research has been focused on the role of metal ions in the fibrillization of amyloidogenic peptides.*

Ann Tiiman

***Ann Tiiman** (b. Karafin) is a doctoral student in the Department of Gene Technology at the Tallinn University of Technology. She has been studying the factors affecting the fibrillation of Alzheimer's amyloid peptide since 2007.*

This journal is © The Royal Society of Chemistry 2011

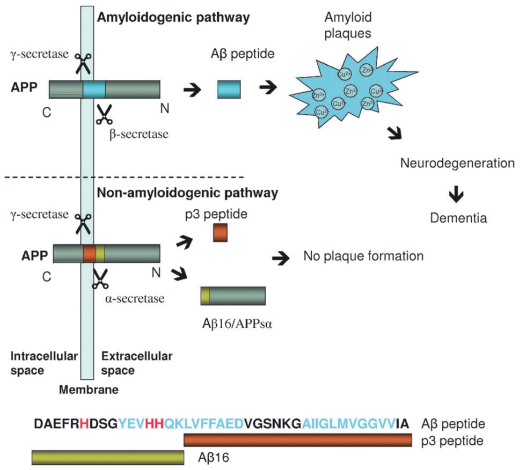

Fig. 1 The amyloid cascade in AD. Formation of Aβ peptide by amyloidogenic cleavage of APP, formation of fibrillar "nucleus" or metal-induced Aβ aggregates, their evolution to Cu(II) containing redox-active amyloid plaques leading to neurodegeneration.

corresponding to Aβ residues 17–40 (or 42). In the amyloidogenic pathway the APP is first cleaved by β-secretase, allowing its large ectodomain to be shed into the luminal and extracellular fluid and leaving a membrane bound C-terminal fragment that is subsequently cleaved by γ-secretase causing the Aβ peptide to be released. The exact point of cleavage by the γ-secretase determines the length of the Aβ peptide, that is usually composed of either 40 or 42 residues.[2] The production of Aβ is a normal physiological process and it is present in the brain and cerebrospinal fluid throughout life.[3] In most cases AD occurs sporadically, but approximately 5% of AD cases belong to multiple familial forms of early onset disease that are generally caused by mutations in the *APP* gene or genes encoding the enzymes that process the APP (*PSEN1*, *PSEN2*) or protein related to Aβ turnover (*APOE*). Generally these mutations lead to increased production of Aβ, especially the more aggregation-prone $A\beta_{42}$ form, supporting the view that Aβ fibrillation and plaque formation is a key event in AD etiology. The mechanism that triggers the age-dependent Aβ aggregation is still elusive, however, substantial evidence has been gathered suggesting that interactions of Aβ with transition metal ions, especially with biometals Cu(II) and Zn(II), may be involved in the processes leading to Aβ aggregation and toxicity, and the dysregulation of copper and zinc homeostasis in the brain may be linked to the development of AD.[4–10]

The brain comprises 2% of body mass but contains 7.3% of total copper and exhibits the highest rate of oxidative metabolism. As a rule Cu(II) and Zn(II) in the body are tightly bound to enzymes and other proteins, but in the brain they also exist in synaptic vesicles as "free" ions (*e.g.* loosely bound to low affinity ligands, for instance to glutamate) that can be released into the synaptic cleft during neurotransmission.[7,9,11] After excitatory release the concentrations of ionic zinc and copper in the synaptic cleft of glutamaergic neurons located mainly in the cortex and hippocampus may reach 60 μM[12] and 15 μM,[7] respectively. Aβ is also present in the synaptic cleft region where it has the potential to interact with Cu(II) and Zn(II) and form amyloid. In the synaptic cleft area there are also other more potent metal-binding proteins present such as metallothionein-3 (MT-3) released by neuronal cells, which have the potential to suppress metal–Aβ interactions, but MT-3 levels are decreased in AD.[9]

The role of altered metal homeostasis as a pathogenic factor in AD has been intensively studied, moreover, assumption about the causative role of metal ions in AD has laid the basis for the elaboration of the metal chelation therapeutic approach aimed at the elaboration of therapeutic agents, which modulate metal bio-availability in the brain and have the potential to demetallate and dissolve plaques and ameliorate several of the dysfunctional events characteristic of AD.[5,13,14]

To understand the potential of the metal chelating therapeutic approach in AD we have to understand the role of metal ions in amyloid plaque formation, which considers both—interaction of metal ions with Aβ peptides as well as the effect of metal ions on fibrillization and toxicity of Aβ peptides.

As a rule, the following arguments are listed to point out the important role of Cu(II) and Zn(II) ions in plaque formation and toxicity: (i) Zn(II) and Cu(II) levels are elevated in AD brain and enriched in amyloid plaques;[15–18] (ii) metal ions bind to Aβ *in vitro*[19–22] and Aβ directly coordinates the metal ions within the plaques;[23] (iii) Zn(II) and Cu(II) cause Aβ aggregation and may enhance fibril formation *in vitro*;[24–31] (iv) metal ions enhance amyloid formation and plaque load and toxicity in AD model animals;[32–34] (v) Aβ coordination of Cu(II) leads to the generation of ROS that can cause oxidative stress and neurotoxicity;[35,36] (vi) toxicity of the amyloid aggregates depends on their copper content;[31,37–40] (vii) treatment with metal chelators results in the dissolution of aggregated Aβ from AD brain extracts.[13,41]

The direct interaction of transition metal ions with Aβ is by far not the only interaction that can relate Zn(II) and Cu(II) dyshomeostasis in the brain with AD progression (for a review see ref. 6 and 7), however, in the current review we focus solely

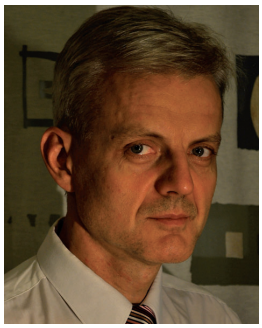

Peep Palumaa

*Dr. **Peep Palumaa** is Professor of genomics and proteomics at the Tallinn University of Technology since 2002. He studied chemistry at Tartu University and got his PhD in 1986 for his studies of the acetylcholinesterase active site. He was a postdoctoral fellow in the Institute of Biochemistry at the University of Zürich at the beginning of the 90s and continued at Tartu University as a senior research scientist and professor of biochemistry. His current research area is structural and medical metalloproteomics with focus on copper chaperons and amyloid peptides.*

on the analysis of this interaction and the role of transition metal ions in the neurotoxicity of the amyloids.

Interactions of monomeric Aβ with Cu(II)

The primary interaction of Aβ peptide with metal ions is the fast formation of a reversible complex where the metal ion is coordinated with metal-ligating groups of the peptide. An exhaustive critical review of the divergent propositions on the structure and affinity of these complexes has recently been given by Faller and Hureau,[42] thus we give only a brief overview of the earlier findings in this field, and provide an alternative explanation for the divergence of the observed metal binding affinities of Aβ in the light of the most recent papers.

Structure of the Cu(II)-Aβ complex

Aβ forms predominantly a mononuclear Cu(II)-Aβ complex with 1 : 1 stoichiometry at physiological pH, and a large set of experimental results indicate that the ligands coordinating the copper ion are either three His side chains or two His and the N-terminal.[42] The presence of all three His residues (His6, His13 and His14) in the Cu(II) coordination sphere is supported mainly by earlier NMR studies[19,43,44] and by using a combination of complementary experimental techniques, namely sedimentation assay, Fourier transform infrared spectroscopy, and X-ray absorption spectroscopy.[45] Involvement of His13 and His14 in Cu(II) binding is also confirmed by ESI MS.[46] Depending on the pH value of the environment the Cu(II)-Aβ complex acquires at least two different structures (Fig. 2).[43,47–49] At higher pH the NMR signals from Asp1 Ala2 and from side chains of all three His residues are affected by copper binding, whereas at pH 6.6 the line broadening observed in $^{13}C[^{1}H]$ NMR spectra supports the involvement of multiple groups in Cu(II) coordination, suggesting the presence of several energetically equivalent (or similar) binding modes.[47] The ε-N atoms of His6, His13 and His14 and an O atom from the carboxylate group of Asp1 were found in the Cu(II) coordination sphere at high pH, and only two His residues at low pH by EPR.[48,49] The transition between the high and low pH forms has a mid-point at pH 8–8.7[43,50] for truncated peptides, but this value may be close to 9 for full-length $A\beta_{42}$.[51] The combination lines that would be expected if several His residues were bound simultaneously to a single Cu(II) ion were not observed in these EPR studies, and it was concluded that at high pH the Cu(II)-Aβ complex is very dynamic and the His residues in the Cu(II) coordination are continuously changing.[52,53] Using hyperfine sublevel coordination (HYSCORE) of Aβ analogues with site-specific ^{15}N labelling, the presence of two forms of the Cu(II)-Aβ complex with His6 as a common and His13 and His14 as alternative ligands at pH 6–7 was confirmed.[52,53] However, in contrast to the study by Dorlet and colleagues, the carboxylate of Asp1 has been found in an equatorial position and coordination of Cu(II) by three His residues has been suggested for component II at pH 8.[48,54]

An important property of the metal ion-Aβ complex is stability in the solution. The copper complex of truncated 1–16 and 1–28 Aβ peptides is usually relatively stable in solution[45] at physiological pH, whereas aggregation and precipitation has often been detected in the case of full-length Aβ.[45,55–57] Since the full-length peptide precipitates at lower pH values in the presence of Cu(II) (precipitation at pH 5.5 is almost immediate[22]), protonation of His residues at slightly acidic pH may lead to the formation of insoluble Cu(II)-Aβ, it can be speculated that the coordination sphere of Cu(II) in Cu(II)-Aβ aggregates may resemble that of the low pH component. The Cu(II)-Aβ complex at physiological pH is tetragonal with four ligands in the equatorial plane and usually one axial ligand.[52] The data on the fourth (and fifth) ligand for Cu(II) is very divergent, suggesting that most likely the Cu(II)-Aβ complex may exist as a mixture of different metalloforms, whereas the distribution between the different forms can be substantially affected by small variations in the environment (pH, peptide and salt concentration, presence of solvents *etc.*) and peptide length and structure. The pleiomorphic, highly dynamic nature of the Cu(II)-Aβ complex might also explain the partially conflicting results in the literature regarding the metal-coordinating groups, since the buffer compounds used can also have a profound influence on the Cu(II) coordination sphere.[42,58] Such a behaviour could be expected since Aβ peptide does not have a "predefined" metal binding site as the metalloproteins do, and the Cu(II)-Aβ complex has a dynamic structure where the dominant set of ligands (two His residues) is complemented with at least two additional ligands. This important feature of the complex has to be considered in the analysis of the Cu(II) binding affinity of Aβ in the presence of low affinity competing ligands.

Aβ can also bind a second Cu(II) ion.[37,42–44,55,59] As a rule, the binding of the second Cu(II) ion is assumed to be

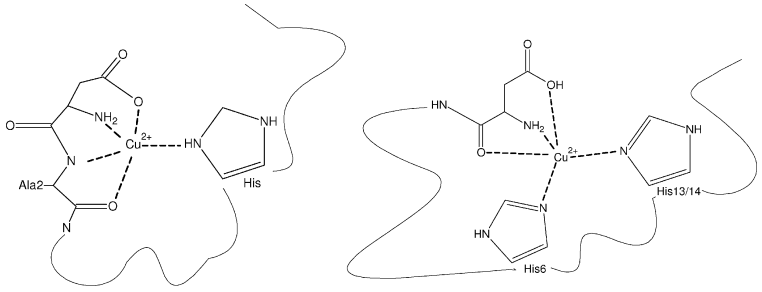

Fig. 2 Schematic presentation of ligands involved in Cu(II) coordination in "high" and "low" pH Cu-Aβ complexes.

 This journal is © The Royal Society of Chemistry 2011

physiologically irrelevant due to the low affinity of the binding. At high Cu(II) concentrations, Aβ can bind as many as four Cu(II) ions.[60]

Metal-binding affinity of Aβ

The metal binding affinity of proteins and peptides is an important parameter in biology, and the quantitative determination of the binding affinity of Aβ peptides helps to assess the significance of metal binding as a potential inducer of pathological Aβ aggregation. Besides some exceptions there is generally no free Cu(II) (or Zn(II)) available in the living organism and, thus, Cu(II) ions can bind *in vivo* only to the peptides that have sufficiently high affinity in order to compete for Cu(II) ions with other metal-binding biomolecules. Disclosing the thermodynamics and kinetics of Cu(II) and Zn(II) binding to Aβ peptides is also crucial for rational design of drug candidates in the framework of metal chelation therapy of AD.

The reported affinity of Aβ towards Cu(II) varies from attomolar[61] to micromolar.[20] It is important to note that the values of the apparent dissociation constant, K_D^{app}, from different laboratories are determined under different environmental conditions and in the presence of different amounts of various Cu(II) binding ligands including buffer components, which have to be taken into account. After the publication of the first buffer independent conditional dissociation constant (K_D) value for Cu(II)-Aβ (equal to 35 nM[62]), the discussion of the Cu(II) binding affinity of Aβ has moved towards the debate over the methods and models for the calculation of conditional constant values and the applicability of compounds used as weak ligands for Cu(II) ions in the experiments.[37,42,63,64] The introduction of the conditional constant concept has resulted in two alternative estimates for K_D values for Cu(II)-Aβ at physiological pH and normal temperature: one in the region of 30–60 nM[37,62–64] and another in the range of 0.1–1 nM or even lower.[51,65,66] Recently, Faller *et al.*[42] have critically analyzed the subject and concluded that the discrepancy between different K_D values reported in the literature arises from the model used for accounting for Cu(II) binding to low-affinity ligands during the calculation of the conditional K_D value. We share the opinion that different K_D values arise mainly from the model used. However, the low estimate of K_D for the Cu(II)-Aβ complex seems to be unreliable for several reasons described below.

Metal ion binding affinity of the Aβ peptide can be determined by several titration methods: (i) spectrofluorimetrically by monitoring the changes in Tyr fluorescence;[20,44,62] (ii) microcalorimetrically;[43,44,66–68] or (iii) using external fluorogenic or colorimetric ion binding dyes as competing ligands.[62,69,70] In principle, the microcalorimetric method is the most accurate, however, due to the high affinity of Aβ towards Cu(II) in comparison to the sensitivity of all applied methods, the measurements have been carried out in the presence of competing low-affinity Cu(II) binding ligands that increase the apparent dissociation constant value to the range suitable for determination. pH buffers (HEPES, Tris, phosphate *etc.*) or amino acids (Gly, His) have been used for this purpose. Phosphate buffer is not suitable for the studies of the effects of Cu(II) (as well as Zn(II)) due to the extremely low solubility of the corresponding phosphates, precipitation of which during the experiments may cause artefacts. HEPES and Tris complexes with Cu(II) are soluble and they stabilize the Cu(II) solutions at neutral pH, making these buffers suitable for the studies of metal-binding affinity.

It has been pointed out that choosing the correct coordination model in K_D calculations is extremely important.[71] The most important feature, besides the correct evaluation of the Cu(II) binding affinity of the "weak" ligand, is the assumption of the presence or absence of ternary complexes. When ternary complexes occur and they are not accounted for in the model used, the affinity of the complex formation would be drastically overestimated. As a rule, the competitive binding models are used in the literature, which do not account for the possibility of ternary complex formation. Verification of the applicability of the model for a particular low-affinity ligand and metal ion is relatively easy: the K_D^{app} values should be determined at different buffer concentrations and the conditional constant calculated must be independent of the buffer concentration. It is also obvious that the K_D values determined in the presence of various low affinity ligands must be similar.

However, the measurements at different buffer concentrations are rather exceptional.[62–64] A good example of K_D determination is presented by Rozga *et al.*[64] who studied the dependence of K_D^{app} on the concentration of HEPES buffer and showed that the K_D value of 57 nM, calculated by using the simple competitive binding (Scheme 1) of Cu(II) to Aβ and to the buffer component is, indeed, independent of the buffer concentration. This value is in good agreement with the average value determined in Tris and HEPES buffers earlier by Tõugu *et al.*[62] Thus, HEPES is suitable for Cu(II)-binding studies in biological systems, since it forms a 1 : 1 complex with Cu(II) and it does not form mixed complexes with amino acids such as Ala, Trp, and His.[72]

On the other hand, the measurements of K_D^{app} in ammonium acetate buffer[63] together with the calculations according to the competition model, do not give a concentration independent K_D value, suggesting the formation of ternary complexes of Cu(II)-Aβ with buffer components.

Faller *et al.*[42] suggested that HEPES is a good buffer for affinity measurements due to 1 : 1 complex formation with copper ions, but its Cu(II)-binding affinity might not be sufficiently high. Tris buffer has a higher Cu(II) binding affinity than HEPES, however, its binding stoichiometry is complex—Cu(II) can bind up to four Tris molecules[63,65] and the application of the N4 model seems relevant. The application of the N4 model to earlier experimental data resulted in an estimate for Aβ Cu(II)-binding affinity, K_D = 0.6 nM, from the data at Tris buffer concentration 10 mM[42] that is in considerably good agreement with the results of calorimetric titrations. However, the recalculation of K_D from Cu(II) binding data at different Tris concentrations from the literature,[43,62,67] according to the N4 model,[65,68] resulted in values that differ even more than the initial apparent constant values,[71] demonstrating clearly that the N4 model without ternary complex assumption is inappropriate. This observation is not surprising since Tris is known to form mixed complexes with various metal ions and ligands.[63] Thus, it can be concluded that the results obtained

A

$$Me^{2+} + A\beta \xleftrightarrow{K_D} Me^{2+} - A\beta$$
$$+$$
$$B$$
$$\downarrow\uparrow K_D^B$$
$$Me^{2+} - B$$

$$K_D = K_D^{app} \Big/ \left(1 + \frac{B}{K_D^B}\right)$$

B

$$Me^{2+} + A\beta \xleftrightarrow{K_D} Me^{2+} - A\beta$$
$$+ \qquad\qquad +$$
$$B \qquad\qquad B$$
$$\downarrow\uparrow K_1^B \qquad\qquad \downarrow\uparrow \alpha K_1^B$$
$$Me^{2+}B + A\beta \xleftrightarrow{\alpha K_D} Me^{2+}B - A\beta$$
$$+$$
$$B$$
$$\downarrow\uparrow K_2^B$$
$$Me^{2+}B_2$$

Scheme 1 The binding of metal ions to Aβ in the presence of low-affinity copper ligands and the definition of apparent (K_D^{app}) and conditional dissociation constants (K_D). Scheme A corresponds exclusively to competitive binding of metal ions to either Aβ or a low-affinity ligand. In the presence of the competing ligand B, the apparent dissociation constant K_D^{app} value determined experimentally is a function of the conditional dissociation constant K_D, dissociation constant of the metal-B complex K_D^B, which can contain more than one ligand and the concentration of ligand B. Scheme B corresponds to ternary complex formation. In this case the K_D^{app} value depends also on the value of α that cannot be determined from independent experiments. K_D is a thermodynamic equilibrium constant that corresponds to the value of apparent constant at zero concentration of competing ligands.

in Tris buffer do not agree with the N4 model, and they also cannot support the low nanomolar K_D value for the Cu(II)-binding affinity of Aβ. Application of the N1 model for Tris-Cu(II) complexes can be used only as a very raw approximation accounting for the ternary complex formation and by assuming that only the Tris molecule with the highest affinity is replaced by Aβ. The results showed that the experimental K_D^{app} values in Tris buffer do not contradict with the Cu(II)-binding affinity of Aβ in a nanomolar range.

The low K_D values close to 1 nM originate from microcalorimetric experiments, where Gly was used as Cu(II) stabilizing compound.[65,68] Using Gly and His as titrants for Cu(II)-Aβ in fluorimetric measurements resulted in a K_D estimate equal to 10 pM.[51] Similarly to Tris, Gly is prone to ternary complex formation with Cu(II) and with other metal ions. Hatcher *et al.* have considered this possibility and made an attempt to prove that ternary complexes do not form by special ESI-MS experiments.[65] In recent years, non-covalent ESI-MS under mild ionization conditions has proved to be a very powerful tool in the studies of strong Cu(I)–protein interactions[73] where the formation of ternary complexes as "adducts" can be detected. However, the ESI-MS method does not detect relatively weak complexes characterized by fast dissociation rates. Thus, the absence of peaks corresponding to Gly-Cu(II)-Aβ in ESI MS spectra cannot be taken as ultimate proof for the absence of such a complex in the solution[65] and other techniques have to be used to determine Gly binding to Cu(II)-Aβ in solution.

In recent competition studies of Aβ affinity towards Cu(II) with three ligands, Gly, His and nitrilotriacetic acid (NTA), the conditional constant value for Cu(II)-$A\beta_{42}$ was estimated to be in the range of 10 pM.[51] However, as these affinities were estimated from the equivalent points of the titration experiments and the whole curves were not analyzed, these results cannot be considered as crucial evidence supporting the pM affinity. It has been pointed out in the literature that NTA is also prone to form ternary complexes.[64]

Since the structure of the Cu(II)-Aβ complex is dynamic and the peptide ligands in the coordination sphere of Cu(II) are in rapid exchange, it has been suggested[37] that the formation of ternary complexes with buffer components is also highly probable. The formation of ternary complexes in ammonium acetate buffer is shown experimentally[63] and this may also occur in the case of other Cu(II) ligands. In Tris buffer, the use of the N4 model results in a 6000-fold difference in K_D values in 10 and 100 mM Tris, which clearly shows that the model is not applicable, *e.g.* not all Tris ligands are replaced by peptide groups during the formation of the Cu(II)-Aβ complex. Application of the N1 model, that can be considered as a rough approximation for accounting for ternary complex formation, resulted in K_D values of 12–90 nM,[42] close to the values observed in HEPES. In the case of HEPES buffer, the absence of ternary complexes has been proved by the measurement of the concentration dependence[64] which resulted in K_D = 57 nM. The measurement of K_D^{app} at various concentrations of the competing ligand is a simple method for proving the model used in K_D determination: the resulting K_D value must be independent of the concentration of the ligand. For glycine as a ligand, these experiments have not been performed so far, and for Tris the N4 model failed the proof.

Thus, in our opinion, the ITC experiments should also be carried out at different Gly concentrations (or Cu(II)-Gly ratios) in order to prove that the model applied actually gives a conditional K_D constant value that does not depend on the Gly concentration.

Cu(II)-binding affinity can be determined by titration with fluorogenic ligands that do not form ternary complexes. Phenyl Green is not a perfect ligand for such a study, however, the changes in fluorescence intensity during the titration of Phenyl Green with Cu(II) ions in the presence of Aβ were in agreement with the K_D^{app} in HEPES buffer and "low" affinity binding was not detected.[62] As there is absolutely no reason to

This journal is © The Royal Society of Chemistry 2011

assume that 10 mM HEPES can cause a 100 000-fold decrease in the Cu(II) binding affinity of Aβ, this observation also supports the K_D value in the range of 30–60 nM. The Cu(II) binding affinities of H6A and H14A mutants of $A\beta_{42}$ are 3–5-fold lower than that of the wild-type and the H13A mutant,[74] which shows that the thermodynamic contribution of His residues to the formation of the Cu(II)-Aβ complex is not very substantial. This observation is in good agreement with the pleiomorphic dynamic nature of the Cu(II)-Aβ complex determined by structural studies. As far as soluble aggregates are concerned, it has been uniformly accepted that binding of Cu(II) to $A\beta_{40}$ and $A\beta_{42}$ is very similar.[37]

It has been known for a long time that, similar to Zn(II) ions, Cu(II) can induce aggregation and precipitation of full-length Aβ,[22,75,76] however, to a smaller extent and more slowly. The co-aggregation of Cu(II) with Aβ can be significant for its role in AD, since during the co-aggregation Cu(II) ions can be kinetically "trapped" in the insoluble Aβ aggregates, which is confirmed by extremely low attomolar affinities of the Cu(II)-$A\beta_{42}$ complex[61] determined in the experiments where peptide has aggregated during prolonged incubation with Cu(II) ions. Most importantly, this property can lead to the appearance of electrochemically active ROS-generating Cu(II) in the plaques of AD patients that cannot be sequestered for instance by MT[39,77] or serum albumin (HSA[38]), and leads to ROS-related neurotoxicity of amyloid plaques, which may play important role in pathology of AD.

Despite the discussion as to whether the conditional binding constant is 50 nM or 50 pM, consensus in affinity studies has been reached in many aspects. First, the Cu(II) binding affinity of Aβ is in a biologically relevant range, Aβ can bind Cu(II) in all forms (monomer, fibril and nonfibrillar aggregate), but under the equilibrium conditions it cannot compete with strong Cu(II) chelators such as MT and HSA. And lastly, the different estimates for the Cu(II) binding affinity of Aβ arise from the model used for accounting for the influence of a competing ligand. It should be noted here that, before the introduction of the concept of a conditional dissociation constant in 2008, the suggested affinity values varied from micro- to attomolar.

Interactions of Aβ with Cu(I)

The amyloid plaques are present in the extracellular space where the stable form of copper is Cu(II), and therefore Cu(II)-Aβ is the predominant form of the complex under physiological conditions outside the cells. However, a number of evidence shows that copper is redox active in the amyloid[78,79] and its redox cycling contributes to the oxidative stress and to neuronal death characteristic of AD.[78,79] Indeed, Cu(II) may be reduced to Cu(I) by the influence of endogeneous reductants such as ascorbic acid, present in CSF at high micromolar concentrations. Studies of Cu(I)-Aβ may substantially contribute to the understanding of the molecular mechanisms of AD, since it can appear in the transient states of redox-cycling leading to the generation of ROS after reaction of Cu(I) with H_2O_2. Cu(I)-Aβ complexes have been studied by making use of truncated peptide, which shows that Cu(I) is coordinated in Cu(I)-$A\beta_{16}$ by the imidazole groups of two histidine residues in a linear fashion,[71,80] whereas the third histidine is also important due to dynamic exchange between several sets of ligands. Thus the Aβ-Cu(I) complex also seems to be pleiomorphic. The changes in the redox potentials show that, from the two forms of copper ions, $A\beta_{40}$ has a higher affinity to Cu(I) ions and the redox properties of the Cu(II)-$A\beta_{40}$ complexes are changing with time during incubation.[81] The affinity of Aβ towards Cu(I) has not been directly determined, but it is assumed to be higher than Aβ affinity towards Cu(II) since the midpoint redox potential of Cu(II)-Aβ/Cu(I)-Aβ is higher than that of free Cu(II)/Cu(I).[80]

A review covering the structural insights and putative mechanisms of Aβ-mediated ROS production by copper ions has recently been published by Hureau and Faller.[82]

Binding of Zn(II) to Aβ

It is commonly accepted that Zn(II) ions form a 1 : 1 complex with Aβ with involvement of the three His residues in the coordination of the Zn(II) ion.[42,83] The complex is a hexa-coordinated bipyramid and structural studies indicate that His6 Nδ, His13, His14 Nε, Asp1 amine, and/or Gln11 carboxylate are bound to Zn^{2+} in the case of human Aβ.[83] However, in contrast to Cu(II) ions, the binding of Zn(II) to Aβ often leads to fast peptide aggregation, the rate and extent of which depend on the peptide length and structure. The Zn(II)-induced Aβ assembly into tinctoral aggregates was first discovered by Bush and colleagues in 1994, where the aggregation was triggered by sub-stoichiometric concentrations of Zn(II).[21,84] However, later it was shown that the effective concentrations of Zn(II) which induce Aβ aggregation are considerably larger (approx. 100 μM).[85–87] $A\beta_{40}$ can aggregate in the presence of Zn(II) ions within milliseconds[88] and the $A\beta_{16}$ form also undergoes fast Zn(II)-induced precipitation, whereas its derivative with protected terminal groups is stable for months under similar conditions.[89,90] Presence of stoichiometric amounts of Zn(II) causes fast precipitation of $A\beta_{40}$ oligomers[91,92] as well as of the $A\beta_{42}$ peptide.[74] Thus, in the case of full-length Aβ peptides the monomeric Zn(II)-Aβ complex is prone to aggregation, which may significantly interfere with the determination of Zn(II) binding affinity. There is evidence suggesting that Zn(II) induces His or Zn(II) cross-linked peptide structures,[45,93] but it is not clear whether the aggregation occurs due to extensive cross-linking or low solubility of the Zn(II)-Aβ complex. Thus, it seems that Zn(II) binding to Aβ cannot be analyzed without accounting for the aggregation of the peptide.

The K_D values of the Zn(II)-Aβ complex reported in the literature vary from 1 to 300 μM. Lower affinity values (K_D = 50–300 μM) were determined from metal ion-induced changes in Tyr fluorescence[20,62] whereas other methods give K_D values in the region of 1–5 μM, which indicates the existence of a tighter complex.[24,69,86,94] In several studies the Zn-binding affinity of Aβ monomers, aggregates and fibrils has been found to be similar,[42,65,95] and it has been concluded that the thermodynamics of metal-transfer reactions from and to Aβ is only slightly dependent on the Aβ aggregation state. At the same time it has been demonstrated that the initial Zn(II)-$A\beta_{40}$ complex with K_D equal to 60 μM undergoes a transition to a

more tightly bound complex with $K_D \approx 2$ μM upon 30 min incubation, leading to formation of nonfibrillar Zn(II)-$A\beta_{40}$ aggregates.[62] A decrease of the K_D value from 7 μM to 2 μM upon aggregation of $A\beta_{40}$ and $A\beta_{42}$ was also observed by Talmard and colleagues.[29] Thus the K_D value for the Zn(II)-Aβ complex apparently depends on the incubation time of the complex, and it can be hypothesized that the Zn(II) binding affinity of Aβ monomers is close to 100 μM and increases to 1–5 μM upon aggregation.

The question whether the Zn(II) binding affinity of Aβ observed is conditional or if it depends on the buffer component(s) and concentration was already raised in the first metal-binding study,[84] where the effect of Tris buffer on Zn(II) binding was observed. However, measurements in 10 mM and 100 mM Tris showed that the difference in the K_D^{app} values was substantially smaller than that predicted from the Zn(II) binding to Tris buffer, suggesting that ternary complexes are formed.[62] The higher affinity of Aβ aggregates towards Zn(II) has to be taken into account in designing metal ion chelators for therapeutic use. However, it should also be considered that the dissociation of metal ions from plaques is not necessarily controlled by thermodynamics, as metal ions might also be kinetically trapped within the plaques.

Effects of Cu(II) and Zn(II) on Aβ aggregation

In vitro the Aβ peptides can be converted into typical amyloid fibrils with a cross-β-sheet structure characteristic to amyloid plaques, whereas the fibrillation shows a sigmoidal time-curve typical for autocatalytic processes. The growth is initiated by the formation of fibrillization nuclei or "seeds". The structure and thermodynamics of the formation of these particles that are unstable by definition remains elusive, however, there is a consensus that these particles are rich in β-sheet secondary structure elements, which form a template for the interaction with incoming peptides through an interchain hydrogen bonding network. A recent kinetic study has revealed that, in the case of Aβ, the critical nuclei may consist of only two peptide molecules.[96] In general, the fibril growth occurs due to the addition of monomers on the growing end of the fibril, and this process is followed by fibril "maturation" *e.g.* bundling and formation of interfibrillar stabilizing interactions. The Aβ fibrillation process can be substantially accelerated by agitation of the incubation mixture and by addition of fragmented preformed Aβ fibrils that act as polymerization "seeds". In agitated solutions the Aβ fibrillization process is fast and highly reproducible.[74,96]

Metal ions like Zn(II) and Cu(II) have a significant influence on the fibrillation of Aβ peptides, however, the studies of their effects have revealed contradictory results about the nature and even the direction of the effects. For instance, Zn(II) has been reported both to inhibit[74,97–101] and to enhance fibril formation.[24–29,102] In the case of native fibrils from post-mortem AD brain tissue, chelation of Zn(II) increases the solubility of Aβ.[41] Both effects, suppression and initialization of Aβ fibrillation, have also been reported for Cu(II).[30,31,55,81,97,100,103–106] In a few cases complex effects have been observed[107] or no influence was detected at all.[108] Recently it was shown that Aβ fibrils are formed in agitated solutions both in the presence and absence of Zn(II) and Cu(II), but not in the presence of clioquinol.[108] NMR studies have shown that Aβ, complexed with either Cu(II) or Zn(II), can attain the aggregation-prone β-strain-turn-β-strain motif similar to that in fibrils.[109] On the other hand it has also been concluded that the binding of Cu(II) to Aβ elongates the time necessary to attain the same β-sheet content as for the metal-free peptide.[81]

One reason for the contradictions is that, in the early papers, the metal-induced aggregation was determined but the nature of the aggregates was not specified. Later it was found that the metal-induced aggregates are predominantly non-fibrillar,[74,97,98,110,111] and currently it is generally accepted that Zn(II) ions induce fast aggregation of both full-length and truncated Aβ peptides into nonfibrillar aggregates. The effects of Zn(II) on Aβ may depend substantially on the Aβ concentration: it has been shown that Zn(II) selectively precipitates oligomers present at high concentrations of Aβ.[91,92] However, Zn(II) also induces lateral aggregation of Aβ fibrils[112] and, in some cases, enhanced formation of fibrillar structures in the presence of metal ions has been observed.[24,107]

Cu(II) ions can also induce Aβ aggregation,[22,61,113] however their presence inhibits Zn(II)-induced aggregation of Aβ peptide[56,104] suggesting that Cu(II)-Aβ is more soluble than its Zn(II) counterpart. The mechanism by which the metal ions induce Aβ aggregation is not clear. The metal-induced conformation can be more prone to aggregation[109] *e.g.* the effect may be kinetic. The effect may also be thermodynamic *e.g.* the metal-Aβ complex may have low solubility. It has been shown that Zn(II), but not Cu(II), induces larger hydrophobic exposures of the Aβ peptide resulting in its destabilization in solution.[111] Aβ peptides with exposed apolar regions might aggregate by the influence of hydrophobic forces, however, bridging of Aβ molecules by metal ions or His residues has also been discussed as a putative mechanism causing metal-induced peptide aggregation.[19,58]

The fibrillation clearly consists of two different processes—nucleation and fibril elongation, and the influence of effectors on these stages can be different. Thus, the answer to the question of whether a compound inhibits or enhances fibrillation may depend on the particular experimental conditions. Biometals, especially Zn(II), are causing fast aggregation of Aβ peptide that can happen in milliseconds.[88] It has been shown that the metal-induced Aβ aggregates are not dead-end products of peptide assembly and they can evolve to Aβ fibrils.[74] The formation of fibrils in the presence of Zn(II) or Cu(II) at 37 °C does not take more than 24 h[108] and the fibrils formed contain the corresponding metal ion.[40] The conversion of initially non-fibrillar metal-induced Aβ aggregates to fibrils can also explain the contradiction between the results of metal ion effects on Aβ fibrillation obtained by different experiments. The fibrillization of Aβ is slow under quiescent solutions in the absence of fibrillar seeds; even $A\beta_{42}$ is stable for several days in the absence of metal ions.[25] As Zn(II) and Cu(II) ions cause fast peptide assembly into metal-induced aggregates that can transform to fibrils within 24 h, the overall fibrillization process under quiescent conditions can be accelerated by metal ions. Indeed, it has been shown recently that fibrillation of Aβ is significantly accelerated by the influence of substoichiometric Cu(II) concentrations, under

 This journal is © The Royal Society of Chemistry 2011

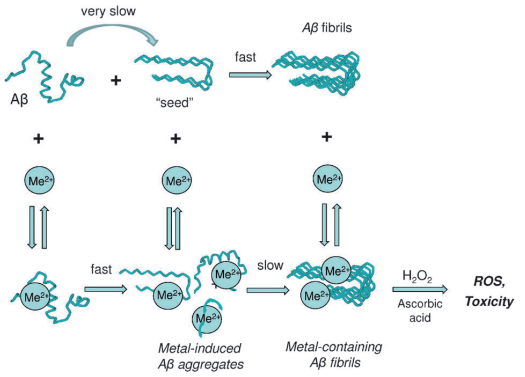

Fig. 3 Fibrillization of Aβ peptide *in vitro* in the presence of metal ions. In the presence of fibrillar nucleus the fibril growth through monomer addition is "fast" (half-life less than one hour). Added metal ions form monomeric complexes with Aβ that precipitate in a non-fibrillar form and also bind to growing fibril ends, thus inhibiting the fast fibrillization process and turning it into a "slow" process that takes a few days. The formation of fibrillar seeds is referred to as "very slow" (it can take several weeks under quiescent conditions). In the absence of seeds the binding of metal ions to Aβ leads to "slow" formation of fibrils, thus increasing the fibrillation rate. Binding of metal ions to fibrils is only partially reversible, the metal ions are "trapped" within matured fibrils.

the conditions where the process in the absence of metal ions is slow (lag period 70–100 h), however, Cu(II) at higher concentrations and Zn(II) still inhibit the fibrillation and result in the formation of nonfibrillar aggregates.[31]

In the presence of pre-formed Aβ seeds and/or agitation[74,114] the fibril growth is fast, and under such "seed-saturated" conditions the metal ions inhibit fibrillization by lowering the concentration of the free peptide due to Me(II)-Aβ complex formation. This seems to be the main effect for Cu(II). Surprisingly, Zn(II), which forms a weaker complex with Aβ than Cu(II), is a more potent inhibitor of Aβ fibrillization than Cu(II) in the agitated conditions.[74] The higher efficiency of Zn(II) as a fibrillization inhibitor can be caused by fast formation of nonfibrillar Zn(II)-Aβ aggregates or by binding of the Zn(II) ion to the growing fibril end, which has been observed recently.[100] The inhibitory effect of metal ions on fast Aβ fibrillization is at least partially "reversible", *e.g.* addition of chelators induced fast fibrillization and the addition of metal ions to "fresh" (but not "aged") fibrils caused their transformation to nonfibrillar aggregates.[74,114] The definition of "fresh" fibrils in this context is arbitrary and depends on the particular experimental conditions, since the loss of fibrillar structure in TEM and lower Thioflavin T binding capacity is also observed for "aged" fibrils.[105] In addition Zn(II) can also induce lateral aggregation of fibrils that occur in plaques.[112] The two different pathways leading to fibril formation *in vitro* in the presence of metal ions described above are summarized in Fig. 3.

Role of His residues in Aβ fibrillization

The role of His residues, mainly His13 that is missing in rodents, has been the focus of intensive research as the His residues may mediate the effects of Zn(II) and Cu(II) on amyloid formation. His residues are involved in metal binding and their environment is rapidly changing during fibril formation.[115,116] It is often taken almost for granted that the replacement of His13 with Ala or Arg completely suppresses the metal induced aggregation of Aβ, however, in the paper[117] which is often cited to confirm this assumption it was demonstrated that the solubility of H13R $A\beta_{28}$ in the phosphate buffer containing high Zn(II) concentration is two times lower than that of wild type $A\beta_{28}$. The relevance of the observed lower solubility of the truncated peptide with His13 in plaque formation is elusive. The replacement of His residues with Ala did not affect the kinetic parameters of Aβ fibrillization and only slightly suppressed the inhibition of fibrillization by metal ions.[74] It seems probable that the part of the Aβ molecule containing His residues is involved in both critical processes of plaque formation—metal binding and fibrillation. However, the energetic contribution of His residues to the stability of the fibrillar state and metal binding seems to be not very significant due to the heterogeneity of the complex structures. A recent study has shown that the key amino acid change responsible for the different Cu(II) binding of human and rodent Aβ peptides is the replacement of Arg5 with Glu and not the H13R substitution.[118]

Molecular background of the metal-chelating therapeutic approach in AD

Considering the perspectives of the metal chelating therapy it is important to find out which step of fibril formation is affected by metal ions *in vivo*. Metal chelating therapy is a relatively new therapeutic approach for AD[41,119] and it was initially assumed that the removal of metal ions from amyloid plaques leads to the solubilisation of the plaques. This hypothesis has been tested on transgenic AD model mice using weak chelators such as clioquinol (CQ) and its second generation derivative (PBT2), which reduced plaque load.[119,120] However, several studies demonstrate that the mechanism of metal chelating therapy is more complex than initially proposed,[121,122] for instance, it has been shown that CQ promotes rather than inhibits the formation of Aβ fibrils *in vitro*.[26] We concluded above as well as in the recent paper[74] that metal ions can enhance or inhibit fibril formation depending on the fibrillation conditions. The same is true for metal chelators *in vitro*: they might demetallate metal-Aβ complexes and solubilize metal induced aggregates to Aβ monomers, which can increase the fibrillation rate in the presence of sufficient amounts of fibrillation seeds or plaques. On the other hand, in the absence of seeds, the metal chelating agents can inhibit fibrillation by preventing the formation of metal induced aggregates that can evolve slowly to fibrillization centers or fibrils.

Under *in vivo* conditions, where the concentration of Aβ is in the nanomolar range,[123] the aggregation of monomeric Aβ molecules is a slow and unlikely process, especially considering the formation of oligomeric nuclei for fibrillation. However, disturbed metal homeostasis and elevated local levels of metal ions may enhance metal-induced assembly of Aβ into non-fibrillar aggregates. If the metal ions are not removed fast

enough by natural metal-buffering proteins such as MTs then nonfibrillar metal-induced aggregates can eventually transform into fibrillar seeds and subsequently to fibrils.[74] Cherny and colleagues[41] demonstrated that selected chelators in their optimal concentrations increase the amount of extractable Aβ from the post-mortem brain from 3 to 10% of the total Aβ, however, it is not excluded that this peptide might originate from nonfibrillar metal-induced aggregates. In AD patients the levels of a brain-specific Zn(II) binding protein, MT-3, are substantially (10-fold) lower than in healthy persons.[124] The lower levels of MT-3 reduce zinc buffering capacity in the regions of zinc-enriched neurons, which may increase the availability of Zn(II) ions to Aβ. Thus, it seems that metal chelators might be useful in preventing amyloid formation; however, when amyloid plaques are already formed their therapeutic potential may be limited as chelators are not able to dissolve fibrillar Aβ. Besides sequestering the metal ions from Aβ, the metal chelators affect all other metal–peptide and metal–protein equilibria, which may exert systematic effects at the cellular and the whole organism level.[7,10]

Toxicity of multimeric forms of Aβ

It is generally accepted that Aβ toxicity is related to the aggregated rather than to the monomeric Aβ form. Different Aβ multimers starting from dimers up to dodecamers have been shown to be cytotoxic. Over the last few years it has been shown that Aβ is most toxic to cell cultures in the form of oligomers generated from supersaturated solutions of the peptide using organic solvents.[3,125,126] Dilution of concentrated solutions of organic compounds in DMSO into water is a well-known procedure for producing emulsions or micelles, however, there is no biological "equivalent" of this procedure in organisms that can lead to similar results. Oligomers are obtained from brain extracts of AD model animals,[127] however, the relation between the artificial toxic oligomers and those observed in brain extracts is not clear. The thermodynamic equilibrium between oligomers and monomers depends, according to the simple equilibrium model, on the peptide concentration in *n*th power, where *n* is the number of monomers in the oligomer. The spontaneous formation of toxic amounts of oligomers (for example dodecamers) in the brain, where the Aβ concentration is approximately 10 nM, is highly improbable, considering that Aβ oligomers are not seen experimentally *in vitro* at peptide concentrations below 10 μM. Moreover, kinetic evidence shows that the minimal structure (stable nucleus) that initiates fibril elongation is a dimer[96] and the growth of individual plaques in model animals is fast,[128] suggesting that fibrillation would out-compete oligomerization at low peptide concentration. These observations suggest that the formation of primary (*e.g.* those forming directly from peptide monomers) Aβ oligomers in the brain has low probability in the amounts sufficient to be toxic. It has been suggested that toxic oligomers can occur in the brain as secondary particles derived from fibrils.[129] Thus, in our opinion the role and especially the origin of Aβ oligomers in AD are still open for debate, and this indirectly supports the view that Aβ fibrils arise from metal-induced Aβ aggregates.

Toxicity of metallated forms of Aβ

It is well established that the ability of Aβ to generate ROS is determined mainly by the presence of redox-active copper ions. Moreover, hydrogen peroxide mediates Aβ toxicity as the antioxidant enzyme catalase can protect cells from Aβ toxicity.[79,130] It should be noted that *in vitro*-generated Aβ fibrils, that exhibit low toxicity in comparison to that of oligomers, are often missing an important characteristic feature of *in vivo* Aβ fibrils: they lack metal ions, which are present in the native amyloid plaques at high millimolar levels.[15–17] The absence of Cu(II) in artificial fibrils tested is especially noteworthy, since an extensive oxidative stress characteristic to the AD brain originates from the redox-active Cu(II) in amyloid plaques. A causative link between Aβ-bound copper and oxidative stress is supported by numerous evidence, however most importantly: (i) the sequestering of Cu(II) ions from Aβ decreases the toxicity of the peptide substantially;[77] (ii) only copper-containing Aβ aggregates are toxic to primary neurons[74] and (iii) in a recent study Sarell and co-workers demonstrated that Cu(II)-containing fibrils are more toxic to PC12 cells than other forms of the peptide.[31]

Cu(II) enrichment in amyloid plaques and the electrochemical activity of Cu(II) bound to Aβ leading to the generation of ROS is well documented. Considering the oxidative stress arising from ROS generated by redox cycling of Cu(II) in amyloid plaques, the main question is not whether the ROS are generated but whether their amount is large enough to cause neurodegeneration. *In vitro* studies have shown that Aβ addition inhibits the rate of ROS generation in Cu(II) containing solutions[131] and reduces the toxicity of metal ions,[132] suggesting that Aβ may help to limit the neurotoxicity of redox metals in the early stages of AD. The ideas regarding a neuroprotective role of Aβ as a sequestrator of redox active ions is not new (for historical background see ref. 133). However, experiments with soluble Cu(II)-Aβ complexes may be biologically irrelevant as there are several proteins in the brain that can sequester Cu(II) from Cu(II)-Aβ complex. The main candidates for this are HSA[37] and MTs.[39,40,77,95] HSA has a considerably higher affinity towards Cu(II) than Aβ, and it is also more abundant in CSF than Aβ and is able to sequester Cu(II) from the Cu(II)-Aβ complex.[37,38] The Zn_7MT is also able to switch three zinc ions for Cu(II) ions initially bound to Aβ and suppress its toxicity *in vitro*.[40,77]

The electrochemically active copper can, however, accumulate in the brain when it is not accessible to these proteins, for instance when it is buried within the network of amyloid fibrils. It has been shown that insoluble *in vitro* generated Cu(II)-$Aβ_{42}$ aggregates are resistant to very potent chelators[22] probably because of kinetic trapping of Cu(II) inside the fibrillar matrix. The assumption of kinetic trapping of the metal ions is also supported by the observation that Zn-MT cannot solubilize or reduce toxicity of already formed Cu(II)-containing fibrils.[40] Cu(II) ions can manifest redox activity only in the presence of reducing agents in the environment, thus they have to be present in cytotoxicity experiments in sufficient amount. It is demonstrated in many reports that Cu-Aβ aggregates are cytotoxic in the presence of ascorbic acid in the concentrations similar to those in CSF.[39,40,77,82,134]

This journal is © The Royal Society of Chemistry 2011

In these experiments ROS are most probably generated by using endogeneous hydrogen peroxide that can freely penetrate cell membranes, the concentration of which can reach up to micromolar in the extracellular space. Thus there is sufficient evidence to assume that the cytotoxicity of Aβ amyloid aggregates is not caused by fibrillar assemblies as such but from buried redox-active metal ions like copper, which in the presence of reducing agents such as ascorbic acid induces ROS generation from endogeneous hydrogen peroxide.

It is known that there is low neurodegeneration around amyloid plaques in the brain of recombinant mice as compared to that in human AD brain.[135] Since the direct measurements of copper content by synchrotron X-ray fluorescence (XRF) microprobes in amyloid plaques from recombinant mice brain show lower copper content than plaques from human AD brain, the lower neurotoxicity can also be correlated with copper content in Aβ plaques.[135]

Moreover, it is demonstrated that upon amyloid plaque formation microglia cells are activated and recruited to the plaque,[128] whereas microglia activation mediates fibrillar amyloid-beta toxicity to neurons.[136] Upon activation the glia cells secrete large amounts of H_2O_2 and NO in a process known as a 'respiratory burst'. Thus, toxicity of activated microglia may arise from increased local levels of hydrogen peroxide around the plaques, which is a substrate for ROS production by amyloid-bound metal ions in a catalytic process.

Concluding remarks

Although the process of Aβ aggregation and its interactions with other biomolecules, including two important biometals, zinc and copper, is intensively studied, the information necessary to develop drugs with disease-modifying effects and a strategy to prevent AD is still missing. To understand the structural basis for the neurotoxicity of Aβ and its metal complexes, and describe the *in vivo* aggregation pathway of Aβ and different intermediates, is probably the most important and most difficult unresolved task in this field. Despite the large inconsistency of the results, some of the most important findings in this field can be highlighted: (i) the affinity of Aβ towards Cu(II) and Zn(II) is sufficiently high to form monomeric complexes with synaptic Cu(II) and Zn(II) ions, however, monomeric Aβ cannot compete with biological metal chelators such as serum albumin and MT-3; (ii) Cu(II)-Aβ complex has a pleiomorphic and highly dynamic structure; (iii) several Aβ forms, monomeric, oligomeric, nonfibrillar and fibrillar, can bind copper whereas the copper ions can be kinetically trapped within the fibrillar Aβ aggregates that makes the complex resistant to metal chelators; (iv) copper ions bound to Aβ are electrochemically active, *e.g.* they can generate ROS in the presence of hydrogen peroxide and reducing agents. In this context the recent observation that Cu(II) bound to Aβ fibrils can also generate ROS might provide a key for understanding the putative role of copper in Aβ toxicity and AD pathology; (v) Zn(II) and Cu(II) inhibit fast "agitation induced" fibrillization of Aβ, however, in the conditions where fibrillization is slow (nonagitated solutions) at least Cu(II) at low concentrations can promote fibrillization and lead to the generation of highly toxic copper-containing fibrillar Aβ forms. In our opinion these results support the opinion that the pathogenic structure that causes the death of neurons in AD can be copper-containing amyloid plaques with fibrillar structure that generate ROS.

References

1 J. A. Hardy and G. A. Higgins, *Science*, 1992, **256**, 184–185.
2 C. Haass and D. J. Selkoe, *Cell*, 1993, **75**, 1039–1042.
3 D. M. Walsh and D. J. Selkoe, *J. Neurochem.*, 2007, **101**, 1172–1184.
4 E. Gaggelli, H. Kozlowski, D. Valensin and G. Valensin, *Chem. Rev.*, 2006, **106**, 1995–2044.
5 P. A. Adlard and A. I. Bush, *J. Alzheimer's Dis.*, 2006, **10**, 145–163.
6 P. Zatta, D. Drago, S. Bolognin and S. L. Sensi, *Trends Pharmacol. Sci.*, 2009, **30**, 346–355.
7 Y. H. Hung, A. I. Bush and R. A. Cherny, *JBIC, J. Biol. Inorg. Chem.*, 2010, **15**, 61–76.
8 P. S. Donnelly, Z. Xiao and A. G. Wedd, *Curr. Opin. Chem. Biol.*, 2007, **11**, 128–133.
9 K. J. Barnham and A. I. Bush, *Curr. Opin. Chem. Biol.*, 2008, **12**, 222–228.
10 S. L. Sensi, P. Paoletti, A. I. Bush and I. Sekler, *Nat. Rev. Neurosci.*, 2009, **10**, 780–U738.
11 M. L. Schlief, A. M. Craig and J. D. Gitlin, *J. Neurosci.*, 2005, **25**, 239–246.
12 A. Hopt, S. Korte, H. Fink, U. Panne, R. Niessner, R. Jahn, H. Kretzschmar and J. Herms, *J. Neurosci. Methods*, 2003, **128**, 159–172.
13 A. I. Bush and R. E. Tanzi, *Neurotherapeutics*, 2008, **5**, 421–432.
14 P. J. Crouch, A. R. White and A. I. Bush, *FEBS J.*, 2007, **274**, 3775–3783.
15 M. A. Lovell, J. D. Robertson, W. J. Teesdale, J. L. Campbell and W. R. Markesbery, *J. Neurol. Sci.*, 1998, **158**, 47–52.
16 L. M. Miller, Q. Wang, T. P. Telivala, R. J. Smith, A. Lanzirotti and J. Miklossy, *J. Struct. Biol.*, 2006, **155**, 30–37.
17 R. Rajendran, R. Minqin, M. D. Ynsa, G. Casadesus, M. A. Smith, G. Perry, B. Halliwell and F. Watt, *Biochem. Biophys. Res. Commun.*, 2009, **382**, 91–95.
18 R. W. Hutchinson, A. G. Cox, C. W. McLeod, P. S. Marshall, A. Harper, E. L. Dawson and D. R. Howlett, *Anal. Biochem.*, 2005, **346**, 225–233.
19 C. C. Curtain, F. Ali, I. Volitakis, R. A. Cherny, R. S. Norton, K. Beyreuther, C. J. Barrow, C. L. Masters, A. I. Bush and K. J. Barnham, *J. Biol. Chem.*, 2001, **276**, 20466–20473.
20 W. Garzon-Rodriguez, A. K. Yatsimirsky and C. G. Glabe, *Bioorg. Med. Chem. Lett.*, 1999, **9**, 2243–2248.
21 A. I. Bush, W. H. Pettingell, Jr., M. D. Paradis and R. E. Tanzi, *J. Biol. Chem.*, 1994, **269**, 12152–12158.
22 C. S. Atwood, R. D. Moir, X. Huang, R. C. Scarpa, N. M. Bacarra, D. M. Romano, M. A. Hartshorn, R. E. Tanzi and A. I. Bush, *J. Biol. Chem.*, 1998, **273**, 12817–12826.
23 J. Dong, C. S. Atwood, V. E. Anderson, S. L. Siedlak, M. A. Smith, G. Perry and P. R. Carey, *Biochemistry*, 2003, **42**, 2768–2773.
24 F. Ricchelli, D. Drago, B. Filippi, G. Tognon and P. Zatta, *Cell. Mol. Life Sci.*, 2005, **62**, 1724–1733.
25 X. Huang, C. S. Atwood, R. D. Moir, M. A. Hartshorn, R. E. Tanzi and A. I. Bush, *JBIC, J. Biol. Inorg. Chem.*, 2004, **9**, 954–960.
26 S. Bolognin, P. Zatta, D. Drago, G. Tognon, P. P. Parnigotto and F. Ricchelli, *NeuroMol. Med.*, 2008, **10**, 322–332.
27 T. Chen, X. Wang, Y. He, C. Zhang, Z. Wu, K. Liao, J. Wang and Z. Guo, *Inorg. Chem.*, 2009, **48**, 5801–5809.
28 C. Rodriguez-Rodriguez, N. Sanchez de Groot, A. Rimola, A. Alvarez-Larena, V. Lloveras, J. Vidal-Gancedo, S. Ventura, J. Vendrell, M. Sodupe and P. Gonzalez-Duarte, *J. Am. Chem. Soc.*, 2009, **131**, 1436–1451.
29 C. Talmard, R. Leuma Yona and P. Faller, *JBIC, J. Biol. Inorg. Chem.*, 2009, **14**, 449–455.
30 D. P. Smith, G. D. Ciccotosto, D. J. Tew, M. T. Fodero-Tavoletti, T. Johanssen, C. L. Masters, K. J. Barnham and R. Cappai, *Biochemistry*, 2007, **46**, 2881–2891.

31 C. J. Sarell, S. R. Wilkinson and J. H. Viles, *J. Biol. Chem.*, 2010, **285**, 41533–41540.
32 J. Y. Lee, T. B. Cole, R. D. Palmiter, S. W. Suh and J. Y. Koh, *Proc. Natl. Acad. Sci. U. S. A.*, 2002, **99**, 7705–7710.
33 D. L. Sparks and B. G. Schreurs, *Proc. Natl. Acad. Sci. U. S. A.*, 2003, **100**, 11065–11069.
34 R. Sanokawa-Akakura, W. Cao, K. Allan, K. Patel, A. Ganesh, G. Heiman, R. Burke, F. W. Kemp, J. D. Bogden, J. Camakaris, R. B. Birge and M. Konsolaki, *PLoS One*, 2010, **5**, e8626.
35 X. Huang, M. P. Cuajungco, C. S. Atwood, M. A. Hartshorn, J. D. Tyndall, G. R. Hanson, K. C. Stokes, M. Leopold, G. Multhaup, L. E. Goldstein, R. C. Scarpa, A. J. Saunders, J. Lim, R. D. Moir, C. Glabe, E. F. Bowden, C. L. Masters, D. P. Fairlie, R. E. Tanzi and A. I. Bush, *J. Biol. Chem.*, 1999, **274**, 37111–37116.
36 D. G. Smith, R. Cappai and K. J. Barnham, *Biochim. Biophys. Acta, Biomembr.*, 2007, **1768**, 1976–1990.
37 M. Rozga and W. Bal, *Chem. Res. Toxicol.*, 2010, **23**, 298–308.
38 L. Perrone, E. Mothes, M. Vignes, A. Mockel, C. Figueroa, M. C. Miquel, M. L. Maddelein and P. Faller, *ChemBioChem*, 2010, **11**, 110–118.
39 G. Meloni, P. Faller and M. Vasak, *J. Biol. Chem.*, 2007, **282**, 16068–16078.
40 R. S. Chung, C. Howells, E. D. Eaton, L. Shabala, K. Zovo, P. Palumaa, R. Sillard, A. Woodhouse, W. R. Bennett, S. Ray, J. C. Vickers and A. K. West, *PLoS ONE*, 2010, **5**.
41 R. A. Cherny, J. T. Legg, C. A. McLean, D. P. Fairlie, X. Huang, C. S. Atwood, K. Beyreuther, R. E. Tanzi, C. L. Masters and A. I. Bush, *J. Biol. Chem.*, 1999, **274**, 23223–23228.
42 P. Faller and C. Hureau, *Dalton Trans.*, 2009, 1080–1094.
43 C. D. Syme, R. C. Nadal, S. E. Rigby and J. H. Viles, *J. Biol. Chem.*, 2004, **279**, 18169–18177.
44 L. Guilloreau, L. Damian, Y. Coppel, H. Mazarguil, M. Winterhalter and P. Faller, *JBIC, J. Biol. Inorg. Chem.*, 2006, **11**, 1024–1038.
45 V. Minicozzi, F. Stellato, M. Comai, M. D. Serra, C. Potrich, W. Meyer-Klaucke and S. Morante, *J. Biol. Chem.*, 2008, **283**, 10784–10792.
46 Y. Lu, M. Prudent, L. Qiao, M. A. Mendez and H. H. Girault, *Metallomics*, 2010, **2**, 474–479.
47 C. Hureau, Y. Coppel, P. Dorlet, P. L. Solari, S. Sayen, E. Guillon, L. Sabater and P. Faller, *Angew. Chem., Int. Ed.*, 2009, **48**, 9522–9525.
48 S. C. Drew, C. L. Masters and K. J. Barnham, *J. Am. Chem. Soc.*, 2009, **131**, 8760–8761.
49 B. K. Shin and S. Saxena, *Biochemistry*, 2008, **47**, 9117–9123.
50 T. Kowalik-Jankowska, M. Ruta-Dolejsz, K. Wisniewska and L. Lankiewicz, *J. Inorg. Biochem.*, 2002, **92**, 1–10.
51 C. J. Sarell, C. D. Syme, S. E. Rigby and J. H. Viles, *Biochemistry*, 2009, **48**, 4388–4402.
52 P. Dorlet, S. Gambarelli, P. Faller and C. Hureau, *Angew. Chem., Int. Ed.*, 2009, **48**, 9273–9276.
53 P. Dorlet, C. Hureau and P. Faller, Eurobic 9: Proceedings of the 9th European Biological Inorganic Chemistry Conference, 2008, 39–45.
54 S. C. Drew, C. J. Noble, C. L. Masters, G. R. Hanson and K. J. Barnham, *J. Am. Chem. Soc.*, 2009, **131**, 1195–1207.
55 S. Jun, J. R. Gillespie, B. K. Shin and S. Saxena, *Biochemistry*, 2009, **48**, 10724–10732.
56 T. Miura, K. Suzuki, N. Kohata and H. Takeuchi, *Biochemistry*, 2000, **39**, 7024–7031.
57 S. Jun and S. Saxena, *Angew. Chem., Int. Ed.*, 2007, **46**, 3959–3961.
58 D. P. Smith, D. G. Smith, C. C. Curtain, J. F. Boas, J. R. Pilbrow, G. D. Ciccotosto, T. L. Lau, D. J. Tew, K. Perez, J. D. Wade, A. I. Bush, S. C. Drew, F. Separovic, C. L. Masters, R. Cappai and K. J. Barnham, *J. Biol. Chem.*, 2006, **281**, 15145–15154.
59 J. W. Karr and V. A. Szalai, *Biochemistry*, 2008, **47**, 5006–5016.
60 C. A. Damante, K. Osz, Z. Nagy, G. Pappalardo, G. Grasso, G. Impellizzeri, E. Rizzarelli and I. Sovago, *Inorg. Chem.*, 2008, **47**, 9669–9683.
61 C. S. Atwood, R. C. Scarpa, X. Huang, R. D. Moir, W. D. Jones, D. P. Fairlie, R. E. Tanzi and A. I. Bush, *J. Neurochem.*, 2000, **75**, 1219–1233.
62 V. Tougu, A. Karafin and P. Palumaa, *J. Neurochem.*, 2008, **104**, 1249–1259.
63 M. Rozga, A. M. Protas, A. Jablonowska, M. Dadlez and W. Bal, *Chem. Commun.*, 2009, 1374–1376.
64 M. Rozga, M. Kloniecki, M. Dadlez and W. Bal, *Chem. Res. Toxicol.*, 2010, **23**, 336–340.
65 L. Q. Hatcher, L. Hong, W. D. Bush, T. Carducci and J. D. Simon, *J. Phys. Chem. B*, 2008, **112**, 8160–8164.
66 Z. Xiao and A. G. Wedd, *Nat. Prod. Rep.*, 2010, **27**, 768–789.
67 J. W. Karr, H. Akintoye, L. J. Kaupp and V. A. Szalai, *Biochemistry*, 2005, **44**, 5478–5487.
68 L. Hong, W. D. Bush, L. Q. Hatcher and J. Simon, *J. Phys. Chem. B*, 2008, **112**, 604–611.
69 C. Talmard, A. Bouzan and P. Faller, *Biochemistry*, 2007, **46**, 13658–13666.
70 Y. Mekmouche, Y. Coppel, K. Hochgrafe, L. Guilloreau, C. Talmard, H. Mazarguil and P. Faller, *ChemBioChem*, 2005, **6**, 1663–1671.
71 C. Hureau, V. Balland, Y. Coppel, P. L. Solari, E. Fonda and P. Faller, *JBIC, J. Biol. Inorg. Chem.*, 2009, **14**, 995–1000.
72 M. Sokolowska and W. Bal, *J. Inorg. Biochem.*, 2005, **99**, 1653–1660.
73 L. Banci, I. Bertini, S. Ciofi-Baffoni, T. Kozyreva, K. Zovo and P. Palumaa, *Nature*, 2010, **465**, 645–U145.
74 V. Tougu, A. Karafin, K. Zovo, R. S. Chung, C. Howells, A. K. West and P. Palumaa, *J. Neurochem.*, 2009, **110**, 1784–1795.
75 X. Huang, C. S. Atwood, R. D. Moir, M. A. Hartshorn, J. P. Vonsattel, R. E. Tanzi and A. I. Bush, *J. Biol. Chem.*, 1997, **272**, 26464–26470.
76 P. W. Mantyh, J. R. Ghilardi, S. Rogers, E. DeMaster, C. J. Allen, E. R. Stimson and J. E. Maggio, *J. Neurochem.*, 1993, **61**, 1171–1174.
77 G. Meloni, V. Sonois, T. Delaine, L. Guilloreau, A. Gillet, J. Teissie, P. Faller and M. Vasak, *Nat. Chem. Biol.*, 2008, **4**, 366–372.
78 X. Huang, C. S. Atwood, M. A. Hartshorn, G. Multhaup, L. E. Goldstein, R. C. Scarpa, M. P. Cuajungco, D. N. Gray, J. Lim, R. D. Moir, R. E. Tanzi and A. I. Bush, *Biochemistry*, 1999, **38**, 7609–7616.
79 C. Opazo, X. Huang, R. A. Cherny, R. D. Moir, A. E. Roher, A. R. White, R. Cappai, C. L. Masters, R. E. Tanzi, N. C. Inestrosa and A. I. Bush, *J. Biol. Chem.*, 2002, **277**, 40302–40308.
80 J. Shearer and V. A. Szalai, *J. Am. Chem. Soc.*, 2008, **130**, 17826–17835.
81 M. Brzyska, K. Trzesniewska, A. Wieckowska, A. Szczepankiewicz and D. Elbaum, *ChemBioChem*, 2009, **10**, 1045–1055.
82 C. Hureau and P. Faller, *Biochimie*, 2009, **91**, 1212–1217.
83 E. Gaggelli, A. Janicka-Klos, E. Jankowska, H. Kozlowski, C. Migliorini, E. Molteni, D. Valensin, G. Valensin and E. Wieczerzak, *J. Phys. Chem. B*, 2008, **112**, 100–109.
84 A. I. Bush, W. H. Pettingell, G. Multhaup, M. d Paradis, J. P. Vonsattel, J. F. Gusella, K. Beyreuther, C. L. Masters and R. E. Tanzi, *Science*, 1994, **265**, 1464–1467.
85 W. P. Esler, E. R. Stimson, J. M. Jennings, J. R. Ghilardi, P. W. Mantyh and J. E. Maggio, *J. Neurochem.*, 1996, **66**, 723–732.
86 A. Clements, D. Allsop, D. M. Walsh and C. H. Williams, *J. Neurochem.*, 1996, **66**, 740–747.
87 A. M. Brown, D. M. Tummolo, K. J. Rhodes, J. R. Hofmann, J. S. Jacobsen and J. Sonnenberg-Reines, *J. Neurochem.*, 1997, **69**, 1204–1212.
88 D. Noy, I. Solomonov, O. Sinkevich, T. Arad, K. Kjaer and I. Sagi, *J. Am. Chem. Soc.*, 2008, **130**, 1376–1383.
89 S. A. Kozin, S. Zirah, S. Rebuffat, G. H. Hoa and P. Debey, *Biochem. Biophys. Res. Commun.*, 2001, **285**, 959–964.
90 S. Zirah, S. A. Kozin, A. K. Mazur, A. Blond, M. Cheminant, I. Segalas-Milazzo, P. Debey and S. Rebuffat, *J. Biol. Chem.*, 2006, **281**, 2151–2161.
91 K. Garai, B. Sahoo, S. K. Kaushalya, R. Desai and S. Maiti, *Biochemistry*, 2007, **46**, 10655–10663.
92 K. Garai, P. Sengupta, B. Sahoo and S. Maiti, *Biochem. Biophys. Res. Commun.*, 2006, **345**, 210–215.
93 Y. Miller, B. Ma and R. Nussinov, *Proc. Natl. Acad. Sci. U. S. A.*, 2010, **107**, 9490–9495.
94 J. Danielsson, R. Pierattelli, L. Banci and A. Graslund, *FEBS J.*, 2007, **274**, 46–59.

 This journal is © The Royal Society of Chemistry 2011

95 P. Faller, *ChemBioChem*, 2009, **10**, 2837–2845.
96 E. Hellstrand, B. Boland, D. M. Walsh and S. Linse, *ACS Chem. Neurosci.*, 2009, **1**, 13–18.
97 Y. Yoshiike, K. Tanemura, O. Murayama, T. Akagi, M. Murayama, S. Sato, X. Sun, N. Tanaka and A. Takashima, *J. Biol. Chem.*, 2001, **276**, 32293–32299.
98 B. Raman, T. Ban, K. Yamaguchi, M. Sakai, T. Kawai, H. Naiki and Y. Goto, *J. Biol. Chem.*, 2005, **280**, 16157–16162.
99 E. House, J. Collingwood, A. Khan, O. Korchazkina, G. Berthon and C. Exley, *J. Alzheimer's Dis.*, 2004, **6**, 291–301.
100 M. Innocenti, E. Salvietti, M. Guidotti, A. Casini, S. Bellandi, M. L. Foresti, C. Gabbiani, A. Pozzi, P. Zatta and L. Messori, *J. Alzheimer's Dis.*, 2010, **19**, 1223–1229.
101 J. Ryu, K. Girigoswami, C. Ha, S. H. Ku and C. B. Park, *Biochemistry*, 2008, **47**, 5328–5335.
102 J. Durand, G. Meloni, C. Talmard, M. Vasak and P. Faller, *Metallomics*, 2010.
103 J. Zou, K. Kajita and N. Sugimoto, *Angew. Chem., Int. Ed.*, 2001, **40**, 2274–2277.
104 K. Suzuki, T. Miura and H. Takeuchi, *Biochem. Biophys. Res. Commun.*, 2001, **285**, 991–996.
105 E. House, M. Mold, J. Collingwood, A. Baldwin, S. Goodwin and C. Exley, *J. Alzheimer's Dis.*, 2009, **18**, 811–817.
106 X. Dai, Y. Sun, Z. Gao and Z. Jiang, *J. Mol. Neurosci.*, 2010, **41**, 66–73.
107 G. M. Klug, D. Losic, S. S. Subasinghe, M. I. Aguilar, L. L. Martin and D. H. Small, *Eur. J. Biochem.*, 2003, **270**, 4282–4293.
108 A. M. Mancino, S. S. Hindo, A. Kochi and M. H. Lim, *Inorg. Chem.*, 2009, **48**, 9596–9598.
109 A. Olofsson, M. Lindhagen-Persson, M. Vestling, A. E. Sauer-Eriksson and A. Ohman, *FEBS J.*, 2009, **276**, 4051–4060.
110 C. Ha, J. Ryu and C. B. Park, *Biochemistry*, 2007, **46**, 6118–6125.
111 W. T. Chen, Y. H. Liao, H. M. Yu, I. H. Cheng and Y. R. Chen, *J. Biol. Chem.*, 2011.
112 D. S. Yang, J. McLaurin, K. Qin, D. Westaway and P. E. Fraser, *Eur. J. Biochem.*, 2000, **267**, 6692–6698.
113 M. F. Ahmad, D. Singh, A. Taiyab, T. Ramakrishna, B. Raman and C. M. Rao, *J. Mol. Biol.*, 2008, **382**, 812–824.
114 K. Zovo, E. Helk, A. Karafin, V. Tõugu and P. Palumaa, *Anal. Chem.*, 2010, **82**, 8558–8565.
115 L. Hou, H. Shao, Y. Zhang, H. Li, N. K. Menon, E. B. Neuhaus, J. M. Brewer, I. J. Byeon, D. G. Ray, M. P. Vitek, T. Iwashita, R. A. Makula, A. B. Przybyla and M. G. Zagorski, *J. Am. Chem. Soc.*, 2004, **126**, 1992–2005.
116 J. Dong, J. E. Shokes, R. A. Scott and D. G. Lynn, *J. Am. Chem. Soc.*, 2006, **128**, 3540–3542.
117 S. T. Liu, G. Howlett and C. J. Barrow, *Biochemistry*, 1999, **38**, 9373–9378.
118 L. Hong, T. M. Carducci, W. D. Bush, C. G. Dudzik, G. L. Millhauser and J. D. Simon, *J. Phys. Chem. B*, 2010, **114**, 11261–11271.
119 R. A. Cherny, C. S. Atwood, M. E. Xilinas, D. N. Gray, W. D. Jones, C. A. McLean, K. J. Barnham, I. Volitakis, F. W. Fraser, Y. Kim, X. Huang, L. E. Goldstein, R. D. Moir, J. T. Lim, K. Beyreuther, H. Zheng, R. E. Tanzi, C. L. Masters and A. I. Bush, *Neuron*, 2001, **30**, 665–676.
120 P. A. Adlard, R. A. Cherny, D. I. Finkelstein, E. Gautier, E. Robb, M. Cortes, I. Volitakis, X. Liu, J. P. Smith, K. Perez, K. Laughton, Q. X. Li, S. A. Charman, J. A. Nicolazzo, S. Wilkins, K. Deleva, T. Lynch, G. Kok, C. W. Ritchie, R. E. Tanzi, R. Cappai, C. L. Masters, K. J. Barnham and A. I. Bush, *Neuron*, 2008, **59**, 43–55.
121 A. R. White, T. Du, K. M. Laughton, I. Volitakis, R. A. Sharples, M. E. Xilinas, D. E. Hoke, R. M. Holsinger, G. Evin, R. A. Cherny, A. F. Hill, K. J. Barnham, Q. X. Li, A. I. Bush and C. L. Masters, *J. Biol. Chem.*, 2006, **281**, 17670–17680.
122 P. J. Crouch, D. J. Tew, T. Du, D. N. Nguyen, A. Caragounis, G. Filiz, R. E. Blake, I. A. Trounce, C. P. Soon, K. Laughton, K. A. Perez, Q. X. Li, R. A. Cherny, C. L. Masters, K. J. Barnham and A. R. White, *J. Neurochem.*, 2009, **108**, 1198–1207.
123 M. Sjogren, H. Vanderstichele, H. Agren, O. Zachrisson, M. Edsbagge, C. Wikkelso, I. Skoog, A. Wallin, L. O. Wahlund, J. Marcusson, K. Nagga, N. Andreasen, P. Davidsson, E. Vanmechelen and K. Blennow, *Clin. Chem.*, 2001, **47**, 1776–1781.
124 W. H. Yu, W. J. Lukiw, C. Bergeron, H. B. Niznik and P. E. Fraser, *Brain Res.*, 2001, **894**, 37–45.
125 M. P. Lambert, A. K. Barlow, B. A. Chromy, C. Edwards, R. Freed, M. Liosatos, T. E. Morgan, I. Rozovsky, B. Trommer, K. L. Viola, P. Wals, C. Zhang, C. E. Finch, G. A. Krafft and W. L. Klein, *Proc. Natl. Acad. Sci. U. S. A.*, 1998, **95**, 6448–6453.
126 W. B. Stine, Jr., K. N. Dahlgren, G. A. Krafft and M. J. LaDu, *J. Biol. Chem.*, 2003, **278**, 11612–11622.
127 S. Lesne, M. T. Koh, L. Kotilinek, R. Kayed, C. G. Glabe, A. Yang, M. Gallagher and K. H. Ashe, *Nature*, 2006, **440**, 352–357.
128 M. Meyer-Luehmann, T. L. Spires-Jones, C. Prada, M. Garcia-Alloza, A. de Calignon, A. Rozkalne, J. Koenigsknecht-Talboo, D. M. Holtzman, B. J. Bacskai and B. T. Hyman, *Nature*, 2008, **451**, 720–U725.
129 I. C. Martins, I. Kuperstein, H. Wilkinson, E. Maes, M. Vanbrabant, W. Jonckheere, P. Van Gelder, D. Hartmann, R. D'Hooge, B. De Strooper, J. Schymkowitz and F. Rousseau, *EMBO J.*, 2008, **27**, 224–233.
130 C. Behl, J. B. Davis, R. Lesley and D. Schubert, *Cell*, 1994, **77**, 817–827.
131 R. Baruch-Suchodolsky and B. Fischer, *Biochemistry*, 2008, **47**, 7796–7806.
132 G. M. Bishop and S. R. Robinson, *Brain Pathol.*, 2004, **14**, 448–452.
133 A. Kontush and C. S. Atwood, *Brain Res. Rev.*, 2004, **46**, 118–120.
134 L. Guilloreau, S. Combalbert, A. Sournia-Saquet, H. Mazarguil and P. Faller, *ChemBioChem*, 2007, **8**, 1317–1325.
135 A. C. Leskovjan, A. Lanzirotti and L. M. Miller, *NeuroImage*, 2009, **47**, 1215–1220.
136 E. Leung, L. Guo, J. Bu, M. Maloof, J. E. Khoury and C. Geula, *Neurobiol. Aging*, 2009.

CURRICULUM VITAE

Name: Ann Tiiman (b. Karafin)
Date of birth: 03.10.1984
Citizenship: Estonian

CONTACT INFORMATION

Address: Department of Gene Technology, Tallinn University of Technology, Akadeemia tee 15, 12618, Tallinn, Estonia
Phone: +372 620 4412
E-mail: tiimanann@gmail.com

EDUCATION

2009-2012 Tallinn University of Technology, PhD student
2007-2009 Tallinn University of Technology, Master degree
„Zn(II) and Cu(II) induced aggregation and fibrillization of Alzheimer's amyloid peptide"
2003-2007 Tallinn University of Technology, Bachelor degree
„The interactions of zinc and copper ions with Alzheimer's amyloid-β peptide"

AWARDS

2011 Tiina Mõis scholarship
2010 Estonian Biochemical Society Student Prize, I award
2010 World Federation of Scientists scholarship
2009 Estonian National Competition of Student Research Works, III place
2009 Estonian Academy of Sciences Student research contest, II award
2008 Estonian Biochemical Student Prize, I award
2007 Estonian National Competition of Student Research Works, III place

CONFERENCES

09. 04. 2010 Oral presentation „ Zn(II) and Cu(II)-induced nonfibrillar aggregates of amyloid-β peptide are transformed to amyloid fibrils, both spontaneously and under the influence of metal chelators" annual meeting of Estonian Biochemical Society, Tartu, Estonia
11-15.03. 2009 poster presentation „ Monitoring of A-beta fibrillization using an improved fluorimetric method" 9th international Conference AD/PD, Prague, Czech Republic
28.06. – 3.07.2008 poster presentation „Interactions of zinc (II) and copper (II) to the full-length Alzheimer's amyloid-β peptide *in vitro*, 33rd FEBS Congress & 11th IUBMB Conference, Athens, Greece
11.04.2008 Oral presentation „Binding of zinc(II) and copper (II) to the full length Alzheimer amyloid-beta peptide", annual meeting of Estonian Biochemical Society, Tartu, Estonia

EMPLOYMENT

01.02.2010 – 01.06.2010 Tallinn University of Technology, Faculty of Science, specialist

2006-2008 Tallinn University of Technology, Faculty of Science, specialist

ELULOOKIRJELDUS

Nimi: Ann Tiiman (s. Karafin)
Sünniaeg: 03.10.1984
Kodakondsus: Eesti

KONTAKTANDMED

Aadress: Geenitehnoloogia instituut, Tallinna Tehnikaülikool, Akadeemia tee 15, 12618, Tallinn, Eesti
Telefon: +372 620 4412
E-post: tiimanann@gmail.com

HARIDUSKÄIK

2009-2012 Tallinna Tehnikaülikool, doktorant
2007-2009 Tallinna Tehnikaülikool, magistri kraad
„Alzheimeri amüloid-beeta peptiidi fibrillatsioon ja agregatsioon Zn(II) ja Cu (II) toimel“
2003-2007 Tallinna Tehnikaülikool, bakalaureuse kraad
„Tsink- ja vaskioonide interaktsioonid Alzheimeri amüloid-β peptiidiga“

TUNNUSTUSED

2011 Tiina Mõisa nimeline stipendium
2010 Eesti Biokeemia Seltsi üliõpilaste teadustööde konkurss, I auhind
2010 World Federation of Scientists stipendium
2009 Eesti üliõpilaste teadustööde riiklik konkurss, III koht
2009 Eesti Teaduste Akadeemia üliõpilastööde konkurss, II auhind
2008 Eesti Biokeemia seltsi üliõpilaste teadustööde konkurss, I auhind
2007 Eesti üliõpilaste teadustööde riiklik konkurss, III koht

OSALEMINE KONVERENTSIDEL

09. 04. 2010 Suuline ettekanne „ Zn(II) and Cu(II)-induced nonfibrillar aggregates of amyloid-β peptide are transformed to amyloid fibrils, both spontaneously and under the influence of metal chelators“ Eesti Biokeemia seltsi aastakoosolek, Tartu
11-15.03. 2009 posterettekanne „ Monitoring of A-beta fibrillization using an improved fluorimetric method“ 9th international Conference AD/PD, Praha, Tšehhi
28.06. – 3.07.2008 posterettekanne „Interactions of zinc (II) and copper (II) to the full-length Alzheimer`s amyloid-β peptide *in vitro*, 33rd FEBS Congress & 11th IUBMB Conference, Ateena, Kreeka
11.04.2008 Suuline ettekanne „Binding of zinc(II) and copper (II) to the full length Alzheimer amyloid-beta peptide“, Eesti Biokeemia seltsi aastakoosolek, Tartu

TÖÖKOGEMUS

01.02.2010 - 01.06.2010 Tallina Tehnikaülikool, genoomika ja proteoomika õppetool, spetsialist

2006-2008 Tallina Tehnikaülikool, genoomika ja proteoomika õppetool, spetsialist

LIST OF PUBLICATIONS

Tõugu, V., **A. Tiiman** and P. Palumaa (2011). "Interactions of Zn(II) and Cu(II) Ions with Alzheimer's Amyloid-Beta Peptide. Metal Ion Binding, Contribution to Fibrillization and Toxicity." Metallomics **3**(3): 250-261

Zovo, K., E. Helk, **A. Karafin**, V. Tõugu and P. Palumaa (2010). "Label-Free High-Throughput Screening Assay for Inhibitors of Alzheimer's Amyloid-B Peptide Aggregation Based on MALDI MS." Anal. Chem. **82**(20): 8558-8565.

Tõugu, V., **A. Karafin**, K. Zovo, R. S. Chung, C. Howells, A. K. West and P. Palumaa (2009). "Zn(II)- and Cu(II)-Induced Non-Fibrillar Aggregates of Amyloid-Beta (1-42) Peptide Are Transformed to Amyloid Fibrils, Both Spontaneously and under the Influence of Metal Chelators." J. Neurochem. **110**(6): 1784-1795.

Karafin, A., P. Palumaa and V. Tõugu (2009). "Monitoring of Amyloid-Beta Fibrillization Using an Improved Fluorimetric Method." New Trends Alzheimer Parkinson Relat. Disord.: AD/PD 2009, 9th , Medimond 255-261.

Tõugu, V., **A. Karafin** and P. Palumaa (2008). "Binding of Zinc(II) and Copper(II) to the Full-Length Alzheimer's Amyloid-Beta Peptide." J. Neurochem. **104**(5): 1249-1259.

DISSERTATIONS DEFENDED AT TALLINN UNIVERSITY OF TECHNOLOGY ON *NATURAL AND EXACT SCIENCES*

1. **Olav Kongas**. Nonlinear Dynamics in Modeling Cardiac Arrhytmias. 1998.
2. **Kalju Vanatalu**. Optimization of Processes of Microbial Biosynthesis of Isotopically Labeled Biomolecules and Their Complexes. 1999.
3. **Ahto Buldas**. An Algebraic Approach to the Structure of Graphs. 1999.
4. **Monika Drews**. A Metabolic Study of Insect Cells in Batch and Continuous Culture: Application of Chemostat and Turbidostat to the Production of Recombinant Proteins. 1999.
5. **Eola Valdre**. Endothelial-Specific Regulation of Vessel Formation: Role of Receptor Tyrosine Kinases. 2000.
6. **Kalju Lott**. Doping and Defect Thermodynamic Equilibrium in ZnS. 2000.
7. **Reet Koljak**. Novel Fatty Acid Dioxygenases from the Corals *Plexaura homomalla* and *Gersemia fruticosa.* 2001.
8. **Anne Paju**. Asymmetric oxidation of Prochiral and Racemic Ketones by Using Sharpless Catalyst. 2001.
9. **Marko Vendelin**. Cardiac Mechanoenergetics *in silico*. 2001.
10. **Pearu Peterson**. Multi-Soliton Interactions and the Inverse Problem of Wave Crest. 2001.
11. **Anne Menert**. Microcalorimetry of Anaerobic Digestion. 2001.
12. **Toomas Tiivel**. The Role of the Mitochondrial Outer Membrane in *in vivo* Regulation of Respiration in Normal Heart and Skeletal Muscle Cell. 2002.
13. **Olle Hints**. Ordovician Scolecodonts of Estonia and Neighbouring Areas: Taxonomy, Distribution, Palaeoecology, and Application. 2002.
14. **Jaak Nõlvak**. Chitinozoan Biostratigrapy in the Ordovician of Baltoscandia. 2002.
15. **Liivi Kluge**. On Algebraic Structure of Pre-Operad. 2002.
16. **Jaanus Lass**. Biosignal Interpretation: Study of Cardiac Arrhytmias and Electromagnetic Field Effects on Human Nervous System. 2002.
17. **Janek Peterson**. Synthesis, Structural Characterization and Modification of PAMAM Dendrimers. 2002.
18. **Merike Vaher**. Room Temperature Ionic Liquids as Background Electrolyte Additives in Capillary Electrophoresis. 2002.
19. **Valdek Mikli**. Electron Microscopy and Image Analysis Study of Powdered Hardmetal Materials and Optoelectronic Thin Films. 2003.
20. **Mart Viljus**. The Microstructure and Properties of Fine-Grained Cermets. 2003.

21. **Signe Kask**. Identification and Characterization of Dairy-Related *Lactobacillus.* 2003.
22. **Tiiu-Mai Laht**. Influence of Microstructure of the Curd on Enzymatic and Microbiological Processes in Swiss-Type Cheese. 2003.
23. **Anne Kuusksalu**. 2–5A Synthetase in the Marine Sponge *Geodia cydonium*. 2003.
24. **Sergei Bereznev**. Solar Cells Based on Polycristalline Copper-Indium Chalcogenides and Conductive Polymers. 2003.
25. **Kadri Kriis**. Asymmetric Synthesis of C_2-Symmetric Bimorpholines and Their Application as Chiral Ligands in the Transfer Hydrogenation of Aromatic Ketones. 2004.
26. **Jekaterina Reut**. Polypyrrole Coatings on Conducting and Insulating Substracts. 2004.
27. **Sven Nõmm**. Realization and Identification of Discrete-Time Nonlinear Systems. 2004.
28. **Olga Kijatkina**. Deposition of Copper Indium Disulphide Films by Chemical Spray Pyrolysis. 2004.
29. **Gert Tamberg**. On Sampling Operators Defined by Rogosinski, Hann and Blackman Windows. 2004.
30. **Monika Übner**. Interaction of Humic Substances with Metal Cations. 2004.
31. **Kaarel Adamberg**. Growth Characteristics of Non-Starter Lactic Acid Bacteria from Cheese. 2004.
32. **Imre Vallikivi**. Lipase-Catalysed Reactions of Prostaglandins. 2004.
33. **Merike Peld**. Substituted Apatites as Sorbents for Heavy Metals. 2005.
34. **Vitali Syritski**. Study of Synthesis and Redox Switching of Polypyrrole and Poly(3,4-ethylenedioxythiophene) by Using *in-situ* Techniques. 2004.
35. **Lee Põllumaa**. Evaluation of Ecotoxicological Effects Related to Oil Shale Industry. 2004.
36. **Riina Aav**. Synthesis of 9,11-Secosterols Intermediates. 2005.
37. **Andres Braunbrück**. Wave Interaction in Weakly Inhomogeneous Materials. 2005.
38. **Robert Kitt**. Generalised Scale-Invariance in Financial Time Series. 2005.
39. **Juss Pavelson**. Mesoscale Physical Processes and the Related Impact on the Summer Nutrient Fields and Phytoplankton Blooms in the Western Gulf of Finland. 2005.
40. **Olari Ilison**. Solitons and Solitary Waves in Media with Higher Order Dispersive and Nonlinear Effects. 2005.
41. **Maksim Säkki**. Intermittency and Long-Range Structurization of Heart Rate. 2005.

42. **Enli Kiipli**. Modelling Seawater Chemistry of the East Baltic Basin in the Late Ordovician–Early Silurian. 2005.
43. **Igor Golovtsov**. Modification of Conductive Properties and Processability of Polyparaphenylene, Polypyrrole and polyaniline. 2005.
44. **Katrin Laos**. Interaction Between Furcellaran and the Globular Proteins (Bovine Serum Albumin β-Lactoglobulin). 2005.
45. **Arvo Mere**. Structural and Electrical Properties of Spray Deposited Copper Indium Disulphide Films for Solar Cells. 2006.
46. **Sille Ehala**. Development and Application of Various On- and Off-Line Analytical Methods for the Analysis of Bioactive Compounds. 2006.
47. **Maria Kulp**. Capillary Electrophoretic Monitoring of Biochemical Reaction Kinetics. 2006.
48. **Anu Aaspõllu.** Proteinases from *Vipera lebetina* Snake Venom Affecting Hemostasis. 2006.
49. **Lyudmila Chekulayeva**. Photosensitized Inactivation of Tumor Cells by Porphyrins and Chlorins. 2006.
50. **Merle Uudsemaa**. Quantum-Chemical Modeling of Solvated First Row Transition Metal Ions. 2006.
51. **Tagli Pitsi**. Nutrition Situation of Pre-School Children in Estonia from 1995 to 2004. 2006.
52. **Angela Ivask**. Luminescent Recombinant Sensor Bacteria for the Analysis of Bioavailable Heavy Metals. 2006.
53. **Tiina Lõugas**. Study on Physico-Chemical Properties and Some Bioactive Compounds of Sea Buckthorn (*Hippophae rhamnoides* L.). 2006.
54. **Kaja Kasemets**. Effect of Changing Environmental Conditions on the Fermentative Growth of *Saccharomyces cerevisae* S288C: Auxo-accelerostat Study. 2006.
55. **Ildar Nisamedtinov**. Application of ^{13}C and Fluorescence Labeling in Metabolic Studies of *Saccharomyces* spp. 2006.
56. **Alar Leibak**. On Additive Generalisation of Voronoï's Theory of Perfect Forms over Algebraic Number Fields. 2006.
57. **Andri Jagomägi**. Photoluminescence of Chalcopyrite Tellurides. 2006.
58. **Tõnu Martma**. Application of Carbon Isotopes to the Study of the Ordovician and Silurian of the Baltic. 2006.
59. **Marit Kauk**. Chemical Composition of $CuInSe_2$ Monograin Powders for Solar Cell Application. 2006.
60. **Julia Kois**. Electrochemical Deposition of $CuInSe_2$ Thin Films for Photovoltaic Applications. 2006.
61. **Ilona Oja Açik**. Sol-Gel Deposition of Titanium Dioxide Films. 2007.

62. **Tiia Anmann**. Integrated and Organized Cellular Bioenergetic Systems in Heart and Brain. 2007.
63. **Katrin Trummal**. Purification, Characterization and Specificity Studies of Metalloproteinases from *Vipera lebetina* Snake Venom. 2007.
64. **Gennadi Lessin**. Biochemical Definition of Coastal Zone Using Numerical Modeling and Measurement Data. 2007.
65. **Enno Pais**. Inverse problems to determine non-homogeneous degenerate memory kernels in heat flow. 2007.
66. **Maria Borissova**. Capillary Electrophoresis on Alkylimidazolium Salts. 2007.
67. **Karin Valmsen**. Prostaglandin Synthesis in the Coral *Plexaura homomalla*: Control of Prostaglandin Stereochemistry at Carbon 15 by Cyclooxygenases. 2007.
68. **Kristjan Piirimäe**. Long-Term Changes of Nutrient Fluxes in the Drainage Basin of the Gulf of Finland – Application of the PolFlow Model. 2007.
69. **Tatjana Dedova**. Chemical Spray Pyrolysis Deposition of Zinc Sulfide Thin Films and Zinc Oxide Nanostructured Layers. 2007.
70. **Katrin Tomson**. Production of Labelled Recombinant Proteins in Fed-Batch Systems in *Escherichia coli*. 2007.
71. **Cecilia Sarmiento**. Suppressors of RNA Silencing in Plants. 2008.
72. **Vilja Mardla**. Inhibition of Platelet Aggregation with Combination of Antiplatelet Agents. 2008.
73. **Maie Bachmann**. Effect of Modulated Microwave Radiation on Human Resting Electroencephalographic Signal. 2008.
74. **Dan Hüvonen**. Terahertz Spectroscopy of Low-Dimensional Spin Systems. 2008.
75. **Ly Villo**. Stereoselective Chemoenzymatic Synthesis of Deoxy Sugar Esters Involving *Candida antarctica* Lipase B. 2008.
76. **Johan Anton**. Technology of Integrated Photoelasticity for Residual Stress Measurement in Glass Articles of Axisymmetric Shape. 2008.
77. **Olga Volobujeva**. SEM Study of Selenization of Different Thin Metallic Films. 2008.
78. **Artur Jõgi**. Synthesis of 4'-Substituted 2,3'-dideoxynucleoside Analogues. 2008.
79. **Mario Kadastik**. Doubly Charged Higgs Boson Decays and Implications on Neutrino Physics. 2008.
80. **Fernando Pérez-Caballero**. Carbon Aerogels from 5-Methylresorcinol-Formaldehyde Gels. 2008.
81. **Sirje Vaask**. The Comparability, Reproducibility and Validity of Estonian Food Consumption Surveys. 2008.

82. **Anna Menaker**. Electrosynthesized Conducting Polymers, Polypyrrole and Poly(3,4-ethylenedioxythiophene), for Molecular Imprinting. 2009.
83. **Lauri Ilison**. Solitons and Solitary Waves in Hierarchical Korteweg-de Vries Type Systems. 2009.
84. **Kaia Ernits**. Study of In_2S_3 and ZnS Thin Films Deposited by Ultrasonic Spray Pyrolysis and Chemical Deposition. 2009.
85. **Veljo Sinivee**. Portable Spectrometer for Ionizing Radiation "Gammamapper". 2009.
86. **Jüri Virkepu**. On Lagrange Formalism for Lie Theory and Operadic Harmonic Oscillator in Low Dimensions. 2009.
87. **Marko Piirsoo**. Deciphering Molecular Basis of Schwann Cell Development. 2009.
88. **Kati Helmja**. Determination of Phenolic Compounds and Their Antioxidative Capability in Plant Extracts. 2010.
89. **Merike Sõmera**. Sobemoviruses: Genomic Organization, Potential for Recombination and Necessity of P1 in Systemic Infection. 2010.
90. **Kristjan Laes**. Preparation and Impedance Spectroscopy of Hybrid Structures Based on $CuIn_3Se_5$ Photoabsorber. 2010.
91. **Kristin Lippur**. Asymmetric Synthesis of 2,2'-Bimorpholine and its 5,5'-Substituted Derivatives. 2010.
92. **Merike Luman**. Dialysis Dose and Nutrition Assessment by an Optical Method. 2010.
93. **Mihhail Berezovski**. Numerical Simulation of Wave Propagation in Heterogeneous and Microstructured Materials. 2010.
94. **Tamara Aid-Pavlidis**. Structure and Regulation of BDNF Gene. 2010.
95. **Olga Bragina**. The Role of Sonic Hedgehog Pathway in Neuro- and Tumorigenesis. 2010.
96. **Merle Randrüüt**. Wave Propagation in Microstructured Solids: Solitary and Periodic Waves. 2010.
97. **Marju Laars**. Asymmetric Organocatalytic Michael and Aldol Reactions Mediated by Cyclic Amines. 2010.
98. **Maarja Grossberg**. Optical Properties of Multinary Semiconductor Compounds for Photovoltaic Applications. 2010.
99. **Alla Maloverjan**. Vertebrate Homologues of Drosophila Fused Kinase and Their Role in Sonic Hedgehog Signalling Pathway. 2010.
100. **Priit Pruunsild**. Neuronal Activity-Dependent Transcription Factors and Regulation of Human *BDNF* Gene. 2010.
101. **Tatjana Knjazeva**. New Approaches in Capillary Electrophoresis for Separation and Study of Proteins. 2011.

102. **Atanas Katerski**. Chemical Composition of Sprayed Copper Indium Disulfide Films for Nanostructured Solar Cells. 2011.
103. **Kristi Timmo.** Formation of Properties of $CuInSe_2$ and $Cu_2ZnSn(S,Se)_4$ Monograin Powders Synthesized in Molten KI. 2011.
104. **Kert Tamm**. Wave Propagation and Interaction in Mindlin-Type Microstructured Solids: Numerical Simulation. 2011.
105. **Adrian Popp**. Ordovician Proetid Trilobites in Baltoscandia and Germany. 2011.
106. **Ove Pärn**. Sea Ice Deformation Events in the Gulf of Finland and This Impact on Shipping. 2011.
107. **Germo Väli**. Numerical Experiments on Matter Transport in the Baltic Sea. 2011.
108. **Andrus Seiman**. Point-of-Care Analyser Based on Capillary Electrophoresis. 2011.
109. **Olga Katargina**. Tick-Borne Pathogens Circulating in Estonia (Tick-Borne Encephalitis Virus, *Anaplasma phagocytophilum*, *Babesia* Species): Their Prevalence and Genetic Characterization. 2011.
110. **Ingrid Sumeri**. The Study of Probiotic Bacteria in Human Gastrointestinal Tract Simulator. 2011.
111. **Kairit Zovo**. Functional Characterization of Cellular Copper Proteome. 2011.
112. **Natalja Makarytsheva**. Analysis of Organic Species in Sediments and Soil by High Performance Separation Methods. 2011.
113. **Monika Mortimer**. Evaluation of the Biological Effects of Engineered Nanoparticles on Unicellular Pro- and Eukaryotic Organisms. 2011.
114. **Kersti Tepp**. Molecular System Bioenergetics of Cardiac Cells: Quantitative Analysis of Structure-Function Relationship. 2011.
115. **Anna-Liisa Peikolainen**. Organic Aerogels Based on 5-Methylresorcinol. 2011.
116. **Leeli Amon**. Palaeoecological Reconstruction of Late-Glacial Vegetation Dynamics in Eastern Baltic Area: A View Based on Plant Macrofossil Analysis. 2011.
117. **Tanel Peets**. Dispersion Analysis of Wave Motion in Microstructured Solids. 2011.
118. **Liina Kaupmees**. Selenization of Molybdenum as Contact Material in Solar Cells. 2011.
119. **Allan Olspert**. Properties of VPg and Coat Protein of Sobemoviruses. 2011.
120. **Kadri Koppel**. Food Category Appraisal Using Sensory Methods. 2011.
121. **Jelena Gorbatšova**. Development of Methods for CE Analysis of Plant Phenolics and Vitamins. 2011.
122. **Karin Viipsi**. Impact of EDTA and Humic Substances on the Removal of Cd and Zn from Aqueous Solutions by Apatite. 2012.
123. **David Schryer**. Metabolic Flux Analysis of Compartmentalized Systems Using Dynamic Isotopologue Modeling. 2012.
124. **Ardo Illaste**. Analysis of Molecular Movements in Cardiac Myocytes. 2012.
125. **Indrek Reile**. 3-Alkylcyclopentane-1,2-Diones in Asymmetric Oxidation and Alkylation Reactions. 2012.

126. **Tatjana Tamberg**. Some Classes of Finite 2-Groups and Their Endomorphism Semigroups. 2012.
127. **Taavi Liblik**. Variability of Thermohaline Structure in the Gulf of Finland in Summer. 2012.
128. **Priidik Lagemaa**. Operational Forecasting in Estonian Marine Waters. 2012.
129. **Andrei Errapart**. Photoelastic Tomography in Linear and Non-linear Approximation. 2012.
130. **Külliki Krabbi**. Biochemical Diagnosis of Classical Galactosemia and Mucopolysaccharidoses in Estonia. 2012.
131. **Kristel Kaseleht**. Identification of Aroma Compounds in Food using SPME-GC/MS and GC-Olfactometry. 2012.
132. **Kristel Kodar**. Immunoglobulin G Glycosylation Profiling in Patients with Gastric Cancer. 2012.
133. **Kai Rosin**. Solar Radiation and Wind as Agents of the Formation of the Radiation Regime in Water Bodies. 2012.